Volume 86 (1), March Spec. Issue 2020

Proceedings of the Indian National Science Academy

Special Issue : 36th IGC 2020 **Geoscience Research in India: The Indian Report to IUGS 2016-2020 (Part II)**

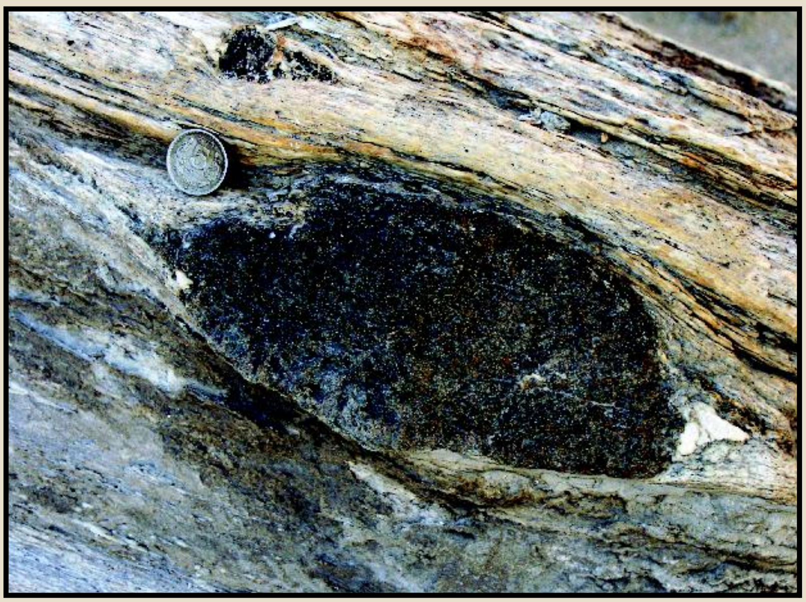

Guest Editors
A K Jain and D M Banerjee

Full text available at: http://www.insa.nic.in

PROCEEDINGS OF THE INDIAN NATIONAL SCIENCE ACADEMY

Proc Indian Natn Sci Acad **86** No. 1 March 2020 pp. 775-875

DOI: 10.16943/ptinsa/2020/49834

The Indian Subcontinent: Its Tectonics

A K JAIN[1,*] and D M BANERJEE[2,*]
CSIR-Central Building Research Institute, Roorkee 247 667, India
Department of Geology, University of Delhi, Delhi 110 007, India

A new geological and tectonic map of the India Subcontinent is presented with a brief description of its various elements. The map cover parts of India, Bhutan, Nepal, Sri Lanka, Bangladesh, Myanmar, and Pakistan and some of the offshore regions. The Extra-Peninsular region includes the Cenozoic Himalayan Orogen in Pakistan, India Nepal, Bhutan and its possible extension into Myanmar. This belt is separated fronm the Peninsular region by the vast late Cenozoic-Pleistocene Indo-Gangetoc-Brahmaputra Basin. The Peninsular India is mostly composed of six Archean-Proterozoic cratonic nuclei with indications of Hadean elements in Singhbhum. Proterozoic mobile belts surround these nuclei; hence the peninsular part might have been a single continent till end of Proterozoic. Deformation and metamorphism gradually decreased in their intensity, when vast Proterozoic sedimentary basins evolved over the Indian cratons and mobile belts unconformably. Paleo-Mesozoic rifts created the coal-bearing Gondwana basins, followed by marine transgressions before the onset of extensive Deccan volcanic eruptions in the western parts of the continent.

Renewed northward movement of main Gondwan fragment as the part of the Indian Plate and its convergence with the Asian Plate caused the closure of the Tethyan Ocean in the north along the Indus-Tsangpo Suture Zone and evolution of the Himalayan Orogen during the Cenozoic when northern Indian margin was remobilized, deformed and metamorphosed. Uplift, exhumation and erosion of this mountain caused vast transportation of sediments in the Himalayan foreland basins and the Indo-Gangetic-Brahmaputra Basin. Northward movement of the Indian Plate was partitioned into dextral transpresional tectonics and eastward subduction in the Myanmar-Andaman.

Keywords: **Geology and Tectonics; India; Bhutan; Nepal; Sri Lanka; Bangla Desh; Myanmar and Their Various Tectonic Elements; Geological and Tectonic Map**

Introduction

The Indian Subcontinent is composed of the continental lithosphere and constitutes one of the very significant components of the Indian Plate as a part of the Gondwanaland that broke into fragments at ~100 Ma and started moving northwards. The Indian Plate includes most of South Asia—the Indian Subcontinent —and a portion of the basin under the Indian Ocean, parts of Tibet (South China) and western Indonesia, and extending up to the Indus-Tsangpo Suture Zone which marks the boundary of this plate with the northern Asian Plate. The plate has a convergent margin along the Himalaya in the north, transform margins in the west and the east, and the oceanic ridge in the Indian Ocean (Fig. 1).

We have defined the Indian Subcontinent as the southern part of Asia comprising India, Pakistan, Nepal, Bhutan, Bangladesh, Sri Lanka, and Myanmar, though Tibet, once considered a part of this Subcontinent, was linked to this landmass before Permian. Although Myanmar, traditionally linked to the Indian Subcontinent, has many tectonic commonalities with the terrains of Thailand and Malaysia. All these countries share many geological features that transgress political boundaries. In other words, the evolutionary history of this south Asian geographic segment is common, represented today by trans-country mountain ranges, rivers, coastline, and desert.

We have classified these terrains confined by the Himalayan orogen, Trans-Himalaya, and the Karakoram in the north, Kirthar and Sulaiman ranges in the northwest and west, Indo-Myanmar Ranges including Patkai, Naga, Arakan Yoma Mountains in the east extending into the Gulf of Thailand through the Bay of Bengal.

**Author for Correspondence: E-mail: himalfes@gmail.com; dhirajmohanbanerjee@gmail.com*

A realization has emerged that a common geological and tectonic map of all the countries making the continental lithosphere of the Indian Plate has not been recently published when many of these countries are organizing and participating in the 36th International Geological Congress (IGC) in Mach; 2020, Delhi India. This write-up provides a summary account of various geological and tectonic elements, constituting the Indian Subcontinent. Traditionally, it is sub-divided into (i) Peninsular India with uplands and seacoasts, (ii) Exta-Peninsula region of the Himalayan Range including ranges in Pakistan and Myanmar, and (iii) The Indus-Ganga-Brahmaputra Plain sandwiched between the two.

Geological and Tectonic Elements of the Map

Compiled geological and tectonic map incorporates the following distinct units which are linked with each other in space and time: (i) Indian Cratons, (ii) Tectonics of Sri Lanka, (iii) Proterozoic Mobile Belts, (iv) Proterozoic 'Purana' Sedimentary Basins, (v) Tectonics of the Himalaya, (vi) Trans-Himalaya and Karakoram, (vii) Deccan Traps, (viii) Tectonics of Western Margin of India, (ix) Geology and Tectonics of Bangladesh, (x) Geology and Tectonics of Myanmar, and (xi) Geology and Tectonics of Pakistan (Plate 1 in folder).

Indian Cratons

The Precambrian Peninsular India is comprised of six ancient cratonic nuclei that were formed with a prolonged geological history spanning the Archean and Paleoproterozoic era (Fig. 1). These are classified into the North Indian Block (NIB) and the South Indian

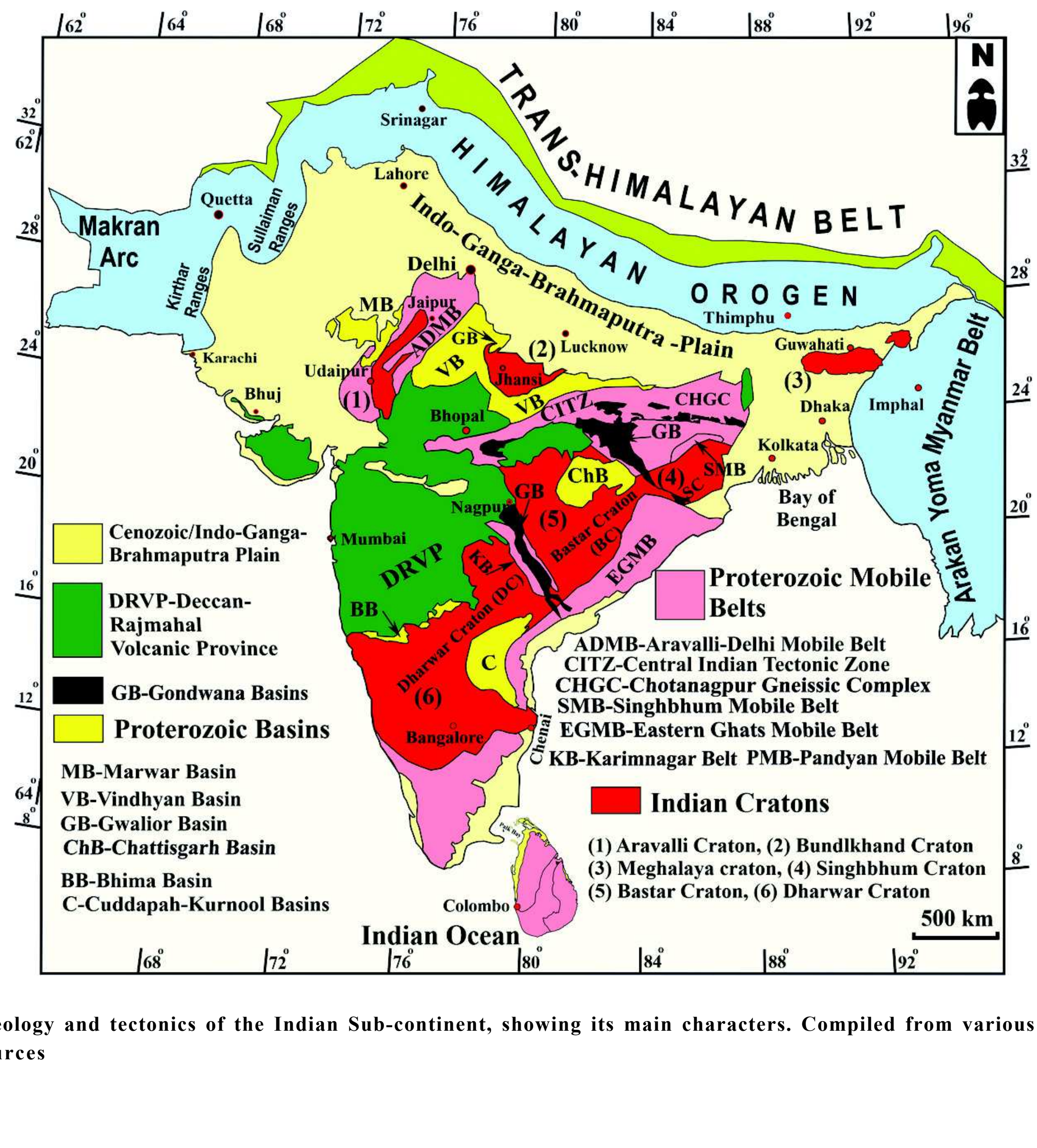

Fig. 1: Geology and tectonics of the Indian Sub-continent, showing its main characters. Compiled from various published sources

Block (SIB) (Naqvi and Rogers, 1987). The former comprises of the Bundelkhand and Aravalli Cratons and the latter is made up of the Dharwar, Bastar and Singhbhum cratons; these are all surrounded by younger Proterozoic Fold Belts. A prominent ENE-WSW trending Central India Tectonic Zone (CITZ) separates these blocks whose fabric extends eastward through Chhotanagpur Plateau, while the isolated Meghalaya makes the sixth craton (Sharma, 2009).

Aravalli Craton

The Aravalli Craton with highly complex geological history is identified as the Banded Gneissic Complex (BGC) (Heron, 1953) The southeastern boundary of this craton hugs the Vindhyan sedimentary basin and Deccan Volcanics across the northwest-directed Great Boundary Fault (GBF). It is surrounded mostly by the Proterozoic Aravalli Supergroup belt, while in the northwest Sandmata Complex is juxtaposed against the Delhi Supergroup.

The Aravalli Craton is comprised of the following units (Sharma and Mondal, 2019, and references therein): (i) Banded Gneissic Complex (BGC-I and BGC-II) of 3.5–3.2 Ga, (ii) volcano-sedimentary belts of 2.8 Ga, and (iii) calc-alkaline to high-K Berach granitoid. Fareeduddin and Banerjee (2020) have critically evaluated validity of view of term 'Banded Gneissic Complex' (BGC) in view various provisions in the stratigraphic codes.

Banded Gneissic Complex (BGC): The BGC is made up of granite gneisses, migmatites, metasedimentary enclave and metabasics (Heron, 1953). Gupta *et al*. (1997) classified pre-Aravalli gneissic granitoids under the Mangalwar Complex of the Bhilwara Supergroup. Roy (1988) named the pre-Aravalli granite-gneiss-amphibolite bodies as the Mewar Gneiss. The BGC occurring to the north and south of Nathdwara, Udaipur valley shows marked differences in contact relationship, metamorphism and age. These were identified as the BGC-I in the south and named as the Bhilwara Gneiss (Gupta, 1934), with tonalite–trondjhemite–granite, gneiss–migmatite-granitoid–amphibolite as the 3.3-3.2 Ga nuclei (Wiedenbeck and Goswami, 1994). The BGC-II is exposed north of Nathdwara as a single crustal block with granite magmatism and metamorphism at 2.54–2.45 Ga. There are conflicting interpretations of the BGC, from a Proterozoic migmatized Aravalli and Raialo (Naha and Halyburton, 1974) to a remobilized Archean entity (Sharma, 1988; Roy *et al*., 2005). Different stages of structural and metamorphic transformations have largely obliterated the original protolith history (Bhowmick and Dasgupta, 2012).

The Aravalli Craton experienced tectonothermal events during the Proterozoic orogeny (ca.1.7 Ga) (Buick *et al*., 2006), when the BGC-I domain remained unaffected, while the BGC-II was largely reworked (Roy *et al*., 2005). Oldest zircon of 3491 ± 7 Ma was derived from the volcanics at the culminating phase of the BGC (McKenzie *et al*., 2013). Gopalan *et al*. (1990) measured a 3.31 ± 0.07 Ga Sm-Nd isochron age from the Ahar River granite and a younger isochron age of 2.83 ± 0.05 Ga for mafic amphibolites within the gneisses of the 2.95 Ga Untala granitoid. Similarities in ages of gneisses and associated amphibolites suggest that mafic volcanism is synchronous to the granitic protoliths. U-Pb-Hf isotope studies by Kaur *et al*. (2019) reveal that the TTG precursors of gneissic complex intruded during the Paleoarchean (3.31 Ga) and Neoarchean (2563-2548 Ma).

On the other hand, the BGC-II yields largely Proterozoic ages (~1.7 Ga) with sporadic Archean remnants (Buick *et al*., 2006; Dharma Rao *et al*., 2011). The Proterozoic tectono-thermal events did not leave any imprint on the BGC-I cratonic component. In Central Rajasthan, the BGC-II reveals two contrasting metamorphic histories: (i) distinct litho-tectonic domain of the Sandmata Complex with granulite facies metamorphosed pelites, charnockite, calc-silicates, minor mafic dykes and intrusive granitoids, and (ii) Mangalwar Complex (MC) of amphibolite facies assemblage within trondhejemite-tonalite gneisses (TTG), calc-silicates and meta-sediments (Gupta, 1934; Gupta *et al*., 1980, 1997). The Banas Dislocation Zone (BDZ) delimits the MC to its north while the BGC-I and the Aravalli Supergroup lies to its south (Sinha-Roy *et al*., 1998). The Sandmata granulites are polymetamorphic, with an early medium-pressure granulite facies metamorphism in the stability field of sillimanite. On the other hand, Mangalwar Complex is monocyclic having suffered only one high-pressure metamorphism (Bhowmick and Dasgupta, 2012). On culmination of the granitic activity these basement gneisses exhibit telltale evidence of rifting, volcanism, exhumation and erosion, followed by weathering and development of aluminous paleosol on top of the intermittent mafic volcanics (Banerjee, 1996; Pandit *et al.*, 2008). Between Hindoli-Jahajpur succession and the Mangalwar Complex, the BDZ is developed as a thrust contact and restricts the domain of the Delwara Dislocation Zone and Rakhabdeo Suture in the north (Sinha-Roy and Malhotra, 1989). The Sandmata Complex is juxtaposed against the Aravalli mobile belt due to the Kaliguman (Shear) Zone and the Delwara Dislocation Zone. In south, the Rakhabdeo Lineament abuts against north Gujarat Suture (Sant and Karanth, 1993) or extends up to western end of the Son-Narmada Fault in northern Gujarat.

Volcano-sedimentary Belt (2.8 Ga): Large linear Archean metasedimentaries overlie the BGC as dismembered remnants in the southeast and northeast of Udaipur (Roy and Jhakar, 2002), while Sinha-Roy *et al*. (1993) interpolated large-scale Archaean granite-greenstone set up within the Aravalli Craton. The Hindoli Group is also interpreted as a secondary greenstone belt juxtaposed with the Mangalwar terrane with a prominent DSZ. Low grade Jahajpur Formation and Hindoli Group pass into amphibolite grade migmatite of the Mangalwar Complex and are either considered equivalent to Aravallis of the Girwa Valley or the oldest unit in the metasedimntary succession.

Berach Granite: It crops out close to the GBF near Chittaurgarh and has either been interpreted as the basement for the overlying Aravalli metasediments or last phase of cratonization event (Sinha-Roy, 1985). Mondal and Raza (2013) consider these 2506-2580 granites as intrusive into the BGC due to partial melting of metasomatized subcontinental lithospheric mantle. The Untala Granitoid, however, was derived from an already evolved Paleoarchean crust, intruded by ~3100 Ma granite and reworked in the Neoarchean (Kaur *et al*., 2019).

While nuclei of the Indian Plate that are conventionally grouped together in the Ur assembly include the cratons of Dharwar, new radiometric dates favour grouping of Bundelkhand–Aravalli nucleus also as part of the Ur supercontinent (Mondal, 2009).

Bundelkhand Craton (BC)

The triangular-shaped Bundelkhand Craton covers an area of about 26,000 km2 and is separated from the Aravalli Craton by the Great Boundary Fault (GBF). Low grade Paleoproterozoic metasedimentaries of the Bijawar (=Sonrai) and Gwalior Basins occur on the margin of this craton, while unmetamorphosed sedimentary rocks of the Vindhyan basin wrap the craton in the north, southwest and west. NE-SW trending Aravalli–Delhi Fold Belt (ADFB) and the ENE-WSW trending Central Indian Tectonic Zone (CITZ) directly overlie this craton. The southern margin of the craton shows a steep gravity gradient which reflects presence of the nearby Son-Narmada Fault (Ramakrishnan and Vaidyanadhan, 2008).

Stratigraphic and Tectonic Units: The Bundelkhand Craton consists of following three distinct litho-tectonic uits:

(i) **Bundelkhand Gneissic Complex:** Vast track of the BC are covered by light coloured, highly deformed and layered 3.2–3.3, 2.7 and 2.5 Ga TTG ($^{207}Pb/^{206}Pb$ isotopic data of Gopalan *et al*., 1990), with the oldest felsic crust of 3551 ± 6 Ma, having Hf model ages between 3.80 Ga and 3.95 Ga (Kaur *et al*., 2016). The gneiss from Mahoba and Kuraicha yielded 3270 ± 3 Ma and 3297 ± 8 Ma ages for zircon (Mondal *et al*., 2002). Four Paleoarchean magmatic episodes have been identified within the BC at ca. 3.55, 3.44–3.40, 3.30 and 3.20 Ga at regular intervals of 100–150 Myr with reworking of older mafic and felsic crust between 3.55 and 3.20 Ga (Kaur *et al*., 2016).

(ii) **Bundelkhand Greenstone Belts:** Malviya *et al*. (2006) classified the greenstone belts into two complexes, viz. the Central Bundelkhand (Babina and Mauranipur belts) and the Southern Bundelkhand (Girar and Madaura belts) complex. The Babina–Mauranipur–Mahoba greenstone belt comprises disrupted sequences of amphibolites, banded iron formation, pillow basalts, komatiitic basalts, calc-silicate rocks, white schists, quartzites, anatectic granites, metapelites and ~3.55 to 3.20 Ga TTG intrusives (Absar *et al*., 2009).

Within the Babina belt, ultramafics (peridotite, dunite and pyroxenite) retain their primary geochemical signatures, while pillow lavas and volcanics are subalkalic, and low-K tholeiitic basaltic andesite. BIF is associated with metamorphosed arenites, pelites, marble and calc-silicates. The Mauranipur supracrustals represent an Archean ophiolite sequence in an island arc setting of converging plates (Malviya *et al*., 2006). Babina greenstone calc-alkaline felsic dacites have U-Pb Shrimp zircon age of 2542 ± 17 Ma. Arkose, greywacke and mafic-rich metapelites were derived from the erosion of young TTG and granitic batholithic rocks (Raza and Mondal, 2018). In Lalitpur region, volcanogenic Mehroni Group is represented by meta-sedimentaries, gneisses and meta-volcanics of the Kuraicha Formation of conglomerate, marble, BHQ and intercalated basalt. High-pressure metamorphism affected the Babina belt with the development of corundum-bearing phlogopite-chlorite schists.

The Bansi Rhyolite yielded Pb-Pb zircon age of 2517 ± 7 Ma (Mondal *et al*., 2002), like the Bundelkhand Granite.

(iii) **Bundelkhand Igneous Complex:** After the emplacement of the TTGs between 3.5-3.3 and 2.7 Ga, and after a time gap of about 130 Ma (Joshi *et al*., 2017), the BC witnessed widespread intrusion of the Bundelkhand Igneous Complex containing coarse to fine grained and grey to pink granites between 2.58 and 2.45 Ga (Sm-Nd isotopic and U-Pb-zircon ages) with interlayered contemporaneous rhyolite as dykes and sills (Mondal *et al*., 2002; Joshi *et al*., 2017; Kaur *et al*., 2016; Verma *et al*., 2016).

(iv) **Mafic dykes and Quartz Reefs:** NW–SE, to WSW–ENE and NE–SW trending mafic dykes intrude the BC as the youngest magmatic activity and display chilled margins with an aphanitic groundmass of plagioclase microlite laths, granular Fe–Ti oxides and fine clinopyroxene needles (Basu, 1986). Laser ablation $^{40}Ar/^{39}Ar$ dates suggested their emplacement in two phases at 2.15 Ga and 2.09 Ga (Rao *et al*., 2005). The NW–SE trending dykes yielded a U–Pb concordia age of 1979 ± 8 Ma and a mean $^{207}Pb/^{206}Pb$ age of 1113 ± 7 Ma for ENE–WSW trending confirming at least two distinct dyke emplacement events within the BC (Pradhan *et al*., 2012). A U–Pb rutile age of 2100 ± 11 Ma was interpreted as a minimum age of emplacement for a metamorphosed dyke (French *et al*., 2008). High precision U–Pb baddeleyite and zircon ages indicated emplacement of two unmetamorphosed dolerite dykes at 1891.1 ± 0.9 and 1888 ± 1.4 Ma (Meert *et al*., 2011). These dykes apparently represent a post-cratonization event. Giant quartz veins (GQV)/ quartz reefs constitute spectacular landforms in the BC due to their resistance to erosion, homogeneous distribution and NE–SW trending preferred orientation (Basu, 1986). Brittle and brittle–ductile shear zones controlled the distribution of these reefs which were emplaced in an extensional phase (Roday *et al*., 1995).

Regional Deformation Pattern: At least three phases of folding in the supracrustal rocks are evident (Roday *et al*., 1995). The ~2.5 Ga granitoids exhibit submagmatic fabric unaffected by later deformation events. Gneissic foliation plane is folded by later folds with N-S trending axial plane foliation, while hook-shaped folds indicate coaxial character of two deformation events.

The BC is Dissected by Three Major E-W Trending Ductile Shear Zones: Raksa Tectonic Zone–RTZ, Madura Tectonic Zone–MTZ and Bundelkhand Tectonic Zone–BTZ; the oldest vertical BTZ shear system is marked by mylonites having alternating ultramylonite (dark) and mylonite foliated layers with sinistral shear sense (Pati *et al*., 1997).

Dhala Impact Crater: Deeply eroded Dhala Crater is a near-circular structure of ~11 km diameter in western parts of the BC and has been interpreted either as a cryptovolcanic explosion structure (cauldron structure) or world's seventh oldest meteoritic impact structure (Pati *et al*., 2017). The crater has a distinct (i) central elevated area (CEA) of the Paleoproterozoic Vindhyan Supergroup, (ii) pre-Vindhyan flat-lying alternating argillaceous-arenaceous sediments and lateritized conglomerate, and (iii) rings of impact melt veins and large breccia on the impacted Archean granitoids (Pati *et al*., 2008).

Crustal Evolution: U-Pb zircon dating from the Bundelkhand Craton indicate the presence of ~3.55 Ga TTG (Kaur *et al*., 2016), though presence of zircon xenocrysts of 3.59 Ga and zircon Hf model age (two-stage) up to 3.95 Ga suggest an older crust formation history around Eoarchean (Saha *et al*., 2011; Kaur *et al*., 2016). In this craton the Neoarchaean is marked by appearance of a variety of mantle- and crust-derived granitoids including TTGs, sanukitoids, granites, anatectic K-rich leucogranites and A-type granites (Kaur *et al*., 2016). The 2.51 Ga K-rich anatectic leucogranites mark the reworking and cratonization of Archean crust.

Meghalaya Craton (MC)

Sharma (2009) named the Precambrian succession of the Shillong-Mikir Hills as a distinct Meghalaya Craton (MC) with an exposed area of approximately 33,000 km^2. ENE-trending and rectangular-shaped plateau is extensively covered by the Holocene alluvium of the Brahmaputra River. E-W trending Dauki fault system, NE trending Haflong Fault, the Jamuna Fault/NW-SE trending Kopili Fault, E-W trending Brahmaputra Fault System (the Oldham Fault) provide the physical limits of this craton on all sides, with the Cretaceous Sylhet Trap (133–100 Ma) in the south. Geologically, the following units characterize the Meghalaya Craton:

Archean Gneissic Complex: It consists of granite gneiss, augen gneiss, and upper amphibolite to granulite facies metamorphics. Cordierite–sillimanite±corumdum gneiss/schist, quartz–feldspar orthogneiss, amphibolite, granulite and biotite± hornblende schists are dominant lithologies of the craton (Hussain *et al*., 2019), and are intimately associated with granite gneiss in the Khasi Hills. Bidyananda and Deomurari (2007) obtained ^{207}Pb/^{206}Pb zircon Neoarchean–Paleoproterozoic (2637 ± 55, 2230 ± 13 Ma) ages from quartzo-feldspathic gneiss for the core-rim, while other zircon grains ranged between 1.98 and 1.67 Ga. Thermal overprinting during Proterozoic ~1.7 Ga was reported by Rb-Sr dating of granitoids. A gneissic sample from Rhesu area of Garo Hills yielded ^{207}Pb/^{206}Pb zircon ages between 1.84 and 1.54 Ga. Mesoproterozoic granulite facies metapelites of Garo-Goalpara Hills) show monazite age of 1596 ± 15 Ma with its rims having younger ages of 1032 to 1273 Ma (Chatterjee *et al*., 2007). A charnockite from Nongstoin–Riangdo road gave zircon ages between 1.28 and 1.08 Ga, like the Neoproterozoic imprints from the Eastern Ghats (Bidyananda and Deomurari, 2007). Metapelites have counterclockwise pressure–temperature path and near-peak conditions of 7–8 kbar and 850^{o}C. In the Sonapahar granulite facies, enclaves of corundum–spinel–sapphirine metapelites occur within the granite–granodiorite suite. Homogenous monazite grains in granulite facies metapelites yielded tightly clustered date at 500 ± 14 Ma which nearly coincides with ~480 Ma Rb-Sr dates of the porphyritic granite that intruded the Meghalaya gneiss complex (Chatterjee *et al*., 2007).

Proterozoic Shillong Group: The Archean Gneissic Complex is unconformably overlain by NE-SW trending Proterozoic Shillong Group, containing mica schist, phyllite, quartzite and slate. The maximum time limit of the Shillong Group is given by Rb-Sr whole-rock isochron age of 1150 ± 26 Ma granite gneiss that occurs at the base of the Shillong Group (see Ghosh *et al*., 1991). Maximum depositional age of the Shillong Group cover is indicated by the youngest detrital zircon of 1.48 Ga (Bidyananda and Deomurari, 2007). Yin *et al*. (2010) noted Pb-Pb zircons ages from 3.3 to 1.1 Ga, with two sub-groups of 1.1 ± 1.25 and 1.5 ± 1.75 Ga. The Proterozoic hornblende gabbros of the Khasi Greenstone belt are best exposed in East Khasi Hills as lensoidal intrusives within the low-grade Shillong Group (Mazumder, 1986).

Late Neoproterozoic–Paleozoic Granitoids: The intrusive Mylliem granite has the Rb-Sr whole-rock isochron age of 607 ± 13.14 Ma (Chimote *et al*., 1988). Pink granite from Songsak of East Garo hills of 500 ± 40 Ma, Kyrdem (479 ± 26 Ma), Nongpoh (550 ± 15 Ma), Mylliem (607 ± 13 Ma) and South Khasi (690 ± 19 Ma) represent widespread magmatism during 600-500 Ma (Ghosh *et al*., 2005).

U-Pb SHRIMP zircon geochemistry and geochronology of the Rongjeng, Guwahati and Longavalli granite gneisses, and Sonsak, Kaziranga, South Khasi, Kyrdem and Nongpoh granitoids provide two distinct age groups: (i) 1778 ± 37 Ma, and (ii) 535 ± 11 Ma to 516 ± 9.0 Ma. The Cambrian granite plutons intruded the basement granite gneisses and the Shillong Group. Mafic to porphyritic microgranular enclaves of almost the same age (519.5 ± 9.7 Ma) occur within the South Khasi granitoid. Chemical (U–Th–Pb) monazite age of 501 ± 5 Ma of mafic magmatic enclaves provides the age of the magma hybridization event in the Nongpoh granitoids (Sadiq *et al*., 2017). In the Mikir (Karbi) Hills, late phase A-type bimodal granitoids profusely intrude the Shillong Group along with dolerite and amphibolites (metabasalts) of 515.1 ± 3.3 Ma age. The West Garo pluton is A-Type post-tectonic biotite-monzogranite and biotite-syenogranite with low Ca, alkaline and peraluminous character (Choudhury *et al*., 2012), and Rb-Sr age of 616 ± 86 Ma.

Carbonatite Complexes: The Meghalaya Craton witnessed an Early Cretaceous (105–107 Ma) igneous activity along N-S and E-W trending fractures, which controlled the emplacement of four ultramafic-alkaline-carbonatite complexes (UACC) (Sadiq *et al*., 2014). The Sung Valley carbonatite was emplaced into the Proterozoic Shillong Group and consists of ultramafics, alkaline rocks and carbonatites; the latter are the youngest intrusive phase classified as calcite carbonatite.

Sung Valley and Jasra UACC intrusions have U–Pb ages of 109.1 ± 1.6, 104.0 ± 1.3 and 101.7 ± 3.6 Ma (Srivastava *et al*., 2019) while nepheline syenite and perovskite in the Jasra clinopyroxenite have U–Pb zircon ages of 106.8 ± 1.5 and 101.6 ± 1.2 Ma.

Sylhet Trap: Outcrops of the Cretaceous Sylhet Traps are restricted to narrow east-west 60x80 km area along the southern edge of the Meghalaya Craton above the eroded Precambrian basement and are overlain by the Cretaceous-Eocene sediments. The Rajmahal Traps, basaltic rocks in subsurface Bengal Basin and the Sylhet Traps bear strong geochemical similarity and belong to a Large Igneous Province (LIP), which is related to the Kerguelen hotspot activity during the Early Cretaceous that affected the Archean East Indian cratonic margin (Baksi, 1995; Kent *et al*., 2002).

Tectonics: Seismically active Shillong Plateau (Meghalaya Craton) was affected by steep southerly-dipping Oldham Fault and the northerly-dipping Dauki-Dapsi Thrust. Due to the uplift of the Shillong Plateau, the Brahmaputra River was deflected northward and westward (Govin *et al*., 2018). Magnetotelluric imaging suggested the Meghalaya Craton to have been thrust over the Sylhet basin sediments. E-W trending Dauki Fault Zone (DFZ), located along southern margin of the craton, separates the plateau of about 1.2 to 1.5 km elevation from the sea-level exposures of Sylhet/Bangladesh Plains sediments. It merges with the NE-trending Haflong thrust belt. The Barapani Shear Zone (BSZ) trends NE-SW within the Shillong Group metamorphics and is characterized by distinct curviplanar landform features indicating its sinistral strike-slip character (Das *et al*., 1995). The Urn Ngot fault (UGF) trending N-S with dextral strike-slip controls the flow of river for more than 30 km before taking a westward turn and entering Bangladesh. The UGF intersects the Barapani Shear Zone in the north. The Jamuna Fault and Dudhnai Faults trend N-S, while the Kopili and the Guwahati Faults trend NW-SE.

Bastar Craton (BC)

Eastern and southeastern boundaries of the Bastar Craton show thrust contacts with the prominent Proterozoic Eastern Ghats Mobile Belt (EGMB). In the north lies the ENE-trending Central Indian Tectonic Zone–CITZ (Roy and Hanuma Prasad, 2003). The NW-trending Pranhita–Godavari and Mahanadi rift zones bound the craton on its southwestern and northeastern margins, respectively. The Deccan Traps cover its westernmost parts. The craton essentially is comprised of (i) Oldest gneissic complex with TTG suite, (ii) Proterozoic supracrustal volcano-sedimentary greenstone mobile belts, (iii) Paleoproterozoic younger granitoid intrusives, (iv) Granulite belts, (v) Mafic dike swarms, and (vi) Proterozoic sedimentary basins.

Sukma–Amgaon TTG Complex: The Sukma Gneiss is dominated by the TTG suite (Sukma Granite–I) and a K-rich granite (Sukma Granite–II), granulite, gabbro and gabbroic anorthosites. Tonalite gneiss yielded a U–Pb upper intercept age of 3561 ± 11 Ma (Ghosh, 2004), which is the oldest age of gneissic protolith obtained so far. A whole-rock 3018 ± 61 Ma Pb-Pb crystallization age for gneisses from the Sukma area reveal two generations of gneisses at 3.6-3.5 and 3.0 Ga (Sarkar *et al*., 1990). Engulfed within the vast Archaean TTG sequence are ancient supracrustals of the Sukma Group and Amgaon Group.

Supracrustal Volcano-sedimentary Greenstone Belts: This craton incorporates the Bengpal–Sukma belt in south, Kotri–Dongargarh belt in north and center, the Sonakhan belt in the east, the Amgaon belt in west, and the Chilpi belt in north and numerous scattered enclaves. The Bengpal Group unconformably overlies the Sukma Group, and contains amygdaloidal meta-basalts with intercalated schists, interlayered immature arkose, quartz- and lithic wackes, metapelites and the BIF. The Sukma Group consists of sillimanite quartzite, cordierite-sillimanite, cordierite anthophyllite rocks, calc-gneisses and widespread BIF. The sequence is intruded by granites. Unconformably overlying the Bengpal Group schists are the scattered BIFs (Bailaddila Group) within the gneisses, with the earliest deformation phase marked by isoclinal folds and later tight to open folds.

Largest Kotri-Dongargarh supracrustal belt unconformably overlies the Archean Sukma Gneiss/ Amgaon Gneiss, whose oldest Nandgaon Group is associated with bimodal volcanics. The lower felsic unit constitutes the Bijli Formation having WR Rb–Sr isochron ages of 2180 ± 25 and 2503 ± 35 Ma. The upper mafic unit forms the Pitepani Formation. The Dongarhgarh volcanics date 2465 ± 22 and 2270 ± 90 Ma (Krishnamurthy *et al*., 1988). The Nandgaon Group is intruded by the Dongargarh Granite (2465 ± 22 Ma) in the south and the Malanjkhand Granite (2490 ± 8 Ma) in the north. Intrusion of high-Mg mafic dykes of ~2450 Ma are found in both granites. The younger greenstone belts of the Bailadila, Sonakhan, and Abujhmar Groups comprise mafic and felsic volcanics and metasedimentary sequence containing the BIF. The craton was involved in another orogenic event marked by granulite facies metamorphism at the end Archaean time (2672 ± 54 Ma), followed by intrusion of alkali feldspar megacrystic granites and pink granites-the Sukma Granite, Keskal, Darbha, Sitagaon, Dongargarh and Malanjkhand granitoids of 2450-2650 Ma age (Mohanty, 2015).

The Neoarchean Sonakhan Greenstone Belt (SGB) is dominated by basalt, andesite, dacite, rhyolite and volcano-sedimentary rocks. In lower parts, the Baghmara Formation contains an association of entirely basaltic volcanics in lower unit, while upper unit comprised of basalt-andesite-dacite-rhyolite (BADR) series (Mondal and Raza, 2009).

Granites, Granulites and Dikes: N-S trending Malanjkhand Granitoid (MG), occurring along a 500 km^2 long pluton in Balaghat district, intrudes the older Amgaon schist/gneiss, and is exposed in northwest and west of the pluton. The Nandgaon Group bimodal volcano-sedimentary lithounits are exposed in the southern and eastern margins of the pluton. The MG is overlain by the Chilpi metasediments in its southeastern and western parts and is composed mainly of granodiorite to granite, linked with the Central Indian Tectonic Zone–CITZ (Yedekar *et al*., 1990; Jain *et al*., 1995). Based on WR Rb-Sr isochron age of 2347 ± 16 and $^{207}Pb/^{206}Pb$ zircon data from the MG, granitic activity is indicated at ca 2.48 Ga, while WR Rb-Sr ages are 2362 ± 58, 2467 ± 38 and 2243 ± 217 Ma (ca 2.4 Ga) indicating hydrothermal overprinting (Panigrahi *et al*., 1993). The Dongargarh Granite intrudes both the Nandgaon and the Amgaon gneiss and is nonconformably overlain by the Khairagarh Group. The Kanker Granite is peraluminous and silicic (SiO2=66–76 wt%) granite with a U-Pb zircon age of 2480 ± 3 Ma. Two granulite belts of Bastar Craton are the Bhopalpatnam granulite belt (BGB) and the Kondagaon granulite belt (KGB). Several NW-SE trending dike swarms are mafic to sub-alkaline with medium to high-grade metamorphism of ~2.9 Ga (BD1) and 1.88–1.89 Ga (BD2) along with ~2.4–2.5 Ga (BN) boninite–norite and tholeiitic dikes (Srivastava and Gautam, 2016, and references therein).

The Bastar Craton is dotted with numerous Proterozoic sedimentary basins like Chattisgarh, Khariar, Ampani, Keskar, Singanpur, Abujhmar, Indravati and Sabari basins (Ramakrishnan and Vaidyanadhan, 2008).

Singhbhum Craton (SC)

Pear-shaped Singhbhum Craton (SC), also known as the Singhbhum–Orissa Craton, encompasses N-S elongated body of approximately 50, 000 km^2 in Jharkhand, Orrisa and near-by regions in Eastern India. It is a complex of numerous lithounits of different ages and evolved during the Singhbhum Orogeny (Saha, 1994). It is divided into the following associations: (i) Older Metamorphic Group (OMG), (ii) Singhbhum Granite (SG) pluton, (iii) Iron Ore Group (IOG), (iv) Dhanjori and Simlipal Volcanics, (v) Newer Dolerite Dykes, (vi) Kolhan Group sediments. Tectonically, the Singhbhum Craton is limited by two major thrust zones: (i) Singhbhum Shear Zone (SBSZ) (also known as the Copper Belt Thrust) along its northern margin with the Singhbhum Mobile Belt (SMB), and (ii) the Sukinda Thrust (ST) along its southern margin against the Eastern Ghats Mobile

Belt.

Older Metamorphic Group (OMG-~3.5Ga): The OMG consists of intensely deformed fuchsite-bearing quartzite, mica schist, ortho- and para-amphibolite and calc-silicates with steeply plunging to vertical sheath folds (Roy and Bhattacharya, 2012). Quartz-kyanite, sillimanite-muscovite, quartz-feldspar aggregates and fuchsite-bearing quartzite indicate metamorphosed clay and regolith palaeosols having 'granite protoliths' (cf., Misra, 2006). Low-K tholeiitic (LKT) amphibolite of the OMG and amphibolites are enriched in large ion lithophile elements (LILE). Detrital zircon of the OMG metasediments yielded 3627 ± 39 Ma and ca. 3550 Ma ages and two younger clusters of 3.4 and 3.2 Ga (Goswami *et al*., 1995; Mondal *et al*., 2007), thus establishing the oldest maximum depositional age of the OMG sediments around 3.5 Ga on an unknown granitic basement. The younger ages were taken as metamorphic events.

Older Metamorphic Tonalite Gneiss (OMTG-3.45-3.30 Ga): The Older Metamorphic Tonalite Gneiss (OMTG) consists of enclaves of tonalite gneiss and quartz-feldspathic rocks with tectonically interleaved amphibolites (Saha, 1994). For the OMTG age data include Pb-Pb isochron of 3664 ± 79 Ma (Ghosh *et al*., 1996). These also include whole-rock Rb–Sr and Pb/Pb isochron ages of 3280 ± 130 and 3378 ± 98 Ma for the OMTG, 3448 ± 2.2 Ma U-Pb TIMS zircon age and ca. 3380 Ma Pb-Pb whole-rock age of 'tonalite-xenolith', 3442 ± 26 Ma Pb-Pb age of granitoid, 3457 ± 35 Ma and 3437 ± 9 Ma Pb-Pb zircon ages (Misra *et al*., 1999), U-Pb SHRIMP zircon age at 3380 ± 11 Ma for the tonalitic gneiss, 3448 ± 19 and 3527 ± 17 Ma U-Pb zircon ages of tonalitic gneiss from the northernmost part (Acharyya *et al*., 2010), and $^{207}Pb/^{206}Pb$ SHRIMP zircon age of 3.45 Ga from tonalite gneiss. $^{207}Pb/^{206}Pb$ ion probe zircon ages of the OMTG also cluster around 3.2 Ga, which is considered as growth during metamorphism (Mishra *et al*., 1999). In agreement with this age, are monazite ages of 3306 ± 22 Ma from the OMTG as crystallized during metamorphism (Prabhakar and Bhattacharya, 2013).

Hadean–Archean Cratonic Crust: Tonalite gneiss of the OMTG sequence from the Champua revealed 4.24-4.03 Ga xenocrystic zircons, indicating records of oldest precursor of the Hadean age from Singhbhum (Chaudhury *et al*., 2018). In addition, one single Hadean zircon is recorded with ε $^{207}Pb/^{206}Pb$ age of 4015 ± 9 Ma in modern sediments of the Baitarani River, draining the Singhbhum craton (Miller *et al*., 2018). Initial eHf of –5.30 in this grain indicate an episode of Hadean felsic crust formation in the Singhbhum craton. Sreenivas *et al*. (2019) discovered detrital zircon grains of 3.95 Ga and 2.91 Ga from the quartzite and dacite from the Iron Ore Group. In combination with the above reported Hadean, Eoarchean xenocrystic (up to 4.24 Ga) and modern detritus zircon grains from the Singhbhum craton, it is likely that the Eoarchean crust was generated by recycling of the Hadean felsic crust.

Singhbhum Granite (SG) Pluton: The SC incorporates an elongated outcrop of the Singhbhum Granite (SG) complex in central parts of nearly 12 separate magmatic bodies (Saha, 1994). Three multi-stage emplacements of granitic phases have been distinguished within the SG pluton: SG I (3.35 Ga), SG II (3.1 Ga), and SG III (2.9 Ga), spanning a long period of about 500 Ma. Phase-I SG intrusions are relatively K-poor granodiorite-tronjodiorite, while the Phase-II and Phase-III plutons are granodiorite grading to adamellite and leucogranite. Two distinct types of granitoids (Type A and Type B) have been identified with magma originated by shallow melting of a juvenile mafic source. Second phase at 3.35 Ga exhibits variable geochemical signatures due to high temperature melting of a heterogeneous, juvenile source of tonalites and mafics at lower crustal depth (Dey *et al*., 2017). ~3.30 Ga non-porphyritic ferroan, silica-rich biotite granite was formed by high-pressure melting of a tonalite-dominated source. Episodic plume-related mafic-ultramafic magma underplating and intraplating in an oceanic plateau setting is suggested as the possible mechanism for formation of these granitoids (Dey *et al*., 2017). Erosion of the Precambrian Singhbhum Craton from Keonjhar produced pyrophyllite-bearing paleosol between 3.29 and 3.02 Ga, prior (Mukhopadhyay *et al*., 2014).

Iron Ore Group: Surrounding central Singhbhum gneissic Craton and non-conformably overlying it, three extensive belts of the Iron Ore Group (IOG) contains massive pillow basalt, dacite, pyroclastics and ultramafics in the lower parts, and predominantly BIF sequence in the upper parts

(Mukhopadhyay *et al*., 2012; references therein). Mukhopadhyay *et al*. (2008) obtained zircon U-Pb age of 3507 ± 3 Ma from of the Tomka-Daitari belt. Zircon U-Pb age of 3392 ± 25 Ma from a tuff of the Jamda-Koira belt (Basu *et al*., 2008) and ~3.3 to 3.17 ± 0.1 Ga granite intrusions in the Gorumahisani-Badampahar belt (Saha, 1994; Nelson *et al*., 2014) brackets age of the IOG between 3.4 and 3.1 Ga.

Volcanics: Simlipal Volcanics: In the southeastern parts of the Singhbhum Craton, tholeiite and andesitic basalts, spilitic lavas and tuffs make the bulk of the volcanic succession with dunite to quartz diorite at the top. The Simlipal basin represents explosive volcanism in deep marine conditions on a continental platform (Saha, 1994). Dhanjori Volcanics: Volcano-sedimentary Dhanjori Volcanics unconformably overlies the SG along its northeastern margin near the SSZ (Majumdar and Sarkar, 2004). These volcanics contain metasediments, ultramafics, tuff, and metabasalts. Misra and Johnson (2005) obtained Pb-Pb and Sm-Nd whole-rock isochron ages of 2794 ± 210 and 2787 ± 270 Ma, respectively from these volcanics. Ongarbira Volcanics: Unconformably overlying the SC the Ongarbira sequence is comprised of ultramafic lavas at the base, followed upwards by pillowed tholeiitic basalts. These are intercalated with thin bands of quartzite and slate; and have suffered greenschist metamorphism. (Blackburn and Srivastava, 1994). Jagannathpur Volcanics: On the southwestern flank of the craton, these volcanics were emplaced in the Noamundi basin, and are weakly metamorphosed komatiitic to tholeiitic basalts. Misra and Johnson (2005) obtained a WR Pb-Pb isochron of 2250 ± 81 Ma as the formation age for these volcanics. Malangtoli Volcanics: These volcanics span in southwestern parts to the west of Keonjhar and range from basalt to andesite of the tholeiite to calc-alkaline series.

Newer Dolerite Dyke Swarm (NDDS): The Singhbhum Granite pluton exhibits the Newer Dolerite Dyke Swarm (NDDS) which intruded in NNE-SSW, N-S, NNW-SSE and WNW-ESE directions (Bose, 2008). Most of the dykes are of quartz dolerite with small occurrences of norite, granophyre, microgranite and syenodiorite. $^{207}Pb/^{206}Pb$ baddeleyite ages on these dykes revealed the following groups: (i) 2800.2 ± 0.7 Ma to 2750 ± 0.9 Ma NNE-SSW trending dykes (ii) 2.25 Ga baddeleyite age of NE-SW to ENE-WSW trending Kaptipada swarm, and (iii) younger WNW-ENE trending 'newer dolerite' Pipilia dyke swarm of ~1765 Ma (Srivastava *et al*., 2016; Kumar *et al*., 2017).

Post-Singhbhum Granite Intrusions: Bonai Granite: It is separated from the main Singhbhum Granite batholith by the IOG supracrustal belt and shows two phases with the Phase-I as migmatitic Bonai granite (3369 ± 57 Ma, Pb-Pb WR age) and the Phase-II porphyritic Bonai granite (3163 ± 126 Ma Pb-Pb WR age) (Sengupta *et al*., 1996). Nilgiri Granite: Separated from the main SG by a narrow strip of 3–8 km wide IOG phyllite and quartzite, this body of granite is composed of the TTG to granite in southeastern parts of the craton (Saha, 1994). The Nilgiri pluton is intruded by the Mayurbhanj Granite along its margin. For the second and third phases of the Mayurbhanj granite, in-situ Pb-Pb zircon ages are 3080 ± 8 Ma and 3092 ± 5 Ma, respectively (Misra and Johnson, 2005). Soda Granite: Along the SSZ, this granite dates 2220 ± 54 Ma (Pb-Pb WR isochron age) and has been interpreted as the age of emplacement/crystallization of this body.

Dharwar Craton (DC)

The Dharwar Craton is the largest and one of the best-investigated Archean cratonic block of the Indian Subcontinent in an area of about 0.45 million km^2 with a crustal record from ca. 3.6 to 2.5 Ga. In the north, it is overlain by narrow Proterozoic sedimentary Kaladgi and Bhima Basins and Cretaceous Deccan Traps, while Karimnagar granulite belt makes its northeastern periphery. The eastern margin is covered by the Proterozoic Cuddapah basin, while the Pan-African Pandyan Mobile Belt (PMB) is juxtaposed along its southern margin. The region south of the orthopyroxene isograd and including the PMB is also called the South Granulite Terrain (SGT) (Ramakrishnan and Vaidyanadhan, 2008).The Dharwar Craton is sub-divided into the Western Dharwar Craton (WDC) and the Eastern Dharwar Craton (EDC) (Swami Nath *et al*., 1976; Naqvi and Rogers, 1987), which are separated by the Chitradurga Shear Zone (Radhakrishna and Naqvi, 1986). Based on new data, the EDC is further sub-divided into the Central Dharwar Craton (CDP) having significant component of >3.0 Ga old crust and remobilization at 2.56–2.51 Ga.

TTG-type Gneisses: A suite of migmatitic TTG-type gneiss with numerous enclaves appear to be the oldest sequence in the WDC along Gorur-Hassan-Holenarsipur region. U-Pb zircon ages range from 3607 ± 16 Ma to 3280 ± 5 Ma, with diapiric trondhjemites intrusions into the TTG gneisses and greenstones around ca. 3223-3178 Ma (Guitreau *et al*., 2017). The migmatitic gneisses comprise two different compositional types: low-Al, gneiss and high-Al gneisses (Jayananda *et al*., 2015). Guitreau *et al*. (2017) obtained magmatic zircons of 3410.8 ± 3.6 Ma age from granitic gneiss of the Holenarsipur Schist Belt (HSB) with inherited zircons of 3295 ± 18 to 3607 ± 16 Ma within a 3178 ± 10 Ma trondhjemitic gneiss and biotite-rich enclave.

Dharwar Batholith: To the east of the Chitradurga greenstone belt, the Dharwar Batholith of the EDC contains greenstones, banded grey to dark grey gneisses, migmatite and trondhjemite-grey granodiorite (Chadwick *et al*., 2000). East of Chitradurga shear zone, the EDC shows an increase of transitional TTGs with tonalitic to granodioritic phases. The process of accretion was at ca. 3.45-3.23 Ga in the WDC with remnants of ca. 3.60 Ga (Maibam *et al*., 2016; Guitreau *et al*., 2017), in the central parts it was at ca. 3.30-3.00 Ga; the transitional TTGs were emplaced at ca. 2700-2560 Ma (Balakrishnan *et al*., 1999; Maibam *et al*., 2016), and the gneisses were accreted during 2.70-2.55 Ga in the EDC (Krogstad *et al*., 1991; Dey *et al*., 2016).

Dharwar Greenstone Belts: The following greenstone belts characterize the DC: (i) Sargur Group greenstone belt (3.4-3.1 Ga-WDC): The WDC greenstone belt contains linear ultramafic-mafic volcanics with quartzite-carbonate-pelite and BIF with dominant komatiite and komatiite basalt, spinifex textured flows and pillows/pillow breccia (Jayananda *et al*., 2016). These erupted between 3.38 and 2.56 Ga (Jayananda, 2020, and references therein). Al-depleted Barberton–type and Al-undepleted Munro-type komatiites are also recognized in this region (Tushipokla and Jayananda, 2013). (ii) Dharwar Supergroup greenstone belts (2.9-2.7 Ga-WDC): The younger Dharwar Supergroup comprises lower Bababudan Group and upper Chitradurga Group, corresponding to two age groups of volcanics: (a) ca. 3.0–2.9 Ga Kudremukh greenstone belt of high-Mg basalts with minor komatiite and boninite, and (b) 2.74–2.67 Ga Chitradurga–Gadag greenstone belt. (iii) Greenstone Belts from central Dharwar: Major greenstone belts include Ramagiri, Penakacherla, Sandur, Kustagi and Hungund belts with pillowed metabasalts, greywacke and felsic volcanics make the bulk of these belts. (iv) Eastern Dharwar greenstone belts (2.7-2.5 Ga): Numerous high-Mg basaltic greenstone belts dominate the eastern Dharawar with small amounts of komatiite and intermediate to felsic volcanics/pyroclastics along with greywacke-argillite, carbonate and BIFs. These range in age from ~2.7-2.56 Ga (Jayananda *et al*., 2018 and references therein). N-S trending narrow linear Kolar and Hutti Greenstone Belt (KGB) has gold mineralization in volcanics, quartz-carbonate veins and stratiform sulphide lodes in BIF along with shear zones. Rajamani *et al*. (1985) reported komatiitic to tholeiitic amphibolite from the KGB. Amphibolite and gneiss terranes across the KGB were juxtaposed by horizontal E-W compression between 2530 and 2420 Ma along this belt, which sutured discrete crustal terranes on its either sides (Krogstad *et al*., 1989).

Closepet Granite and Other Plutons: The Late Archaean Closepet Granite is an elongated N-S to NNW-SSE trending arcuate batholith along the eastern sheared margin with the Western Dharwar Craton (Moyen *et al*., 2003). The exposed body is divided into northern and southern parts, separated by the Sandur Schist belt and crops out along crustal cross-section of about 10–13 km in depth. The Closepet Granite has been dated as 2513 ± 5 Ma (Friend and Nutman, 1991) and is a part of widespread Neoarchaean 2.68 to 2.52 Ga plutonism and mark the stabilization of the Eastern Craton (Maibam *et al*., 2011; Jayananda *et al*., 2020).

Major Shear Zones: The Dharwar Craton is dissected by major shear zones which play an important role in the reconstructions of the continental assembly. Drury *et al*. (1984) produced some of the early geological maps of the shear zones while Jain *et al*. (2003) determined ductile shearing zones. Ramakrishnan (2003) recognized shear zones of Balehonnur, Babubudan, Chitradurga Boundary, Chitradurga, Mettur, Cuddapah Eastern Margin, Nallamalai, Eastern Ghats, Bhavani, Moyar, Noyil-Cauveri, Palghat-Cauveri, and Achankovil. The Chitradurga Shear Zone separates the Eastern Dharwar Craton (EDC) from the Western Dharwar

Craton (WDC). The E-W trending Moyar Shear Zone (MSZ) is characterized by clockwise deflection of NNE-trending fabric of the Northern massifs which possesses very steep east-west foliations and steeply to moderately plunging lineation (Jain *et al*., 2003). The Nilgiri Massif (NM) is marked by another prominent almost ENE-trending Bhavani Shear Zone (BSZ) along its southern margin and possibly truncated by the MSZ around Bhavani Sagar and Satyamangalam. Numerous shear criteria within the shear zone reveal its distinct sinistral ductile character with steep mylonitic foliation dipping towards northwest and bear strong gently plunging lineation towards SW. Extensive low-lying expanse around Coimbatore-Namakkal-Tiruchirappalli is characterized by E-W trending Palghat-Cauvery Shear Zone (PCSZ) (Drury *et al*., 1984). The Cauvery River flows along distinct E-W trending major shear zone boundary from south of Namakkal to Tiruchirapalli. Sigmoidal bending of NE-trends of Kollimalai and Pachaimalai hills along their southern margins indicates the presence of a distinct large-scale dextral shear zone. Within the PCSZ, main foliation trends almost E-W with subordinate orientation towards NE and N and is marked by E or W gently plunging mineral lineation (Jain *et al*., 2003). These shear zone record UHT and HP metamorphism.

Proterozoic Mafic Dikes: These dykes trend orthogonal to the regional trend of the Dharwar Craton in an area of 140, 000 km^2 with ages ranging between 2.43 and 2.10 Ga with some ages clustering around 1.85 Ga (French *et al*., 2008; Soderlund *et al*., 2019; Srivastava *et al*., 2019). Söderlund *et al*. (2019) have provided many U-Pb baddeleyite ages (ID-TIMS) between 2.37 and 1.79 Ga on the mafic dykes across the eastern Dharwar Craton.

Deformation: Two contrasting large-scale deformation patterns characterize the Dharwar Craton: (i) elongate domes and basins in the WDC Paleo- to Mesoarchean gneiss and greenstone belts preserving the 'dome and keel' structural pattern related to vertical tectonics and, ii) superposed N-S trending strike-slip ductile shear zones both in the WDC and the EDC, preserving evidence of the Neoarchean convergent tectonics(Chadwick *et al*., 2000; Jayananda *et al*., 2020).

Metamorphism: Progressive regional metamorphism (~2.50 Ga) in the DC reveals a continuous increase in P–T conditions from north to the south from greenschist facies to amphibolite and granulite facies (Pichamuthu, 1965; Janardhan *et al*., 1982; Raase *et al*., 1986). A N-S traverse through Chitradurga, Sargur and Nilgiri Hills indicated greenschist facies (4-5 kbar/~500^{o}C) progressing to amphibolite (5-7 kbar/600^{o}C) and then granulite (8-9 kbar/800-850^{o}C) facies (Raase *et al*. 1986).

Three cratonic blocks reveal contrasting metamorphic record and thermal history. The WDC preserves garnet-kyanite assemblage denoting two thermal events at ca. 3100 and 2500 Ma. The southern parts of the Chitradurga Shear Zone record peak metamorphic conditions of ~10 kbar/~820–875°C, while. U–Pb zircon and Pb–Pb monazite geochronology indicates crystallization of parent mafic magmas at c. 2.61–2.51 Ga and subsequent regional metamorphism of these intrusives into garnet-amphibolite and garnet-granulite facies at c. 2.48–2.44 Ga.

The CDC show progressive increase of metamorphism from greenschist facies in the Sandur greenstone belt in the north to granulite facies in Kabbaldurga to the south (Pichamuthu, 1965), where orthopyroxene-sillimanite and spinel-quartz assemblages indicate moderate to low pressure-high temperature assemblages. The central block is affected by an upper amphibolite to granulite facies metamorphism close to 3211-3160 Ma and 2640-2610 Ma. In Kabbaldurga–BR Hills region, in-situ monazite dating together with Sm-Nd garnet-whole-rock isochron ages indicate three thermal events at ca. 3211-3160 Ma, 2640-2610 Ma and 2520-2450 Ma (Peucat *et al*., 2013).

The Archean Hutti-Maski greenstone belt of the EDC had undergone mid-amphibolite facies metamorphism at ca. 2564 ± 12 Ma with PT increase up to ~6 kbar and ~620^{o}C and post-peak near-isothermal decompression (Hazarika *et al*., 2015). In comparison, the Kolar greenstone belt underwent a lower amphibolite facies metamorphism at ca. 2546 ± 12 Ma and PT increase up to ~4.6 kbar/~600^{o}C, followed by decompressional cooling. The ages of felsic volcanism are constrained at ca. 2669 ± 22 Ma and 2661 ± 32 Ma in the Hutti-Maski and Kolar belts, respectively (Hazarika *et al*., 2015). Cordierite-andalusite-biotite assemblage in pelites indicate low pressure-low to moderate temperature in western margin of Kolar Greenstone Belt. U-Pb monazite and zircon ages from the EDC indicate that it was involved only in one thermal event around 2.50-2.53 Ga (Peucat *et al*., 2013).

Crustal Evolution: The process based crustal evolution models for Dharwar Craton are: (i) back-arc marginal basins for the E-W trending greenstone belts and north-verging subduction zones serving as crustal scale shear zones which got tectonically modified by N-S trending shear systems, (ii) mantle plumes in shallow subduction zones in the EDC for the evolution of greenstone belts (Dey *et al*., 2018; Jayananda *et al*., 2018, 2020). Such greenstone belts of the EDC are interpreted as composite tectonostratigraphic terranes of accreted plume-derived and convergent margin-derived magmatic sequences. Associated alkaline basalts record subduction-recycling of Mesoarchean oceanic crust. The CDC grew along the margin of already existing ca. 3.4-3.0 Ga WDC microcontinent through hotspot and active margin setting. In the oceanic environments, hotspot magmatism generated komatiite to basaltic magmatism (Naqvi *et al*., 2002) possibly as oceanic islands. Westward subduction of intervening oceanic crust along the margin of microcontinent generated arc crust and led to slab breakoff causing melting of the base of the arc crust as well as surrounding sub-arc mantle, resulting in magmatic protoliths of transitional TTGs (Jayananda *et al*., 2018). The 2.7 Ga komatiite to basaltic rocks probably formed in hot spot environment (Dey *et al*., 2018). Assembly of the EDC, CDC and the WDC during 2.58-2.54 Ga triggered mantle upwelling, melting and generation of sanukitoid magma which was emplaced into the CDC as well as newly formed greenstone-transitional TTG crust (Jayananda *et al*., 2018). This upwelling caused crustal reworking and high-T and low-P metamorphism and cratonization of Archean crust. (iii) Greenstone belts containing komatiite, tholeiite and intrusive calc-alkaline gneiss serve as suture zones at ~ 2.5 Ga between two continental blocks is an Archean examples of plate tectonics and arc accretion, (Krogstad *et al*.,1989). (iv) This model includes gravitational 'sagduction' of greenstone belts into gneissic basement and tectonic sliding along the margins of the WDC (Chardon *et al*., 1996). Dome and-basin structures in the older belts are associated with diapiric-type gravitational instabilities. (v) Convergent tectonic model with the WDC is considering the foreland marginal basins (schist belt) and the EDC with greenstone belts as intra-arc basins, accreted on to the former at ~2.75-2.51 Ga (Chadwick *et al*., 2000). (vi) Continental rift model for the evolution of EDC schist belts as rifted small ocean basins that closed by NE-SW compression (Ramakrishnan, 1987).

Based on age zonation patterns, crustal thickness, metamorphic records, cratonization and assembly of micro-blocks into cratonization, most tectonic models invoked westward convergence of oceanic lithosphere, however a few studies also proposed an eastward subduction. Further, it is likely that both the WDC and EDC accreted simultaneously (Maibam *et al*., 2016), although thermal history, U-Pb zircon data and Nd-Hf isotopes indicate their independent geological evolution (Dey *et al*., 2018; Jayananda *et al*., 2018).

Proterozoic Mobile Belts

The Proterozoic Mobile Belts are associated with the six Indian Cratons and are named as the Aravalli-Delhi Mobile Belt (ADMB), the Central Indian Tectonic Zone (CITZ)/or the Satpura Mobile Belt (SMB), the Singhbhum Mobile Belt (SMB), the Eastern Ghats Mobile Belt (EGMB), Nellore Mobile Belt, Pranhita-Godavari Belt and the Pandyan Mobile Belt (PMB) (Fig. 1).

Aravalli-Delhi Mobile Belt (ADMB)

In parts of Gujarat and Rajasthan of western India, NE-SW trending ~800 km long Aravalli Mountain Range represents an ancient mountain chain with well-preserved records of ~3 Ga years of the Precambrian evolutionary history where the Banded Gneissic Complex (BGC) acted as the basement for the deposition of the Aravalli and Delhi Supergroups as major constituent units of this mobile belt. While Aravalli Supergroup is limited to the south-central and east-central parts of Rajasthan, the Delhi Supergroup has two components, northern and southern belts. Adjacent to the 2.58 Ga old Berach Granite are the Mangalwar Complex and the Sandmata Complex (Sinha-Roy *et al*., 1998).

On the peneplaned BGC surface, end of the Mangalwar Complex is marked with rift-related outpouring of mafic lava, which were identified as high-Mg basalt and originated by decompression melting of the underlying upper mantle (Ahmad and Tarney, 1994; Ahmad *et al*., 2018). It pre-dated the aluminous paleosol horizon of pyrophylite-talc-sericite-chlorite-kyanite schist, located at the base of the arkose-conglomerate-quartz arenite units of the basal Aravalli succession (Roy and Paliwal, 1981; Banerjee, 1996; Sreenivasan *et al*., 2001; Pandit *et al*., 2008; deWall *et al*., 2012). This paleosol unit demarcates the erosional unconformity between the gneissic basement and the clastic units of the Aravalli succession. Lavas around Delwara (ca.2.4 Ga) and basic volcanics occurring within the BGC (Mangalwar Complex) are geochemically identical (Raza and Khan, 1993).

The Aravalli succession of Heron (1953) consist of low-grade metasediments, several generations of granites and basic volcanics, and is distinguished from the overlying metamorphosed Delhi Group of rocks. Heron's (1953) original correlation of the Aravalli succession of the Udaipur valley sequences was revised repeatedly (see Faredduddin and Banerjee, 2020 for references and discussion). Though the BGC as the basement for the deposition of the supracrustals of this region is widely accepted (Sharma, 1988; Roy, 1998; Gupta *et al*., 1997), Naha and Mohanty (1990) suggested that the BGC was a product of granitization of the Aravalli sediments.

The Aravalli Supergroup is exposed between Nathdwara-Bhilwara-Hindoli in the north and northeast and Udaipur-Lonavada belt in the south and southeast, and connected at the Delwara Dislocation Zone (Gupta *et al*., 1980; Sinha Roy *et al*., 1998). Since the cover sequences are separated only in space and not necessarily in time, Fareeduddin and Banerjee (2020) referred the Aravalli supracrustal belts of the Nathdwara-Bhilwara-Hindoli area as the East Aravalli Terrain (EAT) and those between Nathdwara-Udaipur-Lunavada areas ('Aravalli type area') as the South-Central Aravalli Terrain (SCAT).

The EAT in the Rajpura-Dariba area contains metasediments of the Rampura-Agucha belt as stretched, attenuated strips of granulite, gneiss, amphibolite, metapelite, calc-silicates, sulphide ore-bearing zones whose Pb-isotope model ages is 1.8 Ga (Deb *et al*., 1989). This belt is engulfed within migmatite country and deeply affected by the longitudinal shears. The Jahajpur-Hindoli Belt (~400 km long) in the NE is distributed along western and eastern belts (Sinha-Roy and Malhotra, 1988), and is comprised of conglomerate, quartzite phyllite, dolomite, BIF and bimodal volcanics (Malhotra and Pandit, 2000), with greenschist facies metamorphism. The western margin of this sequence in the Bhilwara sector is marked by a discontinuous Delwara Dislocation Zone. Perceptible and progressive increase in the metamorphism from east to west was noted in this sector.

The Bethumni-Sindeswar-Rajpura-Dariba belt is surrounded by migmatized gneiss and meta sediments. Along the Pur Banera-Sawar-Bajta belt medium to high grade metamorphic assemblages was affected by three phases of folding. Refolding (F2) of the F1 folds resulted in plunge inversions, and (ii) late ductile shear zones truncated the late F3 folds (Ray, 1988).

The eastern margin of this group with low-grade metamorphic belt in Jahajpur-Hindoli sector is considered pre-Aravalli by Gupta *et al*. (1980) although Sinha-Roy *et al*. (1998) placed them in the Aravallis. Progressive increase in the metamorphism from east to west was noted in this sector.

The South-Central Aravalli Terrain (SCAT) represents the type section of the Aravalli Supergroup from Nathdwara to Udaipur, Dungarpur, Banswara and Lonavada and is made up of low to very-low grade arenite, limestone, dolomite, metapelite and metavolcanics. The Berach granite exhibits intrusive relationship with the eastern tracts of the Aravalli Supergroup. In Udaipur area, the Ahar River Granite acted as the floor for the Aravalli sedimentaries. Stratigraphic status of the folded Lonavada and Champaner Groups remains poorly defined.

Stratigraphy: The bulk of the Aravalli succession represents two sedimentary packages of marine shelf and deepwater facies (Mathur, 1964; Poddar and Mathur, 1967) that facilitated its division into the lower and upper Aravallis, respectively with the Rakhabdeo Lineament marking a tectonic contact. The Aravalli succession has been divided into smaller units in several ways. Based on variation in stromatolite morphology, formational-level classification led to the identification of a Supergroup with three major Groups Debari, Udaipur and Jharol Groups (Gupta *et al*., 1980, 1997; Banerjee, 1971a, b), followed by adding the Sajjangarh Formation (Banerjee and Bhattacharya, 1994) to six-fold classification (Gupta *et al*., 1980), and numerous such proposals (see Fareeduddin and Banerjee, 2020 for ctitical evaluation). Stratigraphy suggested by Roy and Jakhar (2002) is the most quoted scheme, which has been revised by Purohit *et al*. (2015).

Regional Structure: The ADMB Belt has undergone several tectono-magmatic events although primary sedimentary structures are preserved intact. In the SCAT, three phases of folding (F1, F2, F3) affected the Aravalli succession. The first tectonic episode produced east/west plunging tight isoclinal to reclined folds and slaty cleavage; second generation was open to tight folds while open warps represent the third generation of folds (Roy *et al*., 1998; Roy and Jhakhar, 2002). The reversal of dips of basal quartzite-arkose-conglomerate unit in the Debari sector east of Udaipur was interpreted as the result of listric faulting (Roy, 1988). Intense mylonitization in the uppermost parts of the BGC basement suggest strike-slip movement along shear zones with steeply plunging lineations. The Banas Dislocation Zone (BDZ) separates the Aravalli fold belt and the BGC. The 'hammer-head syncline' in the Kankroli-Rajnagar-Nathdwara sector north of Udaipur is the transition area between EAT and SCAT where two generations of large-scale folding affected the Railos as well as Aravallis (Naha and Mohanty, 1990). Extensive Pb-Zn mineralization is noted in Zawar-Balaria-Mochia mine sectors where intense deformation was recorded along narrow belt of shear zone between basement blocks of Sarara and Babarmal.

Age of the Aravallis: The Aravalli sedimentation started around 2.1-1.9 Ga based on the evidence of ~1.9 Ga Rb-Sr isochron age of the intrusive Darwal Granite near Nathdwara (Choudhary *et al*., 1984). This granite intrudes the migmatite terrain which was erroneously thought to have formed by transformation of the Aravalli sediments. Hence, 1.9 Ga Darwal Granite intruded the migmaites of the BGC and not the Aravalli sedimentaries. On the other hand, whole-rock Sm–Nd model ages of 2.3 and 1.8 Ga for the mafic volcanics within the Mangalwar Complex (Ahmad *et al*., 2008) indicates that the Delwara Volcanics, so far considered to be a part of the basal Aravalli, belongs to the BGC (see Fareeduddin and Banerjee, 2020). A large array of the Pb–Pb model ages of 1.8–1.7 Ga fixes the age of the lower part of the Aravalli succession which overrides the metavolcanics of the BGC (Deb and Thorpe, 2004). Measurement of heavy carbon isotope values for some dolomites and marbles in the Nathdwara area led some workers to assign 2.2–2.0 Ga ages to Aravalli succession, and the carbonate rocks of the Jhamarkotra (Matoon) Formation, in particular (Papineau *et al*., 2009). Despite highly precise U-Pb zircon age data, Wang *et al*. (2018) used wrong physical stratigraphy for making the geological interpretations (see Fareeduddin and Banerjee, 2020). McKenzie *et al*. (2013) presented a detrital zircon age peak at ~1772 Ma and the youngest single grain with $^{207}Pb/^{206}Pb$ age 1762 ± 9 Ma from the rocks below the phosphatic dolomite at Jhamarkotra. Large population of 1.9–1.7 Ga zircon grains in the lower part of the Aravalli succession negates the >2.0 Ga for the basal Aravalli carbonates. The greywakes from the Udaipur Formation, overlying the carbonate rocks of the Matoon (Jhamarkotra) Formation, contain a population of 1.8–1.6 Ga detrital zircon and single youngest zircon with $^{207}Pb/^{206}Pb$ age of 1576 ± 7 Ma (Absar and Sreenivas, 2015). The ~1.7 Ga Pb-Pb model age of base metal ore (Deb *et al*., 1989) and ~1.7 Ga Pb-Pb isochron age of phosphatic dolomite are consistent with the above observation (Banerjee and Russell, 1992). The 1921 ± 67Ma Pb-Pb age of the isotopically heavy dolomite from the Ghasiar area of Nathdwara sector (Saranagi *et al*., 2006) is consistent with the antiquity of these dolomites in comparison to the sensu stricto stromatolitic phosphorite and dolomite of the Matoon (Jhamarkotra) formation.

Sedimentary History: Depositional history of the Aravalli succession started with the formation of a basal paleosol horizon which got covered with fluvio-marine arkose-conglomerate and quartz arenite constituting the Debari Group. The overlying Matoon (Jhamarkotra) Group of carbon and multi-component phyllites, stromatolitic dolomite and phosphorite is followed by laminated graywacke and argillite of the Udaipur Group. Youngest overlying laminated metapelites and dirty sandstones are assigned to the Jharol Group possibly deposited as turbidites in the deeper parts of the Aravalli Sea. Slivers of ultramafics and serpentinite occur as detached linear belt along the Rakhabdeo Lineament and considered to be the result of complete rupturing and asthenospheric upwelling leading to formation of oceanic crust (Sinha-Roy *et al*., 1998). The Salumber-Bhukia-Ghatol belt is the extension of type section of the Girwa valley where high-Mg tholeiitic basalts and komatiites are seen on top of the basement gneisses followed upward by arenites of the Debari Group and then carbonates and argillites of Mukundpura and Jagpura formations (Shekhawat *et al*., 2007).

Delhi Mobile Belt

The Delhi Supergroup consists of the North Delhi Fold Belt (NDFB) and the South Delhi Fold Belt (SDFB), which are separated by two chronologically distinct intrusive magmatic events with a gap ~800 Ma (Gupta *et al*., 1980; Sinha Roy *et al*., 1984). Fareeduddin and Banerjee (2020) suggested that these two Delhi basins evolved diachronously with ENE-WSW to E-W trending Jaipur-Dausa-Alwar transcurrent fault possibly representing the contact between two belts.

Basinal Evolution: The NDFB evolved in fossil grabens and identified as near-independent Lalsot-Bayana, Alwar and Khetri basins. The SDFB has an eastern Bhim Basin and western Sendra Basin, which are separated by the basement gneisses (Ramakrishnan and Vaidyanadhan, 2008). The NDFB shows Paleoproterozoic sources for the detritus and limits the maximum depositional age to c. 1720 Ma for the uppermost Ajabgarh Group (Wang *et al*., 2018), while widespread Mesoproterozoic detritus in the SDFB constrains the initial sedimentation of these units to younger than 1055 Ma. The two may have formed in independent basins and thereby display distinctly different depositional history. In the west, the contact with the Marwar Craton (hypothetical craton) is tectonized and partly marked by the ophiolite-bearing Phulad Lineament. In most part of this belt, the Delhis directly override the BGC (Mangalwar Complex), while the Kaliguman Lineament restricts its spatial distribution in the eastern parts and brings it in direct contact with the Sandmata Complex.

Stratigraphy: The Khetri, Lalsot-Bayana and Alwar basins of the NDFB has the Raialo, Alwar and Ajabgarh Groups in ascending order with predominance of meta-arenites, carbonates and volcanics. The Khetri basin with copper mineralization, metasedimentaries and volcanics represents a fault-bound graben with numerous interbasinal faults and intrusive granites and is divided into two by E-W trending Kantli Fault. A suite of nepheline syenites is found at the contact with the Sandmata Complex. The Khetri and Shyamgarh groups are equivalents of Alwar and Ajabgarhs groups. Tectonics include first generation of flexure folding with a strong axial planar foliation through NW-SE directed horizontal compression. Superposed second folds are coaxial with the first folds and are associated with shearing. The cross folds represent the third phase. The Alwar and Lalsot-Bayana basins show complex polyphase folding. The Raialo Group includes carbonates of Makrana with sandstones and volcanic rocks. and inferred to have deposited in tectonically uplifted basin. The Lalsot-Bayana Basin has conglomerates, quartzite and Jahaj-Govindpur volcanics. Quartzose Alwar Group and argillaceous Ajabgarh Groups constitute two major rock units of this region. Several volcanic and intrusive granite traverse this terrain. On the nothwest margin of the NDFB granulite to upper amphibolite facies rocks occur as tectonic slices.

Age Data: $^{206}Pb/^{207}Pb$ data of igneous zircons from charnockite intruding the granulite facies rocks, yielded an age of 1434.3 ± 0.6 Ma. Detrital zircons from pelitic granulites yielded ages between 1522 Ma and 1000 Ma (Fareeduddin and Kroner, 1998). Magmatic zircon from the Pilwa granite yielded an age of 1128 ± 0.7 Ma. Chemical dating of monazite grains (Bhowmick *et al*., 2018) from the Pilwa-Chinwali granulites recorded three broad age domains: (i) 1305 ± 25 Ma as age of older metamorphism from detrital remnant in pelites, (ii) between 1085 ± 10 Ma and 1010 ± 20 Ma as timing of granulite facies metamorphism, and (iii) 880 ± 35 Ma linked with the timing of Erinpura granite magmatism. Deb and Thorpe (2004) obtained an age of 1745 Ma for the Sedex type Pb-Zn mineralization. Using detrital zircon ages, McKenzie *et al*. (2013) inferred that quartzites of the SDFB strongly differ from the Alwar Group of the “North Delhi Belt”.

Tectonics: West of Udaipur in the southern sector, the Aravalli Mobile Belt (AMB) is in contact with the SDFB. This contact was described as an angular unconformity (Heron, 1953), as sheared unconformity (Naha *et al*., 1984) and as a suture zone (Sinha-Roy, 1988; Sugden and Windley, 1984). Gupta and Bose (2000) inferred that the Aravalli and Delhi Supergroups are not juxtaposed as commonly believed but are separated by the basement complex. NNE-SSW to NE-SW trending SDFB extends from Ajmer in Rajasthan to Himmatnagar in Gujarat and show westward younging of the rock sequence. The Gogunda Group and Kumbhalgarh Group correspond to the Alwar and Ajabgarh Groups. The Rajgarh-Bhim and Barotiya-Sendra Basins contain a prominent Barr Conglomerate, quartzite-phyllite-dolomite and bimodal volcanics. The Phulad Ophiolite is exposed in the western parts of the basin. Among the four phases of folding in the SDFB domain, the first F1 folds are rootless, flattened and geometrically isoclinal with axial planar foliation and lineations, the F2 folds are large and reclined with strong axial planar cleavages, the F3 folds are open to tight, and theF4 folds are cross warps.

Metamorphism: The NKB and SKB of the Khetri Belt represent two metamorphic zones in the NDFB, i.e. andalusite-sillimanite and kyanite-sillimanite, respectively (Faredduddin and Banerjee, 2020 and references therein). In Ajmer-Sambhar Lake sector distinct metamorphic zonation can been seen from east to west: the staurolite-kyanite zone in the east and the sillimanite-muscovite zone in the center (Fareeduddin *et al*., 1995).

Age of the DFB: Initial comprehensive Rb-Sr dating indicated widespread ages between 1340 and 1850 Ma for the granitic plutons of the NDFB (Choudhury *et al*., 1984). Revised and precise zircon age data reveal 1.8–1.7 Ga age for the ADMB (Biju-Sekhar *et al*., 2003; Kaur *et al*., 2011). Youngest zircon age in the Alwar Quartzites is 2110 ± 33 Ma. The identification of 3671 ± 15 Ma old zircon seems to represent the basement for the sediments of 1800-1700 Ma age (Biju Shekhar *et al*., 2003). Kaur *et al.* (2018) recognized at least four different ages of metamorphism (between 1.85 and 980 Ma and one phase of metasomatism (~900-850) based on zircon age data. The Deri-Ambaji Pb-Zn ore in the SDMB is apparently as young as ~1.0 Ga (Deb *et al*., 2001, 2004). Different granitic bodies in the region show Rb/Sb age of 850 ± 50 Ma, while granites at Ambaji are 760 Ma old. The Rb-Sr age of 955 Ma to 740 Ma for the post-Delhi Pali-Sendra-Erinpura granites in the SDFB is complimented by zircon ages of 968 ± 1.2 Ma to 800 ± 2 Ma. The Mt Abu granite is dated 764 ± 3 Ma to 779 ± 16 Ma. The granulite metamorphism and their exhumation have been dated at ~ 800 to 860 Ma and ~800 to 760 Ma, respectively. Monazite date of staurolite schist in this area yielded a pooled age of 980 ± 22 Ma, which is assumed to be the age of peak metamorphism (Bose *et al*., 2017). The $^{206}Pb/^{207}Pb$ data for migmatites is in the range of 1695.7 Ma to 2258.1 Ma and indicate a Paleo-Mesoproterozoic provenance for the sedimentary infills. The youngest age of ~1700 Ma constrain the closing time of this basin and is, therefore, contemporaneous to the Aravallis (Fareeduddin and Kröner, 1998). The supracrustals of Sirohi and Sindreth Groups possibly represents the youngest unit of the Delhi Supergroup.

Magmatism: Widespread Neoproterozoic magmatic bodies in the ADMB extend from the Tosham Volcanics (Haryana) in the north to gabbro-norite plutonic rocks of Balaram, Gujarat in the south. These intrusives are the Ojhar Granite (>960 Ma) in the Aravalli metasediments, Newania carbonatite (955 ± 24 Ma) within pre-Aravallis, the Erinpura granite (990 and 830 Ma) and the Mt. Abu granitoid (800-730 Ma) in the Sirohi Group west of the fold belt (Just *et al*., 2011; Van Lente *et al*., 2009; Pradhan *et al*., 2010; Ashwal *et al*., 2013). U–Pb zircon ages of 987 ± 6.4 and 986.3 ± 2.4 Ma from the Ambaji–Sendra rhyolites (Deb *et al*., 2001) and Deb and Thorpe (2004) are arc related. In the southern part of the Ambaji–Sendra belt U–Pb zircon age of 836 +7/-5 Ma is measurd for Siwaya gneissic granite. Thus, geochronological data from The sediments and intercalated volcanics of ADMB formed between 1240 and 966 Ma (Deb *et al*., 2001), plagiogranite intrusions at 1015 ± 4.4 Ma (Gupta and Bose *et al*., 2013) and calc-alkaline granitoids at 968 ± 1 Ma (Pandit *et al*., 2003) record the evolution of a Neoproterozoic volcanic arc between the Marwar terrane and Aravalli Bundelkhand craton of the NW Indian shield.

Deformation of the ADMB: There is no ambiquity in recognizing polyphase deformation of the Aravalli and Delhi where a minimum of three regional folding phases have been identified (Naha *et al*., 1984;

Roy, 1988; Gupta *et al*., 1995). The E-W trending reclined folds of the first generation in the Aravalli rocks are not seen in the Delhi rocks. NNE-SSW to NE-SW trending folds of the second generation in the Aravalli and older rocks are upright, whereas these structures in the Delhi rocks are of two phases—recumbent folds, followed by coaxial upright folds. This difference in the folding pattern suggest an angular unconformity between the Delhi and Aravalli and related rocks. It is interesting to note that both the basement BGC and overlying Delhis are more metamorphosed than the Aravallis.

Crustal Evolution: One of the earliest tectonic models proposes the ensialic rifting at ca 2000-1900 Ma as cause for the formation of large Aravalli basin, followed by subsidence and crustal shortening (assuming Aravalli orogeny at 1900 Ma) (Sharma, 1995). Using trace element geochemistry and petrofacies analysis Banerjee and Bhattacharya (1989, 1994) applied plate tectonic concepts to assign each of the Aravalli clastic rocks to specific tectonic setting and interpreted the evolution of the Aravalli basin in a passive margin setting which changed to active margin tectonics towards the end phase. Sinha-Roy (2000) visualized Proterozoic development as an aulcogen that widened southwards from a triple junction near Nathdwara and closer at 1800 Ma. Antri-Rakhabdeo suture zone and synkinematic granites (Darwal, Anjana) were tell tale evidence of large-scale tectonics. Another major strike-slip fault emanating from the triple junction opened the Delhi basins in two tectonic domains: (i) the NDFB evolved as fault-bound grabens and half-grabens, as part of aborted rifts were intruded by granites at 1450-1650 Ma, and (ii) the SDFB as a linear belt formed as a transtensional rift. The 1000-1100 Ma old Ranakpur gabbros and co-eval Phulad ophiolite suite/mélange were emplaced and was followed by Sendra-Ambaji and Erinpura granites (900 Ma) due to westward thrusting of the Delhi oceanic crust. Several new publications during recent years focus on the development of individual segments of the ADMB under the overall ambit of the plate-tectonic models envisaged above (see Wang *et al*., 2018; Zhao *et al*., 2018).

Central Indian Tectonic Zone (CITZ)

The Bundelkhand and Bastar Cratons are accreted along an ENE–WSW trending Central Indian Tectonic Zone (CITZ) whose limits are defined by the Son–Narmada North Fault (SNNF) in the north and Central Indian Shear Zone (CIS) in the south (Radhakrishna, 1989). In the east, the CITZ continues into the Chotanagpur Gneissic Complex (CGGC) and further northeast into the Shillong Plateau and Mikir Hills of the Meghalaya Craton. The CITZ comprises Proterozoic supracrustal belts of varying metamorphic grades in a largely undifferentiated gneiss and syn- to post-kinematic granite. These can be differentiated into three prominent components: (i) supracrustal belts of Mahakoshal, Betul and Sausar belts, (ii) granulite belts of Makrohar Granulite (MG), Ramakona–Katangi Granulite (RKG) and Balaghat–Bhandara Granulite (BBG), and (iii) brittle ductile to ductile shear zones of Son–Narmada South Fault (SNSF), Gavilgarh-Tan Shear and Central India Shear.

(i) **Mahakoshal Supracrustal Belt:** Northern parts of the CITZ are represented by ENE-WSW trending Mahakoshal supracrustal belt in a fault-bound asymmetrical rift basin (Roy and Bandyopadhyay, 1990) and includes low-grade metamorphosed quartzite-carbonate-chert-BIF-greywacke-argillite-mafic volcanics. Roy and Devarajan (2000) suggested to be a pericratonic shallow marine basin along southern margin of the Bundelkhand Craton, where it developed with rifting, thermal doming and outpouring of tholeiitic magma, pyroclastic flows and ultramafic intrusives. The upper age of the belt is constrained by ca 1.8 Ga calc-alkaline granite intrusive (Sarkar *et al*., 1998). Granitoid plutons intruding the Parsoi Formation are largely metaluminous. U–Pb SHRIMP zircon $^{206}Pb/^{238}U$ ages for microgranular enclaves (1758 ± 19 Ma) and host granitoid (1753 ± 9.1 Ma) from this pluton support their coeval character. Folding remained upright to slightly overturned with the ENE–WSW trend.

(ii) **Betul Supracrustal Belt (BSB):** Sandwiched between the Mahakoshal belt in the north and Sausar supracrustal belt in the south, the Betul supracrustal belt (BSB) is made up of ENE-WSW trending volcano-sedimentary rocks, mafic–ultramafic rocks and granites along with quartzite, garnetiferous schist, calc-silicates, BIF and bimodal volcanics. Bimodal low K-tholeiitic composition of the lava distinguishes it from the other unimodal mafic volcanics of the region (Bhowmik *et al.*, 2000). Metamorphic grade varies from lower- to middle amphibolite facies. Syn-tectonic granite (ca.1.5 Ga) constrains the upper age of the belt.

(iii) **Sausar Belt:** As a part of the larger CITZ, the Sausar Belt is bounded on the north and south by granulite belts of different age (Roy *et al.*, 2006). On the southern margin of the CITZ the Sausar Fold Belt (SFB) is distinctly devoid of volcanics and is made up of arenite-carbonate-pelite-Mn-rich lithologies, resting over the Tirodi Biotite Gneiss (Narayanaswamy *et al.*, 1963; Chattopadhyay *et al.*, 2015). Polymictic conglomerate with clasts of gneisses and granites suggest sedimentation in the shallow shelf environment.

Highly negative $\delta^{13}C$ values of dolomites led Mohanty *et al.* (2015) to propose glacial origin of these rocks which was contested by Chattopadhyay (2015). The contact of the Sausar Group with the Tirodi Gneiss exposes some paleosols (Mohanty and Nanda, 2016) which show characteristic REE abundance typical of an oxygen-deficient basin. According to Yedekar *et al.* (1990), the Sausars were deposited on the passive margin of the Bundelkhand Craton implying provenance to the north.

Four phases of deformation are recorded with an early southward thrusting and associated recumbent/reclined folds (D1/F1), followed by E-W trending upright/steeply inclined folding (F2) of the thrust allochthon. Minor F3 folds distort the F2 hinges and superposed by late F4 cross-folds. Prograde Barrovian metamorphism is of Late Mesoproterozoic to early Neoproterozoic (ca. 1063-993 Ma) age.

(iv) **Granulite Belts:** The Makrohar Granulite (MG) Belt occurs on southern fringe of the Mahakoshal supracrustal belt and incorporates calc silicates, marble, BIF, metapelites, basic rocks, granites and intrusive gabbro-anorthosite, metamorphosed in amphibolite and granulite facies (Pichai Muthu, 1990). Dating of similar granitic rocks from the adjoining area yielded Rb–Sr ages between ca. 1.7 and 1.5 Ga. The Ramakona–Katangi Granulite Belt (RKG) occurs north of Sausar supracrustal belt with felsic migmatitic gneisses, mafic granulites, cordierite gneisses and garnetiferous metadolerite (Bhowmik *et al.*, 2000). This belt yields ca.1043 Ma and 955 Ma EPMA monazite age peaks, 938 Ma SHRIMP U-Pb zircon age from magmatic charnockite (Bhowmick *et al.*, 2012), monazite ages of ca. 945 Ma from a syntectonic (syn-D2) granite and ca. 928 Ma from a post-tectonic granite intrusive (Chattopadhaya *et al.*, 2015). Ductile shear zones mark the contact between the granulites and Sausar supracrustal belt. Three stages of metamorphic evolution were marked by distinct mineralogical assemblages (Bhowmik *et al.*, 2000). These granulites and gneisses form the basement for the Sausar Group. Similarly, four phases of deformation and three phases of metamorphism have been established from metabasics and granulites of the RKG domain (Bhowmik and Roy, 2003). The Tirodi Biotite gneiss, believed to be product of peak metamorphism, yielded a Rb–Sr age of 1525 ± 70 Ma (Sarkar *et al.*, 1986). The southern margin of the CITZ is bordered by the ENE–WSW to NE–SW trending Balaghat–Bhandara Granulite (BBG) Belt, which consists of highly tectonized granulite facies rocks in detached lenses along the CIS (Alam *et al.*, 2017). The BBG belt is also identified as the suture zone between the Bundelkhand and the Bastar Cratons.

Southern margin of the Mahakoshal Supracrustal Belt is marked by a 700 km long E–W to ENE–WSW trending Son-Narmada Fault following the course of these rivers in central India. This Paleoproterozoic shear zone dips to the south at high angle and is intimately related to the opening of the Mahakoshal Basin. In the central part of the CITZ, the Gavilgarh-Tan Shear Zone (GTSZ) is a 900 km long NE–SW to ENE–WSW trending belt, separating the Betul Supracrustal Belt (BSB) from the southerly-located Sausar Supracrustal Belt. The GTSZ is represented by intensely mylonitized granites and gneisses and characterized by large-scale ENE–WSW trending concordant granitic plutons/sheets (Roy and Hanuma Prasad, 2001). The eastern part of this linear structure is expressed as a ductile shear zone. The northern margin of the Bastar Craton is delimited by the Central

Indian Shear Zone (CIS) which trends NE-SW in the western part and WNW-ESE in the east. The DSS profile reflects its south dipping nature although surface rocks dip sub-vertically. In the western part, the CIS separates the northern Betul Supracrustal Belt (BSB) from the southern gneissic complex of the BC on the east. The available radiometric dates, though meager, indicate a broad polarity in the granitic magmatism, with successive younger phases encountered towards south.

Tectonic Models: Yedekar *et al*. (1990) proposed a plate tectonic model for the evolution of the CITZ, in which a southerly dipping subduction of the Bundelkhand Craton was invoked below the Bastar Craton. This model considers BSB as an obducted granulitic oceanic crust, which was exhumed during collisional orogeny. Later workers rejected this proposition as this model does not explain the evolution of the RKG belt, the MG belt, the Betul Supracrustal Belt and the vast expanse of Mesoproterozoic (ca. 1.8–1.0 Ga) granitic magmatism lying to the north of the CIS. Roy and Hanuma Prasad (2003) proposed a north-directed subduction of the oceanic crust of the Bastar Craton below the Bundelkhand. Since, this basin was situated in an arc environment, it may be considered as coeval with the Mahakoshal basin of the back-arc. The basin closed at ca.1.5 Ga, as recorded by syn-tectonic granitic rocks. This event was also accompanied by large-scale mantle melting, which resulted in copious hydrous ultramafic–mafic magmatism. The Sausar basin was closed perhaps at ca. 1.1 Ga, due to continued south-directed thrusting. The closing phase was also marked by the emplacement of profuse granitic rocks. Based on deep seismic reflection and magnetotelluric data acquired across the CITZ, Mall *et al*. (2008) observed reflectivity characteristics dipping towards each other and creating a domal structure across the diffused Central Indian Suture (CIS).

Singhbhum Mobile Belt (SMB)

The Singhbhum Mobile Belt (SMB) is a geological term specific to the ensemble of folded, low to medium grade meta-sedimentary and meta-igneous rocks (1.0–2.4 Ga), sandwiched between the Archaean (>2.4 Ga) Singhbhum Craton in the south, and the Meso/Neo-Proterozoic (0.9–1.7 Ga) Chotanagpur Granite Gneissic Complex in the north with north-dipping ductile shear zones. In the south, the SMB and the Singhbhum Craton are separated by the Singhbhum Shear Zone (Copper Belt Thrust-Mahato *et al*., 2008).

In the Ghatsila Belt a thick sequence of intricately folded and metamorphosed argillite and carbonates belonging to the Gangpur Group is profusely intruded by granite and basic rocks, while the Kunjar Group represents the Gangpur Group in the north and Singhbhum Group and Koira Group in other areas. The Singhbhum Group contains a thick succession of meta-argillite, quartzite and effusive basic volcanics and is divided into a lower fine-grained mica schist of the Chaibasa Formation (~2000-4000 m thick) (Sarkar and Saha, 1983). It displays progressive metamorphic zonation towards the central part. The Chaibasa sandstone is fine-grained, and generally well sorted with well-preserved turbidite structures as well as tidal-flat, fluviatile facies and debris flows (Eriksson and Simpson, 2004). The upper Dhalbhum Formation (~400 m) is magnetite-bearing meta-argillites, quartzites and interstratified basic intrusives and are of fluvial, tidal flat and aeolian origin. The Dalma Formation contain volcanic rocks. A linear belt of granitic rocks is also found emplaced in the Chaibasa Formation near the Singhbhum Shear Zone. The associated Arkasani Granite show Rb-Sr age of 1000-1100 Ma. Another belt of low grade metapelite with rhythmic bands of chert and organic rich beds is the Chandil Formation containing impure carbonates, carbonatite, felsic volcanics, syenite and granite along with welded tuff, rhyolite and dacite. The Chandil sandstones are fluvial deposits and the associated shales are flood plain deposits. Alkali syenite, mafic and ultramafic intrusives and metabasalts are closely intermixed.

The Dhanjori Formation (2.1 Ga) with siliciclastics, volcaniclastic and ultramafic to mafic volcanics is deformed and metamorphosed to greenschist facies (Roy *et al*., 2002). Polymict conglomerate-orthoquartzite of the Dhanjori Basin is positioned between the Singhbhum Craton and Singhbhum Orogen. Gupta *et al*. (1985) divided the Dhanjori Group into (i) a lower formation of pebbly metapelite with ultramafics, and (ii) an upper formation of arkose, conglomerate and metapelites and volcanics of the Dalma lavas. In the west, this succession shows gradational contact with the underlying Koira Group which is intensely folded along the Singhbhum Shear Zone. The Dhanjori lavas are basaltic to andesitic of tholeiitic series with Pb-Pb and Sm-Nd isochron ages of 2820 and 2790 Ma (Ramakrishna and Vaidyanadhan, 2008).

On the eastern margin of the Singhbhum Craton, the Dhanjori Group of metasediments is associated with the Mayurbhanj Granite (Saha, 1994), which is correlatable with the Simlipal Granite (Iyenger and Murthy, 1982) with ages varying from 2084 ± 70 Ma (WR Rb-Sr) to 3008 ± 8 Ma and 3092 ± 5 Ma (Pb-Pb zircon dates). The Sm-Nd isotopic analyses of basic-ultrabasic rocks of the Dhanjori Basin yield an isochron age of 2072 ± 106 Ma indicating their age as early Proterozoic (Roy *et al*., 2002).

A synclinally folded and greenschist facies metamorphosed Dalma Volcanic Formation of volcanics and argillites is developed within the Singhbhum Mobile Belt, which conformably overlies the Dhalbhum Formation (Sengupta *et al*., 2000). A Rb–Sr age of 1487 ± 34 Ma has been determined for the acid tuffs of the Chandil Formation (cf. Sengupta *et al*., 2000). The oval cluster of granite exposures comprising the Kuilapal Granite (cf. Ghosh, 1963; Saha, 1994), exposed within the Chandil supracrustals, has yielded an Rb–Sr whole rock isochron age of 1638 ± 38 Ma (Sengupta *et al*., 1994). A Rb–Sr whole rock isochron of the gabbro–pyroxenite intrusives into the Dalma volcanic rocks yields an age of 1619 ± 38 Ma (Roy *et al*., 2002).

The Chakradharpur Granite Gneiss (CGG) is an isolated granite gneiss within the SMB around Chakradharpur amidst the supracrustal SG which forms the basement for the overlying Singhbhum Group.

The Singhbhum Shear Zone consists of a series of shear zones which at times turn into high angle faults. Extreme ductile shearing and complex deformational history mark this zone with several episodes of metasomatism, migmatization and mineralization of Cu, U, tungsten and apatite. Stratigraphically, rocks of this shear zone overlie the Dhanjori and Koira (IOG) metapelites and are often marked by a sheared conglomerate and, in turn, overlain by the rocks of the Chaibasa Formation. Rocks within the shear zone are represented by argillites and volcanoclastics with abundance of mafic and ultramafic intrusives.

The northern limit of SMB is delineated by the South Purulia Shear Zone (SPSZ) or the Tamar-Porapahar Shear Zone (TPSZ)/lineament where vast expanse of Chhotanagpur Granite Gneiss Complex (CGGC), an extension of the CITZ, abuts against the SMB. A number of small granitoids such as Biramdih, Beldih and Barabazar lie close to the SPSZ. Granites with Pb-Pb isochron age of ca. 1771 Ma were emplaced in rift related environs due to partial melting of stabilized lower/middle crust (initial $^{87}Sr/^{86}Sr$ = 0.7302 ± 0.0066).

Eastern Ghats Mobile Belt (EGMB)

The Eastern Ghat Mobile Belt (EGMB) is predominantly a granulite belt on the margins of the Archean Dharwar–Bastar–Singhbhum Cratons, having a thrust contact (Ramakrishnan and Vaidyanadhan, 2008). The belt is traversed by two Gondwana-bearing NW-SE trending Mahanadi and Godavari Grabens, while the WNW-ESE trending Rengali Belt limits the EGMB in the north, where its contact with the Singhbhum craton is marked by shear zones. The southern limits of the EGMB are vaguely defined in the Nallamalai Hills, where it possibly merges with the Southern Granulite Terrain.

Ramakrishnan *et al*. (1998) proposed the following longitudinal division of the EGMB based on distribution of lithologies: (i) Western Charnockite Zone (WCZ) of charnockite and enderbite with lenses of mafic-ultramafics and minor metapelitic khondalite, (ii) Western Khondalite Zone (WKZ) of dominantly metapelitic khondalite, intercalated quartzite, calc-silicates, marble, and high Mg-Al granulites, (iii) Charnockite-Migmatite Zone (CMZ) of migmatitic gneisses with minor amounts of high Mg-Al granulites and calc-silicates, (iv) Eastern Khondalite zone (EKZ) with lithological similarity with WKZ, but lacking anorthosite, and (v) Transition Zone along the western margin of the EGMB.

Chetty (2017) classified the EGMB into 9 different terranes based on presence of shear zones, lineation, fold patterns and their axial surfaces, while Ricker *et al*. (2001) divided it into Domain I to Domain IV based on Nd-model ages. Dobmeier and Raith (2003) classified the EGMB into 12 crustal provinces and sub-provinces, having distinct lithology, structure, metamorphic grades and geological histories.

Deformation of Western Margin: The Western margin of the EGMB with the Archean Cratons has been called as the West Odisha Boundary Fault, the Eastern Ghats Boundary Shear Zone, the Transition Zone, the Terrane Boundary Shear zone–TBSZ, and the Sileru Shear zone–SSZ (Ramakrishnan and Vaidyanadhan, 2008). West-directed large-scale thrusting of high-grade metamorphosed UHT granulites (charnockite-khondalite) and multi-deformed migmatitic gneisses are thrust westward over hornblende granite and sedimentary rocks of the Bastar Craton. Western margin is marked by alkaline and carbonatite bodies emplaced along a rift zone. The Rangeli Province juxtaposes the EGMB in the north through various dextral shear zones like the Mahanadi Shear Zone (Mahalik, 1994; Mahapatro *et al*., 2009). Within the TBSZ, intense ductile shearing has imbricated different litho-units of the Indian Craton and the EGMB as 'mélange' whose structural geometry reveals its top-to-W/NW overthrust geometry (Biswal *et al*., 2000; Bhadra *et al*., 2004; Sinha *et al*., 2010). This contact is retrogressed with development of quartzo-feldspathic mylonite within the Lakhna Shear Zone. Synkinematically emplaced alkaline intrusives in this belt constrain the age of thrusting ~1.4 Ga (Sarkar and Paul, 1998). In the northwestern margin of the EGMB, garnet-sillimanite-gneisses are folded within calc-gneisses by second generation large-scale NE-SW oriented tight F2 folds which are coaxial to the oldest F1 isoclinal possessing penetrative axial planar foliation S1 (Biswal *et al*., 1998). Fold interference of F1 and F2 produces Type 3 interference pattern. Third generation F3 folds are mostly gentle upright folds.

Deformation within the EGMB: A four-phase deformation history is recorded in the structural architecture of the EGMB. The first three phases were dominated by folding, and the last one by shearing and fracturing. The NE–SW to N–S regional trend is defined by the first- and second-generation folds. The second-phase folding was coaxial with the first, and the fold interference produced hook-shaped structures in the khondalites. The third episode of deformation produced asymmetric folds that gently plunge northeastwards in metapelites and upright disharmonic structures in migmatites (Bhattacharya *et al*., 1994). The generally southeastward- to eastward-dipping rock successions all through their expanse are cut by several ductile and brittle shear zones; the former are associated with mylonites and pseudotachylites.

Metamorphism: Various types of P-T paths for the ultrahigh temperature (UHT) metamorphosed Mg-Al granulites and other lithologies have been inferred from the EGMB from northern parts to extreme south, and are categorized as follows:

(i) the UHT thermal peak >1000^{o}C at 10 kbar and subsequent high-P isobaric cooling (IBC), having clockwise or anti-clockwise path (Bhattacharya and Kar, 2002; Bhattacharya *et al*., 2003; Sarkar *et al*., 2003).

(ii) High-P isobaric cooling (IBC) and subsequent isothermal decompression (ITD) up to 750^{o}C and 5 kbar (Mohan *et al*., 1997; Rickers *et al*., 2001), and

(iii) Isobaric heating–cooling path in the UHT granulites on either side of the Godavari graben, controlled by intrusive plutonic complexes, with thermal peak at 950-1000^{o}C and 6-8 kbar (Bose *et al*., 2000; Dasgupta and Sengupta, 2003).

Petrological studies revealed an early M1 UHT metamorphism with thermal peak at 900–1000^{o}C/8–10 kbar, followed by high pressure isobaric cooling (IBC) to 750–800^{o}C, (Dasgupta and Sengupta, 1995). In Chilka Lake granulites, Sen *et al*. (1995) deduced three phases of isothermal decompression (ITD) paths with two intervening discontinuous isobaric cooling (IBC) paths from peak UHT metamorphism at 8–10 kbar/1000^{o}C down to 4.5 kbar/650^{o}C. In the segment south of the Godavari rift near Kondapalle and Chimakurthy, the EGMB exhibits heating to extreme ~1000°C temperatures and cooling trajectories at different pressures. Two metamorphic events are recorded in the Ongole domain (i) first stage UHT metamorphism at T >950^{o}C, P=6.5–7 kbar from spinel–quartz association (ii) second stage of higher pressure and lower temperature metamorphism at ca. 780^{o}C/9.5 kbar

Age of Metamorphism: Three distinct age groups of the UHT metamorphism are decipherable in the EGMB: the Archaean, Mesproterozoic and Neoproterozoic–Pan-African, though the Neoproterozoic event is the most prolific. In addition, mesoscopic to microscopic structures suggest that the emplacement of charnockite massif was broadly syntectonic with the D1 deformation. Charnockites around Jenapore, Orissa are dated ~3.0 Ga by Sm–Nd, WR Rb–Sr systematics and Pb–Pb zircon methods with Sm–Nd model dates between 3.4 and 3.5 Ga. Khondalite, associated gneiss and granulite from central belt are older than 1.4 Ga anorthosite and alkaline intrusives (Sarkar *et al*., 1981; Ramakrishnan *et al*., 1998), implying the granulite facies metamorphism during this period. The last high-grade metamorphism, superposed on several metamorphism and deformation episodes within central and eastern tectonic units of the northern EGMB, occurred at ca. 960 Ma according to Mezger and Cosca (1999). The Western Charnockite Zone reveals a major thermal event around 1.6 Ga. Discordant sphene ages along a reference line from ca. 935 to 504 Ma indicate a thermal disturbance during a Pan-African deformation phase, as revealed by concordant U–Pb zircon age of 516±1 Ma in a vein. High resolution geochronological data from central segment of the EGMB reveal sustained UHT conditions (T >900ºC) for >50 My between ca 970 and 930 Ma, using $^{207}Pb/^{206}Pb$ zircon and monazite ages, and perhaps for as long as 200 My from ca 1130 to 930 Ma. Two metamorphic events in the Ongole domain, dated by in situ U-Pb monazite, appear to be separated by 60–80 Ma when HT-LP and second metamorphisms occurred at ca. 1620 and 1540 Ma, respectively (Sarkar *et al*., 2014).

Igneous Plutons: The western margin of the EGMB has nepheline syenite, hornblende syenite, and quartz syenite plutons, like those of the Khariar Alkaline Complex in the west or the Prakasan alkaline province south of Godavari Graben. These bodies are either emplaced (i) in a paleo-rift at the Indian cratonic margin, (ii) syntectonic during thrusting and shearing (iii) generated by mantle melting in the presence of CO_2 fluid (Banerjee *et al*., 2013), or (iv) emplaced before the crustal reworking. Massive anorthosites are mapped along its northern margin (Sarkar *et al*., 1981), while Leelanandam (1998) reported a layered igneous complex of anorthosite-gabbro- pyroxenite-chromitite from Kondapalle area in southern EGMB.

Other Proterozoic Mobile Belts

The Dharwar and Bastar Cratons are separated from each other along a NW–SE trending tectonic element with the intervening Pranhita–Godavari Valley basin along which two Karimnagar and the Bhopalpatnam granulites belts (KGB and BGB) are well exposed (Joy *et al*., 2018).

The **Karimnagar Granulite Belt** (KGB) contains coarse-grained unfoliated charnockite with a wide variety of high-grade enclaves of charnockite-enderbite gneiss, ultrabasicbasic granulite, amphibolite, calc-granulite, sapphirine-orthopyroxene-cordierite-bearing pelites and a variety of psammites. The KGB is characterized by at least two deformation phases of refolding in isoclinal style with axial planar foliation (Rajesham *et al*., 1993). SHRIMP U-Pb zircon geochronologic data suggest a Neoarchaean (2604 ± 25 Ma) age for the timing of high temperature metamorphism and accretion of the terrane and Neoproterozoic thermal overprint around 638 Ma.

The **Bhopalpatanam granulite belt (BGP)** lies on the western edge of the Bastar craton on the northeastern rim of the Pranhita-Godavari rift zone and is composed of two pyroxene granulites, ultramafics, quartzite, calc-silicate rocks, Mg–Al metapelites (Vansutre and Hari, 2010). Santosh *et al*. (2004) reported zircon (EPMA) ages from the KGB with the cores recording ages of up to 3.1 Ga and rims with ages of 2.6 Ga. In contrast, the cores of zircons recovered from the BGB demonstrate core ages of 1.9 Ga and the rims of 1.6–1.7 Ga.

The **Nellore–Khammam schist belt (NKSB)** comprise of schistose terrane and separates the marginally metamorphosed and deformed intracratonic Proterozoic Cuddapah basin to the west and the Ongole domain of the EGMB (Hari Prasad *et al*., 2000). In the northern sector it is called the Khammam schist belt (Ramam and Murty, 1997; Okudaira *et al*., 2001), occurring between the EGMB and the Pranhita-Godavari valley sedimentaries. The NKSB is divided into two sedimentary stratigraphic units. The Vinjamuru Group is made up of rocks of amphibolite facies showing characters of a volcano-sedimentary assemblage (Sain *et al*., 2017) with gabbro yielding WR Sm–Nd isotope age of 2654 ± 100 Ma and a 1911 ± 88 Ma isochron age (Vadlamani, 2010). The andesites and rhyolites of the Vinjamuru Group are ~1868 and 1771–1791 Ma (Vadlamani *et al*., 2012). The Vinukonda Granite intrusive in the

Vinjamuru Group is dated as ~1590 Ma (U–Pb zircon TIMS; Dobmeier *et al*., 2006) and represents the minimum age of the Vinjamuru Group. The anorthosite assemblage of Chimalpahad in the NKSB has yielded Sm-Nd model age of ~1170 Ma. Yoshida *et al*. (1996) reported 1126 Ma isochron age of metapelite from the Khammam area. Based on Sm–Nd mineral isochron of 824 ± 53 Ma, Okudaira *et al*. (2001) interpreted metamorphism of these rocks during tectonic accretion of the EGMB to the Dharwar–Bastar craton. The Udaigiri Group is dominated by greenschist facies metamorphism. The only age available from this group is poorly constrained at 1929 ± 130 Ma, based on a single grain xenotime analysis by Das *et al*. (2015). The Prakasam alkaline plutons occurring along the boundary between the Vinjamuru and Ongole domains are dated 1242 and 1369 Ma.

The Kandra Ophiolite Complex (Vijaya Kumar *et al*., 2010) in the south and the Kanigiri ophiolite melange (Dharma Rao *et al*., 2011) in the central part have suffered multiple deformation and metamorphism, and are associated with different granite phases. The granulites of the NKSB facing the Ongole domain were considered Late Paleoproterozoic by Dobmeier and Raith (2003). The Kandra ophiolite complex at 1850–1900 Ma (SHRIMP U–Pb zircon ages; Vijaya Kumar *et al*., 2010) and the Kanigiri complex around 1330 Ma (LA-ICP-MS U–Pb zircon) fixes the time frame of emplacement of these ophiolites.

Pandyan Mobile Belt (PMB)

A distinct domain of gneiss-granulite, called as the Pandyan Mobile Belt (PMB) or Southern Granulite Terrain (SGT), lies to the south of the Palghat-Cauvery Shear Zone (PCSZ) and the Achankovil Shear Zone (ASZ) (Ramakrishnan, 1993). Based on Sm-Nd isotopic signatures (Bhaskar Rao *et al*., 2003) and U-Pb zircon and monazite ages, it is suggested that the boundary of the PMB may be relocated along the newly recognized V-shaped Karur-Kambam-Painavu-Trichur Shear Zone (KKPTSZ) (Ghosh *et al*., 2004). Ramakrishnan and Vaidyanadhan (2008) divided the PMB into (i) Marginal Zone, (ii) Madurai Block or Central Zone, and (iii) Southern Zone (Trivandrum Block or Ponmudi Sub-Block (also known as the Kerala Khondalite Belt) and (iv) Nagercoil Sub-Block.

The Madurai Block was further subdivided into three. The Amravathi sector contains enderbitic charnockite, hornblende-biotite gneiss, lenses of pyroxene granulite and ultramafics, besides garnet-sillimanite gneiss, calc-silicates, quartzite, pink granite and crystalline limestone, having Sm-Nd-WR Pan-African age of 560 ± 17 Ma (Meissner *et al*., 2002). The adjoining Kodaikanal-Anaimalai sector (KA) contains migmatite gneiss with ultramafic and mafic enclaves and quartzite-carbonate-pelite suite. Brown and Raith (1996) recorded sapphirine-bearing, orthopyroxene-sillimanite ± garnet granulite in the Palni Hill Ranges of the Madurai block as evidences of ultrahigh-temperature (UHT) metamorphism. The Tiruchi-Tirunelveli (TT) Sector between the Periyar River and Achankovil SZ is a highly complex association of folded domes and basins, containing quartzite-carbonate-pelite suite (QCP) along with bands of basic granulite and amphibolite. Highly metamorphosed carbonates contain calc-silicates, garnet-sillimanite-graphite gneiss, garnet-cordierite gneiss, cordierite-spinel gneiss, sapphirine gneiss, charnockite, garnet-quartz-feldspar gneiss (leptynites) are the main rock types. Some parts of the block experienced T >1050^{o}C (at 8–10 kbar) UHT metamorphism.

The Trivandrum Block (Santosh, 1996), also termed as the Kerala-Khondalite Belt (Chacko *et al*., 1987) contains metasedimentary migmatitic gneiss, leptynite and granulite facies metapelites (khondalite) with interlayered charnockite, calc–silicates and pyroxene granulite. It is subdivided into the Ponmudi and Nagercoil Sub-blocks. Of interest is the development of incipient charnockite on leptynite (garnet-quartzo-feldspar gneiss), which are also reported from Sri Lanka and Antarctica. Most recent estimates have confirmed peak metamorphic conditions of 830–925°C/6–9 kbar, followed by suprasolidus decompression (Blereau *et al*., 2016). Dominant regional granulite-facies metamorphism and migmatization in the Trivandrum Block is the latest Neoproterozoic to Cambrian in age, though zircon in granitic and charnockitic orthogneiss suggests magmatic protolith ages of 2.1-2.0 Ga, 1.88-1.84 Ga and 1.76 Ga (Kröner *et al*., 2015). Metamorphic ages lie between 570 and 515 Ma (Taylor *et al*., 2014; Whitehouse *et al*., 2014). U-Pb SIMS ages of detrital monazite grains in khondalite yielded a maximum age between 610 and 569 Ma. reveal that original sediments from the Trivandrum Block gneisses were deposited between ~1900 and ~515 Ma (Collins *et al*., 2007). Monazite ages from khondalite are Late Proterozoic/Cambrian (ca. 560–520 Ma) (Santosh *et al*., 2006), while U–Pb zircon metamorphic ages across this block are around 513 ± 6 Ma (Collins *et al*., 2007). The Nagercoil Block preserves massif type charnockites with emplacement ages of 2.1-2.0 Ga and Hf and Nd model ages ranging from Archaean to Palaeoproterozoic (2.8-2.2 Ga) (Kröner *et al*., 2015).

Tectonics: The Karur-Kumbum-Painavu-Trichur Shear Zone trends NE–SW and extends from Karur to Kambam and turns sharply towards NW to Trichur (Ghosh *et al*., 2004). Structural discontinuity across the KKPTSZ is very pronounced in the eastern parts where structural trends are subparallel to the shear zone. Kotamangalam granitic mylonites show polyphase deformation. U-Pb zircon ages of syntectonic granite (567 ± 2 Ma) and sheared Oddhanchatram anorthosite (563 ± 9 Ma) date a major shearing event in the KKPTSZ between ~570–560 Ma. Along the southern edge of the Cardamom Hills charnockite massif a ~10 km wide shear zone, the Achankovil Shear Zone trends from N–S to NW–SE having subvertical to shallow dips with charnockite and paragneiss (Drury and Holt, 1980). A subparallel Tenmala Shear Zone show a sinistral sense of movement. In parts of the AKSZ and TSZ, Ghosh *et al*. (2004) observed similar lithologies.

Proterozoic Intracratonic Basins

Linked to each of the six Indian cratons and associated mobile belts are several undeformed and unmetamorphosed Proterozoic basins whose lower age limits are constrained by ages of the crystalline basement. However, the timeframe of closure time of these basin is still debated based on indigenous Paleozoic biotic remains in some of these basins (Sharma and Singh, 2019 and references therein) in contrast to the ~1000 Ma closure age by paleomagnetic and zircon data (Malone *et al*., 2008; Sahoo *et al*., 2017, and reference therein). A sac term 'Purana Basin' has been applied to all such basin and continue to be used in Indian stratigraphic literature against the IUGS recommendations. Meert and Pandit (2015) treated the term "Purana" chronostratigraphically and identified Purana–I (2.5-1.6 Ga), Purana–II (1.6–1.00 Ga) and Purana–III (900–541 Ma). These independent basins and sub-basins derived their sediments from basement granites and gneisses, hence carry the mineralogical and geochemical signatures of the parent material. Although largely undeformed, folding and thrusting have affected margins of the Cuddapah, Vindhyan and Godavari basins along with granitic activity in parts of Vindhyan basin in eastern end, and emplacement of kimberlite at number of places. Reactivation of the Great Boundary Fault and Central Indian Tectonic Zone are manifestations of Earth's movements during this period of the Peninsular history.

These basins include Marwar Basin (Marwar Craton), Bayana and Vindhyan Basins (BGC-Aravalli-Bundelkhand Craton-Satpura Mobile Belt), Gwalior, Bijawar and Sonrai basins (Bundelkhand Craton), Chattisgarh, Khariar, Indravati, Sukma, Ampani, and Abujamar basins (Bastar Craton) and Pranhita-Godavari Basin (between Bastar and Dharwar Cratons), Cuddapah, Kaladgi, Bhima basins and Papaghani, Kurnool, Palnad, Nallamalai and Srisailam Sub-basins (Dharwar Craton and Eastern Ghats Mobile Belt).

Marwar Basin

In western Rajasthan, felsic Malani Igneous Suite (MIS) is unconformably overlain by the Marwar Supergroup (Marwar Basin), which contains thick sandstone, shale, carbonate and evaporates succession and divisible into clastic Jodhpur Group and Nagaur Group, and a carbonate–evaporite Bilara Group (Pareek, 1984). A subsurface evaporate-rich Hanseran Group is also recognized. Similarity of lithologies with the Late Neoproterozoic to Early Cambrian rocks of Salt Range is significant. The lowest unit of the siliciclastic Jodhpur Group is Sonia Sandstone with the Pokaran Boulder Bed at its base as an eroded outwash deposit which is followed upward by fluvio-marine Girbhakar Sandstone. The overlying Bilara Group contains carbonates and potash-rich cherty foetid limestone and dolomite and reflect intertidal environment with stromatolites. The evaporate-bearing sub-surface carbonates with 7 cycles of dolomite, anhydrite, halite, polyhalite and clay (Kumar, 1999) are named as the Hanseran Evaporite Group and considered coeval with the Bilara Group (Kumar, 1999). Banerjee *et al*. (2007) opined Hanseran evaporates to be younger than the Bilara carbonates. The overlying sandstone, siltstone and shale of the Nagaur Group yielded well-preserved trilobite traces in the Tunklian Sandstone, which is unconformably overlain by the Permo-Carboniferous Bap boulder bed (Pandey and Bahadur, 2009). An isolated Birmania basin comprises of dolomitic Randha and dolo-phosphatic Birmania Formations (Srikantia *et al*., 1969) which directly overlies the MIS. All these unfossiliferous formations are Neoproreozoic-Early Cambrian in age, although Pandey and Bahadur (2009) recorded late Neoproterozoic trace fossils and stromatolites from the Jodhpur Group (<570 Ma; Kumar and Pandey, 2010 and references therein). The discovery of Lower Cambrian trilobite traces like *Cruziana, Rusophycus, Treptichnuspedum* etc. in the Nagaur sandstone is of great stratigraphic significance (Srivastava, 2014). The shifts in the $\delta^{13}C$ carbon isotope spikes in the Bilara carbonates led to relate it to the global end-Neoproterozoic–Early Cambrian carbon isotopic excursion (Pandit *et al*., 2001). Banerjee *et al*. (1998) and Strauss *et al*. (2001) documented sulphur isotopic compositions comparable to globally recognized sulphur isotopic enrichment event at terminal Neoproterozoic.

Age: TIMS U-Pb zircon ages of the Malani rhyolites are 770-750 Ma while U-Pb detrital zircon from the Jodhpur sandstone yielded age peak restricts the provenance to 800-900 Ma age bracket (Malone *et al*., 2008). Detrital zircon populations reveal a large concentration of grains between 700 and 1000 Ma and a small population of young grains with a peak at 540 Ma (McKenzie *et al*., 2011). These sediments were deposited in a rift setting (Cozzi *et al*., 2012). Correlations between the Marwar Supergroup and the Krol-Tal succession of the Lesser Himalaya is supported by nearly identical detrital zircon population variations (McKenzie *et al*., 2011; Hughes *et al*., 2015).

The Marwar Basin sediments were derived from the Erinpura and its equivalent rocks. Correlation of the Bilara carbonates, Hanseran Evaporites, heavy hydrocarbons, phosphatic Birmania rocks (Hughes *et al*., 2015) and Ara Formation (Huqf Supergroup) in south Oman Salt Basin (Banerjee *et al*., 2007) suggests late Neoproterozoic-Early Cambrian age for these sequences. Geophysical probes indicated their vast subsurface expanse in the Rajasthan Shelf (Pareek, 1984; Cozzi *et al*., 2012) with low (<5 degrees) westerly dips of the strata which connects it with the eastern flank of the Indus shelf of the Indo-Arabian Geological Province (Shrivastava, 1992).

Bayana Basin

Attached to the North Delhi Fold Belt, this ~1.8 Ga old NE-SW trending Bayana Basin is made up of fluvial to coastal marine sandstone-conglomerate-volcanic succession. Standard provenance diagnostic petrological, and geochemical data (Raza *et al*., 2012) suggest tectonically controlled sedimentation with major sedimentary fills coming from the gneisses and granites of the BGC, while Singh (1988) indicated the 'Dausa uplift' to be the sediment source terrain.

Gwalior Basin

Nearly E-W trending and ~80 km long unmetamorphosed sedimentary Gwalior Group was deposited along the northern margin of the Bundelkhand Craton showing variable depositional environment. The lower part of the group, the Par Formation, comprises of grit, conglomerate, glauconitic sandstone, stromatolitic limestone. The overlying Morar Formation contains shale, banded chert, volcanic tuff and limestone which are intruded by basic sills and volcanics. Crawford and Compston (1970) reported a Rb–Sr isochron age of 1830 ± 200 Ma for the mafic sill that intrudes the Morar Formation, while Absar *et al*. (2009) bracketed the Gwalior depositional history between 2000 and 1791 Ma. The gabbroic sills yield mineral–whole-rock Sm–Nd isochron corresponding to an age of 2104 ± 23 Ma with model ages of 2.6–1.7 Ga (Samom *et al*., 2017).

Bijawar and Sonrai Basins

On the southeastern margins of the Bundelkhand Craton, the ENE-WSW trending Bijawar Group comprises dolomite, chert breccia and volcano-clastic sediments. Stratigraphically, these rocks are subdivided into the Moli Subgroup and overlying Gangau Subgroup. The Kawar Volcanics with conglomerate at the base is covered by a thick sequence of Bhuson Basalt and followed upward by well-developed grey, white, locally silicified Bajna Dolomite, affected by doleritic Dargawan sills (1789 ± 71 Ma-Rb-Sr age). The Pukhra Sandstone and Malhera Chert Breccia cap the top of the subgroup. The Gangau Subgroup has two subdivisions, a lower

Hirapur Phosphorite Formation and an upper Karri Ferruginous Sandstone Formation.

A detached Sonrai Basin to the west of the Bijawar Basin shows large scale folding with tholeitic Kurrat Basalt (1691 ± 180 Ma-Rb-Sr age) at the base (Haldar and Ghosh, 2000), and the overlying Solda Formation of quartz arenite and ferruginous shale (Prakash *et al*., 1975). The type area of Bijawar Basin around Hirapur and detached Sonrai Basin contains phosphorite and uranium mineralization in different forms and phases (Jha *et al*., 2019).

Vindhyan Basin

A ~5 km thick pile of Mesoproterozoic-Neoproterozoic sedimentary rocks in the central India, designated as the Vindhyan Supergroup, is exposed in a crescent-shaped outcrop around the ~2.5 Ga Bundelkhand Craton. The Vindhyans overlie the Mahakoshal Group in the south, the Chotanagpur gneisses in the east, the Banded Gneissic Complex, Aravallis and Delhis in the west. The Vindhyan succession is exposed in two geographical sectors, the Son valley in the east, and Rajasthan in the west. Direct contact of the two belts with near identical lithology and tectonics remains obscure due to Deccan Volcanics cover. In the Son Valley area around Maihar the entire the Vindhyan succession is exposed with an unconformity between the Lower and Upper Vindhyan.

The Lower Vindhyan comprising of the Semri Group is divisible into seven formations: (i) Conglomeratic Basal Stage, named as the Deoland Formation (cf. Sastry and Moitra, 1984) rests over the Mahakoshal phyllite, and is formed in the marginal coastal environment. (ii) Overlying ~300 m thick Kajrahat Limestone formation consists of shale in the lower part and stromatolitic limestone occurs in the upper part. These stromatolitic limestones represent fluctuating sedimentation milieu on tidal flats of the ancient Vindhyan sea. (iii) The Deonar Formation (~ 300 m thick Porcellanite Formation) is composed of volcanic tuffs, pyroclastics and silicified shales. (iv) About ~100 m thick olive coloured Koldaha Shale overlies the porcellanite-dominant beds. (v) The ~90m thick Salkhan Fawn Limestone is also identified as Bargawan/Chorhat/Tirohan limestone and is prominently stromatolitic. (vi) The Rampur Formation is >100 m glauconitic sandstone overlying the Salkhan Limestone and is same as that of the Chorhat Sandstone, (vii) The Rohtas Limestone is predominantly calcareous with greyish blue and dark compact stromatolitic limestone and is covered by (vii) the Bhagwar Shale Formation with diffused unconformity.

Unconformably overlying the Bhagwar Shale, the Upper Vindhyan is comprised of (i) Kaimur Group of sandstone, shale and a ferruginous conglomeratic bed at the base. The Lower Kaimur Sandstone is locally capped by a breccia horizon (Susnai Breccia), followed by the Ghagghar/Markundi Sandstone and kerogen rich Bijaigarh Shale. The Upper Kaimur Sandstone is also known as Dhandraul Quartzite/ Mangesar Formation. (ii) The Rewa Group with ~ 200 m sandstone-shale succession overlies Kaimur Group. The Panna Shale and the Lower Rewa Sandstone with diamondiferous conglomerate at the bottom were derived from the kimberlite pipes cutting through the Kaimur sandstones. The Govindgarh Sandstone is the uppermost formation. (iii) The Bhander Group occupies the youngest position in the Vindhyan stratigraphy and is made up of shale-limestone-shale-sandstone succession. The Ganurgarh Shale, Sirbu Shale, Bundi Hill Sandstone and Maihar Sandstone and stromatolitic Lakheri Limestone are subdivisions.

Chakraborty (2006) identified five distinct sequences in the Vindhyan Basin: Sequence 1 to Sequence 5 conforming to distinct geological formations of this supergroup. The carbonate facies represents a wide spectrum of depositional facies of supratidal, intertidal, subtidal, lagoonal, estuarine, inner and outer shelf. Carbon and oxygen isotopic studies on various carbonates and organic carbon in the entire Vindhyan succession provided inconsistent results primarily due to diagenetic resetting by isotopically lighter fluids, alteration due to meteoric diagenesis and difficulty in separating dolomite isotopic values from that of primary calcite. Organic geochemistry of carbonaceous laminae in black shales of microbial mat origin at different stratigraphic levels in the Vindhyans, suggest a catagenetic stage of early anthracite formation (Banerjee *et al*., 2006; Dayal *et al*., 2018).

Depositional Environment: The Vindhyan Basin is intracratonic in which entire sedimentary history remained restricted to shallow marine realm.

Black organic shale indicates euxinic milieu, stromatolitic Kajrahat Limestone formed in tidal flats, Porcellanite Formation is pyroclastic, Khenjua Shale is lagoonal, Koldaha Shale shows transitional set up, Fawn Limestone is intertidal, Rampura Formation formed in stormy shelves, Chorhat Sandstone and Rohtas Formation deposited in tidal flats with local turbidites. The Vindhyan Basin is characterized by uniform unimodal westerly to northwesterly paleocurrent patterns (Chanda and Bhattacharya, 1982) suggesting a stable tectonics and persistence of paleoslope. The Upper Vindhyan succession in Rajasthan sector indicate E-W paleoshore line

Basin Evolution: Views regarding the origin of this basin varied from being rift basin (Bose *et al*., 2001, and references therein), foreland basin (Auden, 1933; Raza and Casshyap, 1996); intracratonic basin (Valdiya, 2016), strike-slip basin (Chanda and Bhattacharya, 1982; Crawford and Compston, 1970) and synclise (Chanda and Bhattacharya, 1982). Some researchers believe there must have been two depocenters in a single basin with Bundelkhand granites acting as the extensive intra-basinal horst. High resolution deep seismic reflection studies, well-constrained by gravity, magnetic and magnetotelluric data suggest gradual thickening of the Vindhyan succession towards southeast from Bundi onwards. The NW limit of the Vindhyan Basin is demarcated by the Great Boundary Fault (GBF) that manifests as a 30 km wide NW-dipping thrust fault extending to a depth of 30 km. Bouguer gravity maps reveal a number of elongated highs and lows indicating probable horsts and grabens separating the Son Valley and Rajasthan Vindhyans.

Tectonics: With ~1700 Ma ages now established for the lower Vindhyan sediments, the GBF should be older than that. A linear structure through Jhalawar-Jhansi to the Ganga Valley coincides with Asmara and Jhalawar lineaments. According to Ghosh (1981), the region between these two faults is the basement ridge with ENE-WSW orientation and possibly acted as the divide between the two Vindhyan sectors. This buried ridge seems to join the Faizabad ridge in the Ganga Plain. Airborne magnetic and ground studies reveal large magnetic anomalies representing the horst and graben structure of Paleoproterozoic basement Bijawar and Lower Vindhyan rocks. Das *et al*. (1990) noted an asymmetric graben structure with the southern boundary fault between the Vindhyan and the Mahakoshal as the most prominent linear structure. Using magnetic and electrical methods, Singh and Ghosh (2003) mapped a prominent uplift in the basement to the north of Mirzamurad, followed by steep slope to the south with thicker sediments of the Vindhyans and Bijawar. The 160 m Khairmalia andesite in the Lower Vindhyan suggest the role of tectonic loading and partial melting of the subducting slab in the formation of the Vindhyan Basin (Khan, 2013). It is also stated that although the Vindhyan Basin is an intra-cratonic basin, its genetic evolution suggests a back-arc basin due to continent-continent collision in the Mesoproterozoic. DSS profiles suggest that Vindhyan basin is riddled with deep-seated geofractures.

Age: Doubtful metazoan traces in the Chorhat Sandstones of the Semri Group, erroneous identification of Ediacaran and Lower Cambrian Small Shelly Fauna, microbial assemblages and microfossils extended Vindhyan stratigraphy to Lower Cambrian time (Azmi, 1998; Kumar, 1978; Seilacher *et al*., 1998; Sharma, 2006). Glauconite in Khenjua Formation yielded 1080 ± 40 Ma K-Ar age (Kreuzer *et al*., 1977). Rb-Sr isochron dates of 1140 ± 24 Ma and 1067 ± 31 Ma for the micas in the kimberlite intruding the lower part of the Kaimur sandstone remained in vogue for a long time (Crawford and Compston, 1970). Pb/Pb isochron ages of ca. ~1600-1650 Ma for the Lower Vindhyan Limestone (Sarangi *et al*., 2004) and SHRIMP U-Pb dates for porcellanite hosted zircon of 1628 ± 8 Ma and 1631 ± 1 Ma (Rasmussen *et al*., 2002; Ray *et al*., 2002) acted as the game changer. Dates like 741 ± 9 Ma and 650-750 Ma for the Upper Vindhyan (Ray *et al*., 2003) however remains poorly constrained.

Kolhan Basin

An NNE-SSW trending 60 km long Kolhan Basin is developed over the Singhbhum Craton, where the Kolhan Group was divided into the Mungra Sandstone, stromatolitic Jhinkpari Limestone and Jetia Shale in ascending order (Chakraborty *et al*., 2005). Structurally, this belt consists of (i) domes and basins in the east, (ii) homocline in the west and (iii) a zone of inverted isoclinal folds. The Kolhan Group is also recorded in (i) Nomira Basin and (ii) Mankarchua

Basin (=Kamakhynagar Quartzite). The Kolhan siliciclastics were derived from intensely weathered low-relief granitoids with warm humid paleoclimate and a passive margin or rift tectonic setting (Bandopadhyay and Sengupta, 2004; Sahoo and Das, 2015).

Chattisgarh Basin

The Chhattisgarh Supergroup of the Chhattisgarh Basin in the central India is about 1500 m of clastic and chemical sediments (Naqvi and Rogers, 1987). Murti (1987) identified a lower arenaceous Chandarpur Group, divided into the Lohardih, Chaporadih and Kansa Pather Formations containing conglomeratic, white and brown arkosic sandstone and an upper Raipur Group of limestone–shale, which is divided into the Charmuria, Gunderdehi, Chandi and Tarenga Formations and separated by an unconformity (Patranabis-Deb *et al*., 2007).

Depositional Environment: Conglomerate–shale–sandstone succession represents the proximal facies, while the distal facies is represented by limestone-shale assemblages, deposited on an outer shelf and slope. The Chhattisgarh Supergroup was deposited in two sub-basins, the Hirri in the west and the Bharadwar in the east, separated by the Sonakhan Greenstone Belt, and two proto-basins in the southeast: the Singhora and the Barapahar. Three tectonic settings, an intracratonic sag, rift, and foreland were proposed. The Charmuria and Chandi limestones show heavy $\delta^{13}C$ values of 2.6‰ to 3.6‰, and 3.2‰ to 3.6‰, respectively (George *et al*., 2018), which can be attributed to increased flux of organic carbon burial, consistent with the global late Mesoproterozoic $\delta^{13}C$ profiles.

Age: Authigenic glauconite of the Chapordih Formation yielded K-Ar age of 700-750 Ma (Kreuzer *et al*., 1977). Stromatolitic assemblages suggest Meso-Neoproterozoic ages (Jairaman and Banerjee, 1978). U–Pb SHRIMP ages of zircon in the Sukhda tuff on top of the Chhattisgarh sequence are 1011 ± 19 and 990 ± 23 Ma, and Sapos tuff is 1020 ± 15 Ma suggesting the ~1000 Ma age for the closing of the basin (Patranabis-Deb *et al*., 2007; Bickford *et al*., 2011a, b; Nagaraja Rao *et al*., 1987). Tuffaceous beds at the base of the Singhora and Khariar show zircon crystallization ages as ~1500 Ma (Das *et al*., 2009) and 1405 ± 9 Ma (Bickford *et al*., 2011a).

Indravati and Sukma Basins

Undeformed and unmetamorphosed shallow marine sediments like the Chattisgarh Basin rest over the Bastar Craton. Shallow cross-bedded intertidal terrigenous rocks occur at the bottom and are followed upward by shale-limestone rhythmite. Subdivisions include Tirathgarh, Cherakur, Kanger and Jagdalpur formations (Ramakrishna, 1987).

Age: U–Pb SHRIMP zircon ages from rhyolitic tuff from the top of the Chattisgarh/Indravati sequence (Jagdalpur Formation) point to the closure of the basin at 1001 ± 7 Ma (Bickford *et al*., 2011a, b). Both Indravati and Sukma Basins represent the faulted and eroded remnants of a single continuous Bastar-Chattisgarh superbasin (Ramakrishna, 1987).

Khariar–Ampani Basins

Small independent basins with terrigenous rock successions have distinct peripheral boundary with the Eastern Ghats Mobile Belt and unconformably overlie the Bastar Craton. Datta (1998) subdivided the Khariar succession into three informal units correlatable to the Chandarpur Group of the Chattisgarh Basin. Ratre *et al*. (2010) considered the sediments to be younger than 1460 Ma. The Ampani Basin succession is correlatable to Chattisgarh–Indravati master basin (Balakrishnan and Mahesh Babu, 1987). Attached to the Bastar Craton the Abujhmar Basin occurs on top of the Kotri-Dongargarh orogen. The lower clastic Gundul Formation is covered by the Maspur Basalt (Ramakrishna and Vaidyanadhan, 2008).

Pranhita–Godavari (PG) Basin

NW-SE trending Proterozoic Pranhita–Godavari (PG) Basin records a thick sedimentary pile along the Pranhita–Godavari (PG) valley between the Bastar and Dharwar cratons. The Karimnagar Granulite and the Bhopalpatnam Granulite Belts are exposed on the basin margins and girdled by the Khammam Schist Belt and the Eastern Ghat Mobile Belt. The Godavari Supergroup and the Pakhal Supergroup are major subdivisions. The lower part is dolomitic while the upper part is dominated by arenites. The Pakhals are divided into Mallamalai Group, Mulug Group, Albaka Sandstone and Penganga Group, divided into 10 formations and overlain by Sullavai Group with distinct unconformity (Sreenivasa-Rao, 1987). $^{40}Ar/^{39}Ar$ glauconite plateau ages from Mallampalli, Mulug and Somanpalli sandstones suggest ages of 1686 ± 6 Ma, 1565 ± 6 Ma and 1620 ± 6 Ma, respectively. The Penganga Group of mixed carbonate–siliciclastic lithology show 1200 Ma as the $^{40}Ar/^{39}Ar$ date of glauconite. Fluvial and eolian depositional systems have been reported in this group.

Age: Mathur (1982) reported 1276 ± 30 Ma, 1188 ± 14 Ma and 1142 ± 37 Ma and also one single age of 871 ± 21 Ma for the sandstone and arkosic units. Stromatolite assemblages show Mesoproterozoic affinity. Tectonics involved rifting (Chaudhury *et al*., 2012) and the unconformity-bound sequences provide control on the episodic uplift, erosion and subsidence of the basin.

Kaladgi and Bhima Basins

The Kaladgi and Bhima Basins are placed along the northern margin of the Eastern Dharwar Craton (EDC) (Kale and Phansalkar, 1991), where the former is divided into a lower Kaladgi Subgroup/Bagalkot Group (Jayaprakash *et al*., 1987) with older unit as the Lokapur Group and the upper as the Semikeri Group. The uppermost sequence unconformably overlies the Bagalkot/Kaladgi Group and is called as the Badami Group with the Kerur Formation which comes in sharp contact with the Katagiri Limestone (Saha *et al*., 2016). Both the subgroups are divisible into ten formations. Broadly, three transgressive cycles of sedimentation can be recognized, each floored by the clastic suite of rocks, and grading into cyclic argillite-carbonate suites. Tight, isoclinal to recumbent folding is seen in the central parts of the basin. Multiple co-axial deformations are seen in different phases. The Kerur Formation comprises of poorly sorted and angular clasts as well as subarkose and arenite of shallow marine origin. The palaeoflow is towards SW. The Badami Group show large amplitudes of open folds, and gentle dips. Intraformational conglomerate in the Katagiri Limestone testifies to its penecontemporaneous deformation and basin floor instability.

To the NE of Kaladgi Basin, a limestone-dominated succession of the Bhima Basin overlies the granitic basement rocks of the EDC with a marked unconformity. The Bhima Group is divided into a lower Sedam Subgroup with two significant formations (Rabapalli Formation and Shahbad Limestone), and an upper Andola Subgroup of three formations (Halkal Formation, Katadevarhalli Limestone, and Harwal Shale). The basal conglomerate and grit beds is overlain by quartz arenite, siltstone and shales and in turn topped by cherty limestone along the margins. A recent multipronged geochronological investigation by Joy *et al*. (2019) found U-Pb baddeleyite age of 1861 ± 4 Ma for the dolerite dike in the lower part of the Kaladgi/Bagalkot Group. Paleocurrent analysis indicates a change in the provenance from S to SE to W or NW. U-Th-Pb and Rb-Sr dates indicate that limestone and glauconite bearing sandstones of the Bhima Group and Badami Group were deposited around 800-900 Ma.

Cuddapah Basin

An epicratonic basin bordering the Dharwar Craton exposes a thick sequence of sediments, intrusives and interbedded volcanics, resting over the N-S to NNW-SSE trending EDC (Kale and Phansalkar, 1991; Kale, 2016; Kale *et al*., 2020). The Cuddapah and Nellore Fold Belt constitute a combination of terrains/tectonic blocks that have a common, interlinked evolutionary history spanning the Late Paleoproterozoic to Neoproterozoic (Sesha Sai, 2013; Tripathy *et al*., 2019; Saha and Sain, 2019); the latter is thrust upon the Cuddapah Basin along the Vellikonda Thrust.

The Cuddapah Supergroup is divided into the Papaghni, Chitravati and Nallamalai Groups in an ascending order (Nagaraja Rao, 1987; Kale *et al*., 2020); each separated by an unconformity. Recent workers have shown that deformed Nallamalai Group is bounded by major thrusts hence it is included in the Nallamalai Fold Belt (Tripathy *et al*., 2019). The Papaghani Group rests on the EDC basement complex with an erosional unconformity. The lowest arenaceous Gulcheru Quartzite represents tectonically controlled alluvial fan facies, followed by intertidal flats and carbonate platform. The overlying thick Vempalle Formation consists of laminated cherty, stromatolitic and oolitic dolomite. The sandstones with shallow water sedimentary features, evaporate indicator salt psedomorphs and stromatolitic carbonates indicate intertidal to subtidal environment. Early Proterozoic tholeiitic Kuppalapalle Volcanics have also been identified (French *et al*., 2008). The

Chitravati Group unconformably overlies the Papaghni Group and is subdivided into the Pulivendla Quartzite, Tadpatri Formation and Gandikota Quartzite in ascending order. Mafic sills and dykes are widespread. Pulivendla Quartzite consists of thickly bedded quartz arenite and laterally impersistent conglomerate, derived from the underlying Papaghni Group with a disconformity. The Tadpatri Formation sediments were deposited in the outer shelf environment. The algal dolomites formed in a supratidal to subtidal depositional environment (Mitra *et al.*, 2018). The uppermost Gandikota Quartzite show unconformable relationship with the overlying Bairenkonda Quartzite of Nallamalai Group. Detrital zircon from Gandikota Formation suggests a Mesoproterozoic age (Collins *et al.*, 2015) in contrast to the Paleoproterozoic age given to rest of the Chitravati Group.

The Nallamalai Group displaying green schist facies metamorphism is a tectonically defined segment of the Cuddapah Basin, bounded on either side by the Maidukuru and Vellikonda Thrusts. The contact beween the Chitravati Group and the Nagari Quartzite and its lateral equivalent Bairenkonda Quartzites of the Nallamalai Group is defined by an angular unconformity. Shales, dolomites and quartzites of Cumbum Formation includes folded and faulted lowly metamorphosed Pullampet Slate, Giddalur Quartzite and ferruginous shales and override the Bairenkonda Quartzite with gradational contact. Stromatolitic dolomites are phosphatic along with associated shales (Banerjee and Saigal, 1988). The thick supermature Srisailam Quartzite were deposited by large river system followed by aeolian deposition (Patranabis-Deb *et al.*, 2012). The red-beds indicate deposits after the Great Oxidation Event (GOE).

The Kurnool Group with its six constituent formations in Kurnool subbasin, overlies the Papaghni and Chitravati Groups and onlaps the gneissic basement of the EDC with a major unconformity. The Banganapalle Quartzite rests upon the basement complex with an unconformity. The polymictic conglomerate and cross-stratified sandstone are attributed to alluvial fan and braided fluvial plain environmnts. Stromatolitic Narji Limestone with pyrite indicate local anoxia. The ochre yellow Owk Shale is laterally extensive across the Kurnool subbasin. The succeeding Paniam Quartzite consists of texturally and mineralogically mature sandstone. The overlying Koilkuntala Limestone is followed by Nandyal Shale.

Tectonics: The following sequence of geologically and structurally distinct domains (Kale *et al.*, 2020) along an E-W regional traverse are: (a) East Dharwar Craton block with Archean-Paleoproterozoic mafic dyke swarms. (b) Unconformable capping of Paleo- to Mesoproterozoic Western sub-basins, (c) The Nallamalai Fold Belt (NFB) successions of the western subbasins along its western edge, and (d) Neoarchean metavolcanics of Mesoproterozoic Nellore Schist Belt thrust over the NFB. Geophysical studies across the CB reveal these four juxtaposed terrains have mutually differing crustal characters.

Age: The Papaghni and Chitravati Groups volcanics were emplaced between 1.8 Ga and 1.9 Ga (Sesha Sai *et al.*, 2017). Rb/Sr age (1817 ± 24 Ma) for the Pulivendla sill is in the same range (Bhaskar Rao *et al.*, 1995). Zachariah *et al.* (1999) determined $^{206}Pb/^{204}Pb$ age of the Vempalle and Tadpatri Formations as 1756 ± 29 Ma. The detrital zircons from the siliciclastic sediments yielded U-Pb ages between 2.54 to 0.91 Ga, which represent the ages of the provenance for the Papaghni and Chitravati Groups, possibly from the Dharwar craton (Collins *et al.*, 2015). Sahoo *et al.* (2017) record an age of 2.53 Ga for magmatic zircon, while hydrothermally altered zircons gave concordia ages of 2.32 and 2.12 Ga. U-Th-Pb(total) dating of monazite and uraninite from both the basement and cover in the Palnad Subbasin suggested that the Banganapalle Quartzite may have been deposited between 2.53 and 2.12 Ga. The Nallamalai Group was deposited between 1.68 Ga and 1.59 Ga with inputs from the eastern tectonically active belt (Collins *et al.*, 2015; Sesha Sai *et al.*, 2017). The Srisailam Formation may have been deposited at the same time, further westwards. The Kurnool Group may be reaffirmed as distinctly Neoproterozoic in age, with zircons dated at 913 ± 11 Ma from the Paniam Quartzite. The Vinjamuru Group hosts the 1.9 Ga Kandra ophiolite complex. The Udaigiri domain represents a younger arc that evolved and deformed around 1.3 Ga.

Tectonics of the Himalaya

The E-W trending arcuate Himalayan Mountains run NW–WNW to E–ENE for about 2400 km, with its convexity towards the Indian Peninsula. It is surrounded by the low-lying the Indus–Ganga–Brahmaputra Plain (IGBP) in the south and the Tibetan Plateau in the north (Fig. 1). The main Himalaya Mountain is comprised of at least four almost continuous ranges with distinct geography, geology and tectonics due to southward Cenozoic convergence: (i) the Indus–Ganga–Brahmaputra Plain (IGBP) against the Sub-Himalayan (SH) belt along the Himalayan Frontal Thrust (HFT), (ii) the SH belt against the Lesser Himalaya (LH) sedimentary belt along the Main Boundary Thrust (MBT), (iii) the LH Belt against the Himalayan Metamorphic Belt (HMB) along the Main Central Thrust (MCT), and (iv) the HMB against the Tethyan Himalayan Sequence (THS) along the South Tibetan Detachment Zone (STDS) (Gansser, 1964; Thakur 1993; Hodges 2000, Jain *et al*., 2015; Valdiya, 2016).

Indus–Ganga–Brahmaputra Plain (IGBP)

Largest active foreland basin, the Indo-Gangetic (IGP) in the western parts, and the Brahmaputra and Bengal Basins in the east, is collectively called as the Indus–Ganga–Brahmaputra Plain (IGBP). Arcuate-shaped basin extends 3200 km from Rann of Kutch to Assam, and spans ~550 km in Panjab and about 90 km in the extreme east in about 2.5-million km^2 area of northern Indian subcontinent. It accumulates an enormous quantity of eroded sediments and dissolved materials by large rivers, which also carry the load into mega-fans of the Arabian Sea and the Bay of Bengal. Divided by subtle sub-surface ridges, the IGBP is an amalgamation of the Indus Basin, Ganga Basin, and Brahmaputra Plain (also called as the Assam Basin) and exhibits all significant components of a foreland basin.

The Ganga Plain is marked by three geomorphological zones (i) south-sloping Piedmont Fan Surface (PF) in the north comprising Bhabhar and Terai zones, (ii) Megafan Surface (MF) or Central Alluvial Plain in the middle, and (iii) north-sloping Marginal Plain Upland Surface (MP) in the south. Further, Active Flood Plain Surface (T0), River Valley Terrace Surface (T1), and Upland Interfluve Surface (T2) can also be delineated within the central zone of Megafan Surface. Based on the rate of sedimentation and subsidence history, the Ganga Plain is classified into the Upper, Middle, and Lower units. The entire Ganga Plain is segmented into numerous Precambrian basement tectonic blocks by several longitudinal and transverse faults, developed as a result of neotectonic activities. The basement gently slopes to the north and are found at ~4000 to 6000 m depth near the Himalayan foothills (Sastri *et al*., 1971; Ojha, 2012). Based on gravity anomalies, five basinal depressions are recognizable in the Ganga Valley: the Sahaspur Depression, the Rampur Low, the Sarda Depression, the Gandak Depression, and the Madhubani Depression (Ojha, 2012). Several basement faults like Moradabad fault, Bareilly fault, Lucknow fault, West and East Patna faults and Malda fault (Rao, 1973) are well delineated and seismically active.

The IGBP is referred to as the Foredeep, Rift, Basin, Yoked Basin, Half Graben or Board Shallow basin (Rao, 1973; and references therein). Burbank *et al*. (1992) and Singh *et al*. (1996) suggested that overloading by the Himalaya was responsible for the creation of this basin due to the overriding thrust-fold belt. Gravity measurements across Ganga Plain and Himalaya show deficit of mass below the Ganga Plain and excess of mass below Lesser Himalaya. The present-day near-surface sediments of the basin are of Holocene age; the older Late Quaternary sediments and Siwalik successions are buried below these enormously thick younger sediments (Singh, 1999; Tandon *et al*., 2008).

Cenozoic Himalayan Foreland Basin (HFB)

The Himalayan Foreland Basin (HFB) is an elongated asymmetrical basin between the HFT in the south and the Main Boundary Thrust (MBT) in the north. Sediment pile of this basin extends further south into the IGBP and overlaps the peripheral bulge of the Indian Craton (Kumar, 2020, and references therein). Many transverse basement ridges dissect this basin into several sub-basins and control their sedimentation and tectonics. It evolved with widespread Paleocene-Middle Eocene marine transgression and later fluvial sedimentation, controlled by large southward-flowing river systems from the rising Himalaya (Srikantia and Bhargava, 1998). The following stratigraphic units characterize this belt.

Subathu Formation: The Paleocene-Middle Eocene marine transgression commenced with unconformable deposition of the Subathu Formation over the Proterozoic–Early Paleozoic Lesser

Himalayan and Sub-Himalaya domains. It contains silicified limestone clasts and bauxite at the base, coaly/carbonaceous shale and fossiliferous grey-green shale-siltstone and limestone-sandstone, which grade into variegated purple siltstone-shale (Passage bed) and white sandstone (Bhatia and Bhargava, 2006). It was deposited in euxinic evaporitic lagoons and shallow tidal sea. It is marked by relatively high $\varepsilon_{Nd(t=0)}$ values (~–7.8 to –9) and low $^{87}Sr/^{86}Sr$ ratios (~0.710 to 0.715), with detritus sourced from the proto-Himalaya and ITSZ (Najman *et al*. 2000).

Dagshai Formation: The overlying unfossiliferous Dagshai Formation (=Dharamsala Formation) contains reddish mudstone-siltstone-sandstone alternations. Precise contact relationships between the Subathu and Dagshai Formations are debated since a transition was postulated from marine to fluvial environment (Bhatia and Bhargava, 2006), in contrast to an unconformity with a hiatus of ~10 my to <3 my. Age of the Dagshai Formation is also uncertain: (i) 35.5 ± 6.7 Ma, between <28 and 25 Ma from the 40Ar/39Ar detrital micas, or (ii) base younger than 31 ± 2 Ma from detrital-zircon fission track (ZFT) ages or (iii) 35.5 Ma (Najman, 2006; Jain *et al*., 2009). The $\varepsilon_{Nd(t=0)}$ and 87Sr/86Sr isotopic values range between ~–12.7 to –17.2 and ~0.753 to 0.775, respectively (Najman *et al*., 2000), indicating sources like medium grade metamorphosed HHC.

Kasauli Formation: The overlying Kasauli Formation (~2000 m) contains alternating grey-green sandstone and siltstone-mudstone, which were deposited by migratory braided river system under humid climate. It possesses more metamorphic fragments than older formations, with isotopic characters like the Dagshais. Age of this formation remains uncertain: Lower Miocene (23-16 Ma) from floral and mammal remains, <28 to 22 Ma from 40Ar/39Ar detrital white mica, and 24.9 ± 2.1 to 20.7 ± 3.2 Ma from youngest zircon fission-track (ZFT) peak for the uppermost part (Jain *et al*., 2009).

Siwalik Supergroup: Southerly-flowing fluvial system from the Himalaya deposited over 6 km-thick Miocene-Pleistocene Siwalik Supergroup in the HFB (Kumar, 2020). Many sub-basins like Kangra, Subathu, Dehra Dun mark the HFB due to presence of sub-subsurface ridges and transverse lineaments. Stratigraphically, the Siwalik Supergroup is broadly subdivided into Lower, Middle and Upper Siwalik Subgroups. The Lower Siwalik Subgroup (1800 m thick) of interbedded coarse purple-grey sandstone-brown shale was deposited by highly sinuous meandering rivers in broad muddy flood plains (Singh, 1999), receiving detritus mainly from low-medium grade metamorphosed Himalayan sources between <13 and 9 Ma (cf. Clift, 2017).

About 2.5 km thick Middle Siwalik Subgroup of greyish, mica-rich medium to coarse multi-storied sandstone-siltstone-overbank mudstone were deposited by braided rivers with alluvial fan complexes between 9 and 4.5 Ma. The Upper Siwalik Subgroup of ~2.5 km thick conglomerate-sandstone-mudstone was laid down into coalescing alluvial fans between 4.5 and 1 Ma. Since the HFB detritus was synchronously derived from the Himalaya, it provides an invaluable clue for cooling and exhumation of adjacent rising hinterlands. Detrital 40Ar/39Ar muscovite and ZFT youngest peaks become younger eastwards from 25-20 to 10-8 Ma; this trend is consistent with an eastward-migrating pulse of hinterland cooling (Clift, 2017).

Duns–Late Cenozoic-Holocene Tectonics: The Cenozoic HFB is longitudinally and tectonically dissected by numerous small tectonic intermontane basins containing Late Cenozoic-Holocene sediments, lying over the Siwalik Supergroup. These are bordered by the outer Siwalik Hills on southern sides and the overthrust Lesser/Sub-Himalaya belt in the north along the MBT. Dehra Dun reveals a combined influence of basin margin regime and structures that transect the Dun where foreland propagating Himalayan fold-thrust system is largely controlled by the MBT and the MF) during Pleistocene.

Lesser Himalaya

Lying between the Sub-Himalaya (Outer Himalaya) and the Great Himalaya in the north, the Lesser Himalaya (=Lower Himalaya) is 60 to 80 km wide NW-SE to E-W and WSW-ENE trending belt for nearly 2500 km. Most of the terrain has elevation from 600 to 4,500 m and is highly dissected by south-flowing rivers. Two sedimentary belts characterize the Lesser Himalaya between the Main Boundary Thrust (MBT) and the Munsiari Thrust (MT)/Main Central Thrust (MCT) in Uttarakhand-Nepal: (i) southernmost Neoproterozoic-Early Paleozoic Outer

Lesser Himalayan (oLH) sedimentary belt, and (ii) northernmost Paleoproterozoic- Mesoproterozoic Inner Lesser Himalayan (iLH) sedimentary belt (Valdiya, 1980; Jain *et al*., 2020). These belts are separated by the Lesser Himalayan Crystalline (LHC) nappe.

Outer Lesser Himalayan (oLH) Sedimentary Belt: The oLH Belt of the Shimla-Jaunsar and Blaini-Krol-Tal Groups is exposed between the MBT and Tons Thrust (TT)/North Almora Thrust (NAT). The oldest Shimla Group (=Morar/Chakrata/Dharasu/ Srinagar/Pauri Groups) contains intercalated and alternating greywacke-slate-limestone- dolomite sequences at the base (Srikantia and Bhargava, 1998). Valdiya (1980) interpreted the Shimla Group of Himachal Pradesh and Garhwal as shaly flysch, deposited primarily by NNE-trending lateral turbidity currents originating from the Aravalli-Delhi System, while the overlying Blaini Boulder Beds were considered as slide conglomerates from steep structural slopes. On the contrary, detailed observations by Singh and Mehrajuddin (1978) indicated shelf-mud transition zone of a tidal flat complex for the deposition of the Shimla Group.

Further south, within the Krol Belt, the Neoproterozoic Jaunsar Group is comprised of the Mandhali Formation (conglomerate–limestone–carbonaceous–slate–phyllite), the Chandpur Formation (phyllite–siltstone alternations–metavolcanics) and the Nagthat Formation (quart arenite–slate) in ascending order (Auden, 1934). These rocks crop out in a series of doubly plunging synclines along nearly 280 km long belt between Solan in the NW and Nainital in the SE (Bhargava, 1976). In Kumaon, the oLH belt unconformably overlies the Bhowali Group containing quartzite–dolomitic limestone–slate–metabasalt–metarhyodacite.

The Nagthat siliciclastics reveal extensive development of multistoried medium-to thick-bedded sandstone, conglomerate and siltstone-shale, deposited under shoreface to proximal inner shelf tidal and stormy influence with coarsening upwards prograde stratigraphic sequence in gradual shallowing basin. Their detritus was sourced from the Aravalli-Delhi mountain chain and Bundelkhand granite-gneiss massif during the Neoproterozoic.

The Nagthat Formation is unevenly covered by 200 m thick glacial diamictite, siltstone and sandstone succession of the Blaini Group, representing the Marinoan glaciation of the Cryogenian period with at least two thick and regionally extensive diamictite units, separated by siliciclastics and argillites (Jain, 1981). A glaciogenic origin is supported by the presence of relatively abundant striated clasts and the local preservation of polished and striated pavement on underlying Shimla Group. The cap dolostone is characterized by lighter isotopes of 13δC and 18δO.

Nearly 400 m of shale, siltstone and minor sandstone overlie the Blaini diamictite as Neoproterozoic Infra-Krol Formation. These are followed upwards by predominantly carbonate suite of the overlying Krol Group, which is divided into the Lower (Krol A), Middle (Krol B) and Upper (Krol C, D, E) formations (Auden, 1934). The sequence contains argillaceous limestone interbedded with greenish grey calcareous shale (Krol A), reddish-greyish shale with siltstone and thin layers of dolomite (Krol B), bluish grey limestone and brecciated dolomite (Krol C), dolomitic limestone, stromatolite-bearing cherty dolomite, shale, siltstone and thin sandstone layers (Krol D), and thinly bedded limestone interlayered with calcareous shale, siltstone and dolomite (Krol E). Detailed sequence stratigraphic studies identified several disconformable surfaces indicating interruptions in largely tidal to intertidal sedimentation (Singh, 1980) in a shallow NW-sloping marine Krol Basin.

At the end of the Krol E formation, carbonate deposition was interrupted by development of ~150 m thick euxinic Lower Tal Formation of black shale, chert and organic matter rich phosphorites. Hollow phosphatic tubes of small shelly fauna *Anabarites*, *Protohertzina* and *Maldeotaia* of Tommotian age, pyrite-rich stromatolites and trilobite traces dominated the depositional scene. This Lower Cambrian strata define the Proterozoic-Cambrian boundary (Banerjee *et al*., 1997).

The Tal basin received about 2500 m thick deposits of sandstone and shale under tidal to intertidal environments. Abundant animal trails, syn-sedimentary primary structures in sandstone and reddish-brown shale represent the upper parts of the Lower Cambrian. Uppermost part of the Tal Group shows clean quartz arenite with sedimentary features indicating very shallow water coastal environment of lagoons, tidal flats and shoals (). An unconformity is marked by deposition of Cretaceous Shelly limestone which, in turn, is overlain by the Paleocene Subathu Formation.

oLH sedimentary belt of Sikkim, Bhutan, Arunachal Himalaya-Gondwana Group: The outermost LH Belt contains Damuda Formation of coal-bearing feldspathic sandstone, siltstone, carbonaceous shale, coal lenses/seams with plant fossils and an upper non-coal bearing succession, having characteristic lower Gondwana flora (Lakshminarayan and Singh in Bhargava, 1995). Like the other Gondwana sequences, the Lower Permian marine fossils are associated with sandstone, siltstone and shale intercalations in upper parts of the Setikhola Formation (Joshi in Bhargava, 1995).

Duiri Formation: Further north, the Duiri Formation is named after the Diu Ri valley, and consists of quartzite and boulder slate (diamictite). Greyish boulder slate contains sub-rounded to rounded pebbles and boulders of quartzite, phyllite, slate, dolomite and gneiss in a sandy argillaceous slaty matrix.

Tectonically, the Diuri Formation is bounded by the Buxa Group in the north and the Damudas in the south and resembles the Blaini diamictite and Rangit Pebble slate; the latter are of glacial origin and correlated with Permian Talchir Boulder Bed.

Buxa Group: A thick sequence of dolomite, quartzite and shale into the 'Baxa Series' in western Duars after the famous Buxa Fort. As main repository of dolomite and limestone deposits in Bhutan, this belt extends along the entire foothills with about 1.5 to 6 km thickness. Separated from the Siwalik Group/ Setikhol Formation by the Main Boundary Thrust (MBT), the group has been classified into four formations in ascending order: the Jainti Formation (maroon-purple, green-grey phyllite, metasiltstone and quartzite, and pink-white quartzite), the Manas Formation (white-grey gritty quartzite, creamy dolomite, phyllitic slate and limestone), the Phuntsholing Formation (white-grey quartzite, phyllite and occasional limestone) and the Pangsari Formation (white-cream arenaceous dolomite, phyllite and quartzite) (Tangri in Bhargava, 1995). The upper contact of this group is defined by the Shumar Thrust.

Thungsing Quartzite: A succession containing white, feldspathic, medium to coarse-grained quartzite, occasionally pebbly and conglomeratic have been included in the Thungsing Quartzite with minor slate and phyllite intercalations and considered it separately from the Shumar quartzite.

Further east in Arunachal Pradesh, immediately to the northwest of the Sub-Himalayan Siwalik Belt, the southern front of the Lesser Himalaya is composed of Permian Gondwana Group of the Outer Lesser Himalayan unit, and consists of carbonaceous shale, sandstone and a few coal beds belonging to the Garu (marine) and Khelong (fluvial) sequences.

Lesser Himalayan Crystalline (LHC) nappe

Synformal klippen of the Lesser Himalayan Crystalline (LHC) nappe (Garhwal, Ramgarh, Almora, Baijnath, Askot, Chiplakot, others) are thrust over the LH sedimentary belt (Valdiya, 1980). The lowermost Ramgarh Nappe of the Ramgarh-Debguru-Ulleri-type augen mylonite (ca. 1.85 Ga) is overlain by the Nathuakhan Formation containing quartzite-phyllite with 0.80 Ga youngest detrital zircon (Célérier *et al*., 2009). The Almora Nappe overrides this unit with ca. 1.85 Ga mylonitized granite gneiss along the base, garnetiferous quartzite-schist alternations with 0.85 to 0.58 Ga youngest detrital zircons and 0.55 Ga intrusive granitoids (Trivedi *et al*., 1984).

Inner Lesser Himalayan (iLH) Sedimentary belt

Lying between the North Almora Thrust (NAT) in the south and the Munsiari Thrust (MT)/Vaikrita Thrust (VT)/Main Central Thrust (MCT) in the north, the Proterozoic iLH extends as a linear belt between the Tons and Kali valleys. Because of its unfossiliferous character, facies variations and intricate tectonics, stratigraphic correlations are controversial. This belt extends along the strike into Himachal, Jammu and Kashmir in the west and Nepal, Sikkim, Bhutan and Arunachal in the east.

In Jammu-Kashmir and southern Himachal Pradesh, outermost frontal Paleoproterozoic iLH Shali Belt (Srikantia, 1977) contains quartzite-shale (Sundernagar Formation), mafic volcanics-slate (Mandi-Darla Volcanics) and quartzite-salt-marls-shale-dolomite (Shali Group). These are considered NW extension of the Rautgara of Kumaon. All over this belt, these rocks are intimately interbedded with vesicular basalts and tuffs, exposed from Mandi-Darla in Himachal, Alaknanada valley in Garhwal (the Rudraprayag volcanics) and Bhimtal in Kumaon. This belt regionally dips towards NE and is thrust southwestward over the SH belt in the Punjab Re-entrant along the MBT (Srikantia and Bhargava, 1998). It contains the Tatapani limestone and Deoban Group carbonates within the Kulu-Rampur and other smaller windows along the Sutlej-Tons valleys beneath the Jutogh nappe and MCT zone.

Further southeast in Uttarakhand, vast ~10 km thick extensive iLH Paleoproterozoic sedimentary sequence is developed beneath the overthrust metamorphic nappes. In eastern Kumaon, in immediate vicinity of the NAT, stratigraphically oldest and northerly-dipping Rautgara Formation starts with subgreywacke–slate–conglomerate–mafic flows (Valdiya, 1980). This formation imperceptibly grades into the overlying Thalkedar Dolomite (stromatolite-bearing dolomitic limestone), the Sor Slate (green-brown-black slate), the Gangolihat Formation (stromatolite-bearing carbonates, shale, phosphorite and magnesite), and the Berinag/Garhwal Groups (quartz arenite–mafic flows) (Kumar, 1980). The Deoban Limestone (dolostone) displays prolific development of algal biostromes. Distribution of primary sedimentary structures in the Rautgara, Gangolihat and Berinag Formations suggest subtidal, supratidal and coastal beach depositional environment, respectively, with northerly paleocurrents. These carbonates are correlatable with the Shali Formation in Himachal, the Jammu Limestone and the Sirban Limestone in the Jammu-Kashmir sector. In Himachal, the Berinag-type quartz arenite and metavolcanics are identified as the Rampur Quartzite in the Sutlej Valley, the Manikaran Quartzite in the Beas Valley, the Shalimar Quartzite in the Chenab Valley and the Sauna Formation in Jammu. In the Eastern Himalaya, the Daling Group in Darjeeling area, Samchi-Shumar Group in Bhutan and Miri-Siang Group in Arunachal Pradesh correlate with this group.

Himalayan Metamorphic Belt (HMB)

The Himalayan metamorphism represents one of the most prominent manifestations of the Himalayan orogeny along its entire strike length and, therefore, is most well studied. Core of the Himalayan orogen is mostly comprised of high-grade metamorphic complex with a cover of the Tethyan Himalayan Sequence (THS), and constitutes the "Central Crystalline Axis" of Himadri/Great Himalaya belonging to the Himalayan Metamorphic Belt (HMB). Folded thrust nappe of the HMB extensively covers the LH sedimentary belt and is exposed into the (i) Lesser Himalayan Crystallines (LHC), (ii) Higher Himalayan Crystallines (HHC), and the (iii) Tso Morari Crystallines (TMC) from south to the north. An extensional Zanskar Shear Zone (ZSZ)/South Tibetan Detachment System (STDS) separate this belt from the THS.

LHC Belt: Numerous klippen of low-medium grade metamorphosed LHC—the Salkhala Nappe, Garhwal and Almora Nappe etc. contain highly deformed alternating phyllite and schist. The lowermost Ramgarh Nappe of mylonite orthogneiss (~ca. 1.85 Ga), belonging to the MCTZ, is overlain by quartzite-phyllite of the Nathuakhan Formation, having ~0.80 Ga detrital zircons (Mandal *et al*., 2015). The Almora Nappe overrides this unit with mylonitized granite gneiss (~1.85 Ga) along the base and garnetiferous quartzite-schist alternations with 0.85 to 0.58 Ga youngest detrital zircons and 0.55 Ga intrusive granitoids (Mandal *et al*., 2015).

As a part of the Almora Nappe, regional metamorphism within pelite-psammite sequence of the Askot Klippe exhibit chlorite-biotite-muscovite-garnet-quartz, biotite- muscovite-garnet-quartz, biotite-muscovite-garnet-plagioclase-quartz and K-feldspar-sillimanite-garnet-biotite-plagioclase±cordierite-quartz assemblages, which attained granulite facies metamorphism (Das *et al*., 2019). Disequilibrium textures along garnet-biotite contact indicate beginning of granulite facies metamorphism, which is substantiated by 6.6 kbar/~776ºC for garnet rims. Within the LHC Belt of the Alaknanda valley near Joshimath, Spencer *et al*. (2012) recorded P-T conditions of ~5 kbar and ~550ºC below the MCT, while a sudden jump takes place across it to ~14 kbar and 850ºC.

An integrated P-T path of the LH belt comprises garnet-kyanite grade metapelites along the footwall of the MCT from the Arunachal Himalaya (Goswami-Banerjee *et al*., 2014). A near isobaric peak Barrovian metamorphism at P ~8–9 kbar with increase in T-maximum from ~560°C in metagranite through ~590–600°C in lower and middle garnet-zone to ~600–630°C in upper garnet- and kyanite-zone rocks. Metamorphic sequence of the LH Belt additionally records a pre-Barrovian near isobaric thermal gradient in mid crust at ~6 kbar from ~515°C in middle garnet zone to ~560–580°C in the upper garnet- and kyanite zone, adjoining the MCT. A clockwise P–T path is proposed from the studied section of the Arunachal GHS with burial to lower crustal depths, prograde heating leading to kyanite-facies partial melting at T ~750–800°C and steep, near isothermal decompression to mid-crustal depths and subsequent post-decompressional cooling.

HHC Belt: The HHC belt is exposed along numerous sections from Zanskar to Arunachal Himalaya where it reveals classic Himalayan Inverted Metamorphism (HIM) (Jain and Manickavasagam, 1993; Kohn, 2014; Pant *et al*., 2020). This belt is comprised of two litho-tectonic units: (i) a lower Munsiari Group/Lesser Himalayan Crystalline Sequence (LHCS)/Main Central Thrust Zone (MCTZ) of amphibolite, schist and augen mylonite, delimited by the Munsiari Thrust at the base (sensu stricto Main Central Thrust-Heim and Gansser, 1939) and the Vaikrita Thrust at the top, and (ii) the upper main group of High Himalaya Crystalline Sequence (HHCS)/Great Himalayan Sequence (GHS)(also known as the Vaikrita Group in Uttarakhand) is bounded by the MCT (sensu lato)/Vaikrita Thrust at the base and the South Tibetan Detachment System (STDS) near the top (Jain *et al*., 2014).

In the NW Himalaya, the HHC Belt has suffered at least four superposed recognizable deformation (D1–D4) and associated metamorphic events, resulting into its complex history. Out of these, D1 deformation produces isolated, tight and appressed "flame" folds (F1) on lithological banding/metamorphic layering (S0) whose axial-plane foliation S1 parallels this layering. Chlorite, biotite, and quartz are developed along this foliation, indicating lower greenschist facies M1 metamorphism. D2 deformation was most widespread and produced penetrative foliation (S2) paralleling axial surfaces of close to isoclinal, reclined to recumbent F2 folds on S1 foliation or lithological and/or metamorphic layering. S2 foliation dips between 20° and 40° NE. In schist the foliation is composed of S-surfaces that are progressively deflected and become subparallel to the ductile C-foliation of high strain on a scale of millimetres (Jain and Manickavasagam, 1993). In various deformed granitoids, this typically resembles the S-C mylonitic foliation, and regionally records top-to-southwest sense of ductile shearing, which is also evident from asymmetric quartz and feldspar augen, pressure shadows, rotational fabric within porphyroblasts and other shear criteria. Stretching mineral lineation (L2), coaxial to the F2 folds, plunges NE/SW almost down-dip, and was developed on composite S1-S2 and/C-foliation due to preferred orientation of mica, chlorite, tourmaline, amphibole, staurolite, kyanite, sillimanite, quartz, and feldspar during M2 metamorphism.

D3 phase produced isoclinal to tight F3a and superposed F3b folds that plunge gently either NW/SE. The F3b folds are open to closed and are inclined. Development of chlorite at the expense of garnet and biotite, and D3-related foliation have been observed during this deformation. Discrete kinks, tensional gashes, and brittle shear zones represent the youngest D4 deformation event and occasional mineral growths.

The HHC metamorphics are foliated and gneissose from garnet through staurolite-kyanite to sillimanite–K-feldspar grades, and rarely granulite, having garnet, staurolite, kyanite and sillimanite porphyroblastic growths. Muscovite, biotite, quartz, and/or chlorite and chloritoid define the main foliation, which are also sometimes porphyroblastic. Staurolite is subordinate in the middle structural levels in southeast Kashmir and western Garhwal. Chlorite is occasionally retrograde after garnet, staurolite, and biotite in staurolite- kyanite schist. Minor zircon, apatite, and ilmenite are present in the matrix, and as inclusions in biotite and garnet. The mineral assemblages include the following:

(i) Garnet grade: Chlorite–biotite–muscovite–chloritoid–garnet–plagioclase–quartz

(ii) Staurolite-kyanite grade: Biotite–muscovite–garnet–kyanite–quartz±plagioclase±

K-feldspar±staurolite±chlorite

(iii) Sillimanite–muscovite grade: Garnet–biotite–muscovite–kyanite–sillimanite± plagioclase–feldspar–quartz

(iv) Sillimanite–K-feldspar grade: Garnet–biotite–

sillimanite–K-feldspar–plagioclase–quartz±cordierite

In southeast Kashmir along the Chenab Valley, garnet grade within ~500 m of the MCT footwall zone of the iLH records rim 6.5 kbar P and 550°C T, while hanging wall of the MCT in the staurolite-kyanite grade records garnet core T of 500 to 550°C and P of 8.5 kbar; rim data indicate T of 600 to 650°C and P of 8 to 9 kbar (Jain and Manickavasagam 1993; Manickavasagam *et al*., 1999). In sillimanite-muscovite grade, an increase in core T of about 170°C is seen with no significant change in P, but rim data reveal a reduction of about 50°C and 1 to 2 kbar. Garnet cores in sillimanite–K-feldspar grade reveal peak T and P of 780°C and 10 kbar.

Along the Sutlej valleys in Himachal, using overprinted contact metamorphic assemblages on the Paleoproterozoic Jeori-Wangtu granite gneiss/mylonite, Pant *et al*. (2006) demonstrated presence of pre-1800 Ma low-grade regional metamorphism in the Jeori-Wangtu sequence, while a sericite schist records a Paleoproterozoic soil horizon along the basement-cover contact (Bhargava *et al*., 2011). Manickavasagam *et al*. (1999) measured garnet rim data between 490 and 500°C for the garnet to staurolite-kyanite transition zone, and 570 and 590°C and ~8 kbar for staurolite-kyanite grade, exposed between Jhakri and Wangtu in the lower structural levels on footwall of the Vaikrita Thrust. However, above hanging wall of the Vaikrita thrust to the STDS, the HHC records an increasing T of 575 to 620°C and P of ~7 kbar in staurolite-kyanite grade, whereas sillimanite-muscovite grade exhibits 740 to 800°C and ~9 kbar

Along the Bhagirathi valley, Manickavasagam *et al*. (1999) noted rim P-T results as ~5.75 kbar and ~550°C for the garnet grade in pelitic schist on hanging wall of the Munsiari Thrust. Above the Vaikrita Thrust on its hanging wall, garnet cores record 500 to 545°C in staurolite-kyanite grade and ~750°C for sillimanite-muscovite grade in the GHS, garnet rim data reveal 8 to 9 kbar and 600 to 650°C for the staurolite-kyanite grade; and 9 to 11 kbar and ~700 °C for the sillimanite-muscovite grade.

Further southeast along the Alaknanda valley, Spencer *et al*. (2012) recorded dramatic P-T increase across the LHCS from ~5 kbar and ~550°C to ~14 kbar and ~850°C at ~3 km above the MCT in the GHS, though pressures then decrease up section to ~8 kbar in the GHS at nearly constant ~850°C near the STD.

In Darjeeling-Sikkim, progressive increase of both pressure and temperature is recorded with increasing grade and structural levels through the Lesser Himalaya, the MCTZ and the HHC. Following peak metamorphism at 5.8 kbar and 590°C, the LH metamorphics underwent clockwise P-T-t path due to decompression of the crust (Prakash and Tewari, 2016). The MCT zone near Darjeeling revealed polyphase deformation and Barrovian metamorphism with peak P varied from 5.0 to 7.5 kbar and T of 570 to 780°C in garnet and staurolite zones, respectively (Tewari and Prakash, 2016). In the overthrust HHC, migmatite has characteristic biotite±garnet±sillimanite-plagioclase-K-feldspar-quartz assemblage with evidence of extensive partial melting through biotite dehydration reaction (Tewari and Prakash, 2017). Migmatite experienced peak P-T at 7.2 ± 0.5 kbar and 775 ± 20°C, respectively with timing of crustal melting ~21 Ma.

In the MCT zone of upper parts of the Teesta River valley, deformation mechanism differs from that of the underlying LH and overlying HHC sequence, with peak metamorphism of 750-800°C before intense faulting at 20 Ma (450-700°C) and isolated 11 Ma brittle phase.

Ganguly *et al*. (2000) calculated peak metamorphic conditions from the HHC sequence in the Sikkim-Darjeeling section as ~10.4 kbar, 800ºC temperature and extremely rapid (~15 mm/yr) exhumation up to the depth of ~15 km, followed by a much slower process ~2 mm/yr, up to at ~5 km depth. It is proposed that change of exhumation rate might reflect a process of tectonic thinning, followed by erosion and/or horizontal flow at shallow depth and suggests that the HHC exhumed from a depth of ~34 km within ~8 Ma.

Using in situ Th–Pb monazite ages, Mottram *et al*. (2014) observed that peak P–T metamorphic conditions reached earliest in structurally highest part of inverted GHS above the MCT between ~37 and 16 Ma in southerly leading-edge and between ~37 and 14.5 Ma in northern rear-edge of the MCT zone at peak P–T conditions of 10 kbar and ~790ºC.

Tso Morari Crystalline Belt (UHP metamorphism): Eclogite was first reported from the inaccessible Rupshu district of Jammu and Kashmir, followed by their detailed regional geologic description (Srikantia and Bhargava, 1978). Subsequently, the UHP rocks were observed from Kaghan and Neelum valley (Pakistan), and Ama Drime, Nepal, which have wide implications for angle of subduction, P-T-t path of the subducted block and recovery (Leech *et al*., 2005; Epard and Steck, 2008 and references therein).

In the NW Himalaya, the TMC is comprised of ~100x50 km long and NW-SE trending dome of quartzo-feldspathic gneiss, metamorphics and Paleozoic granitoids (Puga, Tanglang La, Polokongka La/Rupshu Granite, respectively), having dispersed small eclogite and garnet amphibolite bodies/lenses (Thakur, 1993; Jain *et al*., 2003; Leech *et al*., 2005). It is a UHP eclogite-gneiss-greenschist complex in southeastern Ladakh beneath the THS cover to the south of the ITSZ. Presence of coesite-bearing eclogite within the TMC and Kaghan (Pakistan) provides undisputed evidence that leading edge of the ICL subducted beneath the ITSZ to ~120 km depth in Early Eocene (Leech *et al*., 2005; Guillot *et al*., 2008).

The TMC attained peak P-T conditions for the UHP eclogite-gneiss at 27-39 kbar and 750-850^{o}C at ~55 Ma (de Sigoyer *et al*., 2000), and retrogressed to HP eclogite-facies (20 kbar, 600^{o}C), amphibolite-facies (13 kbar, 600^{o}C), greenschist-facies (4 kbar, 350^{o}C), and finally exhumed to the surface (Guillot *et al*., 1997). U-Pb SHRIMP zircon dates from the TMC pinpoint precise ages of peak UHP metamorphism (53.3 ± 0.7 Ma), HP metamorphism (50.0 ± 0.6 Ma) and amphibolite metamorphism (47.5 ± 0.5 Ma). ~30 Ma age of $^{40}Ar/^{39}Ar$ muscovite and biotite records last stage greenschist metamorphism (Leech *et al*., 2005, 2007). Present dataset reveals that final exhumation of the Tso Morari Complex, including the eclogite, was almost simultaneously with the HHC belt.

Tethyan Himalayan Sequence (THS): The THS is typically developed beyond the Great Himalaya on northern passive margin of the Paleoproterozoic-Neoproterozoic Indian Plate during Cambrian to Paleogene/Lower Eocene, and represents a vast sedimentary ~10 km thick pile, deposited in the vast Tethyan Ocean (Bhargava, 2008; Bhargava and Singh, 2020). It rests over the HHC Belt in several disconnected basins. The THS commenced with eruptions of the Khewra Traps and Singhi bi-modal Volcanics in Salt Range and Bhutan, respectively in a rift basin. The Cambrian Kunzam La Formation has remarkable lithological similarity from Kashmir to Bhutan and deposited in subtidal to locally supratidal environments, except in Nepal. This sedimentation ranged up to Middle Cambrian; a part of late Cambrian is preserved only in Kashmir and Bhutan. A widespread regression commenced in late Cambrian and culminated in early Ordovician due to the Kurgiakh Orogeny, which has caused the uplift and erosion of highlands to produce conglomerate at the base of Ordovician.

The Early Ordovician (Thango Formation) is mainly arenaceous with a basal conglomerate up to Nepal, while in Bhutan sedimentation seems to have commenced in Late Ordovician. During this period, carbonates (Takche/Shiala/Yong Formations) have conspicuous build-ups in Kashmir-Spiti-Kinnaur-Garhwal-Bhutan, and imperceptibly pass into another carbonate succession in Early Silurian and may be extending into the Wenlock.

Regression in the Wenlock caused disconformity between the Early Silurian and Early Devonian; this break is more pronounced in western Spiti-Lahul-Zanskar. The Early/Middle Devonian transgression deposited the Muth Formation from Kashmir to Uttarakhand. In Nepal, it was somewhat deeper, while it was delayed in Bhutan; therefore, deposition commenced in Late Devonian. Elsewhere, sediments grade into siliciclastic-carbonate sequence of the Lipak Formation/Syringothyris Limestone, which range from Givetian to Tournaisian. The later part is siliciclastic of the Po Formation/Fenestella Shale of Visean age. There was another uplift during which these sediments contributed clasts to the Late Carboniferous-Early Permian conglomerate (Ganmachidam Formation). In Nepal, the Givetian sediments are disconformably overlain by the Permian. The Early Permian witnessed another transgression (Gechang Formation), which coincided with rifting in Gondwanaland. During the Middle Permian, parts of Kashmir and Zanskar were sites of volcanicity; elsewhere this was a period of non-deposition. Several lacustrine basins were formed in Kashmir (Nishat Bagh/Mammal Formations) during this volcanism. The Gungri/Zewan Formation represented a more extensive transgression during Wuchiapingian. Except in Kashmir, the Late Changhsingian sediments are absent in other parts with distinct break along the Permian-Triassic interval.

The Triassic sediments (Lilang Supergroup) are mainly shallow marine carbonate-dominated, followed by rapid deepening, which lasted up to Carnian (Chomule Formation/Hedenstromia Beds). Thereafter, the basin gradually shallowed during Middle Norian for extensive coral reef growths, which terminated due to further basin shallowing. There was a minor flooding in lower Upper Norian (Alaror Formation/ Monotis Shale) after which late Norian shallowed to beach environment (Nunuluka Formation/Quartzite Series). The Rhaetic witnessed another flooding and resulted in deposition of overlapped Para Formation/ Megalodon Limestone. Thereafter, there was a break between the Liassic and Oxfordian (the Upper Callovian break). The Oxfordian to Valanginian Spiti Formation contains ammonoid-bearing black shale throughout the Tethyan sections. In the upper parts, it develops sandstone beds, which pass into the Late Valanginian/Early Huaterivian to Albian Giumal Formation. The sandstone is conformably overlain by limestone and shale of the Chikkim Formation of Campanian/Early Maastrichtian. This part of the Tethyan sequence is absent in Kashmir and Bhutan.

In Zanskar, the ophiolite nappes were emplaced onto the Cretaceous sediments, while deep-facies exotic blocks characterize the Malla Johar nappe in Uttarakhand. Only in Zanskar, the Thanetian to Early Ypresian Kelcha Formation is preserved, and overlain by paralic to fluvial fining-up arenaceous Dunbar Formation (Late Ypresian-Lutetian age). There is hiatus between the Cretaceous and Thanetian sediments, as the Danian element is missing.

Since the THS is also observed within the Lesser Himalayan domain, Myrow *et al*. (2003) and Bhargava and Singh (2020) summarized three models: (i) deposition in two separate tectonic domains, separated by lofty rock barrier, (ii) one single large basin, and (iii) two basins developed at different locations and large scale thrusting along the Main Central Thrust.

Tectonic Boundaries

The India-Asia convergence has produced the following orogen-scale main thrust systems: (i) Quaternary Main Frontal Thrust (MFT)/Himalayan Frontal Thrust (HFT), (ii) Middle Miocene Main Boundary Thrust (MBT), and (iii) Early Miocene Main Central Thrust (MCT) (Thakur, 1993; Hodges, 2000; Yin, 2006; Robinson *et al*., 2006). An extensional South Tibetan Detachment System (STDS) separates the northern margin of the GHS from the Tethyan Himalayan Sequence (Burchfiel and Royden, 1985). These boundaries appear to merge with the blind Main Himalayan Thrust (MHT) (Nabelek *et al*., 2009).

Main Frontal Thrust (MFT): The MFT (=HFT) is the youngest and outermost tectonic boundary between the Indus-Ganga-Brahmaputra Plain and Cenozoic Sub-Himalayan (SH) Siwalik Belt, developed during the Quaternary (Jayangondaperumal *et al*., 2018; Thakur *et al*., 2020). It generates and maintains active, modern Himalayan deformation and topographic front, and is the near-surface expression of the MHT. Thus, the MHT-MFT deformation boundary is the contemporary India-Asia plate interface along which the Indian continental lithosphere subducts beneath Asia (Jain, 2017). Since the youngest Siwalik Group has yielded a 0.5 Ma paleomagnetic age in the western Himalaya, it is likely that the MFT has evolved progressively during later parts of Pleistocene-Holocene and caused deformation in the Sub-Himalaya. Growth of longitudinal, front-parallel intermontane valleys (the Duns) are controlled by imbricated thrust system. The Duns occupy synclinal troughs in the evolving Sub-Himalayan fold-thrust systems and were filled by post-Siwalik piedmont sediments in piggy-back basins during the late Quaternary–Holocene period (Aitchison *et al*., 2007).

The MHT-MFT fault system periodically releases strain during great (M >8) earthquakes and transfers strain during movements along these surfaces, hence this deformation zone is significant for the Himalayan tectonics and natural hazards (Jayangondaperumal *et al*., 2018 and references therein). Outermost surface exposures of the Upper Siwalik typically access small fraction of fault zone and its minor splays in trench. The frontal Siwalik Ranges are marked by anticlinal ridges and in many places by synformal depressions of intermontane basins called duns, such as Soan dun and Dehradun in India and several duns in Nepal. Some of these anticlines are located around Surin Mastgarh, Janauri, Chandigarh and Mohand.

Main Boundary Thrust (MBT): The MBT is one of the major north-dipping Himalayan thrusts, developed during Middle Cenozoic, and forms the present-day structural and orographic boundary between the Sub- and Lesser Himalaya (Valdiya, 1980). Originally, it was defined as the fault contact between the older Tertiary sequence (Subatbu-Dagshai-Kasauli) of the Sub-Himalaya and the Siwalik and called as the 'Main Boundary Fault'. This thrust is called as the (i) 'Boundary Fault' between the Murree and Siwalik from NW syntaxis to Jammu–Poonch, (ii) Riasi Thrust and Murree Thrust, (iii) 'Main Boundary Fault' between Subathu, Murree and Jammu limestone inliers from the Siwalik, (iv) 'Palampur Thrust' between lower Tertiary Dharamsala from underlying Neogene Siwalik in Kangra, (v) 'Bilaspur Thrust' separating Proterozoic limestone, lower Tertiary Subathu and Dharamsala from the Siwalik in Bilaspur area, (vi) 'Nahan Thrust' between Lower Siwalik (Nahan Formation) and overlying lower Tertiary and stromatolite bearing-limestone around Nahan and Yamuna R. See Thakur (2010) for further details regarding newly identified Medlicott-Wadia Thrust (MWT).

Main Central Thrust (MCT): The MCT is one of the most significant and largest tectonic discontinuities as a ductile shear zones in the Himalaya, extending for nearly 2500 km along its entire length from Pakistan, western Zanskar, Nepal, Bhutan, Arunachal Pradesh, and even into the Myanmar (Thakur, 1993; Hodges, 2000; Searle *et al*., 2008; Yin, 2006; Valdiya, 2016). Heim and Gansser (1939) first introduced this term in Garhwal for 'a sharp contact where northerly-dipping crystallines rest over the metamorphosed limestone (p. 78)'. The crystalline rocks were called as the 'Crystalline Central Zone', and noted that this thrust mass 'represents an enormous deep-rooted body of 10-15 km thick crystalline rocks, which must have been at a depth of 30 km below the surface at ~700°C and thrust southwest after the deposition of the Cretaceous flysch (p. 225)'. It is, therefore, evident that there was only one thrust recognized by Heim and Gansser (1939) on regional scale. Since then, the MCT has been investigated by various workers along its entire length. Definition of the MCT has undergone numerous changes with time due to difficulties in its recognition (see Searle *et al*., 2008; Martin, 2017; Carosi *et al*., 2018; Jain *et al*., 2020).

Two distinct MCT are now recognized throughout the Himalaya: the Ramgarh/Munsiari and Vaikrita Thrusts in the NW Himalaya (Valdiya, 1980; Sheshrtha *et al*., 2015; Mukherjee *et al*., 2019; Jain *et al*., 2020), the MCT-1 and the MCT-2 in Nepal (Arita, 1983), bounding a package of rocks in the MCTZ. Time span of the MCT activity ranges from 23–20 to 15 Ma in different parts of the belt down to a reported c. 3 Ma in central Nepal (see Montomoli *et al*., 2015 for an updated review). Montemagni *et al*. (2019) recorded three different biotite–muscovite growths and recrystallization episodes along the Vaikrita Thrust in the Dhauli Ganga valley, viz. a relict mica-1 and mica-2 along the main mylonitic foliation and mica-3 in coronitic garnet during its breakdown. Step-ages of biotite between 8.6 and 16 Ma and muscovite between 3.6 and 7.8 Ma reflect sample-specific recrystallization markers, hence these ages were linked to the activity along the Vaikrita Thrust at least from 9 to 6 Ma at c. 600°C and termination by 6 Ma.

South Tibetan Detachment System (STDS): After the recognition of an extensional fault system in southern Tibet within the contractional Himalayan orogen, the STDS is now ubiquitously documented from western parts, Nepal, Sikkim and Bhutan (Herren, 1987; Burchfiel *et al*., 1992; Patel *et al*., 1993; Iaccarino *et al*., 2017). Many north-dipping parallel low- to steep dipping normal faults of the STDS exhibit top-to-the-north normal shear sense and juxtapose the THS against the HHC belt/Tibetan Slab (Burchfiel *et al*., 1992). At places, these reveal brittle normal faults, detachment faults between the unmetamorphosed/poorly metamorphosed THS and underlying metamorphics, and ductile STDS-controlled shear zone on top of the HHC (Leloup *et al*., 2010). In addition, the STDS also revealed an older top-to-the SW thrust shear sense, superposed by top-to-the-north normal faulting in Zanskar (Patel *et al*., 1993). Throughout the Himalaya, the STDS is now a well-established top-to-the-north-down structure, having ductile to brittle normal shear zones of variable thickness, separating medium- to high-grade GHS in the footwall from the THS in the hanging wall.

Timing of the N-S extension along the STDS has been critically assessed and reviewed by Leloup *et al*. (2010) and Iaccarino *et al*. (2017), who observed that it was initiated at ~26–24 Ma, ceased at ~20 Ma in Zanskar, and became gradually younger eastwards between 15–16 Ma with the transition to brittle-ductile deformation at 13.9 Ma in western Bhutan.

Main Himalayan Thrust: Schulte-Pelkum *et al*. (2005) and Nabelek *et al*. (2009) observed a detachment surface separating the underthrust Indian Plate and the Himalaya hanging wall wedge in Nepal and called it as the Main Himalayan Thrust (MHT). An anisotropic zone was detected along this surface (Schulte-Pelkum *et al*., 2005), where a northward dipping low velocity zone (LVZ) is caused by aqueous fluids resulting from dewatering of underthrust sediments (Nabelek *et al*., 2009).

Majority of earthquakes define a narrow belt between north-dipping MBT and the MCT and are essentially controlled by a mid-crustal ramp within the MHT along which the Indian Plate underthrusts southern Tibet at about 10o (Seeber and Armbruster, 1981; Ni and Barazangi, 1984; Nelson *et al*., 1996). This surface dips at ~15° from about 10 to 20-km depth within the Himalaya and controls focal mechanisms not only of shallow ($\lesssim$30°) earthquakes but also the great Himalayan earthquakes of M>8 (Ni and Barazangi, 1984). Outer seismic mid-crustal ramp extends into an aseismic 30-40 km deep seismic reflector, imaged in the INDEPTH experiment further north (Zhao *et al*., 1993). Seismic observations from the 25 April 2015, Mw 7.8 Gorkha earthquake in Nepal, their integration with geology and deep structures led Hubbard *et al*. (2016) to postulate that the slip patch closely matches an oval shaped, gently dipping MHT fault surface bounded on all sides by steeper ramps.

Recent observations on thermochronological and cooling age patterns, uplift and exhumation rates in different parts of NW- and NE-Himalaya reveal their controls due to structural positions of dome/window/synform, klippen/nappe structures and thrusting/back-thrusting along different major faults (See Thiede *et al*., 2017; Gavillot *et al*., 2018; Patel and ManMohan, 2020). In many instances these surface structures appear to reflect the geometry and kinematics of the MHT with development of duplexes over the ramp of the MHT. Exhumation patterns are controlled by local tectonics that is dictated by the subsurface geometry of the MHT and its associated structures (Thiede *et al*., 2017; Gavillot *et al*., 2018). Plots of thermochronological ages have been examined to understand how duplex over the MHT ramp or surface breaking fault emerging over the MHT influenced the patterns of thermochronological ages and exhumation rates (Patel and ManMohan, 2020).

Himalayan Magmatism

The Himalayan Orogen witnessed episodic magmatism since Paleoproterozoic as (i) Paleoproterozoic magmatic arc and associated granite-mafic bodies, (ii) Neoproterozoic granitoids, (iii) Cambro-Ordovician granitoids, (iv) Permian mafic volcanism and related granitoids, and (v) Cenozoic granitoids (Singh, 2020, and references therein).

Paleoproterozoic Magmatic Arc and Columbia Supercontinent Assembly: The Paleoproterozoic magmatic bodies occur in far-travelled intensely mylonitized Main Central Thrust Zone (MCTZ), whose remnants are observed in the Munsiari Group, Askot–Baijnath–Chiplakot nappe, basal Almora Nappe mylonite and Ramgarh mylonite in Uttarakhand and Ramgarh thrust zone in Nepal and Eastern Himalaya. A belt of such mylonitized magmatic bodies represents the Late Paleoproterozoic magmatic arc with 207Pb/206Pb zircon ages between 1.95 and 1.87 Ga and average whole-rock $\varepsilon_{Nd(0)}$ –25 value from Uttarakhand, Nepal, Sikkim, Bhutan ad Arunachal Pradesh (Mukherjee *et al*., 2019; Jain *et al*., 2020, and references therein).

Northern margin of the Indian Plate witnessed various tectonic set-ups since Paleoprotozoic; the oldest amongst these is the evolution of the Paleoprotozoic iLH basin with the Munsiari magmatic arc that separates the oLH and the GHS belts on either side. Kohn *et al*. (2010) visualized a Paleoprotezoic arc system and argued that linear belts of magmatic and clastic metasediments developed in a very short duration of about 100 Mya only. Mukherjee *et al*. (2019) and Jain *et al*. (2020) opined that granitoids of the Munsiari, Chiplakot, Askot, Ramgarh and basal Almora klippen were generated by subduction-related hydrous partial melting of the Paleoproterozoic mafic source and sediments and is similar to an Andean-type magmatic arc-back-arc system on the Indian northern margin in the Columbia

Supercontinent set-up (Rogers and Santosh, 2002; Hou *et al*., 2008). Break-up of the Columbian supercontinent separated the Indian craton with its northern margin becoming passive as it drifted away and reassembled to form the Rodinia Supercontinent during the Neoproterozoic with the loss of major part of this magmatic arc.

Rodinia (Neoproterozoic) and Magmatism: During the breakup of Rodinia, magmatic bodies with 'within plate granite' (WPG) field characters have played an important role in Greater India domain and indicate the presence of a passive northern margin during the Neoproterozoic (Singh *et al*., 2002). Such ~0.90-0.80 Ga isolated granite intrusives are now recognized at many localities, including Dalhousie, Dhauladhar, Mandi and Chor (see Mukherjee *et al*., 2019; Jain *et al*., 2020 for more details; Dhiman and Singh, 2020). Tectonic setting of the Neoproterozoic magmatism within the GHS is possibly linked either to intracontinental rifting due to superplume beneath the Rodinia Supercontinent or crustal anataxis during syn- to post-collisional crustal thickening during the Neoproterozoic.

Gondwana Amalgamation and Cambro-Ordovician Granitoids: The Cambro-Ordovician magmatism in the Himalaya is widely manifested as two-mica granite pluton emplacements within the LH Granitic Belt, the HHC Belt and near the South Tibetan Detachment System (STDS) because of the Kurgiakh Orogeny (Srikantia, 1977). Numerous such granite bodies occur as discontinuous gneissic culminations/ domes within the THS north of the STDS as independent plutons like the Kaghan, Nyimaling, Tso Morari, Rupshu, Jispa, Kade, Kokhsar, to name a few.

Pangaea Supercontinent and Permian Magmatism: The Himalayan Orogen is also affected by widespread mafic volcanism and Permian plutons which appear to be controlled by opening of the Neo-Tethyan Ocean between ~300 and 250 Ma in the Pangaea Supercontinent (Zhao *et al*., 2018, and references therein). Some such granitoids in the NW Himalaya are Maklad granite, Parkachic and Sanko in Zanskar, and Yunam Granite in Upper Lahaul. The Early Permian 290 Ma Panjal Traps (Phe Volcanics and the Abor Volcanics in Eastern Himalaya) are the largest contiguous outcroppings of volcanics (basaltic, andesitic and silicic) within the Himalaya that are associated with the Late Palaeozoic Gondwana break-up.

Magmatism during Himalayan Orogenesis: Two stages of granitoid emplacements are associated with the Himalayan orogenesis: (i) subduction of the Neo-Tethyan oceanic crust during Cretaceous, followed by (ii) granitoids originated during the Cenozoic India-Asia convergence (Jain, 2014). As a result of the northward subduction, the Dras Volcanic arc has formed with ages ranging from 105 to 65 Ma. At the same time, the Kohistan arc also developed with calc-alkaline batholith emplacement between 120-85 Ma and development of Trans-Himalayan Batholith representing Andean-type magmatism due to melting of north-dipping Tethyan oceanic crust (Schärer *et al*., 1984). Both the batholiths have developed below an island arc, located along the southern margin of Eurasia. The age of Trans-Himalayan bodies pre-date collision and represent subduction-related magmatism ranging from 102-54 Ma.

This phase was followed by collision-related magmatism of smaller volume forming discontinuous small pluton known as the Higher Himalayan Leucogranites (HHL). These intrude closer to the STDS. These syn-to post-Himalayan leucogranites have attained attention due to their association with collision (Weinberg, 2016; Singh, 2020, and references therein). The Himalayan leucogranites are interpreted to have resulted either from (i) crustal anatectic melting due to fluid migration during intracontinental thrusting along the MCT, (ii) decompressional dehydration melting due to slip along the STDS controlling the emplacement of leucogranite plutons, or (iii) vapor-absent muscovite dehydration melting of metamorphic rocks due to shear heating along continuous active decollement). However, irrespective of the mechanism of its generation, leucogranite belt was emplaced after 24 Ma. U-Th-Pb ages of these HHL range between ~ 24 Ma to 12 Ma and become younger eastwards (Carosi *et al*., 2013, and references therein). In the NW Himalaya (Bhagirathi valley), migmatite in sillimanite-muscovite zone exhibits flowage and in situ melt generation of tourmaline-bearing leucogranite where zircon reveals protracted episodic growth from 46 to 20 Ma with peak metamorphism (Singh, 2019).

Exhumation

The Himalayan Orogen has witnessed variable exhumation due to tectonics and/or coupled monsoon-controlled erosion (Jain *et al*., 2000, 2009; Patel *et al*., 2009; Clift, 2017; Thiede *et al*., 2017; Stubner *et al*., 2018; Patel and ManMohan, 2020). Exhumation patterns from the monsoon-affected NW-Himalaya are compared with monsoon-deficient adjoining regions of the Trans-Himalayan (LB) and the Tso Morari Crystallines (TMC) to provide us inputs regarding role of precipitation and erosion in controlling exhumation.

In the NW Himalaya, the HHC and underlying LH sequences experienced differential exhumation rates during Miocene-Quaternary, and are modelled in tectonic framework of fast exhuming structures, coupled with rapid erosion (Jain *et al*., 2000; Thiede *et al*., 2017; Gavillot *et al*., 2018; Stübner *et al*., 2018). Patel and ManMohan (2020, and references therein) relooked ~800 published 40Ar/39Ar (white mica/biotite), zircon fission track (ZFT), zircon U-Th/He (ZHe), apatite fission track (AFT), and apatite U-Th/He (AHe) from the HHC and the LH Crystalline klippen/nappes from both the NW– and NE Himalaya to observe distinct variations in exhumation patterns, which are controlled by domes/windows, thrusts and extensional faults.

In contrast, the Tso Morari Crystalline (TMC) Belt, lacking monsoonal precipation, underwent a record exhumation till ~48-45 Ma from ~120 to 35 km through HP and amphibolite facies (de Sigoyer *et al*., 2000). Greenschist facies minerals grew at ~8 km between 45 ± 2 and 34 ± 2 Ma. Thus, the TMC witnessed record maximum exhumation rate of 17 mm/yr during ~53 and 50 Ma and subsequent deceleration to 12mm/yr from 50 to 47 Ma, 0.3 mm/yr till 34 ± 2 Ma (ZFT) and further lower rate when it attained ~120^{o}C at 24 ± 2 Ma (AFT) (Guillot *et al*., 2008). Further, the Trans-Himalayan Ladakh Batholith is ideally located for determining the exhumation patterns in dry highlands. It witnessed an Early-Middle Eocene very fast exhumation of 3.5 ± 0.9 mm/yr between 50-45 and 48-45 Ma, and then to 1.2 ± 0.4 mm/yr until 43-42 Ma (ZFT age) (Kumar *et al*., 2018). Exhumation rates finally decreased during Oligocene to a minimum of ~0.1 mm/a before a mild Late Miocene-Holocene acceleration.

Large-scale Himalayan Tectonics

Various models have been proposed for large-scale tectonics of the Himalaya.

Large-scale underthrusting of India: Prior to the advent of Plate Tectonics, Argand (1924) illustrated underthrusting of India beneath Asia and its “collision” with the Asian continent beneath Kun-Lun Mountains, and “not” beneath the Himalaya.

Continent-continent Collision: As a follow-up of Plate Tectonics, Dewey and Bird (1970) formulated concepts of collision-type mountain belts for the Alpine-Himalaya orogen. As India approached and collided with the Asian continent, part of this segment obducted as uppermost ophiolite nappes, which rode southwards over the deformed metamorphosed Indian continent and its platform sediments. Buoyancy caused the uplift of the Himalaya, its extensive erosion, and deposition of molassic sediments into the frontal HFB

Intra-crustal Shortening of Indian Subcontinent by Underthrusting: Geological settings of various Himalayan and Trans-Himalayan tectonic units made Powell and Conaghan (1973, 1975) to visualize that the Himalaya was produced by large-scale underthrusting of the Gondwanian Indian continent beneath Asia along subhorizontal crustal fracture with its suturing with Asia along the ITSZ and not directly by continent-continent collision.

Subducting Indian Continental Crust: This model visualized buoyant rise of detached subducted continental crustal slice to upper levels by compression and buoyancy along the STDS, possibly due to slab detachment at depth and flowing in a channel as internally soft low-viscosity material (Chemenda *et al*., 2000).

Himalayan Wedge-extrusion Model: The MCT and non-parallel north-dipping normal fault system caused southward extrusion of high-grade Himalayan metamorphic tapered core (Burchfiel and Royden, 1985). Gravitational collapse of over-thickened continental crust was proposed as a mechanism for development of the STDS and synchronous movements along the MCT.

Channel Flow Model: Southward extrusion of high-grade metamorphic rocks and granitic intrusions within the GHS was caused within a low viscosity mid-crustal channel, bounded by the MCT and STDS near the surface (Nelson *et al*., 1996; Beaumont *et al*., 2001). A pressure gradient between Tibet and India caused such movements, enhanced by focused precipitation, erosion and exhumation along southern margin of the Great Himalaya.

Ductile Shear Model: An inverted metamorphism at structurally higher levels across the GHS was explained by ductile shearing of the ICL within a ~20 km thick non-coaxial intra-continental ductile shear zone where millimetre-spaced C-foliation sigmoidally bent and transposed S-foliation on small-scale towards southwest (Jain and Manickavasagam, 1993). This model postulated that metamorphic isograd surfaces also underwent small-scale displacements by C-foliation with a cumulative displacement of around 80-120 km. Migmatite and leucogranite were produced during decompressional partial melting in sillimanite-muscovite and sillimanite-K-feldspar isograds in the upper parts.

Southward-propagating 'in-sequence' Ductile Thrusting: 'In-sequence' ductile thrusting produced tectono-metamorphic discontinuities/ductile shear zones since ~40 Ma, with top-to-the-S/SW sense of shear (Carosi *et al*., 2018), and progressively exhumed the GHS from uppermost to the lowermost parts, with intervening Higher Himalayan Discontinuity (HHD). In-sequence shear model brought more metamorphosed tectonic slices from deeper to uppermost structural levels; lowermost unit was juxtaposed at 17-13 Ma along the MCT.

Timing of India-Asia Convergence

Paleomagnetic and other evidences indicated that estimated timing of closure of the Neo-Tethys along the ITSZ and the India-Asia impingement/collision varied between 65 and 35 Ma (Leech *et al*., 2005; Bouilhol *et al*., 2013; Jain, 2014, 2017). Paleomagnetic anomalies in the Indian Ocean point out a slow-down of the Indian Plate around 55 ± 1 Ma due to its impingement (Copley *et al*., 2010, references therein). Paleolatitude evidences reveal an India-Asia suturing of the Himalayan Tethyan succession with Lhasa terrane at 46 ± 8 Ma, when these terranes started overlapping at 22.8 ± 4.2ºN paleolatitude (Dupont-Nivetet *et al*., 2010). Stratigraphically, maximum age of India-Asia collision in the ITSZ (Ladakh) was deciphered at 56.5-54.9, and 50.5 Ma from termination of continuous marine sedimentation, and minimum age of closure of the Tethys, respectively (Garzanti and van Haver, 1988). The ICL travelled to the ITSZ trench at 58 Ma (Garzanti *et al*., 1987). Renewed clastic supply within the Zanskar sequence revealed closure of the Tethys at ~56 Ma (Sciunnach and Garzanti, 2012), though first arrival of Asian-derived detritus in uppermost Tethyan sediments indicated this convergence at ~50 Ma (Najman *et al*., 2010). This timing can, additionally, be resolved by comparing ages of continental subduction (UHP metamorphics–TMC), with oceanic subduction (Ladakh Batholith–LB) across the ITSZ. In the TMC, distinct metamorphic events are decipherable from peak UHP, HP eclogite and amphibolites facies at 53.1 ± 0.7, 50.0 ± 0.6 and 47.5 ± 0.5 Ma, respectively. Multiple pulsative crystallization and emplacement within the LB are recorded between ~100 and 41 Ma, with its peak crystallization at 57.9 ± 0.3 Ma (Jain, 2014). Thus, it is evident that two contrasting deep crustal processes took place ~58 Ma across the ITSZ, leading to the India-Asia contact.

Geological Evolution of the Himalaya

Once the Tethyan oceanic lithosphere subducted and closed the Tethyan Ocean, subsequent convergence of the Indian and Asian Plates caused continental lithospheric subduction through the following stages (cf. Jain, 2014, 2017).

First Stage of Continental Subduction and Rise of the Himalaya in Tso Morari: First stage of continental lithospheric subduction in the Himalaya is recorded along leading edge of the Indian Plate in Tso Morari, where it subducted down to a depth of ~120 km to produce carbonate-coesite-bearing UHP eclogite at >39 kb, >750ºC and 53.1 ± 0.7 Ma, and subsequent retrogression to HP and amphibolite facies ~50.0 and ~48 Ma, respectively (Guillot *et al*., 1997; Leech *et al*., 2005). 40Ar/39Ar mica and ZFT ages caused late stage exhumation and shallow crustal stabilization between 45.0 and 34 ± 2 Ma (ZFT) (Schlup *et al*., 2003). Initially, this exhumation was very fast at a rate of ca. 1.7 cm/yr between 53 and 50 Ma and 1.2 cm/yr between 50 and 47 Ma and then slowed down to ca. 0.3 cm/yr till 35 Ma (Guillot *et al*., 2008).

The Himalaya, therefore, first witnessed its rise and emergence in the Tso Morari region between 53 and 50 Ma when continental crust was exhumed from a depth of ~120 km. This terrane uplifted very fast to near-surface and eroded off to shed detritus into the HFB and the ITSZ basin (Jain *et al*., 2009). This subducting lithospheric slab did not melt till its decompression around 50 Ma after the HP metamorphism. Very steep geometry of the Indian lithosphere and its melting along the ITSZ, thus, explain sharp isotopic changes in the overlying LB along its southern margin.

Second Stage of Continental Subduction–the HHC: Folded HMB slab underwent peak Late Eocene pre-MCT regional Barrovian metamorphism in upper amphibolite facies at 650-700°C, 8-9 kb and around 45-35 Ma (Hodges, 2000). It is likely that the ICL witnessed the development of the proto-MCT at around 45 Ma and underwent shallow continental subduction to a depth of 35 to 25 km after subduction in the Tso Morari region; both the regions witnessed almost simultaneous amphibolite metamorphism at nearly the same time. $^{40}Ar/^{39}Ar$/K-Ar hornblende and muscovite ages gave its cooling through 500 ± 50°C and 350 ± 50°C between 40 and 30 Ma (Sorkhabi *et al*., 1999).

Third Stage of Continental Subduction within the HHC: The Miocene ~25 Ma metamorphism within the HHC belt, and its partial melting led to leucogranite generation between 25-15 Ma, and occasionally during the Eocene-Oligocene (33-23 Ma) (Carosi *et al*., 2018). These melts appear to have evolved in a southward extruding Himalayan orogenic channel, bounded by the MCT and STDS (Jain *et al*., 2005; Grujic, 2006). Subsequent Miocene–Pleistocene exhumation is widespread in the HHC, followed by its extensive erosion to produce detritus for the Cenozoic Himalayan foreland and Indo-Gangetic–Assam/Bengal basins (Hodges, 2000; Yin, 2006); these patterns are either controlled by tectonics, concomitant erosion or a combination of two processes (Jain *et al*., 2000).

Present-day Configuration

During the past two decades, configuration of the Indian Plate beneath the Himalaya and northern regions has been imaged by magnetotelluric profiling, seismic tomography and focal plane mechanism of recent earthquakes. Magnetotelluric (MT) profiles from the NW-Himalaya image the present-day geometry of the Indian Plate (IP) as a northerly gently dipping subducting slab with about 7-km thick veneer of Miocene-Recent conducting sediments (<50 Wm) within the Indo-Gangetic Plains (IGP) and Sub-Himalaya. Their contacts represent fluid-saturated fractured zone of the MHT along which the IP subducts beneath the Himalaya with an intervening ramp near the Higher Himalaya (Miglani *et al*., 2014; Rawat *et al*., 2014). This mid-crustal conductor of low resistivity zone may also indicate partial melt in extreme northeast between Tso Morari and beyond, where its subhorizontal geometry extends beneath high resistive LB and Karakoram (Arora *et al*., 2007).

Seismic tomography, reflection profiles, earthquakes and their fault-plane solutions from the Himalayan arc and Tibet provide constraints present-day configuration of the Indian Plate. In NW-Himalaya, the Moho runs almost parallel below low resistivity layer and defines geometry of the subducting ICL even beyond Karakoram fault. Majority of earthquakes are located within a narrow belt between north dipping MBT and the MCT and are essentially controlled by a mid-crustal ramp within the MHT along which the Indian Plate underthrusts southern Tibet at about 10o (Nelson *et al*., 1996). This surface dips at ~15° from about 10 to 20-km depth within the Himalaya and controls focal mechanisms not only of shallow ($\lesssim$30°) earthquakes but also the great Himalayan earthquakes of M>8 (Ni and Barazangi, 1984). Outer seismic mid-crustal ramp extends into an aseismic 30-40 km deep seismic reflector, imaged in the INDEPTH experiment further north (Zhao *et al*., 1993).

Subducted Indian lower crust does not stop at the ITSZ/IYS but underthrusts and extends northwards beneath the partially molten Asian crust till Bangong-Nujiang Suture (BNS) where both the Indian and Asian lithospheric mantles subduct downwards due to flow (Nábelek *et al*., 2009; Liang *et al*., 2012). Recent deep seismic reflection profiles by Guo *et al*. (2017) across ITSZ further strengthen a crustal-scale outline of the subducting Indian crust.

Thus, critical geological and geophysical evidences from the Himalaya and adjoining mountains lead us to postulate that the Indian continental lithosphere (ICL) subducted and imbricated sequentially in geological past since 58 Ma. The overriding sequences were scrapped, thrust southward along the MCT-MBT systems, and sequentially deformed as crustal wedges in the rising Himalaya whose erosion caused deposition into the frontal Himalayan Foreland basin and the Indo-Gangetic Plains because of tectonics and monsoonal precipitation since Miocene. The Indian and Asian Plates interacted and 'collided' only in the Bangong-Nujiang Suture (BNS), and not beneath the Himalaya.

Trans-Himalayan and Karakoram Ranges

The Himalayan Mountains are bordered on the northwest by the Ladakh, Karakoram, Pamir and the Hindu Kush ranges, while the Tibetan Plateau controls its overall shape in the central part. A 50–60 km wide tectonic valley of the Indus–Tsangpo Suture Zone separates these geographical units throughout the Himalayan ranges from extreme west to the east. These Trans-Himalayan and Karakoram Mountains are drained by the Indus, Shyok, Nubra Rivers and their tributaries in the west, and Tsangpo-Brahmaputra drainage system in the east.

Geology and Tectonics

Vast Tethyan Ocean separated the northern parts of the Indian Plate from the southern Asian Plate (Stampfli and Borel, 2002), and closed along the Shyok Suture Zone (SSZ) and the Indus–Tsangpo Suture Zones (ITSZ) in the south (Searle *et al*., 1987; Rolland *et al*., 2000; Jain and Singh, 2009). These sutures demarcate contact between these plates and delimit the Himalaya. These preserve evidences of (i) initial Late Mesozoic subduction of the Neo–Tethys oceanic lithosphere along the SSZ during the Early Cretaceous-Lower Eocene with intervening intra-oceanic Shyok–Dras Volcanic Arc, (ii) emplacement of the younger calc–alkaline Trans–Himalayan plutons, and (iii) final closure of the Neo–Tethys along the ITSZ (Honegger *et al*., 1982; Searle *et al*., 1987; Rolland *et al*., 2000, Yin, 2006).

Indus–Tsangpo Suture Zone (ITSZ)

Nearly continuous ITSZ signifies the disappearance of the Neo-Tethys oceanic lithosphere by northward subduction of the Indian Plate during Aptian–Albian (120-110 Ma) for more than 2000 km (Maheo *et al*., 2004), indicated by the presence of the ophiolite complexes and associated sediments along its entire length. Two main litho-tectonic associations characterize this zone: (i) southward-obducted Spongtang Ophiolite Nappes, and (ii) steeply dipping main suture zone; the latter contains (a) the Dras Volcanics defining the Upper Jurassic to Upper Cretaceous volcanic island arc, (b) dismembered ophiolite bodies and mélanges such as Nidar ophiolite, and (c) the flysch and molassic fluvial clastic sediments (Gansser, 1964; Honegger *et al*., 1982; Thakur, 1993).

(i) **Spongtang Ophiolite Nappe:** The Kiogarh ophiolite nappe in Uttarakhand, the Spongtang Nappe/Shilakong ophiolite in Zanskar, and the Karzok ophiolite of the Tso Morari are parts of the highest ophiolite nappe, where the oceanic lithosphere is obducted onto the Tethyan Himalayan Sequence (THS) (Reuber, 1986; Srikantia and Razdan, 1981). Gently dipping thrusts bind the Spongtang ophiolite nappe in a NW-SE trending and doubly plunging synform. It is made up of Photang sub-nappe in lower parts and the Spong sub-nappe in upper parts; all having thrust contacts. The lower unit contains basalt, andesite, pillow lavas, agglomerates, tuffaceous sediments, chert, limestone, arenite and serpentinite slivers, while the upper sub-nappe contains mainly ultramafic bodies (Srikantia and Razdan, 1981).

Reuber (1986) opined that it has MORB affinities and originated at mid-oceanic ridge. This crust is thrust over a volcano-sedimentary sequence, which originated in an intra-oceanic supra-subduction zone (Corfield *et al*., 2001). U-Pb zircon dating of plagiogranite indicated an oceanic accretion at 177 Ma (Pedersen *et al*., 2001). Catlos *et al*. (2018) modelled origin of the Spongtang ophiolite along mid-ocean spreading center having spreading rate >2cm/y in the Neo-Tethyan Ocean from Late Triassic to Jurassic, while ridge had increasing influence of subduction by Early Cretaceous; age of latest obduction occurred between 64.3 ± 0.8 Ma to 42.4 ± 0.5 Ma.

(ii) **Indus Tsangpo Suture Zone (ITSZ):** Almost continuous NW-SE trending ITSZ belt is comprised of the following litho-tectonic units (see Figs. 6.2, 6.7 in Thakur, 1993):

(a) **Dras Volcanics:** Two ophiolite belts within the ITSZ are separated by wide exposure of the Dras Volcanics, containing volcanics, pyroclastics, volcaniclastic sediments and radiolarian chert for nearly 400 km. Along the southern contact, the sequence is obliquely thrust over the Kargil molasse as well as the Shergol ophiolite mélange, while the Ladakh Batholith makes the substratum for this formation with an intrusive contact in the north. The southern contact is also tectonic with the overthrust Lamayuru Formation, the ophiolite belt and the Zanskar Supergroup sediments. Reuber (1989) recognized two distinct lithological associations within the Dras sequence: (a) Dras-I containing basalt, basaltic-andesite, black slate and Orbitolina-bearing limestone of Albian-Cenomanian age, and (b) Dras-II of tuffites, ash beds, and breccia.

These rocks overlie ultramafics (harzburgite, dunite, wehrlite, pyroxenite) of the ocean floor sequence. Some dunites contain elongated chromite grains, indicating plastic deformation. Uppermost parts of ophiolite are characterized by bulbous pillow basalt, related to the subduction of the Indian Plate beneath the oceanic margin of the Asian Plate. It is developed as an island arc, characterized by calc-alkaline volcanic suites on oceanic crust (Dietrich *et al*., 1983; Reuber, 1989). It is intruded by granodiorite plutons, dated between 103 and 70 Ma (Honegger *et al*., 1982). South of the Dras arc, volcanics are replaced by the Nindam flysch, corresponding to the fore-arc area, having thick volcano-sedimentary rocks (Clift *et al*., 2000).

(b) **Nidar Ophiolite:** Many ophiolite bodies have been observed within the ITSZ, but the most complete, undeformed and non-imbricated body is exposed at Nidar in SE parts exhibiting upper mantle to supra-ophiolitic sediments of the intra-oceanic volcanic arc affinity (Ahmad *et al*., 2008; Maheo *et al*., 2004). It contains a basal ultramafic unit of chromite-bearing harzburgite and spinel dunite, followed by cumulate gabbro with Sm-Nd WR-mineral age of 139.6 ± 32.2 Ma (initial $^{143}Nd/^{144}Nd$=0.512835± 0.000053, $\varepsilon Nd(t)$=+7.4) (Satoru *et al*., 2001; Ahmad *et al*., 2008), basalt and sheeted dyke complex, pillow lava, thin shale and chert, possessing Hauterinian to Aptian radiolaria (132 ± 2 to 127 ± 1.6 Ma–Early Cretaceous) age (Satoru *et al*., 2001). This belt yielded in situ octahedral diamonds, their graphite pseudomorphs, hydrocarbon (C-H) and hydrogen (H2) fluid inclusions in the UHP peridotitic minerals, indicating their sources from mantle transition zone or base of the upper mantle during upwelling beneath the Neo-Tethys Ocean spreading centre (Das *et al*., 2017).

(c) **Nindam Formation:** A volcano-sedimentary succession within the Shergol ophiolite belt as lateral facies of the Dras Volcanics (Frank *et al*., 1977) is called as the Nindam Formation (Bassoullet *et al*., 1982). It consists of ~3000 m thick alternating sandstone, siltstone and shale with bedded tuffs (Thakur and Misra, 1984). These were derived from a mafic to intermediate volcanic terrain like the Dras during Cretaceous and deposited as distal to proximal turbidites and beds of channel origin (Brookfield and Andrew-Speed, 1984).

(d) **Lamayuru Unit:** Between the Zanskar Supergroup (THS) and Shergol ophiolites, ~3000 m thick Lamayuru and Karamba units were deposited between Permian to Early Cretaceous on the Indian continental slope (Bassoullet *et al*., 1981). These are comprised of shale, siltstone and graded sandstone, and incorporate large ‘exotic’ limestone block as remnants of the Triassic to Upper Cretaceous north-facing Indian passive margin, while ophiolitic mélanges were accreted at trench within the Tethys Ocean to the north, only during latest Cretaceous.

(e) **Indus Group:** Lying between the Ladakh Batholith and the Shergol/Nidar ophiolite/Tso Morari Dome in the south, ~5 km-thick Indus Group trends almost NW-SE within the ITSZ, containing mainly of rhythmically alternating conglomerate, sandstone, siltstone and shale. Brookfield and Andrew-Speed (1984) divided this unit into the Khalsi flysch and the Miru unit, with limestone intercalations (Khalsi limestone), which yielded Aptian to lower Albian fauna; the flysch represents a deep-sea fan to basin plain deposit.

Within the ITS zone the Indus Group sediments represent the final phase of deposition in an actively subsiding Indus Basin, which represents a narrow embayment occupied by a relict shallow tidal sea with prominent energy (Singh *et al*., 2015). It received sediments both from the Ladakh Batholith and Karakoram block in the north and the Indian continental margin and Suture zone deposits in the south by different drainage systems.

(f) **Kargil Formation:** A linear discontinuous sedimentary succession of the Kargil Formation overlies non-conformably the Ladakh Batholith (Brookfield and Andrew-Speed, 1984). Approximately 1700 m thick sequence is divided into the Kargil (conglomerate, green sandstone and purple mudstone), Tharumsa (multi-storey grey sandstone and mudstone) and Pashkyum formations (purple and green sandstone and mudstone) in the ascending order. The sequence was deposited during Oligocene to Pliocene by alluvial fans to braided streams between rising units of the ITSZ and the Ladakh Batholith.

Ladakh Batholith

The Trans Himalayan batholiths, located immediately to the north of the ITSZ for almost entire length of the Himalaya, represent an Andean-type calc-alkaline magmatism due to northward subduction of the Neo-Tethyan oceanic crust during early Cretaceous Lower Eocene (Honegger *et al*., 1982; Schärer *et al*., 1984; Jain *et al*., 2002). This belt is almost continuous as the Kohistan–Deosai Batholith in Pakistan to Ladakh Batholith in India, Kailash tonalite and Gangdese pluton in southern Tibet and the Lohit Batholith in Arunachal Himalaya. Regionally, the ITSZ demarcates its southern margin, while the Main Karakoram Thrust (MKT)/Shyok Suture Zone (SSZ) delimits its northern boundary in Pakistan and India (Rolland *et al*., 2000; Jain *et al*., 2008; Jain and Singh, 2009).

The Ladakh Batholith is a NW-SE trending 600 km long and 30-80 km wide magmatic belt with an exposed thickness of ~3 km (Honegger *et al*., 1982). It consists of gabbro, diorite, granodiorite and granite, and intrudes the Dras volcanics. Northern slopes of this batholith are exposed in contact with the Khardung and Shyok Volcanics along the Shyok Valley. The batholith belongs to the calc-alkaline series, like the Kailash and Lhasa Trans-Himalayan batholiths.

Along the Indus River, north dipping molassic sedimentary sequences partially cover its southern margin and are the eroded material from this uplifted magmatic arc with subordinate components from the passive Indian margin sedimentary succession (Sinclair and Jaffey, 2001). Locally, andesitic to rhyolite volcanics along with volcaniclastic sediments nonconformably overlie the Ladakh Batholith around Khardung near its northern margin with the SSZ (Weinberg and Dunlap, 2000).

Age of Crystallization: Pulsative crystallization and emplacement of the LB occurred in multiple stages at ~100, 72, 67, 58, 51, 41 Ma and younger times, possibly by melting of the earlier phases. The oldest Early Cretaceous magmatism within the LB was around Kargil in its western parts (Honegger *et al*., 1982). Weinberg and Dunlap (2000) obtained SHRIMP U–Pb zircon ages of 58.1 ± 1.6 Ma from its core and relatively younger age of 49.8 ± 0.8 Ma from the rims near Leh and interpreted these as crystallization of the source igneous rocks and a later magmatic phase, respectively. Zircon crystallization ages are 58.4 ± 1.0 and 60.1 ± 0.9 Ma from the southern and northern margins of this batholith, respectively (Singh *et al*., 2007), while these are ~68–66 Ma in extreme north at Hunder along the Shyok valley (Weinberg *et al*., 2000; Upadhyay *et al*., 2008; White *et al*., 2011; Bouilhol *et al*., 2013). Some younger components within the Ladakh Batholith date between 53.4 ± 1.8 and 45.27 ± 0.56 Ma along the southern margin. Relatively low initial 87Sr/86Sr (0.704 ± 0.001) and high 143Nd/144Nd ratios (0.5126) support the derivation of its magma from partial melting of subducting oceanic slab (Honegger *et al*., 1982).

A very detailed SHRIMP U-Pb zircon dating of central segment of the LB revealed that the axis of the batholith has multiple zircon growths between 58 ± 0.8, 56.6 ± 0.9 and 54.8 ± 1.9 Ma between Khardung La and Chang La (Weinberg *et al*., 2000; Upadhyay *et al*., 2008; White *et al*., 2011; Bouilhol *et al*., 2013), followed by multiple rim growths during 62.2 and 48.8 Ma, and another phase at around 15.6 ± 1.0 Ma. Further east, the batholith at Chumathang has zircons of 59.2 ± 0.7 Ma with rim growth at 50.4 ± 2.7, while younger intrusions date around 48.2 ± 0.8 Ma (St-Onge *et al*., 2010; White *et al*., 2011).

In immediate contact with the ITSZ, southernmost parts of the Kohistan-Ladakh-Arc (KLA) between Deosai and Ladakh have yielded in situ U-Pb zircon ages between 102.1 ± 1.2 to 50.3 ± 1.2 Ma (1σ) with homogeneous zircon age population, average 9.4 ± 0.7 εHf(i), weighted mean 2.6 ± 0.7 εNd(i) and 0.703744 to 0.704719 ^{87}Sr/^{86} Sr(i) (Bouilhol *et al*., 2013). In contrast, samples from southern margin are younger to 50.4 ± 1.6 Ma (youngest being 29.6 ± 0.8 in Ladakh), and yield εHf(i) as low as –15, εNd(i) between –9.7 and –3.6 and 87Sr/86 Sr(i) ranging between 0.705862 and 0.713170 (Bouilhol *et al*., 2013). These ages along with a change in isotopic characters were interpreted due to a pre-50.0 Ma intra-Tethyan oceanic arc, where a mixture of components was derived from Enriched-Depleted MORB Mantle (E–DMM) and subducted oceanic lithosphere. The post-50 Ma samples exhibit strong isotopic variability and involvement of additional enriched components, e.g. isotopically evolved crust. A shift in isotopic compositions of the KLA rocks at 50.2 ± 1.5 Ma reflects the India-KLA collision, according to these authors.

Sixty-five published ages from the Trans-Himalayan Ladakh indicate a peak of 57.9 ± 0.3 Ma from the LB with minor peaks at 50.8 and 41.3 Ma (Jain, 2014). U-Pb SHRIMP-II zircon dating from two widely-located samples along the Kharu-Chang La section provide undisputed evidences for almost simultaneous emplacement and crystallization of diorite and granodiorite, as the former gave mean 206Pb/238U age of 58.4 ± 1.0 Ma, and the granodiorite was dated as 60.1 ± 0.9 Ma (Singh *et al*., 2007).

Exhumation Patterns: After the crystallization of the Ladakh Batholith at ~58.0 Ma, it underwent normal magmatic cooling till 45-46 Ma (Rb-Sr and K-Ar biotite cooling ages) (Kumar *et al*., 2017). The batholith witnessed very fast Early–Middle Eocene exhumation which peaked at 3.5 ± 0.9 mm/a between 50–45 Ma (40Ar/39Ar hornblende ages) and 48–45 Ma (Rb–Sr biotite ages) because of the India–Asia convergence, followed by deceleration at a rate of 1.2 ± 0.4 mm/a until 43–42 Ma (zircon FT ages), like the Deosai batholith in the west. Exhumation rates finally decreased during Oligocene to ~0.1 mm/a before a mild late Miocene–Holocene acceleration.

Shyok Suture Zone (SSZ)

In Late Cretaceous to Eocene the Ladakh Batholith intruded the interior of the Dras Island Arc, which is demarcated by another suture zone in the northeast—the Shyok Suture Zone (SSZ) (Weinberg *et al*., 2000). This suture zone was first recognized by Gansser (1977), and contains dismembered ultramafics, gabbro and basalt bodies and sediments with tectonic mélanges of Cretaceous age (Matte *et al*., 1996). It extends beyond Nanga Parbat spur as the Main Karakoram Thrust-MKT (Rolland *et al*., 2000 and references therein), and terminates against the ITSZ in southwestern Tibet.

The SSZ reveals tectonic stacking of the Cretaceous volcano-sedimentary sequences from different volcanic arc and back-arc environments (Rolland *et al*., 2000). In the western part (Skardu area), it can be subdivided into (a) northern group of olistolith basaltic blocks and tuffs, where basalts are produced in back-arc settings, and (b) southern group of predominantly of andesites, having island-arc tholeiite (IAT) to calc-alkaline affinities.

(a) **Shyok–Saltoro–Nubra Sector:** On either side of the Saltoro Range, the SSZ exposes the Khalsar Formation, the Shyok Volcanics, the Hundri Formation, the Saltoro Volcanics, molasses and ophiolites, and the Nubra Formation with tectonic contacts (Thakur, 1993). Near the SSZ, acidic Khardung Volcanics overlying the Ladakh Batholith yielded U-Pb zircon ages between 67.4 ± 1.1 and 60.5 ± 1.3 Ma, thus limiting age of emplacement of batholith as Late Cretaceous–Paleogene (Dunlap and Wysoczanski, 2002). The Khalsar Formation contains calcareous phyllite, chlorite- mica schist with limestone and quartzite, and is tectonically separated from the underlying Khardung Volcanics by the Khalsar Thrust (Thakur, 1993). It is overlain by basalt and andesite of the Shyok Volcanics between Diskit, Hunder and further west along the Shyok River.

Along the southern slopes of the Saltoro Range between Y-junction of the Shyok and Nubra Valleys, a succession of slate, phyllite, limestone, calc schist, marls and chlorite schist is thrust above the Shyok Volcanics, and is called as the Saltoro Flysch/Hundri Formation/ Diskit Formation/Saltoro Formation of

Upper Cretaceous–Lower Eocene age (Thakur, 1993). Predominantly pelitic and low grade metamorphosed Hundri Formation consists of slate, phyllite, quartzite and limestone with Upper Cretaceous–Lower Eocene foraminifera fauna, and is thrust over by a 3000 m-thick coarse clastics of the Saltoro molasse, which is made up of conglomerate, sandstone and variegated shale. Contemporaneous volcanism is represented by a persistent andesite horizon within the molasse. This molasse sequence has youngest detrital zircons population of approximately 92 Ma and a dike of 85 Ma (U/Pb zircon ages) that cuts basal molasse outcrops, implying that deposition of the succession began in the Late Cretaceous (Borneman *et al*., 2015). This minimum age of the SSZ rules out any possibility of an Eocene collision between Kohistan-Ladakh and Asia.

In the Saltoro Hills, the Shyok Volcanics occupy the core of a major synform and is thrust southwards over the Saltoro Formation along a thrust. Large track of the Saltoro Range contains an ophiolite complex of low-grade metamorphosed ultramafics, cumulate to non-cumulate gabbros, diabase, pillow and massive basalt and chert as the Saltoro ophiolite of the North Saltoro belt, possibly as the repetition/correlation of more southerly Biagdang belt (Borneman *et al*., 2015).

Along the Nubra Valley, a succession of volcanics, shale, limestone, conglomerate, slate and imbricated thin serpentinite and peridotite bodies is exposed beneath the overthrust Karakoram Batholith Complex. This long and linear belt has been grouped as the Nubra ophiolitic mélange/Nubra Formation (cf., Thakur, 1993). The Tirit Granite (75–68 Ma) intrudes this sequence. Extensive outcrops of these volcanics are seen in upper reaches of the Nubra Valley, where these override the lithologies of the Karakoram Shear Zone mylonite along a southerly and moderately hading thrust.

(b) **Chang La Sector:** Thick imbricated ultramafics, gabbro, volcanics, conglomerate, sandstone and chert are exposed between Tsoltak and Darbuk, and represents the most accessible cross-section through this suture (Rolland *et al*., 2000). Clastics and limestone alternate with siliceous tuff, tuffaceous mudstone, pyroclastics and basalt between Chang La and Tangtse; limestone intercalations yielded early to middle Albian foraminifers like Mesorbitolina minuta (Douglass), Simplorbitolina sp., M. texana (Roemer) (Matsumaru *et al*., 2006). Ehiro et a1. (2007) discovered Callovian (late Middle Jurassic) ammonoids (Macrocephalites, Jeanneticeras) in the lower parts.

On the left valley slopes of the Tangtse River, diorite-granodiorite belt is intensely sheared within the Karakoram Shear Zone (KSZ) and extends northwestwards along the Shyok Valley, where the Tirit granodiorite intrudes the slate-phyllite sequence of the Karakoram Shear Zone around Tirit–Diskit–Khalsar junction of Nubra–Shyok Rivers.

(c) **Chusul–Dungti Sector:** The SSZ comprises Lower to Middle Cretaceous andesite, dacite and interbedded cherts with Orbitolina-bearing limestone of the Luzarmu Formation, nonconformably overlying the Ladakh Batholith between Chusul–Dungti–Fukche (Thakur and Misra, 1984). It is overlain by thickly bedded limestone, quartzite, sandstone, conglomerate and interbedded volcanics of the Diong Formation (=Hundri Formation). Ophiolite succession follows west of Koyul as a part of the SSZ, which is unconformably overlain by the Kole molassic sediments (Thakur, 1993).

Karakoram Mountains: Southern Margin of the Asian Plate

The Karakoram Fault (KF)/Karakoram Shear Zone (KSZ) demarcates the southern margin of the Asian Plate for nearly 700 km, though it is controversial in its location, sense of shearing, large-scale geometry, offset and timing of initiation of the movement. Largely located within wide valley of the Nubra–Shyok–Indus Rivers, and forming a prominent rectilinear topographic feature, the KF/KSZ is mapped as a dextral strike–slip fault running through these 1-3 km wide valleys (Searle, 1996; Jain and Singh, 2009). High exhumation rates of ~3.0 mm/yr and erosion of about 20 km thick crustal rocks are recorded between 18.0 and 11.3 Ma along this fault, which has partitioned an early transpressional strain associated with the Pangong zone from dominantly dextral strike-slip late phase motion since c. 11 Ma (Searle *et al*., 1998).

Estimates of contemporary and Holocene slip rates along the KF vary from ~30 mm/yr on the basis of offsets of geomorphic features (Matte *et al*., 1996), 10 ± 3 mm/yr since 23–24 Ma (Lacassin *et al*., 2004) to 3–4 mm/yr (Brown *et al*., 2002). Current rates appear to be even as low as 3.4 ± 5 mm/yr from the GPS measurements (Jade *et al*., 2004). Estimates of possible offsets along the KF/KSZ varies between 1000 km to as low as 40 km by changing differen tie points (see Jain and Singh, 2009).

Karakoram Tectonic Units-(a) Karakoram Shear Zone (KSZ): An imbricated and intensely mylonitized granite gneiss, volcanics, conglomerate, slate-phyllite-limestone intercalations, amphibolite and serpentinite intervene the Shyok Suture Zone and the frontal Asian Plate margin along the Nubra–Shyok Valleys for nearly 200 km to form the 1-5 km wide KSZ. In the extreme northwest, this narrow belt deforms the Karakoram Batholith Complex (KBC) around Kubed into augen mylonite, and extends further upstream along the Nubra Valley for another 30 km. Largely covered by alluvium and megafans of transverse tributaries, the KSZ contains massive amygdoidal basalt and andesite, sheared conglomerate, purple and grey-green slate and limestone intercalations. It is overthrust by highly sheared serpentinized ultramafic lenses within the KSZ; all dip gently to moderately between 20 to 50^{o} towards northeast beneath the overthrust KBC. Gently dipping dark pelites demarcate the front of this belt beneath the KBC from Sati to Shyok and further southeast along the Shyok Valley to the U-shape bend (see Van Buer *et al*., 2015).

Within the KSZ, undeformed and fractured Tirit granodiorite intrudes the slate–phyllite–volcanic sequence around Diskit–Khalsar–Tirit junction of the Nubra–Shyok Rivers and extends northwards on western face of the hill between Trisha and Murgi. Subalkaline to calc-alkaline Tirit body is an I-type suite of trondhjemite–tonalite–granodiorite–granite of volcanic arc affinity and solidified at subvolcanic level between 2.5 and 3.5 km thick overburden of the Shyok volcanics. Apophyses of this body are seen at the confluence of the Nubra and Shyok Rivers. Elsewhere, it is intruded by numerous dolerite dykes. U-Pb zircon ages from this granitoid have yielded two mean crystallization ages of an older 109.4 ± 1.1 Ma, and younger 67.32 ± 0.66 Ma phase (Kumar *et al*., 2017); these data bracket the plutonic emplacement within the KSZ around 68 Ma.

In the central Shyok–Tangtse–Chusul sector, the KSZ contains highly mylonitized amphibolite and granite gneiss, derived from granodiorite–diorite suite of the SSZ and granitoids of the KMB, respectively. Alternating ultramylonite and augen mylonite are best exposed along the Tangtse Valley between Darbuk and Tangtse and marked by intense S-C ductile shear fabric, and steeply plunging down-dip stretching mineral lineation. Various kinematic indicators exhibit strong dextral sense of ductile shearing towards southeast with temperature of mylonitization ranging between 300 and 500°C in the upper greenschist facies. (Roy *et al*., 2010). Kinematic vorticity (Wk) analysis along the KSZ indicate distinct pure and simple shear-dominant regimes during different stages of the evolution of the KSZ (Roy *et al*., 2016). Pure shear strain has affected southern edge of the Asian plate when it was initially juxtaposed against the Indian plate around 70 Ma, and changed to simple shear, possibly during its reactivation between 21 and 13 Ma.

The KSZ is intruded by mildly deformed Darbuk granite near confluence of Tangste and Iching Rivers with U-Pb zircon ages of 20.8 ± 0.4 Ma (Jain and Singh, 2008). Thin concordant to discordant sheets of highly deformed folded and undeformed 2-mica and hornblende–bearing granitoids intrude the Tangste mylonite and metamorphics. U–Pb SHRIMP analysis of zircons from these sheets indicate their older crystallization ages of 106.0 ± 2.3 Ma, 72.8 ± 0.9 Ma, 71.4 ± 0.6 Ma and 63.0 ± 0.8 Ma (Reichardt *et al*., 2010), with a younger phase between 22-15 Ma (Boutonnet *et al*., 2012). Still a younger leucogranite veins yielded zircons of 15.68 ± 0.52, 13.73 ± 0.28 Ma, and even 9 Ma (Horton and Leech, 2013).

(b) **Karakoram Batholith Complex (KBC):** Monotonous vertical cliffs of biotite–muscovite granite in upper parts of the Nubra Valley beyond Panamik constitute the main body of the KBC. To the southeast, it intrudes the Karakoram Metamorphic Complex (KMC) as concordant bodies. Two distinct granite suites of I– and S–type affinities are developed within the KBC (Ravikant, 2006): an inner belt of I–type granitoids of quartz monzonite, granodiorite and tonalite with initial $^{87}Sr/^{86}Sr$ values of 0.7061

± 0.0002, and a younger outer peraluminous 2-mica and garnet-bearing S-type granitoids has higher initial 87Sr/86Sr ratios 0.7244 ± 0.0001. The batholith is regionally thrust southwestwards along gently to moderately dipping KSZ along the Nubra and Shyok valleys. In the north it dips vertically at Kubed and then changes its dip to southwest and appears to connect with the Main Karakoram Thrust of the Hunza–Biafond region in the west. In the southeast along the Shyok valley, it dips gently towards northeast and continues for a very long distance until Tangste where it dips again steeply.

Karakoram Metamorphic Complex (KMC): In the Shyok–Pangong Mountain–Phobrang region, southern edge of the Asian Plate is extensively deformed and metamorphosed in two distinct metamorphic belts.

(a) **Tangtse Group:** Southern outer belt is exposed around the U-turn of the Shyok River and occupies the Pangong Mountains between Tangtse gorge and Chusul in immediate vicinity of the KSZ. It is characterized by high-grade sillimanite–K-feldspar-bearing garnetiferous schist and gneiss, amphibolite, hornblende granite gneiss, leucogranite and granulite facies metamorphics (Rolland and Pecher, 2001; Jain *et al*., 2003). Granulite facies metamorphism was attained at PT conditions of 5.5 kbar/800°C and subsequently retrogressed into amphibolite (4–5 kbar/700–750°C) and greenschist facies (3–4 kbar/350–400°C) at 32 Ma, 20–18 and 13.6 ± 0.9 Ma, and finally at 11 Ma, respectively (Rolland *et al*., 2009).

Mica schist and gneiss have undergone partial melting and prolific migmatization in the Pangong Injection Complex along the Tangtse gorge (Jain and Singh, 2009). Numerous dome-shaped and elongated lenses of these biotite-rich granitoids reveal passive melt injection in extensively migmatized rocks. In turn, metamorphics and granitoids are cut by numerous late phase pegmatite veins, which emanate from these bodies along the least-strained southern margin. However, associated calc–silicate and amphibolite in this zone remained unaffected by melting and migmatization. Likewise, leucogranite near Sati in the Tirit sector yielded SHRIMP U-Pb zircon age of 15.0 ± 0.4 Ma age from well-developed zircon rims, with cores ranging between 1437 and 84 Ma (Weinberg *et al*., 2000).

(b) **Pangong Group:** Further northeast in the inner belt of the KMC, the Pangong Group contains mainly slate, mica schist, greenschist/amphibolite and marble, calc–silicate and a band of mylonitized granite gneiss. Low-grade metamorphics with many marble bands are best developed between Phobrang and Pangong Tso and along its banks. Our reconnaissance observations confirm the presence of greenschist/amphibolite and calc-silicates. Metamorphism varies from biotite to sillimanite–muscovite grade within this belt (Jain and Singh, 2008).

Deccan Volcanic Province (DVP)

The DVP is one of the largest continental flood basalt (CFB) provinces of the world, occupying a contiguous exposed area of around 500,000 km^2. Its original extent is speculated to have been more than twice this, from which large parts were either eroded away or downfaulted below the Arabian Sea. Geochronological and paleomagnetic studies demonstrated the proximity of the Indian Plate over the Reunion hotspot (Courtillot *et al*., 1988; Duncan and Pyle, 1988), and the age of the Deccan volcanism straddling the Cretaceous–Paleogene (K-Pg) Boundary. The hot-spot related volcanism, in conjunction with the rifting of the Indian Plate from Madagascar and then Seychelles during the Cretaceous and the position of this province on the western margin of India justify the recognition of the DVP as a CFB-VRM (continental flood basalts on a volcanic rifted margin) province (Bryan and Ernst, 2008).

Flow Characters

Thickness: The DVP has a maximum exposed thickness of more than 1650 m along the Western Ghats Escarpment. Recent drilling in the Koyna-Warna seismic zone yielded an uninterrupted 1251 m thick stack of subhorizontal basaltic flows, demonstrating that the trap-basement contact occurs up to 400 m below msl in this area. The maximum uninterrupted thickness of the Deccan basalts adds up to more than 2000 m, which has also been endorsed by geophysical methods, with an estimated volume of ~2.8×10^5 km^3 for the present-day exposures of DVP, assuming thinning of the pile towards its fringes (Kale *et al.*, 2020). Recent high precision dating has confirmed that this volcanism (including its precursors and late events) lasted between around 70 Ma and 60 Ma, with the main continental flood basalts erupting in a shorter span of less than 5 Myr (Schoene *et al.*, 2019; Sprain *et al.*, 2019).

Volcanic Phases: The Deccan volcanism occurred in not less than 3 phases of tectonic activities (pre-volcanic, syn-volcanic and post-volcanic) (Kale *et al.*, 2019; Schoene *et al.*, 2019; Sprain *et al.*, 2019). The large pre-volcanic phase occurred during the Cretaceous prior to 68 Ma, linked to the passage of the Indian Plate over the Reunion hotspot. Intrusive and dykes (~80 Ma) are widely distributed throughout the Dharwar and Bastar Cratons, rifts of the Mahakoshal belt and Mundwara alkaline complex (Rajasthan). The alkaline plugs, cones and sheet-like intrusions in the Mesozoic sequences in Kutch have been the early signals of a plume-lithosphere interaction and magmatic underplating of the continental crust.

The syn-volcanic events cover the Maastrichtian-Danian eruption of voluminous basaltic flows, associated with dramatic terminal Cretaceous mass extinction. The post-volcanic Cenozoic tectonism appears to include emergence of the western coast of India with associated seafloor spreading and the Quaternary neotectonic activity.

Late Paleozoic–early Mesozoic breakup of Gondwanaland, leading to intracontinental rifts and deposition of fluvio-lacustrine Gondwana Supergroup sediments during Permian-Cretaceous eventually gave way to the breakup of East Gondwana. Linkage of this breakup with the Kerguelen hotspot (Bredow and Steinberge, 2018) is recorded in the 130–115 Ma old Rajmahal–Sylhet Traps. The separation between India and Madagascar between ~88 and ~83 Ma was followed by northward drift of the Indian Plate that resulted in its influence under the Reunion hotspot, opening of the southern Indian Ocean and associated oceanic volcanism (Bhattacharya and Yatheesh, 2015).

Distribution: The Deccan Trap lavas cover a variety of sequences: conceal the Archean gneisses in Malwa Plateau of the Aravalli-Bundelkhand Cratons, Proterozoic Vindhyan Supergroup and the Mahakoshal mobile belt where thin patchy occurrences of the Gondwana and Lameta sediments pop out of the Deccan cover. Patchy exposures of the Late Cretaceous Bagh Group and the Lameta Formation straddle the volcanics along the Narmada valley. At Amarkantak Plateau, Proterozoic mobile belt and Archean gneisses of the Bastar Craton are hidden under the Deccan lavas. Rock sequences of the Dharwar craton, Proterozoic Basins of Kaladgi and Bhima and the Mesozoic rocks of the Kutch and Saurashtra regions underlie the Deccan Basalt.

Late Cretaceous intertrappean sedimentary beds occur interbedded with lava flows in Kutch, Saurashtra, along the Narmada valley and the Amarkantak Plateau. A rich assemblage of Maastrichtian flora and fauna along with dinosaurian egg-clutches have been recorded (Kapur and Khosla, 2018, and references therein).

Flows Geometry: The Deccan Traps essentially display a sheet-like geometry with lateral spread being 50 times larger than the thickness. Individual lava flow ranges in thickness between 5–25 m, although exceptionally thick flows (~100 m) have also been recorded. Uninterrupted lateral continuity across several tens of km is best seen along escarpment faces of hill ranges. Individual lava flows are separated by 'interflow horizons', which contain volcaniclastic tuffaceous material that may not be baked/oxidized and are recognized as 'boles' while some of these are of pedogenic origin (Sayyed, 2014).

Morphological Types: In the DVP, basaltic lava flows display three internal layers, namely the crust, core and base (Kezsthelyi *et al.*, 1999) from top to bottom, respectively. Based on their internal and geometry, Deshmukh (1988) classified the Deccan basaltic flows as (i) compound with multiple units of pāhoehoe lobes, (ii) simple and (iii) áā types. A large variety of morphological types and their lateral transitions were recorded from the DVP. Kale (2020) suggested that the observed morphologies in the DVP represent a continuous variation series between two end members, 'lobate' and 'sheet' flows. The lobate flows are akin to the typical channel-fed pahoehoe flows. When such lobes are emplaced in rapid succession, they may have annealed together into a 'compound' flow. The sheet flows have a much larger aerial spread and may display internal structures comparable to sheet/slabby/rubbly pahoehoe along their length of exposures. The mixed type distribution indicates that both end-member types occur in sub-equal proportions in the sequences.

Volcanism Models: The chemical stratigraphy, established in the western parts of the DVP in the late 1980's, led to the emergence of a central shield volcanic model for this province. This appeared to be consistent with the distribution of the lavas based on the Hawaiian volcanological classification (Deshmukh, 1988). Subsequent workers made assumption of a main volcanic edifice located north of Nasik and overstepping of the chemical formations radially away from it, to model the Deccan volcanism. This monocentric eruptive model did not take on board evidence of the record of several eruptive vents occurring across the DVP (Srinivasan *et al*., 1998). According to Kale *et al*. (2019) the architecture of the Deccan lavas has greater similarities with the Icelandic piles of lavas (e.g. Óskarsson and Riishuus, 2014) than the Hawaiian volcanism. Overall, the morphology and structure of the basaltic lavas in the DVP conform to their subaerial eruption with rare occurrences of subaqueous spilitic pillow lavas. Localized lakes yielded lacustrine inter-trappean sediments. Intrusive dykes, sills and other bodies are well known from various parts of the DVP. In the Narmada valley, the ENE-WSW dyke swarm cuts through not only the basaltic flows, but also their Cretaceous and Proterozoic basement sequences. All the dyke swarms (Sheth *et al*., 2018) in the region are seen cutting across only the basaltic flows except the Satpura dyke which also intrudes the Gondwana sediments. These dyke swarms represent vestiges of the fissures that fed the basaltic flows.

Narmada valley and its southern region appear to be the primary axis along which the earliest Deccan Trap basalts were erupted in an N-S oriented extensional tectonic setting. The anomalous crustal structure along the Narmada valley, manifested as a string of gravity highs, presence of mantle and crustal xenoliths in the dykes occurring along this linear zone and its westward extension in the Saurashtra–Kutch region endorse such a model (Ray *et al*., 2008; Karmalkar *et al*., 2016). The Coastal and Sangamner dyke swarms and the Panvel flexure reflect an E-W oriented extensional system (Dessai and Bertrand, 1995,). It is likely that this stress system is linked to the India-Seychelles rifting and evolution of the western continental margin of the Indian Plate (Misra and Mukherjee, 2017).

Eruption History

The remarkable uniformity in petrochemical composition of these basalt flows is noteworthy. Like other continental flood basalts with zero to negative ε_{Nd} and $^{87}Sr/^{86}Sr > 0.704$, the primary Deccan magmas from enriched mantle sources has been established over the years (Manu Prasanth *et al*., 2019, and references therein). Sheth (2016) discussed the possibility of more than one sub-crustal magma chambers in the evolution of the Deccan lavas. Variable degrees of crustal contamination have been recorded in different parts of the DVP to reflect the heterogeneous nature of the sub-Trappean basement. Non-basaltic rocks (including rhyolites, andesitic tuffs, lamprophyres, andesitic and alkaline basaltic dykes; carbonatites and related igneous complexes like Girnar, Mundhwara and Ambadongar (Chandra, *et al*., 2018) are an integral component of the DVP although they represent less than 5% of its volume. Using the minor variations in the compositional characters of basaltic flows in the western parts of the DVP, chemical stratigraphy was established in the mid-1980's (Cox and Hawkesworth, 1985; Bodas *et al*., 1988; Subbarao and Hooper, 1988) that became the foundation of most of the subsequent models of long distance correlations of lava packets and the eruptive history of this province. Using geochronological and paleomagnetic data, different volcanological models and critical analysis of the chemical database, Kale *et al*. (2019) advocated a sub province-wise stratigraphy of the DVP, without any implied lateral correlations between sub provinces. Geochronological data indicate that volcanism did not occur across the entire province at the same time, as postulated in the monocentric models.

Volcanism in the continental segment of the DVP occurred in not less than three distinct phases (Schoene *et al*., 2019; Sprain *et al*., 2019) but had limited geographic extents during each phase. The oldest and largest eruptive phase (68-66 Ma) spanned the magnetic chrons 30N-29R. This widespread volcanism occurred in Kutch–Saurashtra and the Western DVP, straddles the K-Pg Boundary and may have contributed significantly to the environmental stresses leading to mass extinctions. The next phase occurred in Mandla and Satpura sub provinces during the Danian times between 65.8 Ma and 64.0 Ma corresponding to the magnetic chrons 29N-28R-28N (Shrivastava *et al*., 2014, 2015). The uppermost lava sequences in the Western sub province (with normal polarity) were coeval with this phase of eruptions. The youngest phase of Deccan volcanism occurred in the western edges around Bombay and the offshore region, approximately in the period of 63.5-62.0 Ma. The magnetic polarity data suggest that some of the youngest lavas from the Mandla sub province may have been erupted during this phase, as well. This phase appears to have yielded the non-basaltic volcanic from the DVP.

Post-volcanic Events

Horizontally exposed stacks of lava flows, yielding picturesque cliffs all along the edges of peneplaned plateau, are characters of the DVP that led to it being considered a structurally undeformed and stable continental block. Dipping flows indicate their post-eruptive deformation, viz. the Panvel Flexure near Mumbai (Sukheswala and Poldervaart, 1958), and in the Satpura belt between the Narmada and Tapi river valleys. Seismic events at Koyna (1967: M 6.3), Bhatsa (1983: M 4.2), Killari (1993: M 6.2), Jabalpur (1997: M 5.8) etc. within the Deccan Plateau disrupted the conventional notion of tectonic stability of the DVP.

Zones of Deformation

Earlier studies linked the deformation processes to deep crustal features that were reactivated in response to the clymatogenic uplift of the Deccan Plateau in the post-Trappean times (Radhakrishna, 1993). The geomorphic studies in different parts of the Deccan Traps (e.g., Dikshit, 2001; Kale and Rajaguru, 1987, 1988) attributed several geomorphic anomalies in the DVP to either the step-like erosion of the stack of the basaltic flows or to climate changes.

The geophysical data demonstrate that the sub-trappean basement is fragmented into crustal blocks having differing rheological characters (Raval and Veeraswamy, 2011; Rajaram *et al*., 2017).

Several regional faults of Precambrian origin have been mapped along Son-Narmada Lineament. Bedrock gorges (Murthy *et al*., 2014) are seen cutting through the Precambrian rocks as well as the Deccan Traps. Fault planes dislocating the Deccan Traps have been recorded in the Narmada valley. The >250 km long Tapi Lineament marks the southern boundary of the Satpura horst (Sheth, 2018) separating the Quaternary Tapi alluvium from the Deccan Traps. Stratigraphy of the Deccan Traps north and south of this fault plane is different, indicating that sectors on either side of this fault had diverse eruptive histories during the eruptive phase of the Deccan Traps.

Deformation and dislocation of the basaltic flows is suggestive of relative subsidence of crustal blocks in post-eruptive times along the Son-Narmada Lineament zone due to progressive subsidence in tectonically created intracontinental sinks. A NW-SE trending sub-Trappean rift zone (Kurduwadi Lineament: Brahmam and Negi, 1973) redefined as an intracontinental shear show dominant strike-slip movements (Peshwa and Kale, 1997). The recent seismicity at Killari and around Bhatsa–Vaitarna valleys (Rastogi *et al*., 1986) in Thane district are manifestation of the modern tectonic reactivation of this zone. Based on an integrated geomorphic and structural study of the upland part of the northern Deccan Plateau, Kale *et al*. (2017) concluded that Quaternary movements of crustal blocks along the Kurduwadi lineament are responsible for the anomalous accumulation and localized deformation of the sediments along the Mula and Pravara river valleys that drain this region.

Koyna-Warna Seismic Zone (KWSZ): Following the Earthquake (M=6.3) in the vicinity of the Koyna region in December 1967, this intra-plate seismic event provides a well documented case of reservoir-triggered seismicity. Scientific drilling in this region since 2014 helped in to understand the cause of this (Gupta *et al*., 2017). Re-examination of the geomorphic and geological setup identified several geomorphic anomalies and fracture zones that indicate recent activity (Kale *et al*., 2014). It is evident that the NW-SE trending Chiplun–Warna lineament is a regional zone of shearing that has strong expressions on the Plateau region as well as the coastal tract. Magnetic potential mapping and its correlation with Bouguer gravity data (Rajaram *et al*., 2017) and

LIDAR mapping (Arora *et al*., 2018) are indicative of tectonically active NW-SE trending zone underlying the KWSZ with roots in the Precambrian basement.

Konkan Coastal Belt (KCB)

The KCB is a narrow coastal strip that is less than 100 km at its widest and runs in a N-S direction across more than 400 km within the DVP. It is flanked by the Arabian Sea and the Western Ghats Escarpment (WGE) along its western and eastern margins, respectively. Several lines of evidence including (a) general geomorphic characters of the drainage network, (b) continuity of the lava flow stratigraphy, (c) distribution of laterite caps, (d) physical and geomorphic continuity of the coastal strip southwards beyond the DVP into the basement terrain; etc. have been used by different authors to explain the evolution of this narrow coastal strip. The evolution of this coastal strip has been generally attributed to an erosional retreat of the hypothetical West Coast fault that developed due to the rifting between India and Seychelles (Hooper *et al*., 2010). This model assumes that the lava flows that once covered the present exposures have been eroded away. The N-S oriented coastal dyke swarm in the northern parts of the KCB possibly acted as feeders to the adjoining lava flows (Vanderklyusen *et al*., 2011). The basaltic flows in this belt display a distinctive westerly tilt of 3º–5º while the Panvel flexure have dips up to 20º towards west and give an appearance of being a monoclonal flexure fold and is associated with faulting along strike-slip faults and fracture zones.

Tectonics of Western Margin of India

North-south trending Sahyadri Ranges span more than 1600 km linearly and parallel the western coastline of India to rise to elevations above 2000 m. This range is characterized by steep west-facing escarpments up to 1200 m, leading to it being referred to as the Western Ghats in geological literature. The eastern slopes of the Sahyadri Range are gentler and gradually merge into the peninsular plateau. The emergence of this range is closely associated with the Cenozoic evolution of the western margin of the Indian Subcontinent.

Paleomagnetic and gravity–seismic modeling of structure and evolution of western margin was limited to the offshore shelf region and the continental segments (Radhakrishna, 1993; Calvés *et al*., 2011). The western margin of India can be broadly divided into the following: (i) Western Ghats Escarpment (WGE), (ii) ~100 km wide coastal strip, (iii) Continental shelf, largely above 200 m below msl isobaths, and (iv) Deep marine basins and volcanic submarine plateaus; some of which occur as a string of islands. Radhakrishna and Vaidyanadhan (2011) refer to the linear depression off the continental slope as the Kori–Comorin Depression or Ridge, while parts of this margin that are floored by continental crust are collectively referred to as the Western Continental Margin of India (WCMI). The WCMI displays 3 differing sectors from north to south. The northern sector exposes the Deccan Trap basalts on the continental part in the Sahyadri Ranges as well as the Konkan Coastal Belt (KCB). The wide continental Bombay offshore shelf hosts several petroliferous basins of the Cenozoic age. The central part exposes the Archean Dharwar sequences on the edge of the Mysore plateau is called the Kanara Coastal Belt with a narrow continental shelf. In the southern sector the Nilgiri Hills are amongst the highest hill ranges. Westward narrow Kerala coastal strip displays lagoons and bars and a slender continental shelf.

Offshore Marine Systems

Deep marine features along the western margin of India are a part of the Indian Ocean and the Arabian Sea. Petroliferous basin in the offshore Bombay region is a significant feature (Biswas, 2008). Marine terraces on western continental shelf extend for more than 1300 km in the N-S direction (Wagle *et al*., 1994) with the occurrence of a barrier-reef system at the edge of this shelf (Vora *et al*., 1996). Studies on morphotectonics of the deep marine realm, paleomagnetic characterization of ocean floor strips and intervening volcanic ridge complex provided considerable information from the ocean floor (Desa *et al*., 2019; Yatheesh *et al*., 2019 and references therein).

The Carlsberg Ridge represents the northern extension of the Central Indian Ocean Ridge as an active spreading mid-oceanic ridge (MOR). The Indian MOR displays variable half-spreading rates between 32 to 120 mm per annum (mm/y) in the N-S direction (Desa *et al*., 2019). The Owens Fracture Zone is a transform fault that extends northwards collinear with the Murray Ridge and Chaman Transform Fault that extend further into the Kohistan–Karakoram belt and continues as the WNW-ESE Indus–Tsangpo Suture zone as the western continental boundary of the Indian Plate (Valdiya, 2016).The Chagos–Lakshadweep Ridge (CLR) is recognized by a string of volcanic islands and seamounts extending between the Chagos Archipelago and the Adas Bank (10ºS and 14ºN). Spread N-S for more than 2500 km, this ridge is less than 300 km wide and produced numerous small islands. The Chagos and Maldives archipelagos have the oceanic crust, while the Lakshadweep segment has thin continental crust. More than 80% of CLR occurs at depths of 1000 m below msl, with the small islands and archipelagos rising above the sea. The Laccadive submarine plateau is a significantly large plateau in northern part of the Laccadive basin. The basaltic lavas from this island yield ages of 55–62 Ma, while those in the Chagos archipelago are ~40 Ma (Sheth, 2000; Kale *et al*., 2019). The Laxmi Ridge and Basin Complex are arrays of ridges and rift basins occurring in the northern parts of the Arabian Sea, southwest of the Saurashtra Peninsula as a northward continuation of the Lakshadweep Complex, but has a NW-SE orientation that may be a manifestation of the deflection along the Owen–Murray Fracture zone. Pande *et al*. (2017, 2019) inferred that the voluminous volcanism, recorded along this ridge and in the Panikkar–Raman seamounts and the Wadia Guyot along with the coeval volcanism in Mumbai, represents the syn-rift phase related to the Indo-Seychelles separation which occurred between 62.9 Ma and 62.1 Ma; the original (?syn-rift) flexure enabled accumulation of a thick pile of sediments and gave way to incipient subduction along parts of the basin. The average sedimentation rates ranging between 4 cm/ky and 10 cm/ky display a sudden spike of 58 cm/ky during the Pliocene (Pandey *et al*., 2018).

The Western Continental Shelf of India (WCSI) occupies an offshore area of more than 300, 000 km2 between the western coast and shelf margin with depths up to 200 m below msl. It extends from the traces of the Murray Ridge in the north till south of Kanyakumari along N-S to NNW-SSE for a length of more than 2000 km. The WCSI represents a thinned and stretched continental crust covered by the Cenozoic sediments. Kutch, Cambay, Bombay High and Kerala Konkan Basin are named as potential sources of hydrocarbon resources in this region. The Kutch Basin includes both offshore and onshore sequences ranging in age from Mesozoic to Recent (Chaudhuri *et al*., 2020). The Cambay Basin is a rifted N-S trending basin that extends from the on-land segment in Gujarat to the offshore segment of the Gulf of Khambat. The Bombay High basin and the Kerala Konkan basin extend all along the western shelf region and are notionally divided at the latitude 16ºN.

To the WCSI north of 16ºN, the Northern Shelf is the widest and divided into 3 major blocks, namely the Kutch–Saurashtra Block, Bombay Block, and the Bombay High in the north and the Ratnagiri Block in the south. They host Eocene to Miocene sediments which rest either on the Deccan Basalts or Precambrian Crystallines. The presence of listric faults and roll-over anticlines, series of subparallel normal and reverse faults besides typical rift-bounded sag basins with occasional mud-diapirs are encountered in them. Most of these sediments are derived from stable granite-gneiss continental interiors. Evolution of large homoclinal carbonate banks in the Saurashtra block during the Paleogene period and its onshore representatives suggests that it was largely a stable block without significant tectonism. The Neogene and Quaternary tectonics appear to be largely responsible for the compressive structures present in these sequences along the northern parts of the shelf.

The Central Shelf of the WCSI is 130 to 80 km wide, narrowing progressively southwards, with a smooth surface. Coast-parallel reefs, submarine terraces, rocky islands and sunken structures including paleo-channels characterize this segment. The presence of volcanic islands on the inner shelf near the shoreline is a typical feature of this segment with one exposed in the St. Mary's Islands to be 89–85 Ma old (Pande *et al*., 2001). A part of the shelf is transected by a series of NNW-SSE trending en-echelon faults and fractures that are cross-cut by a set of WNW-ESE trending shear zones. They have controlled linear geometry of the coastline as well as the successive coast-parallel reefs.

The Southern Shelf of the WCSI is the narrowest and connects around the continental tip with the Indo-Sri Lankan shelf. It is flanked on the west by the Laccadive Basin which has the northern part of

Lakshadweep Ridge on its other side. A series of offshore marine terraces (Alleppey–Trivandrum Terrace Complex) rimmed by a stable reef complex creates a local semicircular protrusion of the shelf into the Arabian Sea. The sedimentation on this part of the WCSI appears to have been continuous from the Oligocene onwards, only to be interrupted by either tectonism and or eustatic fluctuations in the sea-level. The carbonate reefs and older sediments are covered by Holocene terrigenous sediments derived from the Precambrian crystalline rocks of the Peninsular hinterland and reworked Cenozoic sediments (Faruque and Ramachandran, 2014). Most of the normal faults in this segment of the shelf strike N-S to NNW-SSE; and are cut across by a series of WNW-ESE to E-W trending shear zones that appear to have extensions on the continental side, representing the shear zones in the Palghat Cauvery Shear.

Western Coastal Belt

The coastal belt along the western continental margin of India can be divided from North to South into the (i) Konkan Coastal Belt (KCB), (ii) Kanara Coastal belt–often called as the Karwar or Goa–Karnataka coast (GKC), and (iii) the Kerala Coast. The rivers that drain this coastal strip have their origin in the WGE and flow westwards into the Arabian Sea. Stretch of the coast between Tapi River and Goa, referred to as the Konkan Coastal Belt (KCB), is entirely underlain by the Deccan Trap basaltic flows, dykes and associated intrusives. The KCB is characterized by rocky coastline, punctuated with estuaries of west-flowing coastal rivers that originate in the WGE.

The northern KCB exposes the oldest and the youngest Deccan Trap lava flows which steepen westwards up to 20° from the axis of monoclinal Panvel Flexure (Sheth, 1998), while Srinivasan (2002) demonstrated the westward downthrow of a series of N-S trending faults as post-Deccan Trap faulting. Southern KCB exposes subhorizontal Deccan Trap flows with extensive lateritic cappings. Studies in the Koyna Warna Seismic Zone indicate the presence of a major regional shear zone from the Precambrian basement, namely the Chiplun–Warna Lineament (Kale, 2014), The Kanara Coast (Goa-Karnataka Coast-GKC) exposes deeply weathered sequences of the Western Dharwar Craton which is capped extensively by laterite, having a number of narrow linear beaches. In this segment rivers flow westwards down the Sahyadri ranges and then across the coastal strip into the Arabian Sea.

St Mary's and adjoining rocky islands near Udupi expose a variety of acidic and basic volcanics (Bhushan *et al*., 2010), which erupted between 89 and 85 Ma as a part of continental magmatism. The Kerala Coastal strip is underlain by the Archaean–Proterozoic gneisses and charnokite–khondalite massif and are separated by E–W trending deep crustal Moyar–Attur, Bhavani and Palghat–Cauvery Shear Zones. On the east, narrow coastal strip is fringed by lateritic plateaux along foothills of the Sahyadri Ranges. Offshore Neogene–Quaternary sequences have small patchy exposures in this coastal strip (Manjunatha and Shankar, 1992; Nair *et al*., 2006), and are commonly flanked by a series of subparallel N-S to NNW-SSE trending normal faults on landward side with progressive westwards downthrow.

Sahyadri Ranges

The Sahyadri Ranges run parallel to the western coastline of India and are characterized by steep escarpment face towering over the western coastal belt, while its eastern slopes are gentler with rugged hilly terrain gradually It is underlain by the Deccan, the Dharwar rocks and the Granulitic Terrain in different sectors. While its western sides display active erosional incision by streams, including well documented examples of river capture, the eastern sides display mature meandering river channels very close to the crest. This geomorphic consistency across bedrock domains with differing ages and structural patterns is indicative of a unified Quaternary denudational history for this mountain range. Three possible origins of this razor-sharp escarpment are (i) Faulting (ii), Erosion, and (iii) Dead cliff (Dikshit, 2001). Epeirogenic uplift was used to explain the uplift history of the Sahyadri (Powar 1993; Radhakrishna 1993). In an attempt the explain a structural model of the Deccan Traps, Widdowson and Cox (1996) speculated that structure may be a combined effect of the original rifting of the western margin of India, crustal doming over a plume-head, coastal monocline and flexure associated with isostatic rebound. Gunnel (2001) and Richards *et al*. (2016) delinked the Sahyadri uplift from the Deccan Traps volcanism.

Geophysical data has demonstrated that continental crust thins out west of the WGE (Singh *et al*., 2007; Nemcok and Rybar, 2017). The offshore structural patterns along the WCSI, transverse strike-slip faults (Misra *et al*., 2014; Rajaram *et al*., 2017) and the subparallel faults controlling the Palaeogene–Neogene sediments along the Kerala coastal belt appear to support the assumption of major continent-scale faulting, located offshore within the shelf. Ajaykumar *et al*. (2017) have inferred that a group of deep-seated fractures were reactivated during episodic break-up of Gondwanaland between ~90 Ma and 65 Ma and led to distension surface faulting and associated dyke emplacement which resulted into sculpted high-relief and rugged terrain of the Southern Sahyadri. The 'step-faulting' model of the KCB along the Panvel flexure (Dessai and Bertrand, 1995; Srinivasan, 2002) and structural patterns recorded in the offshore region are consistent with the 'rift margin' origin for the western coast of India. It is now evident that the Sahyadri Range may have originated earlier but its present physiography represents a surface, drained by antecedent rivers reflecting inherited patterns, which are modified by the Neogene and Quaternary tectonics and climatic changes. Neotectonic activity and recurring seismicity pose doubts about the tectonic stability of this continental block (Valdiya and Samwal, 2017).

The Sahyadri uplift is also linked to the crustal doming related to the Deccan Traps volcanism (Chandrasekharam, 1985; Sheth, 2007; Hooper *et al*., 2010), but fails to explain satisfactorily the uplift history beyond the limits of this volcanism. The 'razor-sharp' WGE does give an impression of being a fault-scarp; but fails to provide any geological evidence of faulting and dislocation along it or in its immediate vicinity.

The chronology of events that have impacted the Western Margin of India is as follows:

The Australia–Antarctica block rifted away from the Indo–Madagascar–Seychelles block during the Aptian–Albian times (~113–118 Ma) in response to the Kerguelan Hotspot, leading to the opening of the Eastern Indian Ocean, eruption of the Rajmahal–Sylhet–Bengal Traps and the evolution of Cretaceous sedimentary basins (Bredow and Steinberger, 2018; Kale *et al*., 2019). Following this, India and Madagascar rifted and eventually drifted apart during the Turonian–Campanian (~90–84 Ma). This led to the northward drift of Greater India, Seychelles and other smaller segments (Yatheesh *et al*., 2013) and its interaction with the Reunion Hotspot during the Maastrichtian (~70 Ma) acting as precursors to the Deccan Volcanism and further separation of the India–Africa blocks, as recorded in the North Arabian and Somali basins (Eagles and Hoang, 2013). The terminal Cretaceous (Late Maastrichtian) Deccan basalts on the continental block took place between 69–65 Ma especially in the Saurashtra High and Somnath Ridge. Early Paleocene separation of India and Seychelles occurred during the second phase of Deccan volcanism (Collier *et al*., 2008) which led to widespread phase of flood basalt volcanism in this province (Renne *et al*., 2015). Non-basaltic volcanics also occur on the westernmost edge of the DVP between 62–60 Ma. The opening of the Laxmi basin, and the subsidence of the WCSI indirectly provides an indicative timing for the emergence of the coastal highlands fringing the continental shelf. The Paleogene syn-rift sediments are dominated by detrital siliciclastics that eventually gave way to calcareous sediments. The large Eocene submarine mass-transport complex at the base of the continental slope (Dailey *et al*., 2019), listric faults, roll-over anticlines, mud-intrusions, and horst-graben structures (Nair and Pandey, 2018) are consistent with the model of evolution of a passive continental margin passing through the rifting and subsequently drifting phases. The volcanic activity in the Lakshadweep ridge during the Late Palaeocene–Early Eocene times (55–62 Ma) is a contemporary ocean floor volcanism. Absence of Trap-derived sediments in the Paleogene sequences on the northern shelf is consistent with easterly tilting of the Indian Peninsula and appears to have occurred during the Early Eocene times (Radhakrishna, 1993). With the establishment of the passive margin continental shelf along the western margin of India, further drifting of the Indian plate is manifested in the ocean-floor with the widening of the Indian Ocean (Bhattacharya and Yatheesh, 2015; Bijesh *et al*., 2018). It is significant to note that there appears to be a close temporal relation between the events of Himalayan collision along northern margin of the Indian Plate and the sea-floor spreading rates in the Indian Ocean. The Late Oligocene corresponds to tectonic movements along the WCSI including some of their onshore exposures along the Kerala coast. The Miocene to Early Pliocene times (~ 22 Ma to 3.6 Ma) represents a period of relative stability with the formation of laterite in the Sahyadri, the coastal belts and formation of peat deposits and reefs along the shelf-edge. Major structural upheavals, both in the offshore and onshore segments, are recorded during the Late Pliocene and Holocene times. They include differential block movements along the WGE and the SONATA as well.

Present-day configuration of the Western Margin of India is a consequence of this long tectonic history, modified by the influences of eustatic sea-level changes, climatic variability over time and finally subjected to various phases of uplift and subsidence. There is no doubt that it is a typical rifted passive margin of a continental block which evolved during the Cenozoic times, but had roots of its origin in the late Mesozoic times.

Tectonics of Sri Lanka

Sri Lanka is located on the southern tip of the Indian sub-continent, with many offshore islands, including the Mannar Island. Three distinct topographic zones characterize Sri Lanka viz., the Central Highlands, the Coastal Plains, and the Coastal Belt.

Highest mountains of the Central Highlands possess north-south trending high plateau and a series of minor rugged highlands, which descend into escarpments and ledges at 400 to 500 meters before sloping down toward the coastal plains. The Coastal Plains (30 and 200 m) are most of the island's surface where ridges and valleys gradually rise to merge with the Central Highlands and produce dissected plains. In southeast parts, change between the two domains is abrupt, and Highlands appear to rise up like a wall. A Coastal Belt, ~ 30 m above sea level surrounding the island, consists of sandy beaches and indented coastal lagoons, including the Jaffna Peninsula. Elsewhere, extensive eroded metamorphic rocks produced dissected coast rocky cliffs, bays, and offshore islands.

Geological Framework

Sri Lanka is comprised of more than 90% Precambrian N-S trending high grade metamorphic and igneous rocks (Fig. 2) with the following characters (Cooray, 1994).

Highland Complex (HC): A sequence of supracrustal association of garnet-sillimanite gneiss, metaquartzite, marble and calc-silicates is interbanded with granitoid orthogneiss and charnockitic gneiss, metamorphosed under upper amphibolite to granulite facies. This belt extends from northeast to southwest through the central highlands. Some klippen of the HC are exposed within the Vijayan Complex at Buttala, Kataragama and Kuta Oya.

Vijayan Complex (VC): Formerly known as the "Eastern Vijayan Complex" in eastern and southeastern parts of the island, the Vijayan Complex (VC) contains granitoids, migmatite and granitic gneiss, with scattered metaquartzite, amphibolite and calc-silicates, metamorphosed under upper amphibolite facies. The boundary between the HC and VC is often interpreted as a west-dipping thrust.

Wanni Complex (WC): Formerly called as the "Western Vijayan Complex", northwestern parts of Sri Lanka consist of migmatite, granitic gneiss, charnockitic gneiss, and minor metasediments (garnet-cordierite gneiss, metaquartzite) and granitoids, metamorphosed under upper amphibolite to granulite facies.

Kadugannawa Complex (KC): Earlier known as the "Kadugannawa Gneiss", this sequence contains hornblende and biotite-hornblende gneiss, hypersthene-bearing gneiss and minor metasediments. These are exposed in elongated doubling-plunging synforms ("Arenas") around Kandy and are metamorphosed under upper amphibolite to granulite facies.

Deformation

High-grade metamorphic terranes, described above, have undergone different deformation histories, though some of the elements remain common.

Structures of the Highland Complex (HC): Berger and Jayasinghe (1976) demonstrated that the HC has undergone polyphase deformation around Kandy with dominant NNW-SSE trending L-S fabric, stretching lineation, boudinage and rootless isoclinal folds; all of these were produced during D1-D2 deformations with coeval granulite facies metamorphism. Subsequent D3 deformation produced open to tight NNW-trending km-scale synforms and antiforms, which refolded these earlier structures. The

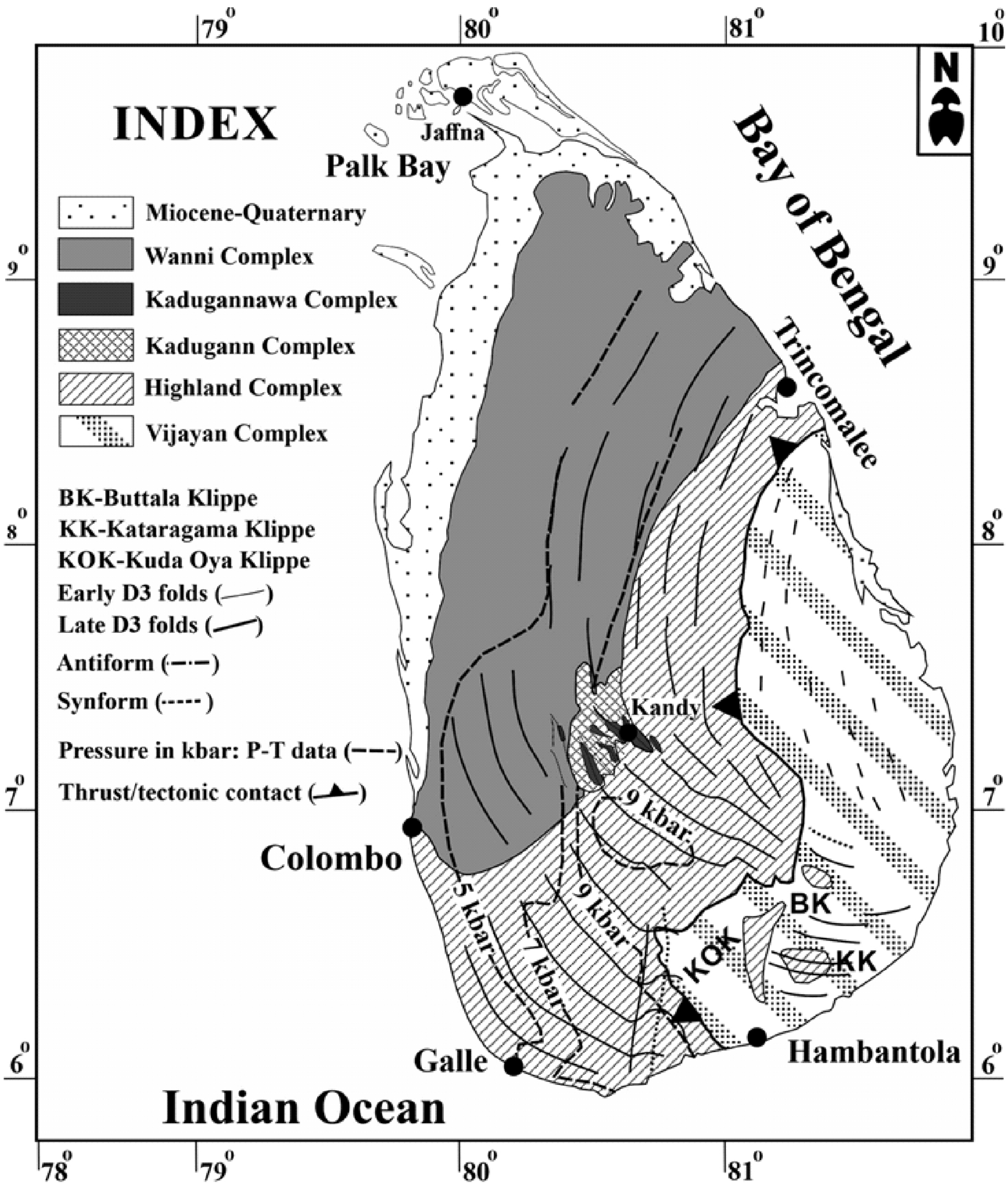

Fig. 2: Simplified geological map of Sri Lanka, showing major boundaries and structural trends along with pressure-temperature of main metamorphism. Redrawn after Compiled after Geological map of Sri Lanka (1982), Kröner *et al.* (1991) and Cooray (1994), Berger and Jayasinghe (1976)

D1 deformation incorporated inclusion trails in garnet porphyroblasts and fold hinges (Mathavan *et al.*, 1999), which is a pre-granulite phase (Kröner *et a1.*, 1994; Kehelpannala, 1997. Shallow-dipping high-grade compositional layering in Sri Lanka were interpreted due to a combination of flattening and noncoaxial deformation during thrusting (Kröner *et al*. 1994).

Structures of the Vijayan Complex (VC): The VC possesses discontinuous and complexly oriented several circular domes. Though there is a distinct break in the structural pattern, some prominent trends of the HC appear to be continuous into the VC. Two deformation phases in the VC produced an early N-S stretching isoclinal folds and later upright folds with the same trend (Kriegsman, 1991).

Structures of the Wanni Complex (WC): Since a large part of the WC possibly represents former Highland Group rocks, it has a similar history between the WC and HC. Prominent and major upright folds in the HC are continuous into the eastern WC, including early structures such as tight to isoclinal folds and strong stretching lineation with identical orientation (Voll and Kleinschrodt, 1991).

Metamorphism

High-grade metamorphism during the Pan-African event at ca. 610–520 Ma has produced widespread granulite-facies assemblages, now retrogressed and affected by extensive late metamorphic K-metasomatism. The VC experienced amphibolite-facies metamorphism, whereas the other complexes underwent granulite-facies metamorphism with a retrograde amphibolite-facies overprint (Kehelpannala 1997). From central parts of the HC, Sajeev *et al*. (2007) record textural and compositional evidences of high-pressure-ultrahigh-temperature (HP-UHT) granulite facies metamorphism and multistage decompression from peak P-T conditions of 12.5 kbar/ 925°C to 844°–982°C or even 9 kbar/1050°C, with two generations of metamorphic zircon overgrowths with contrasting Th/U at 569 ± 5 and 551 ± 7 Ma, (Sanjeev *et al*., 2010).

UHT-controlled metasedimentary and metabasic rocks in western HC range from <8 kbar to >15 kbar and <800 to >1200°C (He *et al*., 2018). Two contrasting P-T-t paths for metasedimentary and meta-igneous rocks indicated a clockwise path for the former with a near-isobaric prograde heating segment, followed by a near-isothermal down-pressure retrograde segment. And, meta-igneous rocks are marked by a near-isobaric cooling path, followed by a P-T decrease after peak metamorphism (He *et al*., 2018). After peak metamorphism, P–T trajectory from prograde to near isobaric cooling seems to occur within a time span from Late Cryogenian to Early Cambrian (ca. 665–500 Ma), coeval with the assembly of the Gondwana Supercontinent (Dharampriya *et al*., 2017). In the eastern parts of the HC, long-lived HT metamorphism lasted possibly longer than 100 Ma between ca. 660 to 520 Ma.

The WC had undergone peak metamorphism around 5-7 kbar/700-830°C (Raase and Schenk 1994). In central WC, incipient charnockite represents granulite formation within host amphibolite facies foliated gneiss along veins, patches, shear zones and foliation planes, thus indicating pervasive fluid influx in the Sri Lankan lower crust (Kehelpannala, 1999).

The Vijayan Complex (VC) has a ~580 Ma Pan-African regional metamorphism (Kröner *et al*., 2013) over the 1100–1000 Ma protolith magmatic bodies - a product of subduction-related magmatism. Minor sedimentary enclaves such as metaquartzite, calc-silicate rocks and marble also occur within the VC, and granitoid gneisses show TTG (tonalite-trondhjemite-granodiorite)-dominated signature.

Geochronology

Extensive LA-ICP-MS U–Pb dating of remnant zircon cores from the HC and WC high-grade metamorphics in Sri Lanka reveals that these domains have distinct characteristics: the HC is dominated by detrital zircon (DZ) ages of ca. 3.50–1.50 Ga from various gneisses, while its igneous bodies intruded ca. 2.00–1.80 Ga (Kitano *et al*., 2018). Kröner *et al*. (1987) identified DZ from metaquartzite of the HC, having U-Pb ages between 3.17 and 2.4 Ga, possibly derived from an unknown Archean terrane. Two pelitic gneisses yielded DZ up to 2.04 Ga with a 1.10 Ga metamorphic event around old cores and new zircon growths. A granite intrusive into the HC granulite records an emplacement age of 1.10–1.00 Ga. Zircons from a metaquartzite xenolith within the VC granitoid are not older than ~1.10 Ga; therefore, it is neither Archean in age nor acted as basement to the HC. Kröner *et al*. (1987) suggested that the VC formed significantly later than the HC and that the two units were brought into contact through post-1.1 Ga thrusting.

The WC terrane appears to be much younger with dominant DZ ages of ca. 1.10–0.70 Ga from paragneiss, indicating their different origins from the HC. Sedimentary sources for the WC were mainly eroded from local late Mesoproterozoic to Neoproterozoic igneous rocks with very minor components from an older 2.50–1.50 Ga craton.

The Vijayan Complex (VC) is tectonically juxtaposed against the HC and has undergone intense ductile deformation of diorite to leucogranite bodies with a distinct calc-alkaline geochemical signature and is interpreted as a magmatic arc. Using U-Pb zircon ages, whole-rock Nd, Hf-in-zircon isotopic systematics and geochemical data, Kröner *et al*. (2013) have undertaken extensive analyses of large section of the Vijayan gneisses, where zircon ages fall predominantly between 1.10 and 1.00 Ga with a few early Neoproterozoic intrusions, and indicate the VC as a Grenville-age magmatic arc. Many zircons experienced minor to significant lead-loss at ~580 Ma. Nd and Hf isotopic data indicate primitive origin for most Vijayan gneisses, but significant variations indicate source heterogeneities and involvement of minor amounts of older continental material (Kröner *et al*. 2013).

Sri Lankan Thrusts and Faults

Kleinschrodt (1994) have opined that granulite-facies HC was thrust onto the Vijayan Complex (amphibolite-facies) along its eastern margin through deep crustal and subhorizontal thrust surface. Open to flexure-slip folds followed thrusting and generated subhorizontal fold envelop, thus thrust must underlie large parts of the HC. Remnants of such thrusts are the occurrences of HC klippen such as the Kataragama klippe, indicating that thrust surface was subhorizontal and can be traced for more than 200 km parallel to the transport direction till the coastal regions. This thrusting appeared to have occurred during retrograde metamorphism and younger than formation of 577 ± 14 Ma old migmatite. Several serpentinite bodies are located near this boundary.

Using zircon-apatite fission track (FT) and apatite (U-Th)/He dating methods, Emmel *et al*. (2012) determined kinematic and thermochronological patterns along brittle faults from southern and southwestern Sri Lanka and observed at least 5 thermal overprinting events at 159 ± 18, 144 ± 14, 120 ± 10, 94 ± 8, and 70 ± 10 Ma due to major N-S trending extension subsequent to the Gondwana breakup. Structural data also indicate variations in stress regime during the Late Jurassic and Late Cretaceous, as Sri Lanka separated from East Antarctica and progressively moved away from Madagascar and the Seychelles microcontinent.

Crustal Evolution

In the KC terrane, magmatic episodes between ca. 1.10 and 0.89 Ga were linked to the breakup of the Rodinia supercontinent as a consequent of large-scale rifting (Kröner *et al*., 2003), while Santosh *et al*. (2014) demonstrated that these Sri Lankan Neoproterozoic magmatic pulses are distinctly linked to convergent margin setting. A single ~610–456 Ma common metamorphic event has affected all these terranes as the consequence of collision of Sri Lankan terranes during the assembly of Gondwana. A double-sided subduction system was proposed by Santosh *et al*. (2014) with the Wanni and Vijayan magmatic arcs, juxtaposed against each other along sutures with metamorphosed Highland accretionary sediments in the center.

Sri Lanka does not record widespread extension-related mafic or bimodal magmatism during mid-Neoproterozoic, hence a Rodinia break-up model becomes untenable (cf., Santosh *et al*., 2014), and propounded accreted oceanic components and arc magmatism in a convergent margin setting. The Wanni and Vijayan complexes are considered as continental arcs underlain by Neoarchean–Paleoproterozoic basement. This study also identifies juvenile magmatic additions during mid-Neoproterozoic and latest Neoproterozoic–Cambrian in post-collisional asthenospheric upwelling, which triggered widespread UHT metamorphism within the HC. Thus, convergent margin processes explain better the Neoproterozoic arc-related magmatic suites in contrast to the existing concepts of linking Sri Lanka with Rodinia rifting, associated with the assembly of Gondwana (Santosh *et al*., 2014).

Among various Gondwanland assemblies, Kitano *et al*. (2018) compared available zircon ages from the VC in Sri Lanka for configuration with neighbouring terranes. Of significance are adjacent terranes to Sri Lanka such as the Southern Granulite Terrane (SGT) of southern India and Lützow-Holm

Complex (LHC) of East Antarctica in the Gondwana reconstructions. However, detrital zircon cores in paragneisses from the HC and WC indicate that protoliths from these terranes correlate closely with the Trivandrum Block, the Achankovil Shear Zone and Southern Madurai Block, respectively (Kitano *et al*., 2018).

Myanmar-its Tectonics

Myanmar (formerly known as Burma) spans for about 2000 km N-S linearly from 28°N to 10°N. It is bordered by India, Bangladesh, the Bay of Bengal and the Andaman Sea on the west, and by Thailand, Laos and China in the east and northeast. The country is located across three tectonic plates-the Indian Plate, the Burma microplate and the Sundaland Plate (Fig. 3). To the west, offshore Indian Plate subducts obliquely beneath Myanmar to constitute the Burma microplate (Fig. 3); a right lateral strike-slip Saiging Fault extends from south to north across more than 1000 km. These tectonic zones are responsible for large earthquakes in the region.

Topographically, Myanmar is composed of central lowlands surrounded by steep, rugged highlands. The highest point is Mount Hkakabo Razi (5881 m) in the far north in Kachin State from where

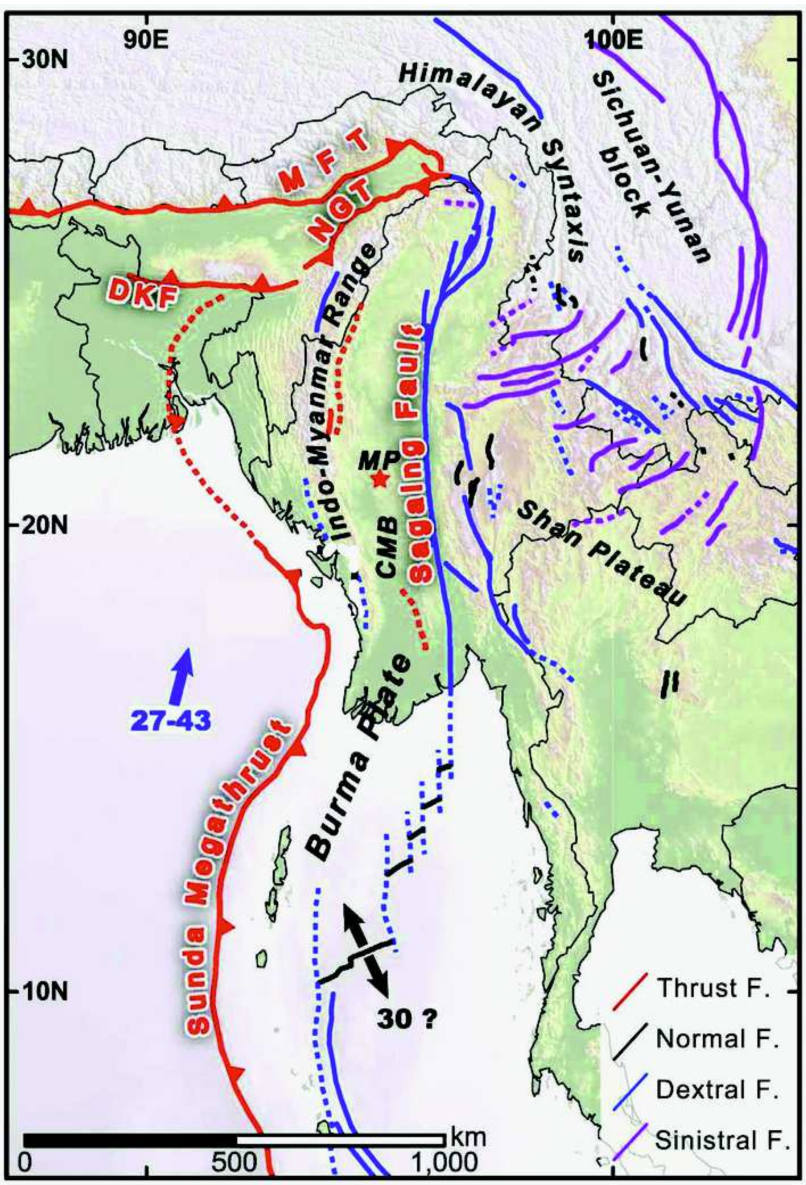

Fig. 3: Regional tectonic map of the Myanmar-Andaman region showing configuration of Myanmar/Burma Plate. Blue arrow: Direction of Indian Plate motion relative to SundaPlate (Socquet*et al*., 2006). Black arrows: Opening direction of the Central Andaman spreading center. Velocities are in mm/yr. Burma Plate (Curray*et al*., 1979) is bounded by the Sunda Megathrust on the west and the Sagaing Fault on the east. DKF-Dauki Fault. MFT-Main Frontal Thrust. NGT-Naga Thrust. CMB-Central Myanmar Basin. MP-Mt. Popa (red star). After Moore *et al.* (2019)

Myanmar slopes southwards to sea level at the Irrawaddy (Ayeyarwady), Salween and Sittang (Sittoung) river deltas in the Andaman Sea. The mountain ranges generally run from north to south with the Patkai Range, the Naga Hills, the Chin Hills and the Rakhine Yoma, located to the west along the borders with India and Bangladesh. Mountain ranges also form the eastern border with China, passing southwards into the highly dissected Shan Plateau at an average elevation of 900 m.

First systematic and comprehensive account of the geology of Central Burma is available after the establishment of the Geological Survey of India in 1851. Subsequently, it became evident that there was excellent oil and natural gas potential in the Cenozoic basins of Central Myanmar, coastal areas along the Bay of Bengal, the Andaman Sea and the offshore islands. Good mineral prospects for tin and tungsten in Kayah and Tanintharyi were established along with for gems in the Mogok area, lead, zinc and silver in the Shan Plateau, gold in the Wuntho Massif in Central Belt and Kachin State, and others. Chhibber (1934a, b) published two volumes on 'The Geology of Burma and The Mineral Resources of Burma', and made fundamental contributions to geology and resources of Myanmar up to 1933.

All the available geological information on India and Myanmar up to the outbreak of the Second World War was included in Pascoe's three volumes on the 'A Manual of the Geology of India and Burma', published in 1950, 1959 and 1964. Since then notable contributions to the geology of Myanmar were made by Tha Hla (1959), Maung Thein and Haq (1970), Maung Thein (1973), and Bender (1983), besides significantly improving our knowledge of the Palaeozoic and Mesozoic stratigraphy, paleontology of the Shan Plateau, strike-slip activity, earthquake disaster potential of the Sagaing Fault. Recent knowledge on geology, tectonics, mineral and energy resources of Myanmar is now available in edited volumes of Geological Society, London, Memoirs by Racey and Ridd (2015) and Barber *et al*. (2017).

Geological and Tectonic Framework

From west to east, Myanmar incorporates the following three arcuate-shaped nearly N-S trending and westward bulging physiographical, geological and tectonic components: (i) the Indo-Myanmar folded mountain ranges comprising Arakan-Yoma mountains, Chin, Naga, Manipur, Lushai and Patkai Hills, passing southwards into the Andaman and Nicobar islands, Sumatra and the Sunda and Banda arcs of Indonesia, (ii) the Myanmar Central Belt (MCB) containing many Cenozoic sub-basins, (iii) Sagaing Fault Zone, and (iv) the Shan Plateau (Fig. 4) (Khin Zaw *et al*., 2017). The Mishmi Hills of Arunachal Himalaya (India) delimit these physiographical regions in the north. The MCB is separated from the Shan plateau by a seismically active Sagaing Fault.

Indo-Burma Folded Mountain Ranges: The Indo-Burma Ranges (IBR), also called as the Indo-Myanmar Ranges (IMR), extend 1300 km N-S and up to 300 km wide and are comprised of an outermost arcuate mountain chain along western Myanmar coast, passing northwards into Bangladesh, Tripura, Manipur and Nagaland (Ghose *et al*., 2014), and southwards into the Andaman-Nicobar islands, Sumatra and further south (Fig. 4). It comprises the Mesozoic and Cenozoic flysch deposits, having several large and smaller ophiolite fragments (Brunnschweiler, 1966, 1974; Rangin, 2017). The ranges initially formed in an accretionary prism setting, then evolved to a sub-aerial fold-and-thrust belt during highly oblique collision between Sundaland and the India Plate (see Kyi Khin *et al*., 2017; Moore *et al*., 2019; Morley *et al*., 2019 for recent details).

Maurin and Rangin (2009) classified the IBR into (i) an IB Outer Wedge, (ii) an Inner IB Wedge, and (iii) the Core of the wedge. Three major faults control the overall geometry of the IB Wedge: (i) west verging Kaladan Thrust from the Andaman Trench to the outer Indo-Burmese Wedge, (ii) the Lelon Fault between the accretionary wedge and metamorphic core, and (iii) the Kabaw Fault between the IB Wedge and the Myanmar central basins.

The IB Outer Wedge progressively narrows down to a few tens of kilometres south of 20oN with dextral transpressive tectonics and en echelon folds, while folds hinges are bent almost ENE near the Dauki Fault. It is a N160oE trending fold-thrust system of the lower Miocene submarine, Upper Miocene shelfal and Plio-Pleistocene fluvial deposits, while the inner wedge of fold-thrust region of mainly Eocene flysch is affected by N-S trending dextral faults; the easternmost core of the wedge is a tectonically complex zone of high grade metamorphics, imbricated with Mesozoic ophiolites and sedimentary sequences of Late Triassic to Late Cretaceous (Bender, 1983). Tectonic, sedimentary and diapiric mélanges characterize the outermost belt where sheared fragments of Cretaceous ophiolites mark the tectonic mélanges within the Eocene turbidite thrust packets of shale-rich beds and thick sandy beds (Moore *et al*., 2019).

The core of the IB Range comprises peridotite, serpentinite, pillow lavas, radiolarian chert, mélange and poorly dated flysch of Late Triassic age (Pane

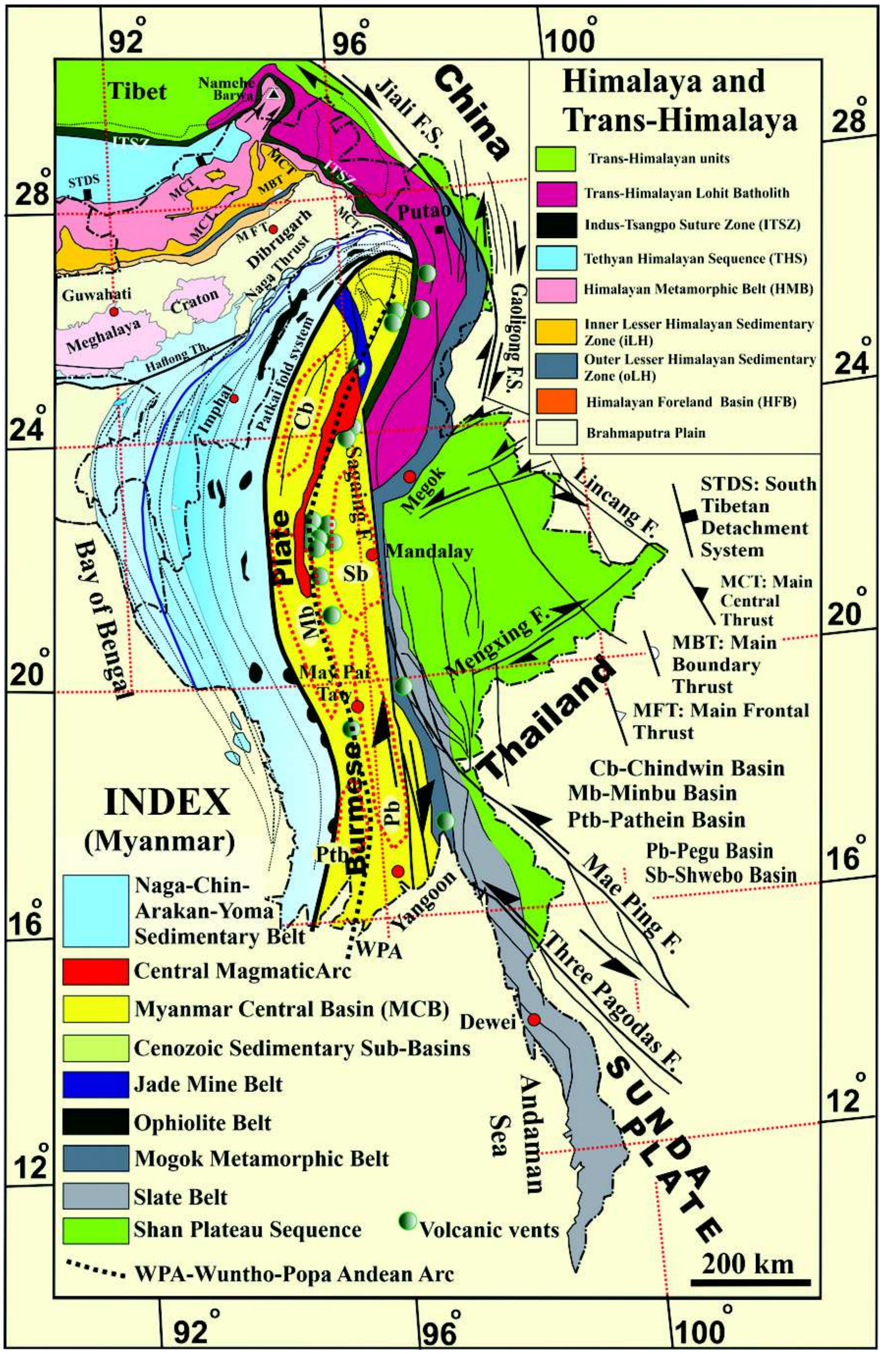

Fig. 4: **Schematic geological map of Myanmar, and its relationship with Eastern Himalaya syntaxis. Approximate locations of the Wuntho-Popa Andean arc (WPA) axis (thick dotted black line) along with sub-basins: the Chindwin, Minbu, and Pathein Basins (Cb, Mb, and Ptb) as forearc, and the Shwebo and Pegu Basins (Sb and Pb) as back-arc basins are after Licht et al. (2018). Redrawn from published sources**

Chaung Formation), and metamorphics including fragments of the metamorphic sole to large ultrabasic bodies. A larger region of southern Chin Hills area is covered by predominantly low-grade metamorphics (Kanpetlet Schists). These mark a broad suture zone of the Tethys ocean and related back-arc basin-derived rock units

Myanmar Central Basin (MCB): Nearly 1100 km long Myanmar Central Basin (MCB) is located immediately east of the IB Belt in the central Myanmar lowlands, and contains a series of Cenozoic petroliferous basins presently affected by an active inversion (Pivnik *et al*., 1998). These basins extend southward in the Andaman Sea and are classically considered as the forearc and back-arc couple basins for the Bengal subduction system with intervening chain of active volcanoes. It is comprised of up to 15 km thick Eocene-Quaternary sedimentary and volcanic rocks in the Western Trough and less than 8 km Miocene–Pliocene sequence in an Eastern Trough over the basement of the Burma plate (Bertrand and Rangin, 2003; Mitchell, 1993). The Kabaw Fault bounds the Central Myanmar Basin on the west and separates it from the Late Mesozoic–Neogene carbonate and flysch forearc accretionary prism and plutonic rocks of the Indo-Burman Ranges (Bender, 1983; Mitchell, 1993; Allen *et al*., 2008). The Mogok Metamorphic Belt occurs as narrow deformational zone (30–40 km wide) between the Central Myanmar Basin and the Shan Plateau of the Sibumasu block (Fig. 4) and is bounded by the Slate Belt in northeastern Myanmar (Mitchell *et al*., 2007).

The MCB is subdivided into smaller sub-basins with underlying narrow steeply and east dipping Burma seismically active subduction zone, characterized by earthquakes extending down to at least 200 km (Guzman-Speziale and Ni, 1996). Above this seismic zone two large calc-alkaline andesite dacite strato-volcanoes (Mounts Popa and Taungthonlon), and the smaller Mount Loimye, were active from Pliocene to recent times (Stephenson and Marshall, 1984) suggesting that the seismic zone may represent a thin slab of subducting Indian oceanic lithosphere that extends north from the Bay of Bengal beneath Bangladesh (Rao and Kalpna, 2005). A belt of Late Cretaceous granodiorites and diorites and Cenozoic volcanics (with associated porphyry and epithermal copper deposits) extending north of Mount Popa (Mitchell, 1993) suggests that this subduction zone may have been relatively long-lived.

Based on sedimentological, geochemical, petrographical, and geochronological data from the Chindwin Basin of the northern part of the Burmese forearc, Licht *et al*. (2018) observed that it behaved as an Andean-type subduction margin until the late middle Eocene, with a forearc basin opened to the trench and fed by denudation of volcanic arc to the east. The Burmese margin changed to an oblique margin ~39–37 million years ago with the forearc basin partitioning into accretionary prism in the west, and synchronously exhumed basement rocks in the east, including coeval high-grade metamorphics.

Sagaing Fault (SF): The Sagaing Fault is a major dextral strike-slip continental transform fault for over 1200 km in Myanmar between the Indian Plate and Sunda Plate (Le Dain *et al*., 1984; Guzmanspeziale and Ni, 1996) and connects spreading centres in the Andaman Sea with the continental convergence zone along the Himalayan front (Fig. 3). On land, it marks the boundary between the Myanmar Central Basin (MCB) in the west and the Shan Scarp in the east (Win Swe, 1972), and crosses through populated cities of Mandalay and Pegu before continuing into the Gulf of Martaban. Different segments of this fault have ruptured in the past in May 1930, Dec 1930, 1931 and 1946 causing severe earthquakes, devastation and tsunami. GPS data in recent past have revealed right-lateral slip rate of 18 mm/yr.

The SF is marked with a low topography west of the Shan Scarp, where a narrow belt of high grade Mogok Metamorphic Belt (Chhibber, 1934) is sandwiched between the two. In its central 700 km long, the fault is remarkably linear between latitude 17^{o}N and 23^{o}N. The fault branches in various splays north of Swebo (22.5^{o}N) and terminates in the Jade Mine belt into a compressive 200-km-wide horse-tail structure. Further north, this fault connects with the Mishmi Thrust as the western extension of the Himalayan Main Central Thrust in Arunachal Pradesh. Southward, the fault terminates again into a horse-tail extensional system connecting to the active Andaman spreading centre (Searle *et al*., 2007; Vigny *et al*., 2003). In its central part, the trace of the fault is distinct from the trace of the faults observed along the foothills of the Shan Scarp.

Major geomorphic features of the Sagaing Fault are the Sittaung/ Ayeyarwaddy deltas in the south, the eastern scarp of the Pegu Yoma, the palaeo-Ayeyarwaddy valley, the modern Ayeyarwaddy valley and the northern basin-and-range topographic domain (Soe Thura Tun and Watkinson, 2017).

The total displacement along the SF remains controversial from an estimate of total 460 km since Miocene (Curray *et al*., 1979), 250 km since post-Lower Miocene (Khin Zaw, 1990) to 100 km with a continuous 20mm/yr right lateral strike slip since 4-5 Ma.

Mogok Metamorphic Belt (MMB): Numerous exposures of metamorphic and intrusive bodies between the Sagaing fault and Shan Plateau belong to the narrow and sigmoidal Mogok Metamorphic Belt (MMB) (Chhibber, 1934). N-S trending belt lies at the foothill of Shan Scarp, and runs over 1500 km with an average width of 25 to 40 km from Putao in the north to the Gulf of Moktama and further southeast in Thailand. The MMB includes mica schists, gneisses, marbles, granulites and rare quartzites, ranging from greenschist to granulite facies, including the Slate Belt adjacent to the Sagaing Fault. These are intruded by deformed granodiorite pluton and pegmatites.

Bertrand *et al*. (2001) have demonstrated various lineation, sheath folds and "pencil-like" mullions as indicative of NNW-SSE directed ductile stretching within the MMB.

Searle *et al*. (2007) suggested the following metamorphic and magmatic events within the MMB: (i) Jurassic–early Cretaceous (171-120 Ma) I-type calc-alkaline subduction-related magmatism for the emplacement of granodiorites and orthogneisses, (ii) Paleocene metamorphism ending with intrusion of cross-cutting post-kinematic biotite granite dikes at ~59 Ma, (iii) main high-temperature sillimanite-muscovite metamorphism peaking at 4.9 kbar/680°C between 45 and 33 Ma to (iv) around 4.4-4.8 kbar/ 606-656°C at 29.3 ± 0.5 Ma, and (v) 24.5 ± 0.3 Ma leucogranite cross-cutting all earlier metamorphic fabrics. Main metamorphic event resulted metamorphic growth of monazite in sillimanite grade and growth of zircon rims at 47-43 Ma, sillimanite+muscovite replacing older andalusite, and synmetamorphic melting producing garnet and tourmaline bearing leucogranites at 45.5 ± 0.6 Ma and 24.5 ± 0.7 Ma.

Bertrand *et al*. (1999, 2001) determined 40Ar/ 39Ar mica cooling ages between Oligocene to Middle Miocene (30 to 18 Ma) along the MMB and confirmed that the MMB cooled diachronously from south to north adjacent to the Sagaing Fault younging northwards.

Shan Plateau: The Shan Plateau (~1000 m elevation) belongs to the Shan-Thai mass as the western edge of the rigid Sundaland block (Mitchell, 1989). It trends NNW-SSE from Yangon to Mandalay, then swings NE-SW from the Mogok Range to western Yunnan (China) and finally trends north to connect with eastern Tibet. The plateau comprises a thick succession of low grade metamorphosed Precambrian, Palaeozoic and Mesozoic predominantly sedimentary rocks. In the westernmost part, the Upper Carboniferous to Lower Permian diamictites or pebbly mudstones belong to the Slate Belt and can be traced into Phuket region of western Thailand. The folding, thrusting and uplifting of the Shan Plateau is coeval with the transpressional deformation along the MCB and the Sagaing Fault.

Based on kinematics, GPS velocity field, and slip rate gradients of the fault systems, Shi *et al*. (2018) interpreted the kinematics and geodynamics of the Shan Plateau and adjoining region due to a curved, southwestward, tongue-like asthenospheric flow. Slip rates for this sinistral fault system increase progressively northwestward towards the Eastern Himalayan Syntaxis (EHS) for about ~700 km long distance to ~12 mm/year before decreasing over the final ~100 km to ~1 mm/year for individual faults towards syntaxis, and matches with the geologic rate averaged over ~10 Ma.

Acknowledgments

Thereturn of the International Geological Congress to the Indian Subcontinent after a lapse of 55 years motivated the authors to compile a Geological and Tectonic Map based on published and unpublished data along with a brief description of the geology of the region. This publication forms Part II of the 36th IGC Special Issue: the Indian Report to IUGS-2016-

2020. The project received wholehearted support of the Indian National Science Academy, New Delhi, and Prof. A K Singhvi, Chair of the National Committee of IUGS and Vice President, INSA in particular. We thank Prof. A K Sood (Past President, INSA), Prof. Chandrima Shaha (Preisdent INSA), Prof. Gadadhar Misra (Vice President Publications, INSA), Prof S Puri, Chief Editor PINSA, for their support at various stages in the preparation this publication. We thank the Editorial Staff of INSA for coordinating the administrative aspects. Shri V K Nair took exceptional care in printing this map. AKJ and DMB thank the INSA for the award of Honorary Scientist Fellowships which made it possible to finalize this work. Dr. N Gopikrishnan, Director, CSIR-Central Building Research Institute, Roorkee, extended the working facilities to AKJ for this work. DMB acknowledges the moral support and working facility provided by the faculty members of the Geology Department of Delhi University. Dr. V S Kale provided inputs to parts dealing with the Deccan Volcanic Province and West Coast. Ms. Gargi Deshmukh, Research Fellow under the Prime Minister Research Fellowship (PMRF) Scheme, took pains in formatting the references within a short time. We also acknowledge numerous unnamed colleagues whose advice was critical to finalization of this map. Vijay Kumar Nair and Richa Sharma are acknowledged for their handling the manuscript.

References

Absar N and Sreenivas B (2015) Petrology and geochemistry of greywackes of the ~1.6 Ga Middle Aravalli Supergroup, northwest India: Evidence for active margin processes *Intern Geol Rev* **57** 134-158

Absar N, Raza M, Roy M, Naqvi S M and Roy A K (2009) Composition and weathering conditions of Paleoproterozoic upper crust of Bundelkhand craton, Central India: records from geochemistry of clastic sediments of 1.9 Ga Gwalior Group *Precamb Res* **168** 313-329

Acharyya S K, Gupta A and Orihashi Y (2010) New U-Pb zircon ages from Paleo-Mesoarchean TTG gneisses of the Singhbhum Craton, eastern India *Geochem J* **44** 81-88

Ahmad I and Mondal M E A (2016) Do the BGC-I and BGC-II domains of the Aravalli craton, northwestern India represent accreted terranes? *Earth Sci India* **9** 167-175

Ahmad I, Mondal M E A, Bhutani R and Satyanarayanan M (2018) Geochemical evolution of the Mangalwar Complex, Aravalli Craton, NW India: Insights from elemental and Nd-isotope geochemistry of the basement gneisses *Geosci Front* **9** 931-942 http://dx.doi.org/10.1016/j.gsf.2017.07.003.

Ahmad T and Tarney J (1994) Geochemistry and petrogenesis of late Archaean Aravalli volcanics, basement enclaves and granitoids, Rajasthan *Precamb Res* **65** 1-23

Ahmad T, Dragusanu C and Tanaka T (2008) Provenance of Proterozoic Basal Aravalli mafic volcanic rocks from Rajasthan, Northwestern India: Nd isotopes evidence for enriched mantle reservoirs *Precamb Res* **162** 150-159

Ahmad T, Tanaka T, Sachan H K, Asahara Y, Islam R and Khanna P P (2008) Geochemical and isotopic constraints on the age and origin of the Nidar ophiolitic complex, Ladakh, India: implication for the Neo-Tethyan subduction along the Indus suture zone *Tectonophysics* **451** 206-224

Ajaykumar P, Rajendran S and Mahadevan T M (2017) Geophysicallineaments of Western Ghatsandadjoining coastal areas of central Kerala and their temporal development *Geosci Front* **8** 1089-1104

Alam M (1972) Tectonic classification of the Bengal Basin *Geol Soc Amer Bull* **83** 519-522

Alam M (1989) Geol and depositional history of Cenozoic sediments of the Bengal Basin of Bangladesh *Palaeogeogr Palaeoclim Palaeoecol* **69** 125-139

Alam M (1997) Bangladesh In: Encyclopedia of European and Asian Regional GeolMoores E M, Fairbridge R W (Eds) *Chapman Hall London* 64-72

Alam M M (1991) Paleoenvironmental study of the Barail succession exposed in northeastern Sylhet, Bangladesh *Bangladesh J Sci Res* **9** 25-32

Alam M M (1995) Tide-dominated sedimentation in the upper tertiary succession of the sitapahar anticline, Bangladesh. In: Tidal Signatures in Modern and Ancient Sediments (Eds: Flemming B W and Bortholma A) *Int Assoc Sediment Spec Publ* **24** 329-341

Alam M, Mustafa A, Joseph R, Curray J R, Chowdhury M L R and Gani M R (2003) An overview of the sedimentary Geol of the Bengal Basin in relation to the regional tectonic framework and basin-fill history *Sedim Geol* **155** 179-208

Alderson A (1991) The Surma Basin, Bangladesh: A palynostratigraphical manual, geological synthesis and comparison with the adjacent hydrocarbon provinces of N.E. India and Myanmar. Geochem Group Project No **4707/003** 1-194

Allen R, Najman Y, Carter A, Barfod D, Bickle M J, Chapman H J, Garzanti E, Vezzoli G, Andò S and Parrish R R (2008) Provenance of the Tertiary sedimentary rocks of the Indo-Burman Ranges, Burma (Myanmar): Burman arc or Himalayan-derived? *J Geol Soc* **165** 1045-1057 https:// doi.org /10 .1144 /0016-76492007-143

Ameen S M M, Hossain M S, Hossain M S, Abdullah R, Bari Z, Uddin M N, Das S C, Tapu A T, Jahan H and Shahriar M S (2016) Deciphering the Precambrian crust between Shillong Mass if and northeast India In: *Intern Assoc Gondwana Res (IAGR) Convention, Trivandum, India* 75-79

Ameen S M M, Khan M S H, Akon E and Kazi A I (1998) Petrography and major oxide chemistry of some Precambrian crystalline rocks from Maddhapara, Dinajpur *Bangladesh Geosci J* **4** 1-19

Ameen S M M, Wilde S A, Kabir M Z, Akon E, Chowdhury K R and Khan M S H (2007) Paleoproterozoic granitoids in the basement of Bangladesh: a piece of the Indian Shield or an exotic fragment of the Gondwanajig saw? *Gondwana Res* **12** 280-387

Argand E (1924) La tectoniquedel' Asie *Proc 13th Intern Geol Cong* **7** 170-372

Arita K (1983) Origin of the inverted metamorphism of the lower Himalaya, central Nepal *Tectonophy* **95** 43-60

Arora B R, Unsworth M J and Rawat G (2007) Deep resistivity structure of the northwest Indian Himalaya and its tectonic implications *Geophys Res Lett* **34** L04307, doi:10.1029/ 2006 L029165

Arora D, Pant N C, Fareeduddin, Sharma S, Raghuram and Sadiq M (2017) Inferring a Neoproterozoic orogeny preceding the Rodinia break-up in the Sirohi Group, NW India. In: Crustal Evolution of India and Antarctica: The Supercontinent Connection (Eds: Pant N C and Dasgupta S) *Geol Soc, London Spec Publ* **457** https://doi.org/10.1144/ SP457.8.

Arora K, Srinu Y, Gopinadh D, Chadha R K, Raza H, Mikhailov V, Ponomarev A, Kiseleva E and Smirnov V (2018) Lineaments in the Deccan Basalts: the basement connection in the Koyna-Warna RTS region *Bull Seism Soc Amer* **108** 2919-2932 doi: 10.1785/0120180011

Ashwal L D, Solanki A M, Pandit M K, Corfu F, Hendriks B W H, Burke K and Torsvik T H (2013) Geochronology and geochemistry of Neoproterozoic Mt. Abu Granitoids, NW India: Regional correlation and implications for Rodinia paleogeography *Precamb Res* **236** 265-281

Auden J B (1933) Vindhyan sedimentation in the Son Valley, Mirzapur District *Mem Geol Surv India* **62**141-240

Auden J B (1934) The geology of the Krol belt *Rec Geol Surv India* **67** 357-454

Azmi R J (1998) Discovery of lower Cambrian small shelly fossils and Brachiopods from the Lower Vindhyan of Son Valley, Central India *J Geol Soc India* **52** 381-389

Bakhtine M I (1966) Major tectonic features of Pakistan: Part II *The Eastern Province Sci Ind* **4** 89-100

Bakshi A K (1995) Petrogenesis and timing of volcanism in the Rajmahal flood basalt Province, northeastern India *Chem Geol* **121** 73-90

Balakrishnan P and Mahesh Babu M (1987) The geology of the Ampani outlier, Kalahandi, Koraput district, Orissa. In: Purana Basins of Peninsular India (Middle to Late Proterozoic) (Ed: Radhakrishna B P) *Mem Geol Soc India* **6** 281-286

Balakrishnan S, Rajamani V and Hanson G N (1999) U-Pb ages for zircon and Titanite from the Ramagiri area, southern India: evidence for accretionary origin of the eastern Dharwar Craton during the late Archean *J Geol* **107** 69-86

Bandopadhyay B C and Sengupta S (2004) The Paleoproterozoic Supracrustal Kolhan Group in Singhbhum Craton, India and the Indo-African Supercontinent *Gond Res* **7** 1228-1235

Bandyopadhyay B K, Chattopadhyay A, Khan A S and Huin A K (2001) Assembly of the Rodinia supercontinent: evidence from the Sakoli and Sausar belts in Central India *Gond Res* **4** 569-570

Banerjee A, Bhattacharya S, Sajeev K and Santosh M (2013) Numerical simulations of CO2 migration during charnockite genesis *Geol* **41** 743-746

Banerjee D M (1996) A Lower Proterozoic Palaeosol at BGC-Aravalli Boundary in South-Central Rajasthan, India *J Geol Soc India* **48** 277-288

Banerjee D M and Bhattacharya P (1989) Petrofacies analysis of the clastic rocks in the Proterozoic Aravalli Basin, Udaipur district, south central Rajasthan *Indian Min* (Spec IGCP 217) **43** 194-225

Banerjee D M and Bhattacharya P (1994) Petrology and geochemistry of graywackes from the Aravalli Supergroup, Rajasthan, India and the tectonic evolution of a Proterozoic Sedimentary basin *Precamb Res* **67** 11-35

Banerjee D M and Saigal N (1988) A study of Proterozoic phosphorite from Chelima-Pacherla area, Kurnool district, Andhra Pradesh, India *J Geol Soc India* **32** 32-39

Banerjee D M, Phukan P, Joachimski M, Kaufman A J, Altermann W, Grover S, Mayr C and Suzane (2007) Evaporite sequence of the Nagaur-Ganganagar basin, Western Rajasthan - new data and new interpretation (Late Extended Abstract). *Intern Conf Precamb Sedi, Tectonics and Second GPSS meeting*, IIT, Bombay, 76-77

Banerjee D M and Russell J (1992) *Pb-Pb dating of Vindhyan stromatolites and a comparison with stromatolitic dates from other Proterozoic terrains*, Seminar on Recent Developments in Vindhyan Geology, Jadavapur University, (Abstract) p.33-34

Banerjee D M, Schidlowski M, Siebert F and Brasier M D (1997) Geochemical changes across the Proterozoic-Cambrian transition in the Durmala phosphorite mine section, Mussoorie Hills, Garhwal Himalaya, India *Palaeogeog Palaeoclim Palaeoeco* **132** 183-194

Banerjee D M, Strauss H, Bhattacharyya S K, Kumar V and Mazumdar A (1998) Isotopic composition of carbonates and sulphates, potash mineralization and basin architecture of the Nagaur-Ganganagar evaporate basin (north-western India) and their implications on the Neoproterozoic exogenic cycle *Miner Mag* **62** 106-107

Banerjee S, Dutta S, Paikary S and Mann U (2006) Stratigraphy, sedimentation and bulk organic geochemistry from the Proterozoic Vindhyan Supergroup (Central India) *J Earth Sys Sci* **45** 37-47

Banerji R K (1981) Cretaceous-Eocene sedimentation, tectonism and biofacies in the Bengal basin, India *Palaeogeogr Palaeoclim Palaeoecol* **34** 57-85

Banerji R K (1984) Post-Eocene biofacies, palaeoenvironments and palaeogeography of the Bengal basin, India *Palaeogeogr, Palaeoclim, Palaeoecol* **45** 49-73

Bangladesh Wikepedia

Barber A J, Khin Zaw and Crow M J (2017) Myanmar: Geol, Resources and Tectonics *Geol Soc London, Mem* **48** https://doi.org/10.1144/M48.1410.2

Bassoullet J P, Colchen M, Juteau T, Marcoux J, Mascle G and Reibel G (1982) Geological studies in the Indus suture zone of Ladakh (Himalayas) *Contrib Himal Geol* **2** 96-124

Bassoullet J P, Colchen M, Marcoux J andMascle G (1981) Field evidences for continental rifting in Triassic time in the Ladakh part of the Indus suture zone *Geol. Ecol. Studies* Qinghai-Xizang Plateau 1, Science Press, Beijing, 579-586

Basu A K (1986) Geology of parts of the Bundelkhand massif, central India *Rec Geol Surv* India **117** 61-124

Basu A R, Bandyopadhyay P K, Chakri R and Zou H (2008) Large 3.4 Ga Algoma type BIF in the Eastern Indian Craton *GeochimCosmochim Acta* **72** A59

Beaumont C, Jamieson R A, Nguyen M H and Lee B (2001) Himalayan tectonics explained by extrusion of a low-viscosity crustal channel coupled to focused surface denudation *Nature* **414** 738-742 doi:10.1038 /414738a

Bender F (1983) Geol of Burma. In: Bannert D (Ed) Beiträgezur Regionalen Geologieder Erde **16**. Gebrüder Born-traeger Berlin 1-293

Berger A R and Jayasinghe N R (1976) Precambrian structure and chronology in the highland series of Sri Lanka *Precamb Res* **3** 559-576

Bertrand G and Rangin C (2003) Tectonics of the western margin of the Shan plateau (central Burma): implication for the India-Indochina oblique convergence since Oligocene *J Asian Earth Sci* **21** 1139-1157 doi:10.1016/S1367-9120(02)00183-9

Bertrand G, Rangin C, Maluski H, Bellon H and the GIAC Scientific Party (2001) Diachronous cooling along the Mogok Metamorphic Belt (Shan scarp, Myanmar): the trace of the northward migration of the Indian syntaxis *J Asian Earth Sci* **19** 649-659

Bertrand G, Rangin C, Maluski H, Han T A, Thein M, Myint O, Maw W and Lwin S (1999) Cenozoic metamorphism along the Shan scarp (Myanmar): evidence for ductile shear along the Sagaing fault or the northward migration of the eastern Himalayan syntaxis? *Geophys Res Lett* **26** 915-918

Bhadra S, Gupta S and Banerjee M (2004) Structural evolution across the Eastern Ghats Mobile Belt-Bastar craton boundary, India: hot over cold thrusting in an ancient collision zone *J Struct Geol* **26** 233-245

Bhargava O N (1995) The Bhutan Himalaya: A Geol Account *Geol Surv India Spec Publ* 1-245

Bhargava O N (2008) An updated introduction to the Spiti geology *J Palaeont Soc India* **53** 93-129

Bhargava O N and Singh B P (2020) Geological evolution of the Tethys Himalaya *Episodes* **43** doi.org/10.18814/epiiugs/2020/020023

Bhargava O N, Kaur G and Deb M (2011) A Paleoproterozoic paleosol horizon in the Lesser Himalaya and its regional implications *J Asian Earth Sci* **42** 1371-1380

Bhaskar Rao Y J, Janardhan A S, Vijaya Kumar T, Narayana B L, Dayal A M, Taylor P N and Chetty T R K (2003) Sm-Nd model ages and Rb-Sr isotopic systematics of Charnockites Gneisses across the Cauvery Shear Zone, southern India: Implications to the Archaean - Neoproterozoic terrane boundary in the Southern Granulite Terrain. In: Tectonics of Southern Granulite Terrain Kuppam-Palani Geotransect (Ed: Ramakrishnan M) *Mem Geol Soc India* **50** 297-317

Bhaskar Rao Y J, Pantulu G V C, Reddy V D and Gopalan K (1995) Time of early sedimentation and volcanism in the Proterozoic Cuddapah basin, South India: evidence from the Rb-Sr age of Pulivendla mafic sill, In: Dyke Swarms of Peninsular India (Ed: Devaraju T C) *Mem Geol Soc India* **33** 329-338

Bhatia S B and Bhargava O N (2006) Biochronological continuity of the Paleocene sediments of the Himalayan Foreland Basin: paleontological and other evidences *J Asian Earth Sci* **26** 477-487

Bhattacharya G C and Yatheesh V (2015) Plate tectonic evolution of the deep ocean basins adjoining the western continental margin of India-a proposed model for the early opening scenario In: Petroleum Geoscience: Indian Contexts (Ed: Mukherjee S) *Springer Intern Publ* Switzerland 1-61

Bhattacharya S and Kar R (2002) High temperature dehydration melting and decompressive P-T path in a granulite complex from the Eastern Ghats, India. *Contrib Min Petrol* **143** 175-191, doi:10.1007/s00410-001-0341-6

Bhattacharya S, Kar R, Teixeira W and Basei M (2003) High-Temperature Crustal Anatexis in a Clockwise P-T Path: Isotopic Evidence from a Granulite-Granitoid Suite in the Eastern Ghats Belt, India *J Geol Soc London* **160** 39-46 doi:10.1144/0016-764902-063

Bhattacharya S, Sen S K and Acharyya A (1994) Structural setting of the Chilka Lake granulite-migmatite-anorthosite suite with emphasis on the time relation of charnockites *Precamb Res* **66** 393-409

Bhowmik S K and Dasgupta S (2012) Tectonothermal evolution of the BGC in central Rajasthan, NW India: present status and correlation *J Asian Earth Sci* **49** 339-348

Bhowmik S K and Roy A (2003) Garnetiferous metabasites from the Sausar Mobile Belt: petrology, P-T path and implications for the tectonothermal evolution of the Central Indian Tectonic Zone *J Petrol* **44** 387-420

Bhowmik S K, Dasgupta S, Baruah S and Kalita D (2018) Thermal history of a Late Mesoproterozoic paired metamorphic belt (?) during Rodinia assembly: New insight from medium-pressure granulites from the Aravalli-Delhi Mobile Belt, Northwestern India *Geosci Front* **9** 335-354

Bhowmik S K, Pal T, Pant N C and Shome S (2000) Implication of Ramakona cordierite gneiss in the crustal evolution of Sausar mobile belt in central India, Precambrian Crust in Eastern and Central India *Geol Surv India, Spec Publ* **57** 131-150

Bhowmik S K, Wilde S A, Bhandari A, Pal T and Pant N C (2012) Growth of the Greater Indian Landmass and its assembly in Rodinia: geochronological evidence from the Central Indian Tectonic Zone *Gond Res* **22** 54-72

Bhushan S K, Rao K N and Vidyadharan K T (2010) Petrography and geochemistry of St.Mary Islands near Malpe, Dakshina Kananada district, Karnataka. *J Geol Soc India* **76** 155-163

Bickford M E, Basu A, Mukherjee A, Hietpas J, Schieber J and Patranabis-Deb S (2011a) New U-Pb SHRIMP zircon ages of the Dhamda Tuff in the Mesoproterozoic Chhattisgarh Basin, peninsular India: stratigraphic implications and significance of a 1-Ga thermal-magmatic event *J Geol* **119** 535-548, doi:10.1086/661193

Bickford M E, Basu A, Mukherjee A, Hietpas J, Schieber J, Patranabis-Deb S, Ray R K, Guhey R, Bhattacharya P and Dhang P C (2011) New U-Pb SHRIMP zircon ages of the Dhamda Tuff in the Mesoproterozoic Chhattisgarh Basin, Peninsular India: stratigraphic implications and significance of a 1-Ga thermal-magmatic event *J Geol* **119** 535-548

Bickford M E, Basu A, Patranabis-Deb S, Dhang P C and Schieber J (2011b) Depositional history of the Chhattisgarh Basin, Central India: Constraints from new SHRIMP zircon ages *J Geol* **119** 33-50 doi: 10.1086/657300

Bidyananda M and Deomurari M P (2007) Geochronological constraints on the evolution of Megahalaya massif, northeastern India: an ion microprobe study *Curr Sci* **93** 1620-1623

Bijesh C M, John Kurian P, Yatheesh V, Tyagi A and Twinkle D (2018) Morphotectonic characteristics, distribution and probable genesis of bathymetric highs off southwest coast of India *Geomorp* **315** 33-44

Biju-Sekhar S, Yokoyama K, Pandit M, Okudaira T, Yoshida M and Santosh M (2003) Late Paleoproterozoic magmatism in Delhi Fold Belt, NW India and its implication: evidence from EPMA chemical ages of zircons *J Asian Earth Sci* **22** 189-207

Biswal T K, Gyani K C, Parthasarathy R and Pant D R (1998) Implications of the geochemistry of the pelitic granulites of the Delhi supergroup, Aravalli Mountain Belt, Northwestern India *Precamb Res* **87** 75-85

Biswal T K, Jena S K, Datta S, Das R and Khan K (2000) Deformation of the terrane boundary shear zone (Lakhna Shear Zone) between the Eastern Ghats Mobile belt and the Bastar craton, in Balangir and Kalahandi districts of Orissa *J Geol Soc India* **55** 367-380

Biswas S K (2008) Petroliferous basins of India-fifty years' history and perspective *Mem Geol Soc India* **66** 159-201

Blackburn W H and Srivastava D C (1994) Geochemistry and tectonic significance of the Ongarbirameta volcanic rocks. Singhbhum District, India *Precamb Res* **67**181-206

Blereau E, Clark C, Taylor R J M, Johnson T E, Fitzsimons I C W and Santosh M (2016) Constraints on the timing and conditions of high-grade metamorphism, charnockite formation and fluid-rock interaction in the Trivandrum Block, southern India *J Metamor Geol* **34** 527-549

Bodas M S, Khadri S F R and Subbarao K V (1988) Geol and stratigraphy of the Jawahar and Igatpuri Formations, Western Ghats lava pile, India *Mem Geol Soc India* **10** 253-280

Borneman N L, Hodges K V, van Soest M C, Bohon W, Wartho J-A, Cronk S S and Ahmad T (2015) Age and structure of the Shyok suture in the Ladakh region of northwestern India: Implications for slip on the Karakoram fault system *Tectonics* **34** 2011-2033 doi: 10.1002/2015TC003933

Bose M K (2008) Proterozoic dykes from Singhbhum granite pluton. In: Indian dykes (Eds: Srivastava R K, Sivaji Ch and Rao C) Narosa Publ New Delhi 413-445

Bose S, Fukuoka M, Sengupta S and Dasgupta S (2000) Evolution of high Mg-Al gran-ulites from Sunkarametta, Eastern Ghats, India: evidence for a lower crustal heating-cooling trajectory *J Metam Geol* **18** 223-240

Bose S, Seth P and Dasgupta N (2017) Meso-neoproterozoic mid-crustal metamorphic record from the Ajmer-Shrinagar section, Rajasthan, India and its implication to assembly of the Greater Indian landmass during the Grenvillian-age orogenesis. In: Crustal Evolution of India and Antarctica: The Supercontinent Connection (Eds: Pant N C and Dasgupta S) *Geol Soc London, Spec Publ* **457** https://doi.org/10.1144/SP457.7

Bouilhol P, Jagoutz O, Hanchar J M and Dudas F O (2013) Dating the India-Eurasia collision through arc magmatic records *Earth Planet Sci Lett* **366** 163-175

Boutonnet E, Leloup P H, Arnaud N, Paquette J-L, Davis W J and Hattori K (2012) Synkinematic magmatism, heterogeneous deformation, and progressive strain localization in a strike-slip shear zone: The case of the right-lateral Karakorum fault. *Tectonics* **31** TC4012 doi: 10.1029/2011TC003049

Brahmam N K and Negi J G (1973) Rift valleys beneath the Deccan Traps (India) *Geophys Res Bull* **11** 207-223

Bredow E and Steinberger B (2018) Variable melt production rate of the Kerguelen Hot Spot due to long-term Plume-Ridge interaction *Geophys Res Lett* **45** 126-136, doi: 10.1002/2017/GL075822

Brookfield M E and Andrew-Speed C P (1984) Sedimentation in high-altitude intermontane basin-The Wakka Chu Molasse (Mid. Tertiary, Northwestern India) *Bull Indian Geol Assoc* **17** 175-193

Brown E T, Bendick R, Bourles D L, Gaur V, Molnar P, Raisbeck G M and Yiou F (2002) Slip rates of the Karakoram fault, Ladakh, India, determined using cosmic ray exposure dating of debris flows and morains *J Geophys Res* **107** 2192 doi: 10.1029/2000JB000100

Brown M and Raith M (1996) First evidence of ultrahigh-temperature decompression from the granulite province of southern India *J Geol Soc* **153** 819-822

Brunnschweiler R O (1966) On the Geol of the Indoburman Ranges *J Geol Soc Australia* **13** 137-194

Brunnschweiler R O (1974) Indoburman Ranges. In: Mesozoic-Cenozoic Orogenic Belts: Data for Orogenic Studies (Eds: Spencer A M) *Geol Soc London Spec Publ* **4** 279-299

Bryan S E and Ernst R E (2008) Revised definition of Large Igneous Provinces (LIPs) *Earth Sci Rev* **86** 175-202

Buick I S, Allen C, Pandit M, Rubatto D and Herman J (2006) The Proterozoic magmatic and metamorphic history of the BGC, central Rajasthan, India: LA-ICP-MS U-Pb zircon constraints *Precamb Res* **151** 119-142

Burbank D W (1992) Causes of recent Himalayan uplift deduced from deposited patterns in the Ganges Basin *Nature* **357** 680-682

Burchfield B C, Zhilang C, Hodges K V, Yuping L, Roden L H, Changong D and Jiene X (1992) The South Tibetan Detachment System, Himalayan Orogen: Extension contemporaneous with parallel to shortening in collisional mountain belt *Geol Soc Amer Bull* **26 9**1-42

Calvés G, Schwab A M, Huuse M, Clift P D, Gaina C, Jolley D, Tabres A R and Inam A (2011) Seismic volcano stratigraphy of the western Indian rifted margin: the pre-Deccanigneous province *J Geophy Res* **116** 1101:28, doi:10.1029/2010JB000862

Carosi R, Montomoli C and Iaccarino S (2018) 20 years of geological mapping of the metamorphic core across Central and Eastern Himalayas *Earth Sci Rev* **177** 124-138

Carosi R, Montomoli C, Rubatto D and Visonà D (2013) Leucogranite intruding the South Tibetan Detachment in western Nepal: implications for exhumation models in the Himalayas *Terra Nova* **25** 478-489, doi:10.1111/ter.12062

Catlos E J, Pease E C, Dygert N, Brookfield M, Schwarz W H, Bhutani R, Pande K and Schmitt A (2018) Nature, Age, and Emplacement of the Spongtang Ophiolite, Ladakh, NW India *J Geol Soc, London* doi: https://doi.org/10.1144/

jgs2018-085

Célérier J, Harrison T M, Webb A A G and Yin A (2009) The Kumaun and Garhwal Lesser Himalaya, India Part 1 Structure and stratigraphy *Geol Soc Amer Bull* **121** 1262-1280

Chacko T, Ravindra Kumar G R and Newton R C (1987) Metamorphic P-T conditions of the Kerala (South India) Khondalite belt: a granulite-facies supracrustal terrain *J Geol* **96** 343-358

Chadwick B, Vasudev V N and Hedge G V (2000) The Dharwar craton, southern India, interpreted as the result of Late Archaean oblique convergence *Precamb Res* **99** 91-101

Chakraborty P P (2006) Outcrop signatures of relative sea-level fall on a siliclastic shelf: Examples from the Rewa Group of Proterozoic Vindhyan basin *J Earth Sys Sci* **115** 23-36

Chakraborty P P, Paul S and Das A (2005) Facies development and depositional environment of the Mungra Sandstone, Kolhan Group, Eastern India *J Geol Soc India* **65** 753-757

Chanda S K and Bhattacharya A (1982) Vindhyan: post Auden developments, In: Geology of Vindhyachal Hindustan Publ Corp New Delhi (Eds: Valdiya K S, Bhatia S B and Gaur V K) 88-101

Chandra J, Paul D, Viladkar S G and Sensarma S (2018) Origin of the Amba Dongar carbonatite complex, India and its possible linkage with the Deccan Large Igneous Province. In: Large Igneous Provinces from Gondwana and adjacent regions (Eds: Sensarma S and Storey B C) *Geol Soc Spec Publ* **463** 137-169

Chandrasekharam D (1985) Structure and evolution of the western continental margin of India deduced from gravity, seismic, geomagnetic and geochronological studies *Phys Earth Planet Int* **81** 186-198

Chardon D, Choukroune P, Jayananda M (1996) Strain patterns, de´collement and incipient sagducted greenstone terrains in the Archaean Dharwar craton (south India) *J Struct Geol* **18** 991-1004

Chatterjee N (2017) Constraints from monaziteandxe no time growth modeling in the MnCKFMASH-PYCe system on the P-T path of a metapelite from Shillong-Meghalaya Plateau: implications for the Indian shield assembly *J Metamor Geol* **35** 393-412

Chatterjee N, Mazumadar A C, Bhattacharya A and Saikia R R (2007) Mesoproterozoic granulites of the Shillong-Meghalaya plateau: Evidence of westward continuation of the Prydz Bay Pan-African suture into northeastern India *Precamb Res* **152** 1-26

Chattopadhyay S, Upadhyay D, Nanda J K, Mezger K, Pruseth K L and Berndt J (2015) Proto-India was a part of Rodinia: evidence from Grenville-age suturing of the Eastern Ghats Province with the Paleoarchean Singhbhum Craton *Precamb Res* **266** 506-529, https://doi.org/10.1016/j.precamres.2015.05.030

Chaudhuri A K, Deb G K, Patranabis-Deb S and Sarkar S (2012) Paleogeographic and tectonic evolution of the Pranhita-Godavari Valley, Central India: a stratigraphic perspective *Amer J Sci* **312** 766-815

Chaudhuri A, Banerjee S and Chauhan G (2020) Compositional evolution of siliciclasticsediments recording tectonic stability of apericratonicrift: Mesozoic Kutch Basin, western India *Marine Petrol* Geol **111** 476-495

Chaudhury T, Wan Y, Mazumder R, Ma M and Liu D (2018) Evidence of Enriched, Hadean Mantle Reservoir from 4.2-4.0 Ga zircon xenocrysts from Paleoarchean TTGs of the Singhbhum Craton, Eastern India *Sci Rep* **8** 7069 doi:10.1038/s41598-018-25494-6

Chemenda A I, Burg J P andMattauer M (2000) Evolutionary model of the Himalaya-Tibet system: geopoem based on new modeling, geological and geophysical data *Earth Planet Sci Lett* **174** 397-409

Chetty T R K (2017) Proterozoic orogens of India. A critical window to Gondwana *Elsevier Inc* 1-395

Chhibber H L (1934a) The Geol of Burma. Macmillan, London

Chhibber H L (1934b) The Mineral Resources of Burma. Macmillan, London

Chimote J S, Pandey B K, Bagchi A K, Basu A N, Gupta J N and Saraswat A C (1988) Rb-Sr whole-rock isochron age for the Mylliem Granite, E.K. Hills, Meghalaya Proc 4th Nat Sym Mass Spectrom, IISC, Bangalore

Choudhary A K, Gopalan K and Sastry C A (1984) Present status of the geochronology of the Precambrian rocks of Rajasthan *Tectonophy* **105** 131-140

Clift P D (2017) Cenozoic sedimentary records of climate-tectonic coupling in the Western Himalaya *Progr Earth Planet Sci* **4** 39 Doi: 10.986/s40645-017-0151-8

Clift P D, Degnan P J, Hannigan R andBlusztajn J (2000) Sedimentary and geochemical evolution of the Dras forearc basin, Indus Suture, Ladakh Himalaya, India *Geol Soc Amer Bull* **112** 450-466

Coffin M F, Pringle M S, Duncan R A, Gladczenko T P, Storey M, Muller R D and Gahagan L A (2002) Kerguelen hotspot magma output since 130 Ma *J Petrol* **43** 1121-1139

Collier J S, Sansom V, Ishizuka O, Taylor R N, Minshull T A and Whitmarsh R B (2008) Age of Sychelles-India break-up. *Earth Planet Sci Lett* **272** 264-277

Collins A S, Patranabis-Deb S, Alexander E, Bertram C N, Falster G M, Gore R J, Mackintosh J, Dhang P C, Saha D, Payne J L, Jourdan F, Backe G, Halverson G P and Wade B P (2015) Detrital mineral age, radiogenic isotopic stratigraphy and tectonic significance of the Cuddapah Basin, India *Gond Res* **28** 1294-1309

Collins A S, Santosh M, Braun I and Clark C (2007) Age and sedimentary provenance of the southern granulites, South India: U-Th-Pb SHRIMP secondary ion mass spectrometry *Precamb Res* **155** 125-138

Cooray P G (1994) The Precambian of Sri Lanka: a historical review *Precamb Res* **66** 3-18

Copley A, Avouac J P and Royer J Y (2010) India-Asia collision and the Cenozoic slowdown of the Indian plate: Implications for the forces driving plate motions *J Geoph Res* **95** B03410, doi:10.1029/2009JB006634

Copley A, Avouac J P and Royer J-Y (2010) India-Asia collision and the Cenozoic slowdown of the Indian plate: Implications for the forces driving plate motions *J Geophys Res* **95** B03410, doi:10.1029/2009JB006634

Corfield R I, Searle M P and Pedersen R B (2001) Tectonic setting and obduction history of the Spontang ophiolite, Ladakh Himalaya, NW India *J Geol* **109** 715-736

Courtillot V, F´eraud G, Maluski H, Vandamme D, Moreau M G and Besse J (1988) Deccan Flood basalts and the Cretaceous/Tertiary boundary *Nature* **333** 843-846

Cox K G and Hawkesworth C J (1985) Geochemical stratigraphy of the Deccan Traps at Mahabaleshwar, Western Ghats, India, with implications for open-system magmatic processes *J Petrol* **26** 355-377

Cozzi A, Rea G and Craig J (2012) From global geology to hydrocarbon exploration: Ediacaran-Early Cambrian petroleum plays of India, Pakistan and Oman. In: Geology and Hydrocarbon Potential of Neoproterozoic-Cambrian Basins in Asia (Eds: Bhat G M, Craig J, Thurow J W, Thusu B and Cozzi A) *Geol Soc London Spec Publ* **366** 131˘162, http://dx.doi.org/10.1144/SP366.14

Crawford A R and Compston W (1970) The age of the Vindhyan system of Peninsular India *Quart J. Geol Soc London* **25** 351-371

Curray J R and Munasinghe T (1991) Origin of the Rajmahal Traps and the 85jE Ridge: preliminary reconstructions of the trace of the Crozet hotspot *Geol* **19** 1237-1240

Curray J R, Emmel F J and Moore D G (2003) The Bengal Fan: morphology, geometry, stratigraphy, history and processes *Marine Petrol Geol* **19** 1191-1223

Curray J R, Emmel F J, Moore D G and Raitt R W (1982) Structure, tectonics and geological history of the northeastern Indian Ocean In: The Ocean Basins and Margins. The Indian Ocean (Eds: Nairn A E M and Stehli F G) *Plenum, New York* **6** 399-450

Curray J R, Moore D G, Lawver L A, Emmel F J and Raitt R W (1979) Tectonics of the Andaman Sea and Burma. In: Geological and Geophysical Investigations of Continental Margins (Eds: Watkins J, Montadert L and Dickenson P W) *Amer Assoc Petrol Geol Mem* **29** 189-198

Dailey S K, Clift P D, Kulhanek D K, Blusztajn J, Routledge C M, and others (2019) Large-scale mass wasting on the Miocenecontinental margin of western India *Geol Soc Amer Bull* **28**, doi:10.1130/B35158

Das B P, Joshi M and Kumar A (2019) Tectonochemistry and P-T Conditions of Ramgarh and Almora Gneisses from Askot Klippe, Kumaun Lesser Himalaya *Acta Geol Sinica* **93** 322-343

Das J D, Saraf A K and Jain A K (1995)Fault tectonics of the Shillong plateau and adjoining regions, north-east India using remote sensing data *Int J Remote Sensing* **16** 1633-1646

Das K, Yokoyama K, Chakraborty P P and Sarkar A (2009) EPMA U-Th-Pb Monazite dating and trace element geochemistry of tuff units from the basal part of Chhattisgarh and Khariar basin, central India: implications for basin initiation and depositional contemporaneity *J Geol* **117** 88-102

Das L K, Mishra D C, Ghosh D and Banerjee B (1990) Geomorphotectonics of the Basement in a part of the Upper Son Valley of the Vindhyan Basin *J Geol Soc India* **35** 445-458

Dasgupta S and Sengupta P (1995) Ultrametamorphism in Precambrian granulite terrains-evidence from Mg-Al granulites and calc-granulites of the Eastern Ghats, India *J Geol* **30** 307-318

Dasgupta S and Sengupta P (2003) Indo-Antarctic correlation: a perspective from the Eastern Ghats granulite belt, India. In: Proterozoic East Gondwana: Supercontinent Assembly and Breakup (Eds: Yoshida M, Windley B F and Dasgupta S) *Geol Soc London, Spec Publ* **206** 131-143

Dasgupta S, Bose S and Das K (2013) Tectonic evolution of the Eastern Ghats Belt, India *Precamb Res* **227** 247-258

Dasgupta P K, Chakrabarti P K and Datta D (1991) Basinward migrating submarine fan environments from the Barail group in the north Cachar Hills, Assam-Arakan Orogen, India. In: Facies Models (Eds: Bouma A H and Carter R M) 195-217Das S, Basu A R and Mukherjee B K (2017) In situ peridotitic diamond in Indus ophiolite sourced from hydrocarbon fluids in the mantle transition zone *Geol*, doi:10.1130/G39100.1

Das S, Shukla D, Bhattacharjee S and Mitra S K (2015) Age constraints of Udayagiri domain of Nellore schist belt by xenotime dating around Pamuru, Prakasam district, Andhra Pradesh *J Geol Soc India* **85** 289-298

Datta B (1998) Stratigraphic and sedimentologic evolution of the Proterozoic siliciclastics in the southern part of Chhattisgarh and Khariar, central India *J Geol Soc India* **51** 345-360

Dayal A M, Devleena M, Kavitha S, Kalpana M S, Patil I J and Sharma M (2018) Organic geochemistry of the Vindhyan sediments: Implication for hydrocarbons *J Asian Earth Sci* **91** 329-338, doi:10.1016/j.jseaes.2014.03.010

de Sigoyer J, Chavagnac V, Blichert-Toft J, Villa I M, Luais B, Guillot S, Cosca M and Mascle G (2000) Dating the Indian continental subduction and collisional thickening in the northwest Himalaya: Multichronology of the Tso Morari eclogites *Geol* **28** 487 490

De Wall H, Pandit M K and Chauhan N K (2012) Paleosol occurrences along the Archean-Proterozoic contact in the Aravalli Craton, NW India *Precamb Res* **216** 120-131

Deb M and Thorpe R I (2004) Geochronological constraints in the Precambrian geology of Rajasthan and their metallogenic implications: Sediment-Hosted Lead-Zinc Sulphide Deposit. Narosa Publishing House New Delhi 246-263

Deb M, Thorpe R I, Cumming G L and Wagner P A (1989) Age, Source and Stratigraphic Implications of Pb Isotope Data for Conformable, Sediment-hosted, Base Metal Deposits in the Proterozoic Aravalli-Delhi Orogenic Belt, Northwestern India *Precamb Res* **43** 1-22

Deb M, Thorpe, R I, Kristic D, Corfu F and Davis D W (2001) Zircon U-Pb and galena Pb-isotope evidence for an approximate 1.0 Ga terrane constituting the western margin of the Aravalli-Delhi orogenic belt, northwestern India *Precamb Res* **108** 195-213

Desa M A, Ramprasad T and Raju K A (2019) An integrated geophysical study east of the southern Chagos Laccadive Ridgecomplex, Central Indian Ocean Basin: Implications for the Rodriguez Triple Junction dynamics in the Late Cretaceous *Marine Geol* **414** 47-63

Deshmukh S S (1988) Petrological variations in compound flows in Deccan Traps and their significance *Mem Geol Soc India* **10** 305-319

Dessai A G and Bertrand H (1995) The "Panvel flexure' along the western Indian continental margin: an extensional fault structure related to Deccan magmatism *Tectonophy* **241** 165-178

Dewey J F and Bird J M (1970) Mountain belts and the new global tectonics *J Geophys Res* **75** 2625 2647

Dey S, Halla J, Kurhila M, Nandy J, Heilimo E and Pal S (2016) Geochronology of Neoarchean granitoids of the NW eastern Dharwar craton: implications for crust formation. In: Crust-Mantle Interactions and Granitoid Diversification: Insights from Archaean Cratons (Eds: Halla J, Whitehouse M J, Ahmad T and Bagai Z) *Geol Soc, London, Spec Publ* **449** http://doi.org/10.1144/SP449.9

Dey S, Topno A, Liu Y and Zong K (2017) Generation and evolution of Palaeoarchaean continental crust in the central part of the Singhbhum craton, eastern India *Precamb Res* **298** 268-291 doi.org/10.1016/j.precamres.2017.06.009

Dey S, Pal S, Balakrishnan S, Halla J, Kurhila M and Heilimo E (2018) Both plume and arc: origin of Neoarchaean crust as recorded in Veligallu greenstone belt, Dharwar craton, India *Precamb Res* doi: https://doi.org/10.1016/j. precamres. 2018. 04.019

Dharma Rao C V, Santosh M and Wu Y (2011) Mesoproterozoic ophiolitic mélange from the SE periphery of the Indian plate: U-Pb zircon ages and tectonic implications *Gond Res* **19** 384-401

Dharma Rao C V, Santosh M, Purohit R, Wang J, Jiang X and Kusky T (2011) LA-ICP-MS U-Pb zircon age constraints on the Paleoproterozoic and Neoarchean history of the Sandmata Complex in Rajasthan within the NW Indian Plate *J Asian Earth Sci* **42** 286-305

Dharmapriya P L, Malaviarachchi S P K, Kriegsman L M, Galli A, Sajeev K and Zhang C (2017) New constraints on the P-T path of HT/UHT metapelites from the Highland Complex of Sri Lanka *Geoscien Front* **8** 1405-1430

Dhiman R and Singh S (2020) Neoproterozoic and Cambro-Ordovician magmatism: episodic growth and reworking of continental crust, Himachal Himalaya, India *Internat Geol Rev*, doi.org/10.1080/00206814.2020.1716399

Dietrich V, Frank W, Gansser A and Honneger K H (1983) A Jurassic-Cretaceous island arc in the Ladakh-Himalayas *J Volcanol Geotherm Res* **18** 405-433

Dikshit K R (2001) The Western Ghat: A geomorphic overview. In: Sahyadri (Eds: Gunnell Y and Radhakrishna B P) *Geol Soc India Mem* **47** 159-183

Dobmeier C and Raith M (2003) Crustal architecture and evolution of the Eastern Ghats Belt and adjacent regions of India. In: Proterozoic east Gondwana: Supercontinent assembly and breakup (Eds: Yoshida M, Windley B F and Dasgupta S) *Geol Soc, London, Spec Publ* **206** 145-168

Dobmeier C, Lutke S, Hammerschmidt K andMezger K (2006) Emplacement and deformation of the Vinukonda meta-granite (Eastern Ghats, India)-implications for the geological evolution of peninsular India and for Rodinia reconstructions *Precamb Res* **146** 165-178

Drury S A and Holt R W (1980) The tectonic framework of the south India craton: A reconnaissance involving Landsat imagery *Tectonophy* **65** T1-T15

Drury S A, Harris N B, Holt R W, Reeves-Smith G J , Wightman R T (1984) Precambrian tectonics and crustal evolution in South India *J Geol* **92** 3-20

Duncan R A and Pyle D G (1988) Rapid eruption of the Deccan Flood Basalt at the Cretaceous -Tertiary Boundary *Nature* **333** 841-843

Dunlap W J and Wysoczanski R (2002) Thermal evidence for early Cretaceous metamorphism in the Shyok suture zone and age of the Khardung volcanic rocks, Ladakh, India *J Asian Earth Sci* **20** 481-490, doi:10.1016/S1367-9120(01)00042-6

Dupont Nivet G, van Hinsbergen D J J and Torsvik T H (2010) Persistently low Asian paleolatitudes: Implications for the India Asia collision history *Tectonics* **29** TC5016, doi:10.1029/2008TC002437

Eagles G and Hoang H H (2013) Cretaceousto present kinematics of the Indian, African and Seychelles plates *Geophy J Int* **196** 1-14,doi:10.1093/gji/ggt372

Ehiro M, Kojima S, Sato T, Ahmad T and Ohtani T (2007) Discovery of Jurassic ammonoids from the Shyok suture zone to the northeast of Chang La pass, Ladakh, northwest India and its tectonic significance *Island Arc* **16** 124-132

Emmel B, Lisker F and Hewawasam T (2012) Thermochronological dating of brittle structures in basement rocks: A case study from the onshore passive margin of SW Sri Lanka *J Geophys Res* **117** B10407, doi:10.1029/2012JB009136

Epard J L and Steck A (2008) Structural development of the Tso Morari ultra-high pressure nappe of the Ladakh Himalaya *Tectonophy* **451** 242-264

Eriksson K A and Simpson E L (2004) Precambrian tidalites: recognition and significance. In: The Precambrian Earth: tempos and events (Eds: Eriksson P G, Altermann W, Nelson D R, Mueller W U and Cateneau O) *Develop Precamb Geol Amsterdam 7 Elsevier Science* **12** 631-642

Evans P (1932) Tertiary succession in Assam *Trans Min Geol Inst India* **27** 155-260

Evans P (1964) Tectonic framework of Assam *J Geol Soc India* **5** 80-96

Fareeduddin and Banerjee D M (2020) Aravalli Craton and Mobile Belt: An update. In: Geodynamic Evolution of Indian Subcontinent (Eds: Faredduddin et al.) *Spec Issue Episodes* **43**

Fareeduddin and Kröner A (1998) Single zircon age constraints on the evolution of Rajasthan granulites. In: Precambrian Rocks of India (Ed: Paliwal B S) 547-556

Fareeduddin, Kirmani T R, Srivastava B L, Reddy A B and Bhattacharya J (1995) Lamprophyre dykes in South Delhi fold belt near Pipela, district Sirohi, Rajasthan *J Geol Soc India* **46** 255-261

Faruque B M and Ramachandran K V (2014) The continental shelf of western India. In: Continental shelves of theWorld: their evolution during the last glacio-eustatic cycle (Eds: Chiocci F L, Chivas A R) *Mem Geol Soc London* **41** 213-220

Frank W, Thoni M and Purtscheller F (1977) Geology and petrography of Kulu-south Lahul area. *Colloq Int CNRS Himalaya* **268** 147-160

French J E, Heaman L M, Chacko T and Srivastava R K (2008) 1891-1883 Ma Southern Bastar-Cuddapah mafic igneous events, India: a newly recognized large igneous province *Precambr Res* **160** 308-322

Friend C R L and Nutman A P (1991) SHRIMP U-Pb geochronology of the Closepet granite and Peninsular gneisses, Karnataka, South of India *J Geol Soc India* **38** 357-368

Ganguly J, Dasgupta S, Cheng W and Neogi S (2000) Exhumation history of a section of the Sikkim Himalaya, India: records in the metamorphic mineral equilibria and compositional zoning of garnet *Earth Planet Sci Lett* **183** 471-486

Gani M R and Alam M M (1999) Trench-slope controlled deep-sea clastics in the exposed lower Surma group in the southeastern fold belt of the Bengal Basin, Bangladesh *Sedim Geol* **127** 221-236

Gansser A (1964) Geology of the Himalayas *Intersci Publ*, John Wiley & Sons Ltd. London 1-289

Garzanti E and van Haver T (1988) The Indus clastics: Forearc basin sedimentation in the Ladakh Himalaya (India) *Sedim Geol* **59** 237 249

Garzanti E, Baud A and Mascle G (1987) Sedimentary record of the northward flight of India and its collision with Eurasia (Ladakh Himalaya, India) *Geodynam Acta* **1** 297 312

Gavillot Y, Meigs A J, Sousa F J, Stockli D, Yule D and Malik M (2018) Late Cenozoic foreland-to-hinterland low-temperature exhumation history of the Kashmir Himalaya *Tectonics* **37** doi.org/10.1029/2017TC004668

George B G, Ray J S, Shukla A D, Chatterjee A, Awasthi N and

Laskar A H (2018) Stratigraphy and geochemistry of the Balwan Limestone, Vindhyan Supergroup, India: Evidence for the Bitter Springs $\delta^{13}C$ anomaly *Precamb Res* **313** 18-30, doi:10.1016/j.precamres.2018.05.008

Ghose N C, Chatterjee N and Fareeduddin (2014) A petrographic atlas of ophiolite: An example from the eastern India-Asia Collision Zone *Springer* 1-234

Ghosh S, Chakraborty S, Bhalla JK, Paul DK, Sarkar A, Bishui PK Gupta SN (1991) Geochronology and geochemistry of granite plutons from East Khasi Hills, Meghalaya. *J Geol Soc India* **73** 331-342

Ghosh D K, Sarkar S N, Saha A K, Ray S L (1996) New insights on the early Archaean crustal evolution in eastern India: re-evaluation of Pb-Pb, Sm-Nd and Rb-Sr geochronology. *Indian Min* **50** 175-188

Ghosh G, Ghosh B and Mukhopadhyay J (2015) Palaeoarchaean-Mesoproterozoic sedimentation and tectonics along the west-northwestern margin of the Singhbhum Granite body, eastern India: a synthesis. In: Precambrian Basins of India: Stratigraphic and Tectonic Context (Eds: Mazumder R and Eriksson P G) *Geol Soc London Mem* **43** 121-138 doi.org/10.1144/M43.9

Ghosh J G (2004) 3.56 Ga tonalite in the central part of the Bastar Craton, India: oldest Indian date. *J Asian Earth Sci* **23** 359-364

Ghosh J G, De Wit M J and Zartman R E (2004) Age and tectonic evolution of Neoproterozoic ductile shear zonesin the Southern Granullite Terrain of India, with implications for Gondwana studies *Tectonics* **23** TC3006, doi 10.1029/2002TC001444

Ghosh S, Fallick A E, Paul D K and Potts P J (2005) Geochemistry and origin of Neoproterozoic granitoids of Meghalaya, Northeast India: implication for linkage with amalgamation of Gondwana Supercontinent *Gond Res* **8** 421-432

Goodbred S L Jr and Kuehl S A (1999) Holocene and modern sediment budgets for the Ganges Brahmaputra river system: evidence for highst and disper salt of lood plain, shelf and deep-seadepocenters *Geol* **27** 559-562

Goodbred S L Jr and Kuehl S A (2000) The significance of large sediment supply, active tectonism and eustasy on marginal sequence development: Late Quaternary Stratigraphy and Evolution of Ganga-Brahmaputra delta *Sedim Geol* **133** 227-248

Gopalan K, Macdougall J, Roy A and Murali A (1990) Sm-Nd evidence for 3.3 Ga old rocks in Rajasthan, northwestern India *Precamb Res* **48** 287-297

Goswami J N, Misra S, Wiedenbeck M, Ray Sla and Saha A K (1995) 3.55 Ga old zircon from Singhbhum-Orissa Iron-Ore craton, eastern India *Curr Sci* **69** 1008-1011

Goswami-Banerjee S, Bhowmik S K, Dasgupta S and Pant N C (2014) Burial of thermally perturbed Lesser Himalayan mid-crust: Evidence from petrochemistry and P-T estimation of the western Arunachal Himalaya, India *Lithos* **208-209** 298-311

Govin G, Najman Y, Copley A, Millar I, van der Beek P, Huyghe P, Grujic D and Davenport J (2018) Timing and mechanism of the rise of the Shillong Plateau in the Himalayan foreland *Geology* **46** 279-282

Graham S A, Dickinson W R and Ingersoll R V (1975) Himalayan-Bengal model for flysch dispersal in the Appalachian-Ouachita system *Geol Soc Amer Bull* **94** 273-286

Grujic D (2006) Channel Flow and continental collision tectonics. In: Channel Flow, Ductile Extrusion and Exhumation in Continental Collision Zones (Eds: Law R D, Searle M P and Godin L) *Geol Soc Spec Publ* **268** 25-37

GSI and ISRO (1994) Project Yasundhara: Generalised geological map Geol Surv India and Indian Space Res Organ Publ

Guillot S, de Sigoyer J, Lardeaux J M and Mascle G (1997) Eclogitic metasediments from the Tso Morari area (Ladakh, Himalaya): evidence for continental subduction during India-Asia convergence *Contrib Mineral Petrol* **128** 197-212

Guillot S, Mahéo G, de Sigoyer J, Hattori K H and Pêcher A (2008) Tethyan and Indian subduction viewed from the Himalayan high-to ultrahigh-pressure metamorphic rocks *Tectonophy* **451** 225-241

Guitreau M, Mukusa S B, Loudin L and Krishnan S (2017) New constraints on early formation of western Dharwarcraton (India) from igneouszircon U-P band Lu-Hf isotopes *Precamb Res* **302** 33-49 doi.org/10.1016/j.precamres.2017.09.016

Gunnell Y (2001b) Morphology and scarprecession rates of the Western Ghats Escarpment *Mem Geol Soc India* **47** 89-117

Guo X, Li W, Gao R, Xu X, Li H, Huang X, Ye Z h, Lu Zh and Klemper S L (2017) Nonuniform subduction of the Indian crust beneath the Himalayas *Sci Rep* **7** 12497, Doi:10.1038/s41598-017-12908-0

Gupta A, Basu A and Ghosh P K (1980) The Proterozoic ultramafic and mafic lavas and tuffs of the Dalma greenstone belt, Singhbhum, eastern India *Can J Earth Sci* **17** 210-231

Gupta H K, Arora K, Rao N P, Roy S, and others (2017) Investigations of continued reservoir triggered seismicity at Koyna, India. In: Tectonics of the Deccan Large Igneous Province (Eds Mukherjee S, Misra A, Calves G and

Nemèok M). *Geol Soc London Spec Pub* **445** 151-188

Gupta P and Bose U (2000) An update on Geology of the Delhi Supergroup in Rajasthan *Geol Surv India Spec Publ* **55** 287-366

Gupta P, Fareeduddin, Reddy M S and Mukhopadhyay K (1995) Stratigraphy and structure of Delhi Supergroup of rocks in central part of Aravalli Range *Rec Geol Surv India* **120** 12-26

Gupta S N, Arora Y K, Mathur R K, Iqbaluddin, Prasad B, Sahai T N and Sharma S B (1980) 1:1000,000 Lithostratigraphic map of Aravalli region, southern Rajasthan and northeastern Gujarat. *Geol Surv India Publ* Calcutta-Hyderabad.

Gupta S N, Arora Y K, Mathur R K, Iqbaluddin, Prasad B, Sahai T N and Sharma S B (1997) Precambrian geology of the Aravalli region, southern Rajasthan and northeastern Gujarat *Mem Geol Surv India* **123** 262

Gupta S N, Arora Y K, Mathur R K, Iqbaluddin, Prasad B, Sahai T N, Sharma S B, Sahai B P and Sharma S B (1980) 1:1000,000 Lithostratigraphic map of Aravalli region, southern Rajasthan and northeastern Gujarat *Geol Surv India* Calcutta-Hyderabad

Gupta S N, Arora Y K, Mathur, R K, Iqbaluddin, Prasad B, Sahai T N and Sharma S B (1997) Precambrian geology of the Aravalli region, southern Rajasthan and northeastern Gujarat. *Mem Geol Survey India* 262pp

Gupta, 1934; Gupta BC (1934) The geology of central Mewar. *Geol Surv India Mem* **65** 107-169

Guzman-Speziale M and Ni J F (1996) Seismicity and active tectonics of the western Sunda Arc. In: The Tectonic Evolution of Asia (Eds: Yin A and Harrison T M) *Cambridge Univ Press* New York 63-84

Haldar D and Ghosh R N (2000) Eruption of Bijawar lava: an example of Precambrian volcanicity under stable cratonic conditions. In: Precambrian Crust in Eastern and Central India *Geol Surv India Hyderabad Spec Publ* **57** 151-170

Hari Prasad B, Okudaira T, Hayasaka Y, Yoshida M and Divi RS (2000) Petrology and geochemistry of amphibolites from the Nellore-Khammam schist belt, SE India *J Geol Soc India* **56** 67-78

Hazarika P, Pruseth K L and Mishra B (2015) Neoarchean Greenstone metamorphism in the Eastern Dharwar Craton, India: Constraints from monazite U-Th-Pb_{total} ages and PT pseudosection calculations *J Geol* **123** 429-461

He X-F, Santosh M, Tsunogae T, Malaviarachchi S P K and Dharmapriya P L (2016) Neoproterozoic arc accretion along the 'eastern suture' in Sri Lanka during Gondwana assembly *Precamb Res* **279** 57-80

Heim A and Gansser A (1939) Central Himalaya Geological Observations of the Swiss Expedition 1936 *Mem de la Socie´te´ Helvetique des Sci Naturelles* **73** Reprint 1975 Hindustan Publ Corp (India) 1-245

Heron A M (1953) The Geology of central Rajputana *Mem Geol Surv India* **79** 1-389

Herren E (1987) Zanskar Shear Zone: northeast-southwest extension within the Higher Himalaya (Ladakh, India) *Geology* **15** 409-413

Hiller K and Elahi M (1988) Structural growth and hydrocarbon entrapment in the Surma basin, Bangladesh In: Petroleum Resources of China and Related Subjects, Houston, Texas (Eds: Wagner H C, Wagner L C, Wang F F H and Wong F L) *Circum-Pacific Council for Energy and Mineral Resources Earth Sci Series* **10** 657-669

Hodges K V (2000) Tectonics of the Himalaya and southern Tibet from two perspectives *Geol Soc Amer Bull* **92** 324-350

Holtrop JF and Keizer J (1970) Some aspects of the stratigraphy and correlation of the Surma basin wells, East Pakistan *ESCAFE Miner Resour Dev Ser* **36** 143-154

Honegger K, Dietrich V, Frank W, Gansser A, Thoni M and Trommsdorff, V (1982) Magmatism and metamorphism in the Ladakh Himalaya the Indus-Tsangpo suture zone *Earth Planet Sci Lett* **60** 253-292

Hooper P, Widdowson M and Kelley S (2010) Tectonic setting and timing of the final Deccan flood basalt eruptions *Geol* **38** 839-842

Horton F and Leech M L (2013) Age and origin of granites in the Karakoram shear zone and Greater Himalaya Sequence, NW India *Lithosph* **5** 300-320, doi:10.1130/L213

Hossain I, Tsunogae T, Rajesh H M, Chen B and Arakawa Y (2007) Palaeoproterozoic U-Pb SHRIMP zirconage from basement rocks in Bangladesh: a possible remnant of the Columbia supercontinent *C R Geoscience* **339** 979-986

Hossain I, Tsunogae T, Tsutsumi Y and Takahashi K (2017) Petrology, geochemistry and LA-ICP-MSU-Pb geochronology of Paleoproterozoic basement rocks in Bangladesh: an evaluation of calc-alkaline magmatism and implication for Columbia supercontinent amalgamation *J Asian Earth Sci* **157** 22-39

Hou G, Santosh M, Qian X, Lister G S and Li J (2008) Conûguration of the Late Paleoproterozoic supercontinent Columbia: Insights from radiating maûc dyke swarms *Gond Res* **14** 395-409

Hubbard J, Almeida R, Foster A, Sapkota S N, Bürgi P and

Tapponnier P (2016) Structural segmentation controlled the 2015 Mw 7.8 Gorkha earthquake rupture in Nepal *Geol* **44** 639-642

Hughes N C, Myrow P M, McKenzie N R, Xiao S, Banerjee D M, Stockli D and Tang Q (2015) Age and implications of the phosphatic Birmania Formation, Rajasthan, India *Precamb Res* **267** 164-173

Hussain M F, Vanthangliana V and Mondal M E A (2019) Geochemical Constraints on the Petrogenesis of the Metasedimentary Rocks Forming the Basement of the Shillong Plateau, Northeast India. In: Geological Evolution of the Precambrian Indian Shield, Society of Earth Scientists Series (Eds: Mondal MEA) Springer https://doi.org/10.1007/978-3-319-89698-4-16

Iaccarino S, Montomoli C, Carosi R, Montemagni C, Massonne H J, Langone A, Jain A K and Visonà D (2017) Pressure-temperature-deformation-time constraints on the South Tibetan Detachment System in the Garhwal Himalaya (NW India) *Tectonics* **36**, doi.org/10.1002/2017TC004566

Imam B (1996) Bangladesher Khaniz Sampad *Mineral Resources of Bangladesh, Bangla Academy, Dhaka*

Islam M S and Tooley M J (1999) Coastal and sealevel changes during the Holocene in Bangladesh *Quatr Intern* **55** 61-75

Israil M, Tyagi D K, Gupta P K and Niwas S (2008) Magnetotelluric investigations for imaging electrical structure of Garhwal Himalayan corridor, Uttarakhand, India *J Earth Sys Sci* **97** 189-200

Iyenger S V P and Murthy Y G K (1982) The evolution of Archean Proterozoic crust in parts of Bihar and Orissa, eastern India *Rec Geol Surv India* **112** 1-5

Jade S, Bhatt B, Yang Z, Bendick R, Gaur V K, Molnar P, Anand M and Kumar D (2004) GPS measurements from the Ladakh Himalaya, India: Preliminary tests of plate-like or continuous deformation in Tibet *Geol Soc Amer Bull* **116** 1385-1391

Jain A K (1981) Stratigraphy, petrography and paleogeography of the Late Paleozoic diamictites of the Lesser Himalaya *Sedi Geol* **30** 43-78

Jain A K (2014) When did India-Asia collide and make the Himalaya? *Curr Sci* **106** 254-266

Jain A K (2017) Continental subduction in the NW-Himalaya and Trans-Himalaya *Ital J Geosci* **136** 89-102, doi: 10.3301/IJG.2015.43

Jain A K (2020) Geological Evolution of the Himalayan Mountains. In: Geodynamics of the Indian Plate: Evolutionary Perspectives (Eds: Tandon S K and Gupta N) *Springer Geol* https://doi.org/10.1007/978-3-030-15989-4-10

Jain A K and Manickavasagam R M (1993) Inverted metamorphism in the intra-continental ductile shear zone during Himalayan collision tectonics *Geol* **21** 407 410

Jain A K and Singh S (2009) Geology and Tectonics of the Southeastern Ladakh and Karakoram *Geol Soc India Bangalore India* 1-179

Jain A K, Kumar D, Singh S, Kumar A and Lal N (2000) Timing, quantification and tectonic modeling of Pliocene Quaternary movements in the NW Himalaya: evidences from fission track dating *Earth Planet Sci Lett* **179** 437-451

Jain A K, Lal N, Sulemani B, Awasthi A K, Singh S, Kumar R and Kumar D (2009) Detrital-zircon fission track geochronology of the Lower Cenozoic sediments, NW Himalayan foreland basin: Clues for exhumation and denudation of the Himalaya during India-Asia collision *Geol Soc Amer Bull* **121** 519-535

Jain A K, Manickavasagam R M, Singh S and Mukherjee S (2005) Himalayan collision zone: new perspectives - its tectonic evolution in a combined ductile shear zone and channel flow model *Himalayan Geol* **26** 1-18

Jain A K, Mukherjee P K and Singhal S (2020) Terrane characterization in the Himalaya since Paleoproterozoic *Episodes* https://doi.org/10.18814/epiiugs/2020/020020

Jain A K, Shrestha M, Seth P, Kanyal L, Carosi R, Montomoli C, Iaccarino S and Mukherjee P K (2014) The Higher Himalayan Crystallines, Alaknanda-Dhauli Ganga Valleys, Garhwal Himalaya, India. In: Geological field trips in the Himalaya, Karakoram and Tibet (Eds: Montomoli C, Carosi R, Law R D, Singh S and Rai S M) *J Virtual Expl* **47** 8, ISSN 1441-8142

Jain A K, Singh S (2008) Tectonics of the southern Asian Plate margin along the Karakoram Shear Zone: Constraints from field observations and U-Pb SHRIMP ages *Tectonophysics* **451** 186-205

Jain A K, Singh S and Manickavasagam R M (2002) Himalayan Collision Tectonics *Gond Res Group Mem* **7** 1-114

Jain A K, Singh S and Manickavasagam R M (2003) Intra continental shear zones in the Southern Granulite Terrain: Their kinematics and evolution *Mem Geol Soc India* **50** 225-253

Jain A K, Singh S, Manickavasagam R M, Joshi M and Verma P K (2003) HIMPROBE Programme: Integrated studies on Geol, petrology, geochronology and geophysics of the Trans-Himalaya and Karakoram *Mem Geol Soc India* **53** 1-56

Jain S C, Nair K K and Yedekar D B (1995) Geology of Son-Narmada-Tapti lineament zone of Central India *Geol Surv India Spec Publ* **10** 1-154

Jain S C, Yedekar D B and Nair K KK (1991) Central Indian Shear Zone: a major Precambrian crustal boundary *J Geol Soc India* **37** 521-548

Jairaman R and Banerjee D M (1978) Studies on the stromatolites from the Raipur area, Chattisgarh Basin, Proccedings Workshop on Stromatolites *Geol Surv India Misc Pub* **44** 57-67

Janardhan A S, Newton R C and Hansen E C (1982) The transformation of amphibolite facies gneiss to charnockite in southern Karnataka and northern Tamil Nadu, India *Contrib Mineral Petrol* **79** 130-149

Jayananda M, Aadhiseshan K R, Kusiak M A, Wilde S A, Sekhamo K-u, Guitreau M, Santosh M and Gireesh R V (2020) Multi-stage crustal growth and Neoarchean geodynamics in the Eastern Dharwar Craton, southern India *Gond Res* **78** 228-260 doi.org/10.1016/j.gr.2019.09.005

Jayananda M, Chardon D, Peucat J-J and Fanning C M (2015) Paleo- to Mesoarchean TTG accretion and continental growth, western Dharwar craton, southern India: SHRIMP U-Pb zircon geochronology, whole-rock geochemistry and Nd-Sr isotopes *Precamb Res* **268** 295-322 http://dx.doi.org/10.1016/j.precamres.2015.07.015

Jayananda M, Duraiswami R A, Aadhiseshan K R, Gireesh R V, Prabhakar B C, Kafo K-u Tushipokla and Namratha R (2016) Physical volcanology and geochemistry of Palaeoarchaean komatiite lava flows from the western Dharwar craton, southern India: implications for Archaean mantle evolution and crustal growth *Int Geol Rev* **58-13** 1569-1595

Jayananda M, Santosh M and Aadhiseshan K R (2018) Formation of Archean continental crust in the Dharwar craton, Southern India *Earth Sci Rev* **181** 12-42

Jayananda M, Tsutsumi Y, Miyazaki T, Gireesh R V, KapfoK-u, Tushipokla, Hidaka H and Kano T (2013) Geochronological constraints on Meso-Neoarchean regional metamorphism and magmatism in the Dharwarcraton, southern India *J Asian Earth Sci* **78** 18-38 http://dx.doi.org/10.1016/j.jseaes.2013.04.033

Jayangondaperumal R, Thakur V C, Joe Vivek, Rao R S and Gupta A K (2018) Active tectonics of Kumaun and Garhwal Himalaya *Springer Natural Hazards* **150** ISBN 978-981-10-8242-9

Jayaprakash A V, Sundaram V, Hans S K and Mishra R N (1987) Geology of the Kaladgi-Badami Basins, Karnataka *Geol Surv India Mem* **6** 201-225

Jha S K, Sharma R and Srivastava J P (2019) Trace element signatures and mineral chemistry of clays associated with the alteration of halos of Paleoproterozoic U mineralization in Bijawars of the Sonrai Basin, Central India *Acta Geochemica* http://doi.org/10.1007/s11631-019-00363-9

Johnson S Y and Alam A M N (1991) Sedimentation and tectonics of the Sylhet Trough, Bangladesh *Geol Soc Amer Bull* **103** 1513-1527

Joshi *et al*., 2017 Joshi KB, Bhattacharjee J, Rai G, Halla J, Ahmad T, Kurhila MI, Heilimo E, Choudhary AK (2017) The diversification of granitoids and plate tectonic implications at the Archaean-Proterozoic boundary in the Bundelkhand craton, Central India. In: Halla J, Whitehouse MJ, Ahmad T, Bagai Z (Eds) Crust-Mantle Interactions and Granitoid Diversification: Insights from Archaean Cratons *Geol Soc London Spec Publ* **449** 123-157 http://doi.org/10.1144/SP449.8

Joy S, Patranabis-Deb S, Saha D, Jelsma H, Maas R, Soderlund Uf, Tappa S, Linde G V, Banerjee A and Krishnan U (2019) Depositional history of cratonic Purana basins in Southern India: A multipronged geochronology approach to the Proterozoic Kaladgi and Bhima Basins *J Geol* 1-13, doi.10.1002/gj.3415

Joy S, Linde G V D, Choudhuri A K, Deb G K and Tappe S (2018) Reassembly of the Dharwar and Bastar cratons at ca. 1 Ga: Evidence from multiple tectonothermal events along the Karimnagar granulite belt and Khammam schist belt, southern India *J Earth Sys Sci* **127** 76, https://doi.org/10.1007/s12040-018-0988-2

Just J, Schulz B, de Wall H, Jourdan F and Pandit M K (2011) Monazite CHIME/EPMA dating of the Erinpura granitoid deformation: implications for neoproterozic tectonothermal evolution of NW India *Gond Res* **19** 402-412

Kabir M Z, Chowdhury K R, Akon E, Kazi A I and Ameen S M M (2001) Petrogenetic study of Precambrian basement rocks from Maddhapara, Dinajpur, Bangladesh *Bangladesh Geosci J* **7** 1-18

Kale V S (2014) Landscapes and Landforms of India *Springer Sci Dordrecht* 1-271

Kale V S (2016) Proterozoic Basins of Peninsular India: Status within the Global Proterozoic Systems *Proc Indian Nat Sci Acad* **82** 461-477

Kale V S (2020) Cretaceous volcanism in Peninsular India: Rajmahal-Sylhet & Deccan Traps. In: Geodynamics of the Indian Plate (Eds: Tandon SK and Gupta N) *Springer*doi: 10.1007/978-3-030-15989-4.8

Kale V S and Phansalkar V G (1991) Purana basins of Peninsular India: A review *Basin Res* **3** 1-36

Kale V S and Rajaguru S N (1987) Late Quaternary alluvial history of the northwestern Deccan upland region *Nature* **325** 612-614

Kale V S and Rajaguru S N (1988) Morphology and denudation chronology of the coastal and upland river basins of western Deccan Trappean landscape (India): A collation *Zeitschrift Geomorph NF* **32** 311-327

Kale V S and Vaidyanadhan R (2014) The Indian Peninsula: geomorphic landscapes. In: Landscapes and Landforms of India (Ed: Kale V S) *Springer Sci* 65-78, doi:10.1007/978/ 94/017/8029/ 2/6

Kale V S, Bodas M S, Chatterjee P and Pande K (2020) Emplacement history and evolution of the Deccan Volcanic Province, India *Episodes* doi: 10.18814/epiugs/2020/20015

Kale V S, Dole G, Shandilya P and Pande K (2019) Stratigraphy and correlations in Deccan Volcanic Province, India: Quo vadis? *Geol Soc Amer Bull,* doi: 10.1130/B35018.1

Kale V S, Dole G, Upasani D and Patil Pillai S (2017) Deccan Plateau uplift: insights from the Western Uplands, Maharashtra, India. In: Tectonics of the Deccan Large Igneous Province (Eds: Mukherjee S, Misra A, Calves G and Nemèok M) *Geol Soc London Spec Publ* **445** 11-46

Kale V S, Saha D, Patranabis-Deb S, Sesha Sai V V, Tripathy V and Pillai S P (2020) Cuddapah Basin, India: A collage of Proterozoic sub-basins and Terranes *Proc Indian Nat Sci Acad Sp Issue* (In Press)

Kapur V V and Khosla A (2018) Faunal elements from the Deccan volcano-sedimentary sequences of India: a reappraisal of biostratigraphic, palaeoecology, and palaeobiogeographic aspects *J Geol* **32**, doi: 10.1002/gj.3379

Karmalkar N R, Duraiswami R A, Jonnalagadda M, Griffin W L, Gregoire M, Benoit M and Delpech G (2016) Magma types and source characterization of the early Deccan magmatism, Kutch Region, NW India: insights from the geochemistry of igneous intrusion. In: Recent studies on the Geol of Kachchh (Ed: Thakkar M G) *Geol Soc India Spec Publ* **6** 193-208

Kaur P, Choudhury N and Elyas N (2018) Origin of trondhjemite and albitite at the expanse of A-type granite, Aravalli Orogen, India: Evidence for new metasomatic replacement fronts *Geosci Front* http://doi.org/10.1016/ j.gsf.2018.09.019

Kaur P, Zeh A and Chaudhri N (2014) Characterisation and U-Pb-Hf record of the 3.55 Ga felsic crust from the Bundelkhand Craton, northern India *Precamb Res* **255** 236-244

Kaur P, ZehA and Choudhuri N (2019) Archean crustal evolution of the Aravalli Banded Gneissic Complex, NW India: Constraints from zircon U-Pb ages, Lu-Hf isotope systematics, and whole-rock geochemistry of granitoids *Precamb Res* **327** 81-102

Kaur P, Zeh A, Chaudhri N, Gerdes A and Okrusch M (2011) Archaean to Palaeoproterozoic crustal evolution of the Aravalli mountain range, NW India, and its hinterland: the U-Pb and Hf isotope record of detrital zircon *Precamb Res* **187** 155-164

Kaur P, Zhe A and Choudhuri N (2016) Unraveling the record of Archaean crustal evolution of the Bundelkhand Craton, northern India using U-Pb zircon-monazite ages, Lu-Hf isotope systematics, and whole-rock geochemistry of granitoids. *Precamb Res* **281** Doi: 10.1016/j.precamres. 2016.06.005

Kehelpannala K V W (1997) Deformation of a high-grade Gondwana fragment, Sri Lanka *Gond Res* **1** 47-68

Kehelpannala K V W (1999) Shear-zone controlled arrested charnockitization, retrogression and metasomatism of high-grade rocks *Gond Res* **2** 573-577

Kent R (1991) Lithospheric uplift in eastern Gondwana: evidence for a long-lived mantle plume system? *Geol* **19** 19-23

Kent R W, Storey M and Saunders A D (2002) Large igneous provinces: Sites of plume impact or plume incubation? *Geology* **20** 891-894

Keszthelyi L, Self S and Thordarson T (1999) Applications of recent studies on the emplacement of basaltic lava flows to the Deccan Traps. In: Deccan Volcanic Province (Ed: Subbarao K V) *Mem Geol Soc India* **43** 485-520

Khan A A (2013) Paleogeography of the Peninsular India vis-à-vis geodynamic Petrotectonic significance of the Vindhyan Basin with special reference to Neo-Meso Proterozoic *J Indian Geol Cong* **5** 65-76

Khan A A and Rahman T (1992) Ananalysis of gravity ûeld and tectonic evaluation of the northwestern partof Bangladesh *Tectonoph* **206** 35l-364

Khan F H (1991) *Geology of Bangladesh, Univ Press Ltd Dhaka*

Khan M R andMuminullah M (1980) Stratigraphy of Bangladesh. *Petrol Min Resour Bangladesh Sem Exhib Dhaka* 35-40

Khandoker R A (1989) Development of major tectonic elements of the Bengal Basin: a platetectonic appraisal *Bangladesh J Sci Res* **7** 221-232

KhinZaw (1990) Geological, petrological and geochemical characteristics of granitoid rocks in Burma: with special reference to the associated W-Sn mineralization and their tectonic setting. *J Southeast Asian Earth Sci* **4** 293-335

KhinZaw, Win Swe, Barber A J, Crow M J and Yin YinNwe (2017). Introduction to the Geol of Myanmar In: Myanmar: Geol, Resources and Tectonics Barber, A J, KhinZaw and Crow M J (Eds) *Geol Soc London Mem* **48** 1-17

Kitano I, Osanai Y, Nakano N, Adachi T and Fitzsimons I C W (2018) Detrital zircon and igneous protolith ages of high-grade metamorphic rocks in the Highland and Wanni Complexes, Sri Lanka: Their geochronological correlation with southern India and East Antarctica *J Asian Earth Sci* **156** 122-144

Kleinschrodt R (1994) Large-scale thrusting in the lower crustal basement of SriLanka *Precamb Res* **66** 39-57

Kohn M J (2014) Himalayan Metamorphism and Its Tectonic Implications *Ann Rev Earth Planet Sci* **42** 381-419

Kohn M J, Paul S K and Corrie S L (2010) The lower Lesser Himalayan sequence: a Paleoproterozoic arc on the northern margin of the Indian plate *Geol Soc Amer Bull* **122** 323-335

Kreuzer H, Karre W, Kurssten M, Schnitzer W A and Srivastava N K (1977) K/Ar dates of two glauconites from the Chanderpur Series, Chattisgarh India. On the stratigraphic Status of the Late Precambrian Basins in Central India *GeolologischeJahrbuch B* **28** 23-36

Kriegsman L (1991) Structural Geol of the Sri Lankan basement - a preliminary review. In: The crystalline crust of Sri Lanka, Part I, Summary of Research of the German-Sri Lankan Consortium (Ed: Kröner A) *Geol Surv Dept Sri Lanka Prof Paper* **5** 52-68

Krishnamurthy P, Chaki A, Pandey B K, Chimote J S and Singh S N (1988) Geochronology of the granite-rhyolite suites of the Dongargarh supergroup central India In: Proc 4th National Symp Mass Spect EPS-2/1-EPS-2/3

Krogstad E J, Balakrishnan B, Mukhopadhyay D K, Rajamani V and Hanson G N (1989) Plate tectonics 2.5 billion years ago: Evidence at Kolar, South India *Science* **243** 1337-1340

Krogstad E J, Hanson G N and Rajamani V (1991) U-Pb ages of zircon and sphene for two gneiss terrains adjacent to the Kolar Schist Belt, south India: Evidence for separate crustal evolution histories *J Geol* **99** 801-816

Kröner A, Cooray P G and Vitanage P W (1991) Lithotectonic subdivision of the Precambrian basement in Sri Lanka. In: The Crystalline Crust of Sri Lanka, Part I, Summary of Research of the German-Sri Lankan Consortium (Ed: Kröner A) *Geol Surv Dept Sri Lanka Prof Paper* **5** 5-21

Kröner A, Jaeckel P and Williams I S (1994) Pb-loss patterns in zircons from a high-grade metamorphic terrain as revealed by different dating methods: U-Pb and Pb-Pb ages for igneous and metamorphic zircons from northern Sri Lanka *Precamb Res* **66** 299-337

Kröner A, Kehelpannala K V W and Hegner E (2003) Ca. 700-1000 Ma magmatic events and Grenvillian-age deformation in Sri Lanka: relevance for Rodinia supercontinent formation and dispersal, and Gondwana amalgamation *J Asian Earth Sci* **22** 279-300

Kröner A, Rojas-Agramonte Y, Kehelpannala K V W, Zack T, Hegner E, Geng H Y, Wong J and Barth M (2013) Age, Nd-Hf isotopes, and geochemistry of the Vijayan Complex of eastern and southern Sri Lanka: A Grenville-age magmatic arc of unknown derivation *Precamb Res* **234** 288-321

Kröner A, Santosh M, Hegner E, Shaji E, Geng H, Wong J, Xie H, Wan Y, Shang C K, Liu D, Sun M and Nandakumar V (2015) Palaeoproterozoic ancestry of Pan-African high-grade granitoids in southern most India: Implications for Gondwan are constructions *Gond Res* **27** 1-37

Kröner A, Williams, I S, Compston W, Baur N, Vitanage P W and Perera L R K (1987) Zircon ion microprobe dating of Precambrian high-grade rocks in Sri Lanka *J Geol* **95** 775-791

Kumar A, Lal N, Jain A K and Sorkhabi R B (l995) Late Cenozoic-Quaternary thermotectonic history of Higher Himalayan Crystallines (HHC) in Kishtwar-Padar-Zanskar region, NW Himalaya: Evidence from fission track ages *J Geol Soc India* **45** 375-39l

Kumar A, Prashuramulu V, Shankar R and Besse J (2017) Evidence for a Neoarchean LIP in the Singhbhum craton, eastern India: implications to Vaalbara supercontinent *Precamb Res* **292** 163-174

Kumar B, Srivastava R K, Jha D K, Pant N C and Bhandaru B K (1990) A revised stratigraphy of rocks of Type Area of the Bijawar Group in Central India *Indian Min* **44** 303-314

Kumar R (2020) Late Cenozoic Himalayan foreland basin: Sedimentologic attributes *Episodes* **43** (1)doi.org/10.18814/epiiugs/2020/020024

Kumar R, Jain A K, Lal N and Singh S (2018) Early-Middle Eocene exhumation of the Trans-Himalayan Ladakh Batholith, and the India-Asia convergence *Curr Sci* **113** 1090-1098

Kumar S (1978) Stromatolites and environment of deposition of the Vindhyan Supergroup of central India *J Paleont Soc India* **21-22** 96-101

Kumar S (1980) Stromatolites and Indian biostratigraphy*J Paleont Soc India* **23-24** 166-183

Kumar S and Pandey S K (2010) Trace fossils from the Nagaur Sandstone, Marwar Supergroup, Dulmera area, Bikaner district, Rajasthan, India *J Asian Earth Sci* **38** 77˘85

Kumar S, Bora S, Sharma U K, Yi K, Kim N (2017) Early Cretaceous subvolcanic calc-alkaline granitoid magmatism in the Nubra-Shyok valley of the Shyok Suture Zone, Ladakh Himalaya, India: Evidence from geochemistry and U-Pb SHRIMP zircon geochronology *Lithos* **277** 33-50 doi:10.1016/j.lithos.2016.11.019

Kumar V (1999) Evolution and Geological set up of the Nagaur-Ganganagar Basin, North Western Rajasthan. In: Geological Evolution of Northwestern (Ed: Paliwal B S) India *Scientific Publ India* 34-60

Kyi Khin, KhinZaw and Lin Thu Aung (2017) Geological and tectonic evolution of the Indo-Myanmar Ranges (IMR) in the Myanmar region. In: Myanmar: Geol, Resources and Tectonics (Eds: Barber A J, KhinZaw and Crow M J) *Geol Soc London, Mem* **48** 65-79 https://doi.org/10.1144/M48.4

Lacassin R, Valli F, Arnaud N, LeloupP H, Paquette J L, Haibing L, Tapponnier P, Chevalier M-L, Guillot S, Maheo G and Zhiqin X (2004) Large-scale geometry, offset and kinematic evolution of the Karakorum fault, Tibet *Earth Planet Sci Lett* **219** 255-269

Lal R K, Ackermand D, Seifert F and Haldar S K (1978) Chemographic relationships in sapphirine-bearing rocks from Sonapahar, Assam, India *Contrib Miner Petrol* **67** 169-187

Le Dain A Y, Tapponnier P and Molnar P (1984) Active faulting and tectonics of Burma and surrounding regions. *J Geophys Res* **89** B1, 453-472

Leech M L, Singh S and Jain A K (2007) Continuous metamorphic zircon growth and interpretation of U-Pb SHRIMP Dating: An Example from the Western Himalaya *Intl Geol Rev* **49** 313-328

Leech M L, Singh S, Jain A K, Klemperer S L and Manickavasagam R M (2005) Early, steep subduction of India beneath Asia required by early UHP metamorphism *Earth Planet Sci Lett* **234** 83-97

Leelanandam C (1998) Alkaline magmatism in the Eastern Ghats Belt—a critique *Geol Surv India Spec Publ* **44** 170-179

Leloup P H, Mahéo G, Arnaud N, Kali E, Boutonnet E, Liu D, Liu X and Haibing L (2010) The South Tibet detachment shear zone in the Dinggye area. Time constraints on extrusion models of the Himalayas *Earth Planet Sci Lett* **292** 1-16 doi: 10.1016/j.epsl.2009.12.035

Liang X, Sandvola E, Chen Y J, Hearn T, Ni J, Klemperer S, Shen Y and Tilmann F (2012) A complex Tibetan upper mantle: A fragmented Indian slab and no south-verging subduction of Eurasian lithosphere *Earth Planet Sci Lett* **333-334** 101-91

Licht A, Dupont-Nivet G, Win Z, Swe H H, Kaythi M, Roperch P, Ugrai T, Littell V, Park D, Westerweel J, Jones D, Poblete F, Wa Aung D, Huang H, Hoorn C and Sein K (2018) Paleogene evolution of the Burmese forearc basin and implications for the history of India-Asia convergence. *Geol Soc Amer Bull* **131** 730-748, doi: 10.1130/b35002.1

Mahalik N K (1994) Geology of the contact between the Eastern Ghats Belt and the north Orissa craton, India *J Geol Soc India* **44** 41-51

Mahapatro S N, Tripathy A K, Nanda J and Roy A (2009) Coexisting ultramylonite and pseudotachylyte from the eastern segment of the Mahanadi shear zone, eastern Ghats Mobile Belt *J Geol Soc India* **74** 679-689

Mahato S, Goona, Bhattacharya A, Mishra B and Bernhardt H-J (2008) Thermo-tectonic evolution of the North Singhbhum Mobile Belt (eastern India): A view from the western part of the belt *Precamb Res* **162** 102-127

Maheo G, Bertrand H, Guillot S, Villa I M, Keller F and Capiez P (2004) The south Ladakh ophiolites (NW Himalaya, India): an intra-oceanic tholeiitic origin with implication for the closure of the Neo-Tethys *Chem Geol* **203** 273-303

Maibam B, Gerdes A, Goswami J N (2016) U"Pb and Hf isotope records in detrital and magmatic zircon from eastern and western Dharwar craton, southern India: Evidence for coeval Archaean crustal evolution *Precamb Res* **275** 496-512, doi.org/10.1016/j.precamres.2016.01.009

Maibam B, Goswami J N and Srinivasan R (2011) Pb-Pb zircon ages of Archaean metasediments and gneisses from the Dharwar craton, southern India: implications for the antiquity of the eastern Dharwar craton *J Earth Syst Sci* **120** 643-661

Majumdar R and Sarkar S (2004) Sedimentation history of the PalaeoproterozoicDhanjori Formation, Singhbhum, India and its implications *Precamb Res* **130** 267-287

Malhotra G and Pandit M K (2000) Geology and mineralisation of Jahazpur belt, southeastern Rajasthan. In: Crustal Evolution and Metallogeny in Northwestern Indian Shield (Ed: Deb M), Narosa Publ House, New Delhi 115-125

Mall D M, Reddy P R and Mooney W D (2008) Collision tectonics of the Central Indian Suture zone as inferred from a deep seismic sounding study *Tectonophy* **460** 116-123

Malone S J, Meert J G, Banerjee D M, Pandit M K, Tamrat E, Kamenov G, Pradhan V R and Sohl L E (2008) Paleomagnetism and detrital zircon geochronology of the Upper Vindhyan sequence, Son Valley and Rajasthan, India: A 1000 Ma closure age for the Purana basins? *Precamb*

Res **164** 137-159

Malviya V P, Arima M, Pati J K and Kaneko Y (2004) First report of metamorphosed basaltic pillow lava from central part of Bundelkhand craton, India: An Island arc setting of possible Late Archean age *Gond Res* **7** 1338-1340

Malviya V P, Arima M, Pati J K and Kaneko Y (2006) Petrology and geochemistry of metamorphosed basaltic pillow lava and basaltic komatiite in the Mauranipur area: subduction related volcanism in the Archean Bundelkhand craton, Central India *J Mineral Petrol Sci* **101** 199-217 doi:10.2465/jmps.101.199

Mandal S, Robinson D M, Khanal S and Das O (2015) Redefining the tectonostratigraphic and structural architecture of the Almora klippe and the Ramgarh-Munsiari Thrust sheet in NW India. In: Tectonics of the Himalaya (Eds: Mukherjee S, Carosi R, van der Beek P A, Mukherjee B K and Robinson D M) *Geol Soc London Spec Publ* **412** 247-269

Manickavasagam R M, Jain A K, Singh S and Asokan A (1999) Metamorphic evolution of the NW-Himalaya, India: Pressure-temperature data, inverted metamorphism, and exhumation in the Kashmir, Himachal, and Garhwal Himalaya In: Himalaya and Tibet: Mountain Roots to Mountain Tops (Eds: Macfarlane A, Sorkhabi R B and Quade J) *Geol Soc Amer Spec Paper* **328** 179-198

Manikyamba C and Kerrich R (2012) Eastern Dharwar Craton, India: continental lithosphere growth by accretion of diverse plume and arc terranes. *Geosci Front* **3** 225-240

Manikyamba C, Kerrich R, Naqvi S M and Ram Mohan M (2004) Geochemical systematics tholeiitic basalts from the 2.7 Ga Ramagiri- Hungund composite greenstone belt, Dharwar Craton *Precamb Res* **134** 21-39

Manjunatha B R and Shankar R (1992) Anoteon the factors controlling the sedimentation rate along the western continental shelf of India *Marine Geol* **104** 219-224

Manu Prasanth M P, Hari K R and Santosh M (2019) Tholeiitic basalts of Deccan large igneous province, India: An overview https://doi.org/10.1002/gj.3497

Martin A J (2017) A review of Himalayan stratigraphy, magmatism, and structure *Gond Res* **49** 42-80 https://doi.org/10.1016/j.gr.2017.04.031

Mathavan V, Prame W K B N and Cooray P G (1999) Geol of the High Grade Proterozoic Terrains of Sri Lanka and the Assembly of Gondwana: an Update on Recent Developments *Gond Res* **2** 237-250

Mathur R K (1964) Systematic geological mapping in parts of Udaipur district, Rajasthan. *Unpubl Progress Report Field Season 1963-64 Geol Surv India*

Mathur S M (1982) Precambrian sedimentary sequence of India: their geochronology and correlation *Precamb Res* **18** 139-144

Matsumaru K, Ehiro M and Kojima S (2006) On *Orbitolina* (Foraminifera) from the Shyok Suture Zone, Kashmir, NW India *J Palaeont Soc India* **51** 43-49

Matte P H, Tapponnier P, Arnaud N, Bourjot L, Avouac J-P, Vidal P H, Liu Q, Pan Y and Wang Y (1996) Tectonics of Western Tibet, between the Tarim and Indus *Earth Planet Sci Lett* **142** 311-220

Maung Thein (1973) A preliminary synthesis of the geological evolution of Burma with reference to the tectonic development of Southeast Asia. *Geol Soc Malaysia Bull* **6** 87-116

Maung Thein and Haq BT (1970) The Pre-Paleozoic and Paleozoic stratigraphy of Burma, a brief review. *Union Burma J Sci Tech* **2** 275-289

Maurin T and Rangin C (2009) Structure and kinematics of the Indo-Burmese Wedge: recent and fast growth of the outer wedge Tectonics 28 TC2010

Mazumder S K (1986) The Precambrian framework of part of the Khasi Hills, Meghalaya *Rec Geol Surv India* **117** 1-59

Mckenzie D and Sclater J G (1971) The evolution of the Indian Ocean since the Late Cretaceous *R Astron Soc Geophys J* **24** 437-528

McKenzie N R, Hughes N C, Myrow P M, Banerjee D M, Deb M and Planavasky N J (2013) New Age constraints for the Proterozoic Aravalli-Delhi successions of India and their implications *Precamb Res* **238** 12-28

McKenzie N R, Hughes N C, Myrow P M, Banerjee D M, Deb M, Planavasky N J, Maheshwari A and Sial A N (2013) New Age constraints for the Proterozoic Aravalli-Delhi successions of India and their implications *Precamb Res* **238** 120-128

McKenzie N R, Hughes N C, Myrow P M, Xiao S and Sharma M (2011) Correlation of Precambrian-Cambrian sedimentary successions across Northern India and the utility of isotopic signatures of Himalayan lithotectonic zones *Earth Planet Sci Lett* **31** 471-483, doi:10.1016/j.epsl.2011.10.027

Meert J G and Pandit M K (2015) The Archaeanand Proterozoichistory of Peninsular India: tectonic framework for Precambrian sedimentary basins in India. In: Precambrian Basins of India: Stratigraphic and Tectonic Context (Eds: Mazumder R and Eriksson P G) *Geol Soc London Mem* **43** 29-54 doi.org/10.1144/ M43.3

Meert J G and Pandit M K (2015) The Archean and Proterozoic history of Peninsular India: tectonic framework for Precambrian Sedimentary basins in India. In: Precambrian Basins of India: Stratigraphic and Tectonic Context, Chapter 3 (Eds: Mazumdar R and Eriksson P G) *Geol Soc London Mem* **43** 29-54

Meert J G, Pandit M K, Pradhan V R and Kamenov G (2011) Preliminary report on the paleomagnetism of 1.88 Ga dykes from the Bastar and Dharwar cratons, Peninsular India *Gond Res* **20** 335-343

Meert J G, Pandit M K, Pradhan V R, Banks J, Sirianni R, Stroud M, Newstead B and Gifford J (2010) Precambrian crustal evolution of Peninsular India: A 3.0 billion year odyssey *J Asian Earth Sci* **39** 483-515

Meißner B, Deters P, Srikantappa C and Kohler H (2002) A reappraisal of the pressure-temperature path of granulites from the Kerala Khondalite Belt, southern India *J Geol* **108** 687-703

Miglani R, Shahrukh M, Israil M, Gupta P K, Varsheney S K and Sokolova E (2014) Geoelectric structure estimated from magnetotelluric data from Uttarakhand Himalaya, India *J Earth Sys Sci* **123** 907-918

Miller S R, Mueller P A, Meert J G, Kamenov G D, Pivarunas A F, Sinha A K and Pandit M K (2018) Detrital Zircons Reveal Evidence of Hadean Crust in the Singhbhum Craton, India *J Geol* **126** 541-552

Misra A A and Mukherjee S (2017) Dyke-brittle shear relationships in the western Deccan strike-slip zone around Mumbai (Maharashtra, India), In: Tectonics of the Deccan Large Igneous Province (Eds: Mukherjee S, Misra A, Calves G and Nemcok M) *Geol Soc London Spec Publ* **445** 269-295

Misra A A, Bhattacharya G, Mukherjee S and Bose N (2014) Near N-Spaleo-extension in the western Deccan region, India: does it link strike-slip tectonics with the India-Seychellesrifting? *Int J Earth Sci* **103** 1645-1680 doi:10.1007/s00531.014-1021-x

Misra S and Johnson P T (2005) Geochronological constraints on evolution of SinghbhumMobile Belt and associated basic volcanics of eastern Indian shield *Gond Res* **8** 129-142

Misra S, Deomurari M P, Wiedenbeck M, Goswami J N, Ray S and Saha A K (1999) 207Pb/206Pb zircon ages and the evolution of the Singhbhum Craton, eastern India: an ion microprobe study *Precamb Res* **93** 139-151

Misra S (2006) Precambrian chronostratigraphic growth of Singhbhum-Orissa craton, eastern Indian shield. *J Geol Soc India* **67** 356-378

Mitchell A H G (1989) Tectonic Evolution of the Tethyan Region In: Tectonic Evolution of the Tethyan Region (Ed Sengor A M C) 567-583 Kluwer Acad Publ doi:10.1007/978-94-009-2253-2-24

Mitchell A H G (1993) Cretaceous-Cenozoic tectonic events in the western Myanmar (Burma)-Assam region *J Geol Soc* **150** 1089-1102 https:// doi.org/10.1144/gsjgs .150.6.1089

Mitchell A H G, Htay M T, Htun K M, Win M N, Oo T and Hlaing T (2007) Rock relationships in the Mogok metamorphic belt, Tatkon to Mandalay, central Myanmar *J Asian Earth Sci* **29** 891-910 https://doi.org/10.1016/j.jseaes.2006.05.009

Mitra R, Chakrabarti G and Shome D (2018) Development of Stromatolites in a mixed siliciclastic carbonate succession: An example from Palaeo-Mesoproterozoic Tadpatri Formation, Cuddapah Basin, India *Int J Res Annual Rev* **5** 1248-1269

Mohan A, Tripathi P and Motoyoshi M (1997) Reaction history of sapphirine granulites and a decompressional P-T path in a granulite complex from the Eastern Ghats *Proc Indian Aca Sci (Earth Planet Sci)* **106** 115-129

Mohanty and Guha, 1990) Mohanty M, Guha DB (1995) Lithotectonic stratigraphy of the dismembered greenstone sequence of the Mangalwar Complex around Lawa-Sardargarh and Parasali areas, Rajsamand District, Rajasthan. *Mem Geol Soc India* **31** 141-162

Mohanty M and Guha D B (1995) Lithotectonic stratigraphy of the dismembered greenstone sequence of the Mangalwar Complex around Lawa-Sardargarh and Parasali areas, Rajsamand District, Rajasthan *Mem Geol Soc India* **31** 141-162

Mohanty S P (2015) Palaeoproterozoic supracrustals of the Bastar Craton: Dongargarh Supergroup and Sausar Group. In: Precambrian Basins of India: Stratigraphic and Tectonic Context (Eds: Mazumder R and Eriksson PG) *Geol Soc, London, Mem* **43** 151-164 http://dx.doi.org/10.1144/M43.11

Mohanty S P and Nanda S (2016) Geochemistry of a paleosol horizon at the base of the Sausar Group, central India: Implications on atmospheric conditions at the Archean-Paleoproterozoic boundary *Geosci Front* **7** 759-773

Mohanty S P, Barik A, Sarangi S and Sarkar A (2015) Carbon and oxygen isotope systematics of a Paleoproterozoic cap-carbonate sequence from the Sausar Group, central India. *Palaeogeog Palaeoclimaet Palaeoeco* **417** 195-209

Mondal M E A (2009) Was Bundelkhand-Aravalli nucleus par of Ur supercontinent? *Curr Sci* **96** 33-35

Mondal M E A and Raza A (2013) Geochemistry of sanukitoid series granitoids from the Neoarchaen Berach granitoid batholiths, Aravalli craton, northwestern Indian shield *Curr Sci* **105** 102-108

Mondal M E A and Raza M (2009) Tectonomagmatic evolution of the Bastar craton of Indian shield through plume-arc interaction: evidence from geochemistry of the mafic and felsic volcanic rocks of Sonakhan greenstone belt. In: (Eds: Ahmad T, Hirsch F and Charusiri P) *J Virtual Expl* **32** 7 doi:10.3809/jvirtex.2009.00245

Mondal M E A, Goswami J N, Deomurari M P and Sharma K K (2002) Ion Microprobe 207Pb/206Pb ages of zircons from Bundelkhand massif, northern India: implications for crustal evolution of the Bundelkhand-Aravalli protocontinent *Precam Res* **117** 85-100

Mondal M E A, Sharma K K, Rahman A and Goswami J N (1998) Ion microprobe Pb207/Pb206 zircon ages for gneiss-granitoid rocks from Bundelkhand massif: evidence for Archaean components *Curr Sci* **74** 70-75

Mondal S K, Frei R and Ripley E M (2007) Os isotope systematics of mesoarcheanchromitite-PGE deposits in the Singhbhum Craton (India): Implications for the evolution of lithospheric mantle *Chem Geol* **244** 391-408

Montemagni C, Montomoli C, Iaccarino S, Carosi R, Jain A K, Massonne H-J and Villa I M (2019) Dating protracted fault activities: microstructures, microchemistry and geochronology of the Vaikrita Thrust, Main Central Thrust zone, Garhwal Himalaya, NW India. In: Crustal Architecture and Evolution of the Himalaya-Karakoram-Tibet Orogen (Eds: Sharma, R., Villa, I M and Kumar, S) *Geol Soc London, Spec Publ* **481** https://doi.org/10.1144/SP481.3

Montomoli C, Carosi R and Iaccarino S (2015) Tectonometamorphic discontinuities in the Greater Himalayan Sequence: a local or a regional feature? In: Tectonics of the Himalaya (Eds: Mukherjee S, Carosi R, van der Beek P A, Mukherjee B K and Robinson D M) *Geol Soc Lond Spec Publ* **412** 25-41

Moore G F, Aung L T, Fukuchi R, Sample J C, Hellebrand E, Kopf A, Naing Win, Than W M and Tun T N (2019) Tectonic, diapiric and sedimentary chaotic rocks of the Rakhine coast, western Myanmar *Gond Res* **74** 126-143

Morley C K, Naing T T, Searle M and Robinson S A (2019) Structural and tectonic development of the Indo-Burma Ranges. *Earth Sci Rev* 102992 doi:10.1016/j.earscirev.2019.102992

Mottram C M, Argles T W, Harris N B W, Parrish R R, Horstwood M S A, Warren C J and Gupta S (2014) Tectonic interleaving along the Main Central Thrust, Sikkim Himalaya *J Geol Soc London* **171** 255-268, doi.org/10.1144/jgs2013-064

Moyen J-F, Nedelec A, Martin H and Jayananda M (2003) Syntectonic granite emplacement at different structural levels: the Closepet granite, South India *J Struct Geol* **25** 611-631

Mukherjee P K, Jain A K, Singhal S, Singha N B, Singh S, Kumud K, Seth P and Patel R C (2019) U-Pb zircon ages and Sm-Nd isotopic characteristics of the Lesser and Great Himalayan sequences, Uttarakhand Himalaya, and their regional tectonic implications *Gond Res* **75** 282-297 doi.org/10.1016/j.gr.2019.06.001

Mukhopadhyay J, Beukes N J, Armstong R A, Zimmermann U, Ghosh G and Medda R A (2008) Dating of the oldest greenstone belt in India: A 3.51 Ga precise U-Pb SHRIMP zircon age for Dacitic Lava of the Southern Iron Ore Group, Singhbhum craton *J Geol* **116** 449-461

Mukhopadhyay J, Crowley Q G, Ghosh S, Ghosh G, Chakrabarti K, Misra B, Heron K and Bose S (2014) Oxygenation of the Archean atmosphere: New paleosol constraints from eastern India *Geology* **42** 923-926 doi:10.1130/G36091.1

Mukhopadhyay J, Ghosh G, Zimmermann U, Guha S and Mukherje T (2012) A 3.51 Ga bimodal volcanic-BIF-ultramafic succession from Singhbhum Craton: implications for Palaeoarchaean geodynamic processes from the oldest greenstone succession of the Indian subcontinent *Geol J* **47** 284-311

Murthy A S N, Sarkar D, Sen M K, Sridher V, Prasad A S SS R S (2014) Mapping the sub-trappean Mesozoic sediments in the western part of the Narmada-Tapi region of Deccan Volcanic Province, India *J Asian Earth Sci* **93** 15-24

Murti K S (1987) Stratigraphy and sedimentation in Chattisgarh Basin in Purana Basins of Peninsular India *Mem Geol Soc India* **6** 239-260

Náblek J, Hetenyi G, Vergne J, Sapkota S, Kafle B, Jiang M, Su H, Chen J, Huang B-S and the HI-CLIMB Team (2009) Underplating in the Himalaya-Tibet collision zone revealed by the Hi-CLIMB experiment *Science* **325** 1371†1374

Nagaraja Rao B K, Ramalingaswamy G, Rajurkar S T and Ravindra Babu B (1987) Stratigraphy, structure and evolution of the Cuddapah basin. In: Purana basins of Peninsular India (Middle to Late Proterozoic) *Mem Geol Soc India* **6** 33-86

Naha K and Halyburton R V (1974) Early Precambrian stratigraphy of central and southern Rajasthan, India *Precamb Res* **1** 55-73

Naha K and Mohanty S (1990) Structural studies in the Pre-Vindhyan rocks of Rajasthan: a summary of work of the last three decades. In: Structure and Tectonics: The Indian Scene (Eds: Naha K, Ghosh S K and Mukhopadhyay D) *Proc Indian Acad Sci* **99** 279-290.

Naha K, Mukhopadhyay D K, Mohanty R, Mitra S K and Biswal T K (1984) Significance of contrast in the early stages of the structural history of the Delhi and the pre-Delhi rock group in the Proterozoic of Rajasthan, western India *Tectonophy* **105** 193-206

Nair K K K, Jain S C and Yedekar D B (1995) Stratigraphy, structure and geochemistry of the Mahakoshal greenstone *Mem Geol Soc India* **37** 403-432

Nair K M, Padmalal D and Kurmaran K P N (2006) Quaternary Geol of south Kerala sedimentary basin-anoutline *J Geol Soc India* **67**165-179

Nair N and Pandey D K (2018) Cenozoic sedimentation in the Mumbai off shorebasin: implications for tectonic evolution of the western continental margin of India *J Asian Earth Sci* **152**132-144

Najman Y (2006) The detrital record of orogenesis: a review of approaches and techniques used in the Himalayan sedimentary basins *Earth Sci Rev* **74** 1-72

Najman Y R, Allen R, Willett E A F, Carter A, Barfod D, Garzanti E, Wijbrans, J, Bickle M J, Vezzoli G, Ando S, Oliver G and Uddin M J (2012) The record of Himalayan erosion preserved in the sedimentary rocks of the Hatia Trough of the Bengal Basin and the Chittagong Hill Tracts, Bangladesh *Basin Res* **24** 499-519 doi:10.1111/j.1365-2117.2011.00540.x

Najman Y, Appel E, Boudagher-Fadel M, Bown P, Carter A, Garzanti E, Godin L, Han J T, Liebke U, Oliver G, Parrish R and Vezzoli G (2010) Timing of India-Asia collision: geological, biostratigraphic, and palaeomagnetic constraints *J Geophys Res* **95** B12416

Naqvi S M and Rogers J J W (1987) Precambrian Geology of India. Oxford Univ Press, New York

Naqvi S M, Manikyamba C, Rao G, Subba Rao D V, Ram Mohan M and Sarma S (2002) Geochemical and isotopic constraints on Neoarchean fossil plumes forthe formation of volcanic rocks of Sandur Greenstone Belt, India *J Geol Soc India* **60** 27-56

Narayanaswamy S, Chakravarthy S C, Vemban N A, Shukla K D, Subramaniam M R, Venkatesh V, Rao G V, Anandalwar M A and Nagarajaiah R A (1963) The geology and manganese ore deposits of the manganese belt in Madhya Pradesh and adjoining parts of Maharastra. Part I: general introduction *Bull Geol Surv India* A-22 (I)

Nasipuri P, Saha L, Xie H, Pati J K, Satyanarayanan M, Sarkar S, Bhandari A and Gaur Y (2019) Paleoarchean crustal evolution of the Bundelkhand craton, north-central India In: Earth's Oldest Rock (Eds: van Kranendonk M, Bennett V, Hoffmann J). Elsevier Amsterdam **2** 793-817

Nayak G K, RaoV K, Rambabu H V and KayalJ R (2008) Pop-up tectonics of the Shillong Plateau in the great 1897 earthquake (Ms 8.7): Insights from the gravity in conjunction with the recent seismological results *Tectonics* **27** TC1018 doi:10.1029/2006TC002027

Nelson D, Bhattacharya H N, Thern E R and Altermann W (2014) Geochemical and ion-microprobe U-Pb zircon constraints on the Archaean evolution of Singhbhum Craton, eastern India *Precamb Res* **255** 412-432

Nelson K D, Zhao W, Brown L D and Indepth Team (1996) Partially molten middle crust beneath southern Tibet: Synthesis of Project INDEPTH results *Science* **274** 1684-1688

Nemcok M and Rybar S (2017) Rift-drift transition in a magma-rich system: the Goprift-Laxmi basin case study: western India. In: Tectonics of the Deccan Large Igneous Province (Eds. Mukherjee S, Misra A, Calves G and Nemcok M) *Geol Soc London Spec Publ* **445** 95-117

Ni J F and Barazangi M (1984) Seismotectonics of the Himalayan collision zone: geometry of the underthrusting Indian plate beneath the Himalaya *J Geophys Res* **89** 947-963

Nutman A P, Chadwick B, Krishna Rao B and Vasudev V N (1996) SHRIMP U/Pb zircon ages of acid volcanic rocks in the Chitradurga and Sandur groups, and granites adjacent to the Sandur Schist belt, Karnataka *J Geol Soc India* **47** 153-164

Ojha P S (2012) Precambrian sedimentary basins of India: an appraisal of their petroleum potential In: Geol and Hydrocarbon Potential of Neoproterozoic-Cambrian Basins in Asia (Eds: Bhat G M, Craig J, Thurow J W, Thusu B and Cozzi A) *Geol Soc London Spec Publ* **366** 19-58, http://dx.doi.org/10.1144/SP366.11

Okudaira T, Hamamoto T, Hari Prasad B and Kumar R (2001) Sm-Nd and Rb-Sr dating of amphibolite from the Nellore-Khammam schist belt, SE India: Constraints on the collision of the Eastern Ghats terrane and Dharwar- Bastar craton *Geol Mag* **138** 495-498

Óskarsson B V and Riishuus M S (2014) The mode of emplacement of Neogene flood basalts in eastern Iceland: facies architecture and structure of simple aphyric basalt groups *J Volcan Geotherm Res* **289** 170-192

Pande K, Sheth H C and Bhutani R (2001) 40Ar-39Arage of the St.Mary's Islands volcanics, southern India: record of India-Madagascar break-upon the Indian subcontinent *Earth Planet Sci Lett* **193** 39-46

Pandey D K and Bahadur T (2009) A Review of The Stratigraphy of Marwar Supergroup Of West-Central Rajasthan *J Geol Soc* India **73** 747-758

Pandey D K, Nair N, Pandey A and Sriram G (2017) Basement tectonics and flexure subsidence along western continental margin of India *Geosci Front* **8** 1009-1024 doi:10.1016/j.gsf.2016.10.006

Pandey D K, Pandey A and Whattam S (2019) Relict subduction initiation along a passive margin in the northwest Indian Ocean *Nature Comm* **10** doi:10.1038/s41476-019-10227-8

Pandey D K, Pandey A, Clift P D, Nair N, Ramesh P, Kulhanek D K and Yadav R (2018) Flexure subsidence analysis of the Laxmibasin, Arabian Sea and its tectonic implications. *Geol Mag* **14** doi:10.1017/S001675818000833

Pandit M K, Carter L M, Ashwal L D, Tucker R D, Torsvik T H, Jamtveit B and Bhushan S K (2003) Age, petrogenesis and significance of 1 Ga granitoids and related rocks from the Sendra area, Aravalli Craton, NW India *J Asian Earth Sci* **22** 363-381

Pandit M K, de Wall H and Chauhan N K (2008) Paleosol at the Archean-Proterozoic contact in NW India revisited: evidence for oxidizing conditions during paleoweathering? *J Earth Sys Sci* **117** 201-209

Pandit M K, Sial A N, Jamrani S S and Ferreira V P (2001) Carbon isotopic profile across Bilara Group rocks of Trans-Aravalli Marwar Supergroup in western India: implications for Neoproterozoic-Cambrian transition *Gond Res* **4** 387-394

Panigrahi M K, Mookherjee A, Pantulu G V C and Gopalan K (1993) Granitoids around Malanjkhand copper deposit: types and age relationship. Proceedings of the Indian Academy of Science *Earth Plan Sci Lett* **102** 399-413

Pant N C, Kundu A, Kumar R, Dorka B S and Prasher S (2006) Paleoproterozoic metamorphism in the Jeori-Wangtu Gneissic Crystallines (JWGC), Western Himalaya *J Asian Earth Sci* **26** 585-604

Pant N C, Singh P and Jain A K (2020) A Re-look at the Himalayan metamorphism *Episodes* **43** doi.org/10.18814/epiiugs/2020/020022

Papineau D, Purohit R, Goldgerg T, Pi D, Shields D A, Bhu H, Steele A and Fogel M L (2009) High primary productivity and nitrogen cycling after the Paleoproterozoic phosphogenic event in the Aravalli Supergroup, India *Precamb Res* **171** 37-56

Pareek H S (1984) Pre-Quaternary geology and mineral resources of Northwestern Rajasthan *Mem Geol Surv India* **115** 1-99

Patel R C and ManMohan (2020) Mio-Pliocene Tectonics and Exhumation Histories of the NW- and NE-Himalaya *Episodes* **43** doi.org/10.18814/epiiugs/2020/020019

Patel R C, Adlakha V, Lal N, Singh P and Kumar Y (2009) Spatiotemporal variation in exhumation of the Crystallines in the NW-Himalaya, India: Constraints from Fission Track dating analysis *Tectonophy* **504** 1-13

Patel R C, Singh S, Asokan A, Manickavasagam R M and Jain A K (1993) Extensional tectonics in the collisional Zanskar Himalayan belt. In: Himalayan Tectonics (Eds: Treloar P J and Searle M P) *Spec Publ Geol Soc London* **74** 445-459

Pati J K, Reimold W U, Koeberl C and Pati P (2008) The Dhala structure, Bundelkhand craton, Central India—Eroded remnant of a large Paleoproterozoic impact structure. *Meteoritics Planet Sci* **43** 1383-1398

Pati J K (2005) The Dhala Structure, Bundelkhand craton, Central India—A new large Paleoproterozoic impact structure (abstract) *Meteoritics Planet Sci* **40** A121

Pati J K, Qu W J, Koeberl C, Reimold W U, Chakarvorty M and Schmitt R T (2017) Geochemical evidence of an extraterrestrial component in impact melt breccia from the Paleoproterozoic Dhala impact structure, India *Meteoritics Planet Sci* 1-15 doi: 10.1111/maps.12826

Pati J K, Raju S, Pruseth K L, Magngain V D and Shankar R (1997) Gold Mineralization in parts of Bundelkhand Granitoid Complex (BGC) *J Geol Soc India* **50** 601-606

Patranabis-Deb S, Bickford M E, Hill B, Chaudhuri A K and Basu A (2007) SHRIMP ages of zircon in the uppermost tuff in Chattisgarh Basin in Central India require ~500 Ma adjustment in Indian Proterozoic stratigraphy *J Geol* **115** 407-415, doi:10.1086/518049.

Patranabis-Deb S, Saha D and Tripathy V (2012) Basin stratigraphy, sea-level fluctuations and their global tectonic connections-evidence from the Proterozoic Cuddapah Basin *J Geol* **47** 263-283, DOI: 101002/gj1347

Patriat P and Achache J (1984) India-Eurasia collision chronology has implications for crustal shortening and driving mechanism of plates *Nature* **311** 615-621, doi:10.1038/311615a0

Paul D D and Lian H M (1975) Offshore basins of southwest Asia-Bay of Bengal to South Sea *Proc 9th World Petrol Congress Tokyo* **3** 1107-1121

Pedersen R B, Searle M P and Corfield R I (2001) U-Pb zircon ages from the Spontang Ophiolite, Ladakh Himalaya *J Geol Soc London* **158** 513-520

Peshwa V V and Kale V S (1997) Neotectonics of the Deccan Trap Province: Focus on the Kurduwadi Lineament *J*

Geophys **18** 77-86

Peucat J-J, Jayananda M, Chardon D, Capdevila R, Fanning MC, Paquette J-L (2013) The lower crust of Dharwar craton, south India: Patchwork of Archean granulitic domains *Precamb Res* **227**4-29 http://dx.doi.org/10.1016/j. precamres.2012.06.009

Pichai Muthu R (1990) The occurrence of gabbroic anorthosites in Makrohar area, Sidhi district, Madhya Pradesh. Precambrian of Central India *Geol Surv India Spec Publ* **28** 320-331

Pichamuthu C S (1965) Regional metamorphism and charnockitisation in Mysore state India *Indian Min* **6** 116-126

Pivnik D A, Nahm J, Tucker R S, Smith G O, Nyein K, Nyunt M and Maung P H (1998) Polyphase deformation in a fore-arc/back-arc basin, Salin subbasin, Myanmar (Burma) *Amer Assoc Petrol Geol Bull* **82** 1837-1856

Poddar B C and Mathur R K (1967) A note on the repetitious sequence of greywacke-slate-phyllite in the Aravalli system around Udaipur, Rajasthan *Bull Geol Soc India* **2** 83-87

Powar K B (1993) Geomorphological evolution of the Konkan coastal belt and adjoining Sahyadriuplands with reference to Quaternary uplift. *Curr Sci* **64** 793-796

Powell C McA and Conaghan P J (1973) Plate tectonics and the Himalayas *Earth Planet Sci Lett* **20** 1-12, doi: 10.1016/0012-821X(73)90134-9

Powell C McA and Conaghan P J (1975) Tectonic models of the Tibetan plateau *Geol* **3** 727-731.doi:10.1130/0091-7613(1975)3<727:TMOTTP>2.0.CO;2

Prabhakar N and Bhattacharya A (2013) Paleoarchean partial convective overturn in the Singhbhum Craton, Eastern India *Precamb Res* **231** 106-121

Pradhan V R, Meert J G, Pandit M K, Kamenov G and Mondal M E A (2012) Paleomagnetic and geochronological studies of the mafic dyke swarms of Bundelkhand craton, central India: implications for the tectonic evolution and paleogeographic reconstructions *Precamb Res* **198-199** 51-76

Pradhan V R, Meert J G, Pandit M K, Kamenov G, Gregory L C and Malone S J (2010) India's changing place in global Proterozoic reconstructions: A review of geochronologic constraints and paleomagnetic poles from the Dharwar, Bundelkhand and Marwarcratons *J Geo dynam* **50** 224-242

Prakash D and Tewari S (2016) Garnet-staurolite-mica schist from RangliRangliot, Eastern Himalaya: Constraints from phase equilibria and Thermobarometry *J Geol Soc India* **87** 679-690

Prakash R, Swarup P and Srivastava R N (1975) Geology and mineralization in the southern part of Bundelkhand in Lalitpur district, Uttar Pradesh *J Geol Soc India* **16** 143-156

Purohit R, Bhu H, Sarkar A and Ram J (2015) Evolution of the ultramafic rocks of the Rakhabdeev and Jharol Belts in southeastern Rajasthan, India: New evidences from the imagery mapping. petro-mineralogical and OH stable isotope studies *J Geol Soc India* **85** 331-338

Quazi A H (1986) Geological framework of Bangladesh *GEOSEA V Proc vol. II. Geol Soc Malaysia Bull* **20** 73-80

Raase P and Schenk V (1994) Petrology of granulite facies metapelites of the Highland Complex, Sri Lanka: implication for the metamorphic zonation and the P-T path *Precamb Res* **66** 265-294

Raase P, Raith M, Ackermand D and Lal R K (1986) Progressive metamorphism of mafic rocks from greenschist to granulite facies in the Dharwar craton of South India *J Geol* **94** 261-282

Racey A and Ridd M F (2015) Petroleum Geol of Myanmar *Geol Soc, London, Mem* **45** http://mem.lyellcollection.org/content/45/1.toc

Radhakishna B P (1989) Suspect tectonostratigraphic terrain elements in the Indian subcontinent *J Geol Soc India* **34** 1-24

Radhakrishna B P (1993) Neogene uplift and geomorphic rejuvenation of the Indian Peninsula *Curr Sci* **64** 787-793

Radhakrishna B P and Naqvi S M (1986) Precambrian continental crust of India and its evolution *J Geol* **94**145-166

Radhakrishna B P and Vaidyanadhan R (2011) Geol of Karnataka *Geol Soc India Bangalore*

Raja Rao C S, Poddar B C, Basu K K and Dutta A (1971) Precambrian stratigraphy of Rajasthan-A review *Rec Geol Surv India* **101** 60-79

Rajamani V, Shivkumar K, Hanson G N and Shirey S B (1985) Geochemistry and petrogenesis of amphibolites, Kolar Schist Belt, South India: Evidence for komatiitic magma derived by low percentage of melting of the mantle *J Petrol* **96** 92-123

Rajaram M, Anand S P, Erram V C and Shinde B N (2017) Insight into the structure below the Deccan Trap covered region of Maharashtra, India from geopotential data. In: Tectonics of the Deccan Large Igneous Province (Eds: Mukherjee S, Misra A, Calves G, Nemèok M) *Geol Soc London Spec Publ* **445** 219-236

Rajesham T, Bhaskar Rao Y J and Murti K S (1993) The Karimnagar granulite terrane-a new sapphirine bearing granulite province, south India *J Geol Soc India* **4** 51-59

Raju A T R (1968) Geological evolution of Assam and Cambay Basins of India *Amer Assoc Petr Geol Bull* **52** 2422-2437

Ramachandra H M and Roy A (2001) Evolution of the Bhandara-Balaghat granulite belt along the southern margin of the Sausar mobile belt of central India *J Earth Sys Sci* **110** 351-368

Ramakrishna M (1987) Stratigraphy, Sedimentary Environment and Evolution of Late Proterozoic Indravati Basin, Central India, In: Purana Basins of Peninsular India *Mem Geol Soc India* **6** 139-160

Ramakrishnan M (1987) Tectonic evolution of Proterozoic-type platform-fold belts of Archean age in Western Dharwar Craton *Indian Min* **27** 1-9

Ramakrishnan M (1993) Tectonic evolution of the granulite terranes of southern India *Mem Geol Soc India* **25** 35-44

Ramakrishnan M (2003) Craton-mobile relationsinSouthern Granulite Terrain *Mem Geol Soc India* **50** 1-24

Ramakrishnan M and Vaidyanadhan R (2008) Geology of India *Geol Soc India* Bangalore **1** 556

Ramakrishnan M, Nanda J K and Augustine P F (1998) Geological evolution of the Proterozoic Eastern Ghats Mobile Belt *Geol Surv India Spl Publ* **44** 1-21

Ramam P K and Murty V N (1997) Geology of Andhra Pradesh *Geol Soc India Bangalore India*

Rangin C (2017) Active and recent tectonics of the Burma Platelet in Myanmar. In: Myanmar-Geol, Resources and Tectonics (Eds: Barber A J, KhinZaw and Crow M J) *Geol Soc London, Mem* **48** 53-64, https://doi.org/10.1144/M48.3

Rao J M, Pooranchandra Rao G V S, Widdowson M and Kelley SP (2005) Evolution of Proterozoic mafic dyke swarms of the Bundelkhand granite massif, central India *Curr Sci* **88** 502-506

Rao M B R (1973) The subsurface Geol of Indo-Gangetic Plains *J Geol Soc India* **14** 217-242

Rao N P and Kalpna (2005) Deformation of the subducted Indian lithospheric slab in the Burmese arc *Geophys Res Lett* **32** L05301, doi:10.1029/2004GL022034

Rashid H (1991) *Geography of Bangladesh, Univ Press Ltd, Dhaka*

Rasmussen B, Bose P K, Sarkar S, Banerjee S, Fletcher I R and McNaughton N J (2002) 1.6 Ga U-Pb zircon age for the Chorhat Sandstone, Lower Vindhyan, India: Possible implications for early evolution of animals *Geol* **30** 103-106

Rastogi B K, Chadha R K and Raju I P (1986) Seismicity near Bhatsa reservoir, Maharastra, India *Physics Earth Planet Interiors* **44** 179-199

Ratre K, De Waele B, Biswal T K and Sinha S (2010) SHRIMP geochronology for the1450 Ma Lakhna dyke swarm: its implication for the presence of Eoarchaean crust in the Bastar Craton and 1450-517 Ma depositional age for Purana basin (Khariar), Eastern Indian Peninsula *J Asian Earth Sci* **39** 565-577

Raval U and Veeraswamy K (2011) Mapping of tectonic corridors through hidden parts of the Greater Dharwar terrane, Southern India *J Asian Earth Sci* **43** 1210-1225

Ravikant V (2006) Utility of Rb-Sr geochronology in constraining Miocene and Cretaceous events in the eastern Karakoram, Ladakh, India *J Asian Earth Sci* **27** 534-543

Rawat G, Arora B R and Gupta P K (2014) Electrical resistivity cross-section across the Garhwal Himalaya: Proxy to ûuid-seismicity linkage *Tectonophy* **637** 68-710

Ray J S, Martin M W, Veizer J and Bowring S A (2002) U-Pb zircon dating and Sr isotope systematics of the Vindhyan Supergroup, India *Geol* **30** 131-134

Ray J S, Veizer J and Davis W J (2003) C, O, Sr and Pb isotope systematics of carbonate sequences of the Vindhyan Supergroup, India: Age, diagenesis, correlations and implications for global events *Precamb Res* **121** 103-140

Ray J, Saha A, Koeberl C, Thoni M, Ganguly S and Hazra S (2013) Geochemistry and petrogenesis of Proterozoic mafic rocks from east Khasi Hills, Shillong Plateau, northeastern India *Precamb Res* **230** 119-137

Ray R, Shukla A D, Sheth H C, Ray J S, Duraiswami R A, Vanderkluysen L, Rautela C S and Mallik J (2008) Highly heterogeneous Precambrian basement under the central Deccan Traps, India: direct evidence from xenoliths in dykes *Gond Res* **13** 375-385

Raza A and Mondal MEA (2018) Geochemistry of the Archaean metasedimentary rocks of the Bundelkhand Mauranipur-Babina greenstone belt, central India: Implications for provenance characteristics *J Indian Assoc Sedimen* **35** 57-76

Raza M and Casshyap S M (1996) A tectono-sedimentary model of evolution of Middle Proterozoic Vindhyan Basin *Mem Geol Soc India* **36** 287-300

Raza M and Khan M S (1993) Geochemical characterization of the Delwara volcanic: evidence for the origin of Aravalli basin by extensional rifting. In: Rift basins and Aulacogens (Ed: Casshyap S M) Gyanodaya Prakashan, Nainital India 119-129

Raza M, Ahmad A H M, Shamim Khan M and Khan F (2012) Geochemistry and detrital modes of Proterozoic sedimentary rocks, Bayana Basin, north Delhi fold belt: implications for provenance and source-area weathering *Int Geol Rev* **54** 111-129

Reichardt H, Weinberg R F, Andersson U B and Fanning C M (2010) Hybridization of granitic magmas in the source: The origin of the Karakoram Batholith, Ladakh, NW India *Lithos* **116** 249-272, doi:10.1016/j.lithos.2009.11.013.

Renne P R, Sprain C J, Richards M A, Self S, Vanderkluysen L and Pande K (2015) State shift in Deccan Volcanismat the Cretaceous-Paleogene boundary possibly induced by impact *Science* **350** 76-78

Reuber I (1986) Geometry of accretion, oceanic thrusting of the Spontang Ophiolite, Ladakh-Himalaya *Nature* **321** 592-596

Reuber I (1989) The Dras arc: two successive volcanic events on eroded oceanic crust *Tectonophysics* **161** 93-106

Richards F D, Hoggard M J and White N J (2016) Cenozoicepeirogeny of the Indian peninsula *Geochem Geophy Geosys* **17** 4920-4954, doi:10.1002/2016gc006545

Rickers K, Mezger K and Raith M M (2001) Evolution of the continental crust in the Proterozoic Eastern Ghats Belt, India and new constraints for Rodinia reconstruction: implications from Sm-Nd, Rb-Sr and Pb-Pb isotopes *Precamb Res* **112** 183-212

Robinson D M, DeCelles P G, and Copeland P (2006) Tectonic evolution of the Himalayan thrust belt in western Nepal: Implications for channel flow models *Geol Soc Amer Bull* **118** 865-885, https:// doi .org /10 .1130 /B25911 .1

Roday P P, Diwan P and Singh S (1995) A synkinematic model of emplacement of quartz reefsand subsequent deformation patterns in the central Indian Bundelkhand batholith Proc Indian Acad Sci (Earth Planet Sci) **104** 465-468

Rogers J J W and Santosh M (2002) Configuration of Columbia, a Mesoproterozoic supercontinent *Gond Res* **5** 5-22

Rolland Y and Pecher A (2001) The Pangong granulites of the Karakoram Fault (Western Tibet): vertical extrusion within a lithospheric-scale fault? *Comptes Rendus de l'Acad Sci Paris* **332** 363-370

Rolland Y, Mahéo G, Pêcher A and Villa I M (2009) Syn-kinematic emplacement of the Pangong metamorphic and magmatic complex along the Karakorum Fault (N Ladakh) *J Asian Earth Sci* **34** 10-25, doi:10.1016/j.jseaes.2008.03.009

Rolland Y, Pêcher A and Picard C (2000) Middle Cretaceous back-arc formation and arc evolution along the Asian margin: the Shyok Suture Zone in northern Ladakh (NW Himalaya) *Tectonophysics* **325** 145-173

Rolland Y, Picard C, Pêcher A, Lapierre H, Bosch D and Keller F (2002) The cretaceous Ladakh arc of NW Himalaya-slab melting and melt-mantle interaction during fast northward drift of Indian Plate *Chem Geol* **182** 139-178

Rollinson H R, Windley B F and Ramakrishnan M (1981) Contrasting high and intermediate pressures of metamorphism in the Archaean Sargur Schists of southern India *Contrib Mineral Petrol* **76** 420-429

Roy A and Devarajan M K (2000) A reappraisal of the stratigraphy and tectonics of the Proterozoic Mahakoshal belt, Central India. Precambrian Crust in Eastern and Central India. UNESCO-IUGS-IGCP-368 *Geol Surv India Spec Publ* **17** 79-97

Roy A and Hanuma Prasad (2003) Tectonothermal events in Central Indian Tectonic Zone (CITZ) and its implications in Rodinian crustal assembly *J Asian Earth Sci* **22** 115-129

Roy A and Hanuma Prasad M (2001) Precambrian of Central India: a possible Tectonic model *Geol Surv India Spec Publ* **64** 177-197

Roy A and Hanuma Prasad M (2003) Tectonothermal events in Central Indian Tectonic Zone (CITZ) and its implications in Rodinian crustal assembly *J Asian Earth Sci* **22** 115-129

Roy A B (1988) Stratigraphic and tectonic framework of the Aravalli Mountain range *Geol Soc India Mem* **7** 3-31

Roy A B and Bhattacharya H N (2012) Tectonostratigraphic and Geochronologic Reappraisal Constraining the Growth and Evolution of Singhbhum Archaean Craton, Eastern India *J Geol Soc India* **80** 455-469

Roy A B and Chatterjee A (2015) Tectonic frame work and evolutionary history of the Bengal Basin in the Indian subcontinent *Curr Sci* **109** 271-279

Roy A B and Jakhar S R (2002) Geology of Rajasthan: Precambrian to Recent Sci Publ Jodhpur, India, 421p

Roy A B and Jakhar S R (2002) Geology of Rajasthan: Precambrian to Recent. Scientific Publisher Jodhpur, India **421**

Roy A B and Kröner A (1996) Single zircon evaporation ages constraining the growth of the Archaean Aravalli craton, northwestern Indian shield *Geol Mag* **133** 333-342

Roy A B and Paliwal B S (1981) Evolution of the lower Proterozoic epicontinental deposits: stromatolite bearing Aravalli rocks of Udaipur, Rajasthan, India *Precamb Res* **14** 49-74

Roy A B, Kröner A, Bhattacharya P K and Rathore S (2005) Metamorphic evolution and zircon geochronology of early Proterozoic granulites in the Aravalli Mountains of northwestern India *Geol Mag* **142** 287-302

Roy A S, Jeykumar S, Aggarwal S K and Ebihara M (2002) Sm Nd age and mantle source characteristics of the Dhanjori volcanic rocks, Eastern India *J Geochem* **36** 503-518

Roy A, Sengupta S and Mandal A (2008) Synchronous development of mylonite and pseudotachylyte: an example from the Chitradurga Eastern Margin Shear Zone, Karnataka *J Geol Soc India* **72** 447-457

Roy AB (1988) Stratigraphic and tectonic framework of the Aravalli mountain range *Mem Geol Soc India* **7** 3-32

Roy P, Jain A K and Singh S (2010) Microstructures of mylonites along the Karakoram Shear Zone, Tangste Valley, Pangong Mountains, Karakoram *J Geol Soc India* **75** 679-694, doi:10.1007/s12594-010-0065-1

Roy P, Jain A K and Singh S (2016) Kinematic Vorticity Analysis along the Karakoram Shear Zone, Pangong Mountains, Karakoram: Implications for the India-Asia Tectonics *J Geol Soc India* **87** 249-260

Sadiq M, Ranjith A and Umrao RK (2014) REE Mineralization in the Carbonatites of the Sung Valley Ultramafic-Alkaline-Carbonatite Complex, Meghalaya, India *Cent Eur J Geosci* **6** 457-475 doi: 10.2478/s13533-012-0191-y

Sadiq M, Umrao R K, Sharma B B, Chakraborti S, Bhattacharyya S and Kundu A (2017) Mineralogy, geochemistry and geochronology of mafic magmatic enclaves and their significance in evolution of Nongpoh granitoids, Meghalaya, NE India. In: Sensarma S, Storey BC (eds) Large Igneous Provinces from Gondwana and Adjacent Regions *Geol Soc London Spec Publ* **463** doi.org/10.1144/SP463.2

Saha A K (1994) Crustal evolution of Singhbhum, North Orissa, Eastern India *Mem Geol Soc India* **27** 341

Saha D and Sain A (2019) Multiple convergences along an Archean craton margin: clues from Proterozoic ophiolite remnants, granites and granulite domains along the SE margin of India *J Geodyn,* doi: 101016/jjog201804004

Saha D, Bhowmik S K, Bose S and Sajeev K (2016) Proterozoic tectonics and trans-Indian mobile belts: A status report *Proc Indian Nat Sci Acad* **82** 445-460

Saha L, Pant N C, Pati J K, Upadhyaya D, Berndt J, Bhattacharya A and Satyanarayan M (2011) Neoarchean high pressure margarite-phengitic muscovite- chlorite corona mantled corundum in quartz-free high-Mg, Al phlogopite-chlorite schists from the Bundelkhand craton, north-central India *Contrib Miner Petrol* **161** 511-530

Sahoo D, Pruseth K L, Upadhyay D, Ranjan S, Pal D C, Banerjee R and Gupta S (2017) New constraints from zircon, monazite and uraninite dating on the commencement of sedimentation in the Cuddapah basin, India *Geol Mag* **147** 1230-1246, doi: 101017/S0016756817000140

Sahoo S R and Das S (2015) Kolhan Sedimentation in Chaibasa-Noamundi Basin, Jharkhand, India: A Critical Observation through Lithofacies Analysis *Intern J Earth Sci Engin* **8** 60-66

Sain A, Saha D, Joy S, Jelsma H and Armstrong R (2017) New SHRIMP age and microstructures from a deformed Atype granite, Kanigiri, Southern India: Constraining the hiatus between orogenic closure and post-orogenic rifting *J Geol* **125** 241-259

Sajeev K, Osanai Y, Connolly J A D, Suzuki S, Ishioka J, Kagami H and Rino S (2007) Extreme crustal metamorphism during a Neoproterozoic event in Sri Lanka, A study of dry mafic granulites *J Geol* **115** 563-582

Sajeev K, Williams I S and Osanai Y (2010) Sensitive high-resolution ion microprobe U-Pb dating of prograde and retrograde ultrahigh-temperature metamorphism as exemplified by Sri Lankan granulites *Geol* **38** 971-974

Samom J D, Ahmad T and Choudhary A K (2017) Geochemical and Sm-Nd isotopic constraints on the petrogenesis and tectonic setting of the Proterozoic mafic magmatism of the Gwalior Basin, central India: the influence of Large Igneous Provinces on Proterozoic crustal evolution. In: Large Igneous Provinces from Gondwana and Adjacent Regions (Eds: Sensarma S and Storey B C) *Geol Soc London Spec Publ* **463** https://doi.org/10.1144/SP463.10

Sant D A and Karanth R V (1993) Drainage evolution of the Lower Narmada Valley, Western India *Geomoph* **8** 221-244

Santosh M (1996) The Trivandrum and Nagercoil Granulite Blocks *Gond Res Group Mem* **3** 243-277

Santosh M, Morimoto T and Tsutsumi Y (2006) Geochronology of the Khondalite belt of Trivandrum Block, southern India: electron probe ages and implications for Gondwana tectonics *Gond Res* **9** 261-278

Santosh M, Tsunogae T, Malaviarachchi S P K, Zhang Z, Ding H, Tang L and Dharmapriya P L (2014) Neoproterozoic crustal evolution in Sri Lanka: Insights from petrologic, geochemical and zircon U-Pb and Lu-Hf isotopic data and implications for Gondwana assembly *Precamb Res* **255** 1-29

Santosh M, Yokoyama K and Acharyya S K (2004) Geochronology and Tectonic Evolution of Karimnagar and Bhopalpatnam Granulite Belts, Central India *Gond Res* **7** 501-18

Sarangi S, Gopalan K and Kumar S (2004) Pb-Pb age of earliest megascopic, eukaryotic alga bearing Rohtas Formation, Vindhyan Supergroup, India: Implications for Precambrian atmospheric oxygen evolution *Precamb Res* **132** 107-121

Sarangi S, Gopalan K, Roy A B, Sreenivas B and Sharma S D (2006) Pb-Pb age of carbonates of Jhamarkotra Formation: constraints on the age of Aravalli Supergroup, Rajasthan *J Geol Soc India* **67** 442-446

Sarkar A and Paul D K (1998) Geochronology of the Eastern Ghats Precambrian Mobile Belt—a review *Geol Surv India Spl Publ* **44** 51-86

Sarkar A, Bhanumathi L and Balasubrahmanyan M N (1981) Petrology, geochemistry and geochronology of the Chilka Lake igneous complex, Orissa State, India *Lithos* **14** 93-111

Sarkar A, Boda M S, Kundu H K, Mamgain V V and Ravishankar (1998) Geochronology and geochemistry of Mesoproterozoic intrusive plutonites from the eastern segment of the Mahakoshal greenstone belt, Central India. *IGCP-368 Sem Precamb Crust in Eastern and Central India,* Bhubaneshwar 82-85

Sarkar A, Sarkar G, Paul D K and Mitra N D (1990) Precambrian geochronology of central Indian shield: a review *Geol Surv India Hyderabad Spec Publ* **28** 453-482

Sarkar S N and Saha A K (1983) Structure and Tectonics of the Singhbhum-Orissa Iron Ore Craton, eastern India. Recent Res Geol Hind Publ Corp Delhi **10** 1-25

Sarkar S, Santosh M, Dasgupta S and Fukuoka M (2003) Very high density CO_2 associated with ultrahigh temperature metamorphism in the Eastern Ghats granulite belt, India *Geol* **31** 51-54

Sarkar T and Schenk V (2014) Two-stage granulite formation in a Proterozoic magmatic arc (Ongole domain of the Eastern Ghats Belt, India): Part 1. Petrology and pressure-temperature evolution *Precamb Res* **255** 485-509

Sarkar T, Schenk V, Appel P, Berndt J and Sengupta P (2014) Two-stage granulite formation in a Proterozoic magmatic arc (Ongole domain of the Eastern Ghats Belt, India): Part 2, LA-ICP-MS zircon dating and texturally controlled in-situ monazite dating *Precamb Res* http://dx.doi.org/10.1016/j.precamres.2014.05.024

Sastri V V, Bhandari L L, Raju A T R and Datta A K (1971) Tectonics framework and subsurface stratigraphy of the Ganga basin *J Geol Soc India* **12** 222-233

Sastry M V A and Moitra A (1984) Vindhyan Stratigraphy-A Review *Geol Surv India Mem* **116** 109-148

Satoru K, Ahmad T, Tanaka T, Bagati T N, Mishra M, Kumar R, Islam R and Khanna P P (2001) Early Cretaceous radiolarians from the Indus suture zone, Ladakh, northern India *News Osaka Micropaleont (NOM) Spec* **12** 257-270

Sayyed M G R (2014) Flood basalt hosted paleosols: potential paleoclimatic indicators of global climate change *Geosci Front* **5** 79-799, doi: 10.1015/j.gsf.2013.08.005

Schärer U, Hamet J and Allegre C J (1984) The Trans-Himalaya (Gangdese) plutonism in the Ladakh region: a U-Pb and Rb-Sr study *Earth Planet Sci Lett* **67** 327-339

Schlup M, Carter A, Cosca M and Steck A (2003) Exhumation history of eastern Ladakh revealed by $^{40}Ar/^{39}Ar$ and fission track ages: the Indus river-Tso Morari transect, NW Himalaya *J Geol Soc London* **160** 385-399

Schoene B, Eddy M P, Samperton K M, Keller C B, Keller G, Adatte T and Khadri S F R (2019) U-Pb constraints on pulsed eruption of the Deccan Traps across the end-Cretaceous mass extinction *Science* **363** 862-866

Schulte-Pelkum V, Monsalve G, Sheehan A, Pandey MR, Sapkota S, Bilham R and Wu F (2005) Imaging the Indian subcontinent beneath the Himalaya *Nature* **435** 1222-1225

Sciunnach D and Garzanti E (2012) Subsidence history of the Tethys Himalaya *Earth-Science Rev* **111** 179-198

Sclater J G andFisher R L (1974) Evolution of the east central Indian Ocean, with emphasis on the tectonic setting of the Ninety East Ridge *Geol Soc Amer Bull* **85** 683-702

Searle M P (1996) Geological evidence against large scale pre-Holocene offsets along the Karakoram Fault: implications for the limited extrusion of the Tibetan Plateau *Tectonics* **15** 171-186

Searle M P, Law R D, Godin L, Larson K P, Streule M J, Cottle J M and Jessup M J (2008) Defining the Himalayan Main Central Thrust in Nepal *J Geol Soc London* **165** 523-534

Searle M P, Noble S R, Cottle J M, Waters D J, Mitchell A H G, Hlaing T and Horstwood M S A (2007) Tectonic evolution of the Mogok Metamorphic Belt, Burma (Myanmar) constrained by U-Th-Pb dating of metamorphic and magmatic rocks. *Tectonics* **26** TC3014, doi:10.1029/2006TC002083

Searle M P, Weinberg, R F and Dunlap W J (1998) Transpressional tectonics along the Karakoram Fault Zone, northern Ladakh. In: Continental Transpressional and Transtensional Tectonics (Eds: Holdsworth R E, Strachan R A and Dewey J E) *Geol Soc, London, Spec Publ* **135** 307-326

Searle M P, Windley B F, Coward M P, Cooper D J W, Rex A J, Rex D, Tingdong L, Xuchang X, Jan M Q, Thakur V C and Kumar S (1987) The closing of the Tethys and the tectonics of the Himalaya *Geol Soc Amer Bull* **98** 678-701

Seilacher A, Bose P K and Pflüger F (1998) Triploblastic animals more than 1 billion years ago: Trace fossil evidence from

India *Science* **282** 80-83

Sen S K, Bhattacharya S and Acharyya A (1995) A Multi-Stage Pressure-Temperature Record in the Chilka Lake Granulites: The Epitome of the Metamorphic Evolution of the Eastern Ghats, India? *J Metamor Geol* **13** 287-298, doi:10.1111/j.1525-1314.1995.tb00219.x

Sengupta S, Corfu F, McNutt R H, Paul D K (1996) Mesoarchaean crustal history of the eastern Indian craton: Sm-Nd and U-Pb isotopic evidence. *Precamb Res* **77** 17-22

Sengupta S (1966) Geological and geophysical studies in the western part of Bengal Basin, India *Amer Assoc Petrol Geol Bull* **50** 1001-1017

Sengupta S, Paul D K, Bishui P K, Gupta S N, Chakraborty R and Sen P (1994) A geochemical and Rb-Sr isotopic study of Kuilapal granite and Arkasoni granophyre from the eastern Indian craton *Indian Min* **48** 77-88

Sengupta S, Sarkar G, Ghosh-Roy A K, Bhaduri S K, Gupta S N and Mandal A (2000) Geochemistry and Rb-Sr Geochronology of acid tuffs from the northern fringe of the Singhbhum craton and their significance in the Precambrian evolution *Indian Miner* **54** 43-56

Sesha Sai V V (2013) Proterozoic granite magmatism along the terrane boundary tectonic zone to the East of Cuddapah Basin, Andhra Pradesh-petrotectonic implications for Precambrian crustal growth in Nellore Schist Belt of Eastern Dharwar Craton *J Geol Soc India* **81** 167-182

Sesha Sai V V, Tripathy V, Bhattacharjee S and Khanna T C (2017) Paleoproterozoic magmatism in the Cuddapah basin India *J Indian Geophys Union* **21** 516-525

Shamsuddin A H M andAbdullah S K M (1997) Geological evolution of the Bengal Basin and its implication in hydrocarbon exploration in Bangladesh *Indian J Geol* **69** 93-121

Sharma K K and Rahman A (2000) The Early Archaean-Paleoproterozoic crustal growth of the Bundelkhand craton, northern Indian shield In: Crustal Evolution and Metallogeny in the Northwestern Indian Shield (Eds: Deb M). Narosa, New Delhi 51-72

Sharma M (2006) Paleobiology of Mesoproterozoic Salkhan Limestone, Semri Group, Rohtas, Bihar, India *J Earth Sys Sci* **115** 67-98

Sharma M and Singh V K (2019) Megascopic carbonaceous remains from Proterozoic basins of India. In: Geological Evolution of the Precambrian Indian Shield (Ed: Mondal M E A) *Soc Earth Sci Series Springer* 725-749, doi:101007/978-3-319-89698-4-27

Sharma R (1988) Patterns of metamorphism in the Precambrian rocks of the Aravalli mountain belt *Mem Geol Soc India* **7** 33-76

Sharma R S (1995) An evolutionary model for the Precambrian crust of Rajasthan: some petrological and geochronological considerations *Geol Soc India* **31** 91-115

Sharma R S (2009) Cratons and fold belts of India Lecture Notes Earth Sci 127, Springer-Verlag Heidelberg 1-304

Sharma R S (2009) Cratons and Fold Belts of India Springer-Verlag, Heidelberg 1-304

Sharma R S and Mondal M E A (2019) Evolution of the Indian Shield: New Approach. In: Geological Evolution of the Precambrian Indian Shield (Eds: Mondal M E A) *Springer Soc Earth Sci Series* doi.org/10.1007/978-3-319-89698-4-2

Shekhawat L S, Pandi M K and Joshi D W (2007) Geology and geochemistry of Paleoproterozoic low-grade metabasic volcanic rocks from Salumber area, Aravalli Supergroup. NW India *J Earth Syst Sci* **116** 511-524

Sheth H C (1998) Are appraisal of the coastal Panvel flexure, Deccan Traps, asalistric-fault controlled reversed rag structure *Tectonophy* **294** 143-149

Sheth H C (2000) The timing of crustal extension, diking and eruption of the Deccan Flood basalts *Int Geol Rev* **42** 1007-1016

Sheth H C (2007) Plume-related regional prevolcanic uplift in the Deccan Traps: Absence of evidence, evidence of absence *Geol Soc Amer Spec Paper* **430**785-813

Sheth H C (2016) Giant plagioclase basalts: Continental flood basalt induced remobilization of anorthositic mushes in a deep crustal sill complex *Geol Soc Amer Bull* **128** 916-925

Sheth H C (2018) Is the Satpura "horst" in fact a compressional uplift? *J Geol Soc India* **91** 391-394

Sheth H, Vanderklyusen L, Demonterova E I, Ivanov A V, Savatenkov V M (2018) Geochemistry and 40Ar/39Ar geochronology of the Nandurbar-Dhule mafic dyke swarm: dyke-sill-flow correlations and stratigraphic development across the Deccan flood basalt province *J Geol* **21**, doi:10.1002/gj.3167

Shi X, Wang Y, Sieh K, Weldon R, Feng L, Chan C-H and Liu-Zeng J (2018) Faultslip and GPS velocities across the Shan Plateau define a curved southwestward crustal motion around the eastern Himalayansyntaxis *J Geophy Res Solid Earth* **123** 2502-2518 doi.org/10.1002/2017 JB015206

Shreshtha M, Jain A K and Singh S (2015) Shear sense analysis of the Higher Himalayan Crystalline Belt and tectonics of the South Tibetan Detachment System, Alaknanda-Dhauli Ganga valleys, Uttarakhand Himalaya *Curr Sci* **108** 1107-

1118

Shrivastava B P (1992) Significance fourth dimensional stratigraphic markers in Paleozoic sediments of West Central Rajasthan-Palaeogeographic implications - Petroleum habitat *Indian J Petrol Geol* **1** 224-244

Shrivastava J P, Duncan R A and Kashyap M (2015) Post-K/Pg younger 40Ar-39Ar ages of the Mandla lavas: implications for the duration of the Deccan volcanism *Lithos* **224** 214-224

Shrivastava J P, Mahoney J J and Kashyap M R (2014) Trace elemental and Nd-Sr-Ph isotopic compositional variation in 37 lava flows of the Mandla lobe and their chemical relation to the western Deccan stratigraphic succession, India *Mineral Petrol* **108** 801-817

Sinclair H D and Jaffey N (2001) Sedimentology of the Indus Group, Ladakh, northern India: implications for the timing of initiation of paleo-Indus River *J Geol Soc London* **158** 151-162

Singh A, Bhushan K, Singh C, Steckler M S, Akhter S H, Seeber L, KimW-Y, TiwariA K and Biswas R (2016) Crustal structure and tectonics of Bangladesh: newconstraints from in version of receiver functions *Tectonophy* **680** 99-112

Singh C L and Ghosh G K (2003) Study of Vindhyan sedimentation, crystalline basement and associated structures below the alluvial tracts of Varanasi region, Uttar Pradesh, by magnetic and electrical methods *J Geol Soc India* **62** 205-214

Singh I B (1979) Environment and age of the Tal Formtion of Mussoorie and Nilkanth area of Garhwal Himalaya *J Palaeont Soc India* **20** 214-225

Singh I B (1980) Sedimentological evolution of the Krol Belt sediments *Himalayan Geol* **8** 657-683

Singh I B (1996) Geological evolution of Ganga Plain-An Overview *J Palaeont Soc India* **41** 99-137

Singh I B (1999) Tectonic control on sedimentation in Ganga Plain Foreland Basin: constraints on the Siwalik sedimentation models. In: Geodynamics of the NW Himalaya (Eds: Jain A K and Manickavasagam R M) *Gond Res Group Mem* **6** 3-37

Singh I B and Merajuddin (1978) Some sedimentological observations of the Chhaosa Formation (Simla Slates) in the Simla Hills *Himalayan Geol* **8** 683-702

Singh I B, Sahni A S, Jain A K, and others (2015) Post-collision sedimentation in the Indus Basin (Ladakh, India): Implications for the evolution of the northern margin of the Indian Plate *J Palaeont Soc India* **60** 97-146

Singh IB (1978) On some sedimentological and palaeoecological aspects of the Subathu-Dagshai-Kasauli succession of Simla Hill *J Palaeont Soc India* **21** 19-28

Singh K, Radhakrishna M and Pant A P (2007) Geophysical structure of the western off-shore basins of India and its implications on the Western Ghats *J Geol Soc India* **70** 445-458

Singh S (2019) Protracted zircon growth in migmatites and *In situ* melt of Higher Himalayan Crystallines: U-Pb ages from Bhagirathi valley, NW Himalaya, India *Geosci Front* **10** 793-809, https://doi.org/10.1016/j.gsf.2017.12.014

Singh S (2020) Himalayan magmatism through space and time *Episodes* **43** doi.org/10.18814/epiiugs/2020/020021

Singh S P (1988) Stratigraphy and sedimentation pattern in the Proterozoic Delhi Supergroup, northwestern India *Mem Geol Soc India* **7** 193-206

Singh S, Barley M E, Brown S J, Jain A K, and Manickavasagam R M (2002) SHRIMP U-Pb in zircon geochronology of the Chor granitoid: Evidence for Neoproterozoic magmatism in the Lesser Himalayan granite belt of NW India *Precamb Res* **118** 285-292. doi:10.1016/S0301-9268(02)00107-9

Singh S, Jain A K and Barley M E (2009) SHRIMP U-Pb c (1860) Ma anorogenic magmatic signatures from the NW Himalaya: implications for Palaeoproterozoic assembly of the Columbia Supercontinent In:Palaeoproterozoic Supercontinents and Global Evolution (Eds: Reddy SM, Mazumdar R, Evans D A D and Collins A S) *Geol Soc London Spec Publ* **323** 283-300

Singh S, Kumar R, Barley M and Jain A K (2007) U-Pb SHRIMP ages and depth of emplacement of Ladakh Batholith, NW Himalaya *J Asian Earth Sci* **30** 490-503

Sinha S, Alsop G I and Biswal T K (2010) The evolution and significance of microfracturing within feldspars in low-grade granitic mylonites: A case study from the Eastern Ghats Mobile Belt, India *J Struct Geol* **32** 1417-1429

Sinha-Roy S (1984) Precambrian crustal crustal interaction in Rajasthan, NW India, Proc. Seminar on Crustal Evolution of Indian Shield and its bearing on metallogeny *Indian J Earth Sci* **11** 84-91

Sinha-Roy S (1985) Granite-greenstone sequence and geotectonic development of SE Rajasthan *Bull Geol Min Metal Soc India* **53** 115-123

Sinha-Roy S (1988) Proterozoic Wilson cycles in Rajasthan. In: Precambrian of the Aravalli mountain range (Ed: Roy A B) *Mem Geol Soc India* **7** 95-108

Sinha-Roy S (2000) Precambrian terrain evolution in Rajasthan *Geol Surv India Spec Publ* **55** 275-286

Sinha-Roy S and Malhotra G (1989) Structural relations of the cover and its basement: an example from Jahajpur belt, Rajasthan *J Geol Soc India* **34** 233-244

Sinha-Roy S, Malhotra G and Mohanty M (1998) Geology of Rajasthan *Geol Soc India* 278p

Sinha-Roy S, Mohanty M and Guha D B (1993) Banas dislocation zone in Nathdwara-Khamor Area, Udaipur district, Rajasthan, and its significance on the basement cover relations in the Aravalli Fold Bel. *Curr Sci* **65** 68-72

Socquet A, Vigny C, Chamot-Rooke N, Simons W, Rangin C and Ambrosius B (2006) India and Sunda plates motion and deformation along their boundary in Myanmar determined by GPS*J Geophy Res Solid Earth* **111** (B5) B05406, doi:10.1029/2005JB003877. ISSN2156-2202.

Söderlund U, Bleeker W, Demirer K, Srivastava R K, Hamilton M A, Nilsson M, Pesonen L, Samal A K, Jayananda M, Ernst RE and Srinivas M (2019) Emplacement ages of Paleoproterozoic mafic dyke swarms in eastern Dharwar craton, India: implications for paleoreconstructions and evidence for a ~30° internal block rotation *Precamb Res* **329** 26-43 doi.org/10.1016/j.precamres.2018.12.017

Soe Thura Tun and Watkinson I M (2017) The Sagaing Fault, Myanmar. In: Myanmar-Geol, Resources and Tectonics (Eds: Barber A J, KhinZaw and Crow M J) *Geol Soc London Mem* **48** 413-441 https://doi.org/10.1144/M48.19

Sorkhabi R B, Stump E, Foland K and Jain A K (1999) Tectonics and cooling history of the Garhwal Higher Himalaya (Bhagirathi Valley): constraints from thermochronological data. In: Geodynamics of the NW Himalaya (Eds: Jain A K and Manickavasagam R M) *Gond Res Group Mem* **6** 2l7-235

Spencer C J, Harris R A and Dorais M J (2012) The metamorphism and exhumation of the Himalayan metamorphic core, eastern Garhwal region, India *Tectonics* **31** TC1007, doi:10.1029/2010TC002853

Sprain C J, Renne P R, Vanderkluysen L, Pande K, Self S and Mittal T (2019) The eruptive tempo of Deccan volcanism in relation to the Cretaceous Paleogene Boundary *Science* **363** 866-870

Sreenivas B, Dey S, Bhaskar Rao Y J, Vijaya Kumar T, Babu EVSSK and Williams I S (2019) A new cache of Eoarchaean detrital zircons from the Singhbhum craton, eastern India and constraints on early Earth geodynamics *Geosci Front* **10** 1359-1370 doi.org/10.1016/j.gsf.2019.02.001

Srikantia B, Sant V N and Sharma S B (1969) Geology and Preliminary assessment of Birmania Phosphorite Deposit, Jaisalmer District *J Mines Metals Fuels* **17** 107-113

Srikantia S V (1977) Sedimentary cycles in the Himalaya and their significance on the orogenic evolution of the mountain belt *Coll Intern Centre Nat Recher Scient* **268** 395-408

Srikantia S V and Bhargava O N (1978) The Indus tectonic belts of Ladakh Himalaya: Its Geol, significance and evolution. In: Tectonic Geol of the Himalaya (Ed: Saklani P S) *Today Tomorrow's Printers Publ* 43-62

Srikantia S V and Bhargava O N (1998) Geol of Himachal Pradesh *Mem Geol Soc India* **406**

Srikantia S V and Razdan M L (1981) Shilakang ophiolite nappe of Zanskar mountains, Ladakh Himalaya *J Geol Soc India* **22** 227-234

Srinivasan R, Jaffri S H, Rao G V and Reddy G K (1998) Phreatomagmatic eruptive center from the Deccan Trap province, Jabalpur, central India *Curr Sci* **74** 787-790

Srinivasan V (2002) Post-Deccan Trap faulting in Raigad and Thana districts of Maharashtra *J Geol Soc India* **59** 23-31

Srinivasa-Rao T (1987) The Pakhal Bason-A Perspective *Geol Soc India, Mem* **6** 161-187

Srivastava P (2014) Largest Ediacaran discs from the Jodhpur Sandstone, Marwar Supergroup, India: Their palaeobiological significance *Geosci Front* **5** 183-191

Srivastava R K and Gautam G C (2016) Petrogenesis and tectonic significance of an Early Paleoproterozoic high Mg boninite norite diorite suite of rocks from the Bastar Craton, Central India *Acta Geol Sinica* **90** 116-116

Srivastava R K, Guarino V, Wu F-Y, Melluso L and Sinha A K (2019) Evidence of sub-continental lithospheric mantle sources and open-system crystallization processes from in-situ U-Pb ages and Nd-Sr-Hf isotope geochemistry of the Cretaceous ultramafic-alkaline-(carbonatite) intrusions from the Shillong Plateau, north-eastern India *Lithos* **330-331** 108-119

Srivastava R K, Söderlund U, Ernst R E, Mondal S K and Samal A K (2016) Neoarchaean-Palaeoproterozoic Mafic Dyke Swarms from the Singhbhum Granite Complex, Singhbhum Craton, Eastern India: Implications for Identification of Large Igneous Provinces and Their Possible Continuation on Other Formerly Adjacent Crustal Blocks *Acta Geol Sinica* **90** 17-18

Stampfli G M and Borel G D (2002) A plate tectonic model for the Paleozoic and Mesozoic constrained by dynamic plate boundaries and restored synthetic oceanic isochrons *Earth Planet Sci Lett* **196** 17-33, doi:10.1016/S0012-821X(01)00588-X

Steckler M S, Akhter S H and Seeber L (2008) Collision of the Ganges-Brahmaputra Delta with the Burma Arc *Earth*

Planet Sci Lett **273** 367-378

Stephenson D and Marshall T R (1984) The petrology and mineralogy of Mt. Popa Volcano and the nature of the late Cenozoic Burma Volcanic Arc. *J Geol Soc, London* **141** 747-762, https://doi.org/10.1144/gsjgs.141.4.0747

St-Onge M R, Rayner N and Searle M P (2010) Zircon age determinations for the Ladakh batholith at Chumathang Northwest India: implications for the age of the India-Asia collision in the Ladakh Himalaya *Tectonophysics* **495** 171-183

Strauss H, Banerjee D M and Kumar V (2001) The sulfur isotopic composition of Neoproterozoic to early Cambrian seawater-evidence from the cyclic Hanseran evaporates, NW India *Chem Geol* **175** 17-28

Stmbner K, Grujic D, Dunkl I, Thiede R and Eugster P (2018) Pliocene episodic exhumation and the significance of the Munsiari thrust in the northwestern Himalaya *Earth Planet Sci Lett* **481** 273-283

Subbarao K V and Hooper P R (1988) Reconnaissance map of the Deccan Basalt Group in the Western Ghats, India: Scale 1: 1,000,000. In: Deccan Flood Basalts (Ed: Subbarao K V) *Mem Geol Soc India* **10** enclosure

Sugden T J and Windley B F (1984) Geotectonic framework of the early-mid Proterozoic Aravalli-Delhi orogenic belt, NW India. In: *Abstracts of the Geol Assoc Canada Program* **9** 109

Sukheswala R N and Poldervaart A (1958) Deccan basalts of the Bombay area *Geol Soc Amer Bull* **69** 1475-1494

Swami Nath J, Ramakrishnan M and Viswanatha M N (1976) Dharwar stratigraphic model and Karnataka craton evolution. *Rec Geol Surv India* **107** 149-175

Tandon S K, Sinha R, Gibling M R, Dasgupta A S and Ghazanfari P (2008) Late Quaternary Evolution of the Ganga Plains: myths and misconceptions, recent developments and future directions*Mem Geol Soc India* **66** 1-41

Tapu A T, Ameen S M M, Abdullah R and Zaman M N (2016) Geochemical evaluation of the diorite basement in Barapaharpur, Rangpur, northwest Bangladesh *Bangladesh Geosci J* **22** 17-36

Taylor R J M, Clark C, Fitzsimons I C W, Santosh M, Hand M, Evans N and McDonald B (2014) Post-peak, fluid-media tedmodification of granulite facieszircon and monazite in the Trivandrum Block, southern India *Contrib Mineral Petrol* **168** 1-17

Tewari S and Prakash D (2016) Geothermobarometry and Barrovian Metamorphism of Darjeeling-Mangpu Region, Eastern Himalaya. In: Geostatistical and Geospatial Approaches for the Characterization of Natural Resources in the Environment (Ed: Raju N J) *Springer Intern Publ* 523-526

Tha Hla (1959) Anoteon the petrology and the provenance of the Webu and Marble (‘Alabaster’) inscriptions tones of the Kyaukse area. *J Burma Res Soc* **42** 113-118

Thakur VC (1993) Geol of the Western Himalaya Pergmon Press, Oxford, New York, 1-355

Thakur V C and Mishra D K (1984) Tectonic framework of Indus and Shyok suture zones in eastern Ladakh, northwest Himalaya *Tectonophysics* **101** 207-220

Thakur V C, Jayangondaperumal R and Malik M A (2010) Redefining Wadia-Medlicott’s Main Boundary Fault from Jhelum to Yamuna: an active fault strand of the Main Boundary Thrust in Northwest Himalaya *Tectonophy* **489** 29-42

Thakur V C, Joshi M and Suresh N (2020) Himalayan collisional tectonics” Linking the Kangra piggy-back Basin with reactivation of the Jawalamukhi Thrust and erosion of Dhauladhar Range, Northwest Himalaya *Episodes* **43** doi.org/10.18814/epiiugs/2020/020019

Tripathy V, Satyapal, Mitra S K and Sesha Sai V V (2019) Fold-Thrust Belt Architecture and Structural Evolution of the Northern Part of the Nallamalai Fold Belt, Cuddapah Basin, Andhra Pradesh, India. In: Tectonics and Structural Geology: Indian Context (Ed: Mukherjee S) *Springer Geol* 219-252

Tushipokla and Jayananda M 2013) Geochemical constraints on komatiite volcanism from Sargur Group Nagamangala greenstone belt, western Dharwar craton, southern India: Implications for Mesoarchean mantle evolution and continental growth *Geosci Front* **4** 321-340

Uddin A and Lundberg N (1999) A paleo-Brahmaputra? Subsurface lithofacies analysis of Miocene deltaic sediments in the Himalayan- Bengal system, Bangladesh *Sed Geol* **123** 239-254

Uddin M N (1994) Structure and sedimentation in the Gondwana basins of Bangladesh *Gondwana Nine, 9th Int Gondwana Symp Hyderabad India* **2** 805-819

Uddin M N andAhmed Z (1989) Palynology of the Kopili formation at GDH-31, Gaibandha District, Bangladesh *Bangladesh J Geol* **8** 31-42

Uddin M N andIslam M S U (1992) Depositional environments of the Gondwana rocks in the Khalashpir basin, Rangpur District, Bangladesh *Bangladesh J Geol* **11** 31-40

Upadhyay R, Frisch W and Siebel W (2008) Tectonic implications of new U-Pb zircon ages of the Ladakh batholith, Indus suture zone, northwest Himalaya, India *Terra Nova* **20** 309-317

Upadhyay R, Sharma B L Jr, Sharma B L and Roy A B (1992) Remnants of greenstone sequence from the Archean rocks of Rajasthan *Curr Sci* **63** 87-92

Vadlamani R (2010) Palaeoproterozoic (1.9 Ga) extension and breakup along the eastern margin of the Eastern Dharwar Craton, SE India: New Sm-Nd isochron age constraints from anorogenic mafic magmatism in the Neoarchean Nellore greenstone belt *J Asian Earth Sci* **37** 67-81

Vadlamani R, KYoner A, Vasudevan D, Wendt I, Tobschall H and Chatterjee C (2012) Zircon evaporation ages and geochemistry of metamorphosed volcanic rocks from the Vinjamuru domain, Krishna Province: Evidence for 1.78 Ga convergent tectonics along the southeastern margin of the Eastern Dharwar Craton *Geol J* **48** 293-309

Valdiya K S (1980) Geol of the Kumuan Lesser Himalaya *Wadia Inst Himalayan Geol Dehra Dun* **291**

Valdiya K S (2016) The Making of India Geodynamic Evolution *Springer* 1-924

Valdiya K S and Samwal J (2017) Neo tectonism in the Indian Subcontinent: Landscape evolution *Elsevier Amsterdam* 4 36

van Buer N J, Jagoutz O, Upadhyay R and Guillong M (2015), Mid-crustal detachment beneath western Tibet exhumed where conjugate Karakoram and Longmu-Gozha Co Faults intersect *Earth Planet Sci Lett* **413** 144-157

Van Lente B, Ashwal L D, Pandit M K, Bowring S A andTorsvik T H (2009) Neoproterozoic hydrothermally altered basaltic rocks from Rajasthan, northwest India: implications for late Precambrian tectonic evolution of the Aravalli craton *Precamb Res* **170** 202-222

Vanderkluysen L, Mahoney J J, Hooper P R, Sheth H C and Ray R (2011) The feeder system of the Deccan Traps (India): Insights from dike geochemistry *J Petrol* **52** 315-343

Vansutre S and Hari K R (2010) Granulite belts of central India with special reference to the Bhopalpatnam Granulite Belt: Significance in crustal evolution and implications for Columbia supercontinent *J Asian Earth Sci* **39** 794-803

Verma S K, Verma S P, Oliveira E P, Singh V K and Moreno J A (2016) LA-SF-ICP-MS zircon U-Pb geochronology of granitic rocks from the central Bundelkhand greenstone complex, Bundelkhand craton, India *J Asian Earth* Sci **118** 125-137

Vigny C, Socquet A, Rangin C, Chamot-Rooke N, Pubellier M, Bouin M, Bertrand G and Becker M (2003) Present-day crustal deformation around Sagaing fault, Myanmar *J Geophys Res* **108** 2533 doi:10.1029/2002JB001999

Vijaya Kumar K, Ernst W G, Leelanandam C, Wooden J L and Grove M J (2010) First Paleoproterozoic ophiolite from Gondwana: Geochronologic-geochemical documentation of ancient oceanic crust from Kandra, SE India *Tectonophy* **487** 22-32

Voll G and Kleinschrodt R (1991) Sri Lanka: structural, magmatic and and metamorphic development of a Gondwana fragment. In: The Crystalline Crust of Sri Lanka, Part I. Summary of Research of the German-Sri Lankan Consortium (Ed: Kröner A) *Geol Surv Dept, Sri Lanka Prof Pap* **5** 22-52

Vora K H, Wagle B G, Veerayya M, Almeida F and Karisidaiah S M (1996) 1300 km longlate Pleistocene-Holoceneshelfedge barrier reef system along the western continental shelf of India: occurrence and significance *Marine Geol* **134** 145-162

Wagle B G, Vora K H, Karisiddaiah S M, Veerayya M and Almeida F (1994) Holocene submarine terraces on the western continental shelf of India: implications for sea-level changes *Marine Geol* **117**207-225

Wang W, Cawood P, Pandit M K and Zhou Mei-Fu (2018) Evolving passive and active margin tectonics of the Paleoproterozoic Aravalli basin, NW India *Geol Soc Amer Bull,* doi: 10:1130/B35027.1.4520573/b35027

Wang Y, Sieh K, Tun ST, Lai K-Y and Myint T (2014) Active tectonics and earthquake potential of the Myanmar region *J Geophy Res* **119** 3767-3822

Wardell A (1999) Barapukuria Coal Deposits, Stage 2, Feasibility Study *Geol Survey Bangladesh-UK Coal Project, No. 4298/7B, Petrobangla, Dhaka*

Weinberg R F (2016) Himalayan leucogranites and migmatites: Nature, timing and duration of anatexis *J Metamor Geol* **34** 821-843 https://doi.org/10.1111/jmg.12204

Weinberg R F and Dunlap J (2000) Growth and deformation of the Ladakh Batholith, Northwest Himalayas: Implications for timing of continental collision and origin of calc-alkaline batholith *J Geol* **108** 303-320

Weinberg R F, Dunlap W J and Whitehouse M (2000) New field structural and geochronological data from the Shyok and Nubra valleys, northern Ladakh: linking Kohistan to Tibet *Geol Soc London Spec Publ* **170** 253-275

White L T, Ahmad T, Ireland T R, Lister G and Forster M A (2011) Deconvolving episodic age spectra from zircons of the Ladakh Batholith, northwest Indian Himalaya *Chem Geol* **289** 179-196

Whitehouse M J, Ravindra-Kumar G R and Rimša A (2014) Behaviour of radiogenic Pbinzir conduring ultra high-temperature metamorphism: anion imaging and iontomography case study from the Kerala Khondalite Belt, southern India *Contrib Mineral Petrol* **168** 1042-1059

Widdowson M and Cox K G (1996) Uplift and erosional history of the Deccan Traps, India: Evidence from laterites and drainage patterns of the Western Ghats and Konkan Coast *Earth Planet Sci Lett* **137** 57-69

Wiedenbeck M and Goswami J N (1994) An ion-probe single zircon 207Pb/206Pb age from the Mewar Gneiss at Jhamarkotra, Rajasthan *Geoch Cosmo Acta* **58** 2135-2141

Win Swe (1972) Strike-slip faulting in central belt of Burma. In: Regional Conference on the Geol of Southeast Asia (Ed: Haile N S). *Geol Soc Malaysia Annex to Newsletter* **34**

Yatheesh V, Dyment J, Bthattacharya G C, Royer J Y, Kamesh Raju K A, Ramprasad T, Chaubey A K, Patriat P, Srinivas K and Choi Y (2019) Detailed structure and plate reconstructions of the Central Indian Ocean between 83.0 and 42.5 Ma (Chrons34and20) *J Geophy Res Solid Earth* **124** 4305-4322doi:10.1029/2018JB016812

Yatheesh V, John K P, Bhattacharya G C and Rajan S (2013) Morpho tectonic architecture of an India-Madagascar breakup related anomalous submarine terrace complex on the southwest continental margin of India *Marine Petrol Geol* **46** 304-318

Yedekar D B, Jain S C, Nair K K K and Dutta K K (1990) The central Indian Collision Suture, in Precambrrian of central India *Geol Surv India Spec Publ* **28** 1-37

Yedekar D B, Jain S C, Nair K K K and Dutta K K (1990) The Central Indian collision suture. Precambrian of Central India *Geol Surv India Spec Publ* **28** 1-37

Yin A (2006) Cenozoic tectonic evolution of the Himalayan orogen as constrained by along-strike variation of structural geometry, exhumation history, and foreland sedimentation *Earth-Sci Rev* **76** 1-31

Yin A, Dubey C S, Webb A A G, Kelty T K, Grove M, Gehrels G E and Burgess W P (2010) Geologic correlation of the Himalayan orogen and Indian craton: Part 1. Structural geology, U-Pb zircon geochronology, and tectonic evolution of the Shillong Plateau and its neighboring regions in NE India *Geol Soc Amer Bull* **122** 336-359 doi: 10.1130/B26460.1

Yoshida M, Bindu R S, Kagami H, Rajesham T, Santosh M and Shirahata H (1996) Geochronologic constraints of granulite terranes of South India and their implications for the Precambrian assembly of Gondwana *J Southeast Asian Earth Sci* **14** 137-147

Zachariah J K, Rao Y B, Srinivasan R and Gopalan K (1999) Pb, Sr and Nd isotope systematics of uranium mineralized stromatolitic dolomites from the Proterozoic Cuddapah Supergroup, south India: Constraints on age and provenance *Chem Geol* **162** 49-64

Zhao G, Wang Y, Huang B, Dong Y, Li S, Zhang G and Yu S (2018) Geological reconstructions of the East Asian blocks: From the breakup of Rodinia to the assembly of Pangaea *Earth-Sci Rev* doi: 10.1016/j.earscirev.2018.10.003

Zhao J-H, Pandit M K, Wang W and Xia X-P (2018) Neoproterozoic tectonothermal evolution of NW India: Evidence from geochemistry and geochronology of granitoids *Lithos* **316-317** 330-347.

Geological and Tectonic Map of the Indian Subcontinent

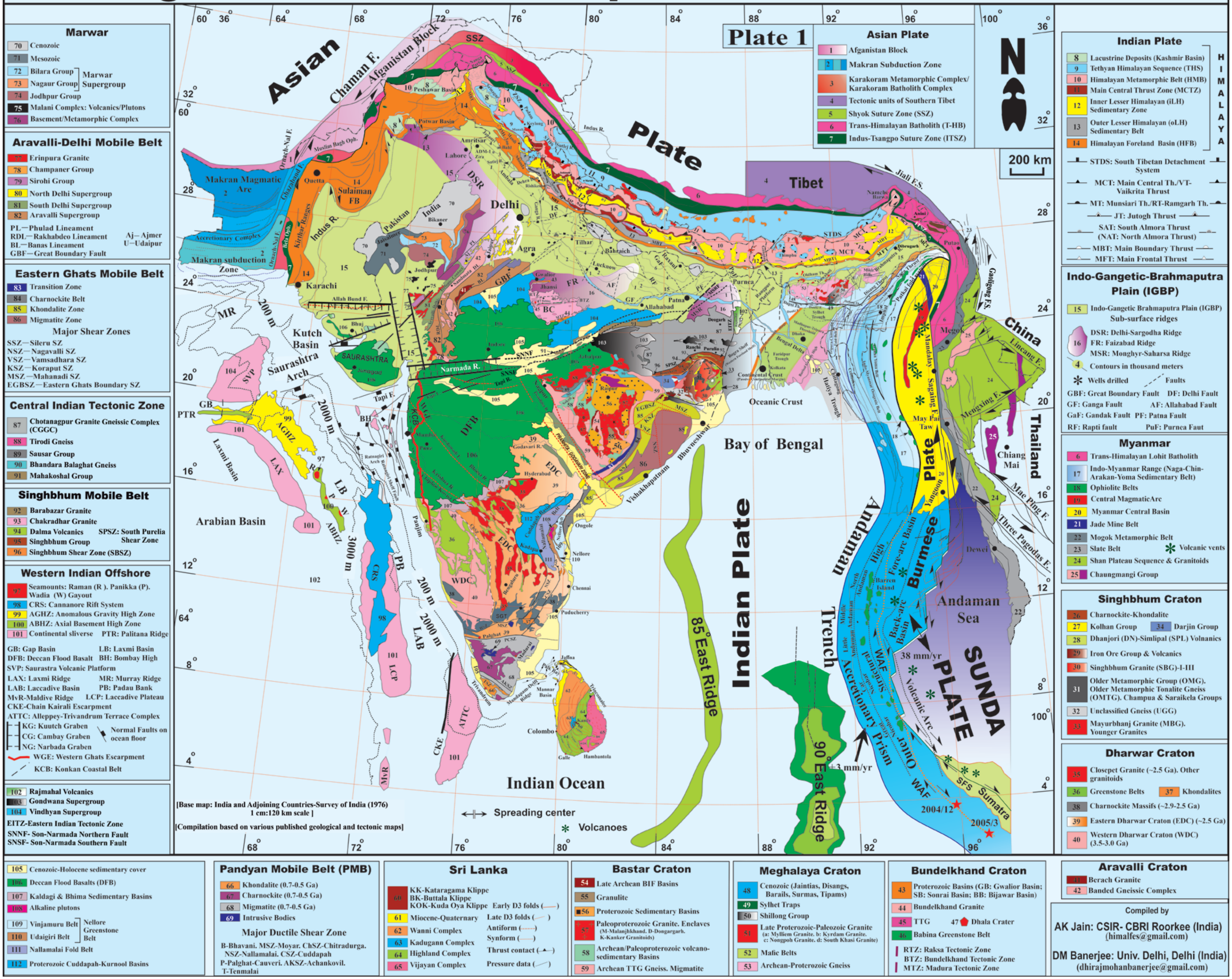

Cite as: Jain A K and Banerjee D M (2020) The Indian Subcontinent: Its Tectonics Map *Proc Indian Natn Sci Acad* **86**: 775-875

Regd. No. 16423/68

ISSN : 2454-9983

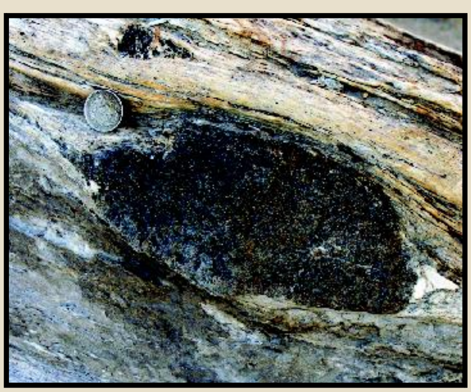

Cover: Asymmetrical eclogite lens in highly sheared gneisses of the Tso Morari Crystallines along leading edge of the Indian continental lithosphere, subducted to a depth of about 120 km around 53 million years (*Photograph courtesy*: AK Jain).

Published by Professor Gadadhar Misra, Vice-President (Publications/Informatics), Indian National Science Academy, Bahadur Shah Zafar Marg, New Delhi 110 002 and printed at Kamala Print-n-Publish, O 96, New Mahavir Nagar, New Delhi 110018, Mob. 9818476511